UC Davis

UC Davis Electronic Theses and Dissertations

Title

Winter Cover Crop Effects on Soil Water Dynamics: A Water Balance Approach in a California Pistachio Orchard

Permalink

https://escholarship.org/uc/item/1k27b0fq

ISBN

9798189233487

Author

Chen, Charlie

Publication Date

2026-06-25

Peer reviewed|Thesis/dissertation

eScholarship.org Powered by the California Digital Library
University of California

Winter Cover Crop Effects on Soil Water Dynamics: A Water Balance Approach in a California Pistachio Orchard

By

CHARLIE HSI-I CHEN

DISSERTATION

Submitted in partial satisfaction of the requirements for the degree of

DOCTOR OF PHILOSOPHY

in

Hydrologic Science

in the

OFFICE OF GRADUATE STUDIES

of the

UNIVERSITY OF CALIFORNIA

DAVIS

Approved:

Isaya Kisekka, Chair

Yufang Jin

Sam Sandoval

Committee in Charge

2026

Copyright 2026
By
Charlie Chen

Table of Contents

Abstract vi
Acknowledgements ix
Chapter 1: Monitoring Depth Matters: Conventional Root-Zone Measurements Miss Deep Soil Water Storage Under Winter Cover Crops in Irrigated Pistachio Orchards 1
Highlights 2
Abstract 3
1. Introduction 5
2. Materials and methods 9
2.1 Study site and orchard management 9
2.2 Experimental design 12
2.3 Precipitation and irrigation 15
2.4 Meteorological variables and evapotranspiration 16
2.5 Soil water balance 17
2.5.1 Neutron probe calibration and measurement 17
2.5.2 Water balance framework 18
2.5.3 Endpoint and interval deep percolation estimation 19
2.5.4 Statistical analysis 20
2.6 Spatiotemporal soil water dynamics 21
3. Results 22
3.1 Seasonal water balance 23
3.1.1 Precipitation and irrigation 23
3.1.2 Evapotranspiration 23
3.1.3 Soil water storage and deep percolation 25
3.1.4 Lower-profile contribution to storage 29
3.1.5 Sensitivity of DP estimates to calculation method 31
3.2 Depth-resolved soil water dynamics 32
3.2.1 Tree-scale three-dimensional soil water distribution 32
3.2.2 Treatment-level vertical soil water redistribution 36
4. Discussion 39
4.1 Synthesis of main findings 39
4.2 Evapotranspiration dynamics under winter cover cropping 39
4.3 Methodological implications for monitoring depth 41
4.4 Methodological implications for deep percolation estimation 45

4.5 Spatial variability across treeline and interrow positions 47
4.6 Implications for SGMA accounting and orchard management 48
4.7 Limitations 49
4.8 Future research 52
5. Conclusions 52
Acknowledgements 54
References 55
Chapter 2: OpenET Model Performance for Water Accounting and Winter Cover Crop Effect Detection in Young Pistachio Orchards 68
Highlights 69
Abstract 70
1. Introduction 72
2. Materials and Methods 79
2.1 Study site and treatments 79
2.2 Eddy covariance measurements and ET_a derivation 84
2.3 OpenET 87
2.4 Reference evapotranspiration and actual crop coefficient calculation 88
2.5 Statistical evaluation 91
3. Results 93
3.1 Climate and atmospheric demand context 93
3.2 Eddy covariance ET_a and the cover crop ET signal 95
3.3 EC-derived actual crop coefficients in young pistachio 98
3.4 OpenET model performance against EC: validation metrics and bias structure 101
3.5 Detection of the cover crop ET signal by RSET 106
3.6 Bi-monthly Ka structure: temporal redistribution between treatments 110
3.7 NDVI verification of cover crop greenness and canopy maturation 116
4. Discussion 121
4.1 Cover crop ET in young pistachio: magnitude and timing 121
4.2 Why OpenET models disagree: model-physics interpretation 126
4.3 Two evaluation skills, two different best models 133
4.4 Comparison with mature and young orchard Kc curves 138
4.5 Practical recommendations for SGMA compliance monitoring 142
4.6 Limitations 147
5. Conclusions 151
Acknowledgements 155

References 156
Chapter 3: APEX simulation of cover cropping in a California pistachio orchard under future climate scenarios 169
Highlights 170
Abstract 171
1. Introduction 172
2. Methods 174
2.1 Online survey 174
2.1.1 IRB approval and survey development 174
2.1.2 Survey design 175
2.1.3 Distribution and recruitment 176
2.1.4 Survey Analysis 176
2.2 APEX Model 177
2.2.1 Study site and experimental design 177
2.2.2 Weather data 179
2.2.3 Measured calibration and validation data 182
2.2.4 APEX model description, setup, and baseline parameters 185
2.2.5 Sensitivity analysis 193
2.2.6 Model evaluation criteria 194
2.2.7 Calibration and validation 195
2.2.8 Climate scenario design 197
3. Results 200
3.1 Survey Results 200
3.1.1 Sample composition 201
3.1.2 Orchard characteristics 203
3.1.3 Reported management practices 205
3.1.4 Report challenges 208
3.1.5 Concerns, benefits, and knowledge gaps 209
3.1.6 Information sources and benefit prioritization 213
3.1.7 Observed yield response and irrigation practices 215
3.1.8 Irrigation and water management 216
3.1.9 Reasons for non-adoption among NC respondents 219
3.2 APEX sensitivity analysis 220
3.3 APEX baseline model outputs 221
3.3.1 Daily scale evaluation 223

3.3.2 Monthly scale evaluation 225
3.3.3 No cover (NC) orchard 227
3.3.4 Cover crop (CC) orchard 232
3.4 Calibration and validation against field observations 234
3.4.1 Calibrated parameter values 243
3.5 Climate scenario outcomes 246
3.5.1 Soil water content and ET 255
3.5.2 Cover crop response under altered climates 257
4. Discussion 259
4.1 Survey findings in the broader context 259
4.2 Calibrated parameter values and sensitivity in the broader APEX literature 264
4.3 Model performance and what we can and cannot conclude 265
4.4 Climate scenario implications, viewed through grower concerns 266
4.5 Grower communication implications 269
4.6 Limitations 270
5. Conclusion 271
Acknowledgements 274
References 275
Chapter 4: Concluding remarks 288
Appendices 292
1. Support Materials for Chapter 1 292
1.1 Empirical Bayesian Kriging (EBK) 292
1.2 Neutron probe 293
1.3 Cosmic Ray 294
1.4 OpenET 297
2. Support Materials for Chapter 2 298
3. Support Materials for Chapter 3 304

Winter Cover Crop Effects on Soil Water Dynamics: A Water Balance Approach in a California Pistachio Orchard

Abstract

California's irrigated agriculture faces tightening water constraints from climate variability, chronic groundwater overdraft, and the Sustainable Groundwater Management Act (SGMA), which requires high- and medium-priority basins to reach sustainability within 20 years. Pistachio (*Pistacia vera*) acreage grew from roughly 25,000 bearing acres in 1979 to over 450,000 in 2023 and is projected to expand by a further 47 percent by 2031, concentrating future water demand in basins now under mandatory groundwater allocations. Winter cover cropping is widely promoted as a climate-smart practice that improves soil structure, infiltration, and nutrient retention, yet California adoption remains below five percent, partly because its water use consequences in a Mediterranean climate are poorly characterized. This dissertation evaluates the soil water, evapotranspiration, and grower-perceived consequences of winter cover cropping in California pistachio orchards using field measurements, remote sensing, surveys, and process-based modeling. ET_a

Chapter 1 quantifies the soil water budget of winter cover cropping in a young commercial pistachio orchard near Davis, California, using paired eddy covariance (EC) towers and 72 neutron probe access tubes (installed to a nominal 3.6 m, standardized to 3.0 m for measurement) across replicated cover crop (CC) and no cover (NC) treatments over three winter and two growing seasons. Cover crops increased actual evapotranspiration (ET_a) by 15 to 30 mm and depleted soil water storage in the upper (0 to 1.2 m) profile, but those losses were largely offset by enhanced storage in the lower (1.2 to 3.0 m) profile, where cover crop soil water content was 8 to 17 percent higher than NC across all five seasons. Post-termination summer ET_a

was 32 to 76 mm lower under CC, consistent with mulch-driven suppression of soil evaporation. Interval-based deep percolation (*DP*) estimates were 1.3 to 7.7 times the conventional endpoint estimates. Rather than removing water from the orchard, CC redistributed it downward into the lower (1.2 to 3.0 m) profile, a pattern invisible at the conventional root zone (0 to 1.2 m) monitoring depth. Accurately characterizing CC water dynamics in deep-rooted perennial systems therefore requires full-profile (0 to 3.0 m) monitoring matched to functional rooting depth, with interval-based water balance accounting.

Chapter 2 evaluates how well remote sensing evapotranspiration (RSET) products perform in young pistachio orchards and whether they can detect treatment-scale differences in actual evapotranspiration (ET_a) between adjacent management systems, both questions directly consequential under SGMA. Daily through seasonal ET_a estimates from six OpenET models and the OpenET Ensemble were compared against eddy covariance measurements from paired CC and NC treatments over three growing and three winter seasons spanning fifth- to seventh-leaf trees. SIMS produced the lowest monthly RMSE (19 mm month^{-1}), outperforming the Ensemble (23 mm month^{-1}), while DisALEXI recovered the CC ET_a signal in six of six seasons (mean absolute deviation 20 mm) versus five of six for SIMS. Actual crop coefficients (K_a) derived from EC measurements rose from 0.57 in fifth leaf (NC) to 0.95 in seventh leaf (NC), filling a gap in the published literature for young California pistachios. No single product served both uses, because the two applications reward different model properties: volumetric water accounting favors the lowest total magnitude error (SIMS), whereas treatment-effect detection favors sensitivity to fine-scale differences between adjacent fields (DisALEXI). Agencies conducting SGMA water accounting should therefore prioritize SIMS, while growers and researchers evaluating cover crop or management effects should prioritize DisALEXI.

Chapter 3 integrates grower perspectives with process-based simulation to project the long-term consequences of winter cover cropping in California pistachio orchards. An Institutional Review Board (IRB) approved online survey of pistachio growers, farm managers, and agronomic advisors provided structured, empirical input on current cover crop practices, perceived benefits, and primary concerns across the production region. The Agricultural Policy/Environmental eXtender (APEX) model was calibrated and validated against measured data from the paired CC and NC treatments of Chapters 1 and 2, including EC-derived ET_a, neutron probe soil water content, leaf area index, cover crop biomass, and pistachio yield. The calibrated model then generated projections of cover crop effects under survey-informed climate scenarios.

Together, these chapters show that winter cover cropping in California pistachio orchards has water consequences that are more nuanced, and more recoverable, than shallow-profile annual system studies suggest, that the RSET models underpinning SGMA accounting differ in their ability to support volumetric accounting versus treatment-effect detection, and that integrating grower perspectives into process-based modeling yields decision-relevant projections of long-term orchard floor management. The cross-chapter contribution is a measurement-to-management framework: field observation reveals where CC water goes, remote sensing determines which tools can track it at scale, and modeling extends both forward in time. This framework supports a more cautious interpretation of CC water costs in deep-rooted perennial systems and clearer guidance for selecting RSET models and designing field measurements for SGMA-era water accounting.

Acknowledgements

I could not have completed this work without the support and encouragement of my mentors, family, friends, my wife, and pets (Cooper, Arya, Haru, and Zeus).

I would like to thank my advisors, Isaya Kisekka and Yufang Jin, for their support and for the freedom they gave me to explore my research interests. I want to especially thank Isaya for taking a chance on me. I did not have the most traditional background for a graduate student in the Hydrologic Sciences Graduate Group (HSGG), so I'm grateful he was willing to take that gamble. I'm also especially grateful to Yufang for the opportunity to intern at the Jet Propulsion Laboratory (JPL) for a summer and a school year. Visiting the JPL campus was a highlight of my time at UC Davis.

I also want to thank my third committee member, Samuel Sandoval Solis, for his mentorship and encouragement throughout my PhD journey.

I want to thank Bullseye Farms, and especially Geoff, Emily, and Danielle, for their cooperation and support. This research would not have been possible without their willingness to let us instrument their field with more sensors than they probably bargained for.

I want to thank my mentor at JPL, Duane Waliser, for the chance to intern with him. I didn't plan on doing an internship, but I'm very glad it happened. It was a great learning experience, and I enjoyed working with everyone on the team, including Nick, Diana, Maia, Michael, and Cynthia.

I want to give a special thank you to everyone in the Kisekka lab who helped with my research over the years: Aaron Guerra, Ali Ghorbanpour, Anish Sapkota, Benny Briggs, Cassandra Bonfil, Felix Ogunmokun, Floyid Nicolas, Gento Shimamura, Ian Gomez, Isabella Burnett, Krista Blide, Matthew Maciosek, Nicolas Almeida, Sidd Dala, Usama Al-Dughaishi,

William Lennon, and Zixuan Gan, for their help with field work. A special shoutout goes to Ian for helping me install the neutron probe access tubes over the summer; I could never have dug all those holes on my own. And to Isabella, thank you for helping with neutron probe data collection for almost an entire year. Every day you spent in the field was another day I had to write, and I needed all the time I could get.

Finally, to my parents, Jennifer and Steven, thank you for everything. And, last but not least, to my wife, Jennie, thank you for your (un)conditional love and support. I'm finally done with school. Forever.

Chapter 1: Monitoring Depth Matters: Conventional Root-Zone Measurements Miss Deep Soil Water Storage Under Winter Cover Crops in Irrigated Pistachio Orchards

Charlie Chen[1], Matthew Roby[2], and Isaya Kisekka[1,3]

[1]Hydrologic Science Program, Department of Land, Air, and Water Resources, University of California, Davis, CA 95616, USA
[2]USDA-ARS Sustainable Agricultural Water Systems Research Unit, Davis, CA, 95616, USA
[3]Department of Biological and Agricultural Engineering, University of California, Davis, CA 95616, USA

This chapter will be submitted for review by the journal Agricultural Water Management. The manuscript, titled *Monitoring Depth Matters: Conventional Root-Zone Measurements Miss Deep Soil Water Storage Under Winter Cover Crops in Irrigated Pistachio Orchards* is prepared by the same co-authors as listed in this chapter.

Highlights

- Cover crops raised winter season ET by 15-30 mm in young pistachio orchards.
- Post-termination mulch cut summer ET by 32-76 mm versus bare ground.
- Cover crops shifted soil water into the lower profile (1.2-3.0 m) for storage.
- Full-profile (3.0 m) monitoring revealed storage invisible at the 1.2 m depth limit.
- Interval deep percolation exceeded endpoint estimates by 1.3-7.7 times.

Abstract

Winter cover crops are widely promoted as a climate-smart conservation practice and are well documented to provide a range of soil health benefits. Adoption in semi-arid regions nonetheless remains limited, in part because most prior studies monitored only the upper 0.9 to 1.2 m of the soil profile and may, therefore, mischaracterize the water cost of cover crops, overlooking water stored and redistributed at greater depth in perennial orchard systems. We quantified how winter cover crops affect full-profile soil water storage, evapotranspiration, and deep percolation in a young irrigated pistachio orchard, pairing eddy covariance (EC) flux towers with 72 3.6 m neutron probe access tubes in cover crop (CC) and no cover (NC) treatments over three winter (2023-24, 2024-25, 2025-26) and two growing (2024, 2025) seasons. Winter cover crops increased actual evapotranspiration (ET_a) by ~15 mm in 2023-24 and ~30 mm in 2024-25, and ~62 mm in 2025-26, with reduced or comparable soil water storage in the upper profile (0 to 1.2 m). That loss was offset by greater or comparable storage in the lower profile (1.2 to 3.0 m), where winter change in storage (ΔS) averaged 60, 44, and 21 mm in CC versus 50, 45, and 13 mm in NC in 2023-24, 2024-25, and 2025-26, respectively. Growing season ET_a (April to October) differed by only ~6 mm between treatments in 2024 but was ~36 mm lower in CC in 2025. After termination, June to October ET_a was lower in CC by 32 mm in 2024 and 76 mm in 2025, consistent with reduced soil evaporation under surface mulch. Because changes in the upper profile under CC were balanced by comparable or greater storage in the lower profile, full-profile ΔS was similar between treatments across all three winters. Short-interval deep percolation (DP) estimates were ~1.3 to 7.7 times the long-interval (endpoint) estimates across winter seasons and depths, indicating that endpoint accounting can substantially underestimate cumulative deep percolation. Full-profile (0.3 to 3.0 m) monitoring thus showed that CC

redistributed soil water into the lower profile rather than removing it from the system, a pattern invisible at conventional (< 1.2 m) measurement depths. These results indicate that shallow monitoring can overestimate the apparent water cost of CC in deep-rooted perennial systems and underscore the importance of matching both monitoring depth and accounting interval to the functional rooting depth.

Keywords: Pistachio; Cover crops; Soil water balance; Deep percolation; Evapotranspiration; Soil water storage

1. Introduction

Water demand now exceeds renewable supply in many highly productive agricultural regions worldwide, a condition the United Nations University Institute for Water, Environment and Health terms "global water bankruptcy" (UNU INWEH and Madani, 2026). In California, this imbalance manifests as recurrent multi-year drought, declining snowpack, and chronic groundwater overdraft, which together threaten the long-term viability of irrigated agriculture in the semi-arid Central Valley (Diffenbaugh et al., 2015; Pathak et al., 2018). Drought has deepened reliance on groundwater, which supplies about 40 percent of total water use in average years and up to 60 percent in critically dry years (DWR, 2025). In response to sustained overdraft, California enacted the Sustainable Groundwater Management Act (SGMA) in 2014, requiring high- and medium-priority basins to reach groundwater sustainability within 20 years (Faunt et al., 2016; Lubell et al., 2020; Borum et al., 2024). As allocations tighten, orchard floor practices that sustain productivity while reducing consumptive use or improving on-farm water storage have drawn growing interest. Perennial tree crops such as pistachio and almond are particularly exposed to these constraints because orchard establishment commits water demand for decades (Mall and Herman, 2019; Baldwin et al., 2020; Kandhway et al., 2025).

Pistachio (*Pistacia vera*) production illustrates this challenge: California grows 99 percent of the U.S. crop, generating over $2.9 billion in revenue in 2023 (CDFA, 2025), and supplies about 41 percent of global production (USDA, 2026). Statewide bearing acreage is projected to rise from 453,750 acres in 2023 to 668,850 acres by 2031, a 47 percent expansion that will sharply increase the orchard area subject to SGMA allocations (Tootelian, 2023). Because pistachio orchards take several years to reach economic production and then remain in

place for decades (Baldwin et al., 2020), decisions made at establishment can shape water outcomes over the life of the orchard.

Winter cover cropping is an orchard floor practice that can advance both soil health and water management. Cover crops (CC) have been shown to improve soil structure (Sainju and Singh, 1997; Blanco-Canqui et al., 2015), enhance infiltration (Blanco-Canqui and Ruis, 2020), reduce runoff and erosion (Joyce et al., 2002), and improve nutrient retention (Unger and Vigil, 1998; Carlisle, 2016; Bergtold et al., 2019; DeVincentis et al., 2020; Borum et al., 2024). They can also deliver broader ecological benefits, including pest suppression, improved soil quality, and nutrient cycling (Snapp et al., 2005; Vukicevich et al., 2016; Koudahe et al., 2022; Vendig et al., 2023; Moore and Norton, 2024). Despite these advantages, adoption in California remains low, largely because of uncertainty about how winter cover crops affect soil water availability and evapotranspiration under semi-arid conditions.

Cover crops generally increase actual evapotranspiration (ET_a) during active growth because they add transpiring biomass (Mitchell et al., 1999; Wang et al., 2021; Garba et al., 2022; Hao et al., 2023). Several studies also report lower soil water content in shallow layers after CC growth, reinforcing the concern that CC may deplete water needed by the main crop (Wyland, 1996; Mitchell et al., 2015; Nielsen et al., 2015; Schomberg et al., 2023). After termination, however, the residue left as surface mulch can suppress soil evaporation later in the season, so the net annual effect depends on the balance between water use during the CC growth phase and water conserved after termination (DeVincentis et al., 2022; Flynn et al., 2025).

Cover crops may also reshape infiltration and water redistribution within the soil profile. In annual systems, cover cropping has been shown to increase infiltration and reduce runoff (Haruna et al., 2022; Joyce et al., 2002). Whether these gains translate into improved water

storage in deep-rooted perennial systems, however, depends on the depth of observation. Most prior studies monitored only the upper 0.9 to 1.2 m of the profile (Mitchell et al., 2015), a depth appropriate for annual crops but likely too shallow to capture the storage zone relevant to orchards with much deeper roots (Goldhamer et al., 1985).

This depth limitation matters. In deep-rooted perennial systems, shallow monitoring can overstate the apparent water cost of winter CC in two ways. First, it misses redistribution below the upper profile (0 to 1.2 m) into the lower profile (1.2 to 3.0 m) accessible to perennial tree roots. Second, it constrains how deep percolation (*DP*) is estimated: because *DP* is typically derived as the residual of the soil water balance, its value depends strongly on the temporal resolution of the storage measurements, and widely spaced endpoint measurements can miss transient drainage events and underestimate the cumulative total.

These two limitations, shallow monitoring depth and reliance on seasonal endpoint accounting, motivate this study. Addressing them together, through depth-resolved monitoring that extends to the functional rooting depth and through interval-based water balance accounting, yields a more complete picture of CC water dynamics in deep-rooted perennial systems and a firmer basis for evaluating cover cropping under SGMA-driven groundwater management.

To address these gaps, we implemented full-profile monitoring from 0.3 to 3.0 m in a young commercial pistachio orchard managed with and without winter cover crops. Paired eddy covariance (EC) flux towers, precipitation and irrigation records, and replicated neutron probe observations were used to construct depth-resolved seasonal water balances across three winters and two growing seasons. The objectives were to (1) quantify the effects of winter CC on seasonal soil water balance components, including actual evapotranspiration (ET_a), deep percolation (*DP*), and change in soil water storage (ΔS); (2) evaluate how winter CC affects the

vertical and spatial distribution of soil water across the full profile; and (3) assess how monitoring depth and temporal resolution shape apparent treatment effects on storage change and deep percolation. We hypothesized that winter CC shifts water downward within the profile, so that apparent water losses in the upper profile are offset by greater storage at depth and by reduced summer evaporation after termination. The following section describes the study site, experimental design, data collection, and soil water balance framework used to evaluate these questions.

2. Materials and methods

2.1 Study site and orchard management

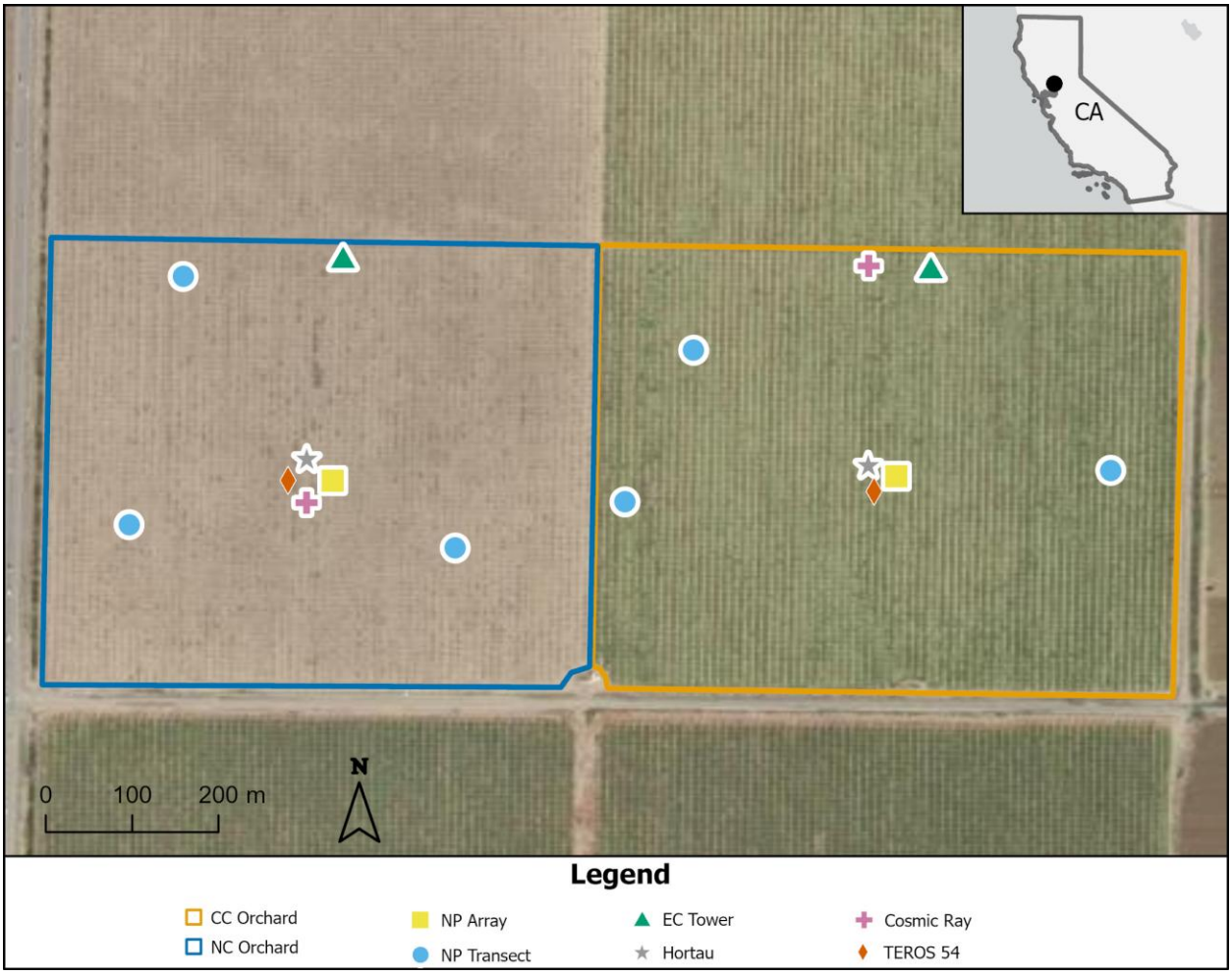


Figure 1. Map of the Bullseye pistachio orchard showing the cover crop (CC) and no cover (NC) treatment quadrants, the eddy covariance flux tower locations in each treatment, the neutron probe access tube locations for the transect and array experiments, and the additional soil moisture sensors (cosmic ray neutron sensor TEROS 54 soil moisture sensors, and Hortau pressure transducers on the irrigation lines) installed in each treatment.

The study was conducted in a 61-ha commercial pistachio orchard (*Pistacia vera*, cultivar 'Golden Hills') located in the southern Sacramento Valley (38.619° N, 121.725° W; Figure 1), approximately 10 km north of Davis, California. The orchard was established in December 2018 with rows oriented north to south, 5.8 m row spacing, and 5.2 m in-row tree spacing, equivalent to 332 trees ha^{-1}. The region has a warm-summer Mediterranean climate. Based on 30-year

records from CIMIS Davis Station 006 (1996 to 2025), mean monthly minimum temperature is 3.6 °C in December and mean monthly maximum temperature is 33.0 °C in July. Mean annual precipitation is 435 mm and falls mainly from November through March, with less than 30 mm of cumulative rainfall from June through October (Table 1).

Table 1. Thirty-year average grass-reference evapotranspiration (ET_o) and precipitation in Davis, CA (1996 to 2025).

	Jan	**Feb**	**Mar**	**Apr**	**May**	**Jun**	**Jul**	**Aug**	**Sep**	**Oct**	**Nov**	**Dec**
Precipitation (mm)	86.0	87.6	56.7	26.4	14.4	2.5	0.1	1.4	5.4	19.6	45.1	89.9
ET_o (mm)	34.8	54.5	95.1	139.0	185.0	208.0	212.0	187.0	146.0	105.0	50.5	32.0

The orchard was divided into four quadrants of about 15 ha each. The two eastern quadrants were managed with winter cover crops (CC), and the two western quadrants were maintained as no cover (NC), with periodic mowing of resident vegetation when needed. Cover crops in the CC quadrants were seeded in late October or early November and terminated in late March or April. Cover crop mixtures included legumes, grains, and brassicas, and species composition and seeding rate varied by season according to grower preference (Table 2). Herbicide was applied to the under-tree strips in both treatments throughout the study; alleyway vegetation was not treated with herbicide.

Table 2. Cover crop mixture composition, seeding rate and date, termination date, and subsequent mowing schedule for the 2023-24, 2024-25, and 2025-26 seasons.

Season	**Composition**	**Seeding rate (kg ha^{-1})**	**Seeding date**	**Termination date**	**Post-termination mowings**
2023-24	23% grain, 25% bell bean, 25% peas, 15% vetch, 2% brassica	50.4	8 Nov 2023	30 Apr 2024	21 Jun 2024; 16 Oct 2024
2024-25	30% bell bean, 30% peas, 20% vetch, 20% rye	44.8	15 Nov 2024	28 Mar 2025	18 May 2025; 24 Jul 2025
2025-26	30% bell bean, 30% peas, 20% vetch, 20% oats	45.0	24 Oct 2025	3 Mar 2026	7 May 2026

According to the National Cooperative Soil Survey (NCSS; https://websoilsurvey.nrcs.usda.gov/app/), soils at the site are mapped mainly as silty clay loams. The NC treatment area is composed of 98 percent Rincon silty clay loam and 2 percent Capay silty clay, whereas the CC treatment area includes 47 percent Sycamore silty clay loam, 34 percent Yolo silt loam, and 19 percent Rincon silty clay loam. To characterize soil texture directly, soil particle size distribution was measured every 0.3 m to a depth of 3.0 m using samples collected during neutron probe access tube installation in 2023. Samples were analyzed with a laser diffraction particle-size analyzer (Partica LA-960, HORIBA, Ltd., Kyoto, Japan). One interrow sample was collected at each depth from each of four installation locations per treatment (n = 4 per depth per treatment). Laboratory analysis classified all four sampled CC locations as silt loam at all depths, which differed from the NRCS surface mosaic. This discrepancy likely reflects the coarse resolution of the soil survey, which cannot resolve fine-scale heterogeneity as well as direct sampling. Treatment means by depth are reported in Table 3.

Table 3. Laboratory-measured soil particle size distribution (clay, silt, and sand, percent by mass) and USDA textural class by depth for the cover crop (CC) and no cover crop (NC) treatments. Values represent the mean of four samples collected at the interrow position from four access tube installation locations per treatment (n = 4 per depth per treatment).

Depth (m)	CC				NC			
	Clay (%)	Silt (%)	Sand (%)	Soil Type	Clay (%)	Silt (%)	Sand (%)	Soil Type
0.3	17.2	67.8	15.0	Silt Loam	28.0	65.8	6.2	Silty Clay Loam
0.6	19.9	68.8	11.2	Silt Loam	30.9	63.7	5.4	Silty Clay Loam
0.9	20.2	67.8	12.0	Silt Loam	31.3	64.6	4.2	Silty Clay Loam
1.2	19.0	60.3	20.7	Silt Loam	29.5	64.3	6.1	Silty Clay Loam
1.5	21.5	62.5	16.0	Silt Loam	25.5	66.0	8.5	Silt Loam
1.8	22.1	67.8	10.2	Silt Loam	25.1	61.7	13.2	Silt Loam
2.1	22.6	67.3	10.0	Silt Loam	25.7	60.1	14.2	Silt Loam
2.4	22.8	62.3	15.0	Silt Loam	24.2	61.3	14.6	Silt Loam
2.7	21.2	57.6	21.3	Silt Loam	24.8	57.4	17.9	Silt Loam
3.0	21.1	56.5	22.4	Silt Loam	18.7	55.2	26.0	Silt Loam

2.2 Experimental design

Detailed soil water monitoring was conducted in the two southern quadrants (one CC, one NC) because they fell within the representative fetch of the EC flux towers. The towers were positioned near the middle of the northern and southern quadrants in each treatment to maintain adequate fetch under both prevailing southerly winds and the northerly wind shift that occurs from late fall through mid-winter. Within each monitored quadrant, two nested experiments were established: a transect experiment to characterize soil water gradients from the tree row to the alleyway center, and an array experiment to resolve three-dimensional soil water distribution around a representative tree (Figure 2).

Each treatment contained four transect locations. At each transect location, four neutron probe access tubes were installed at ~1 m intervals from the tree row to the alleyway center. Transect locations were selected to represent the major mapped soil series present within each treatment. At one of the four transect locations in each treatment, 20 additional tubes were installed in a three-dimensional array around a central tree, resulting in 24 tubes at the array location and four tubes at each of the other three transect locations. The complete design therefore included 36 tubes per treatment and 72 tubes across both treatments.

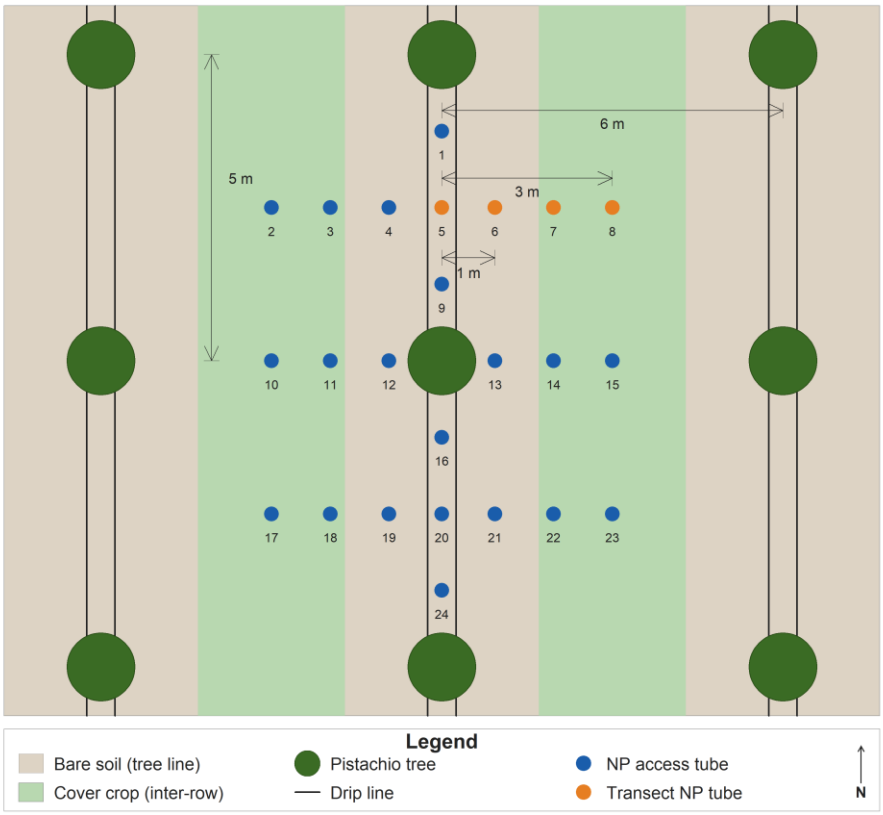


Figure 2. Schematic of the nested experimental design at the array location in each treatment, shown here for the CC treatment (interrow CC shaded green, tree-row bare strip shaded tan). At the array location, 24 neutron probe access tubes were installed to resolve three-dimensional soil water distribution, including an integrated four tube transect (orange) at 1 m intervals from the tree row to the alleyway center. Three additional four tube transects (not shown) were installed elsewhere within each treatment, for a total of 36 tubes per treatment and 72 tubes across both treatments.

All tubes were installed to a nominal length of 3.6 m, but soil accumulation at the base of some tubes prevented consistent access below 3.0 m. Measurements were therefore standardized to a maximum analyzed depth of 3.0 m. Volumetric soil water content (θ, $m^3\ m^{-3}$) was measured with a neutron probe (CPN 503 Elite Hydroprobe, InstroTek, Inc., Raleigh, NC, USA) at all 72 tube locations. Readings were collected at 0.3 m intervals from 0.3 to 3.0 m, yielding 10 measurement depths per tube on each sampling date. Measurements were collected on 13 dates in 2023, 29 dates in 2024, 26 dates in 2025, and 6 dates in 2026 (as of June 2026).

During tube installation in 2023, soil samples were collected at each 0.3 m depth increment for gravimetric water content and soil texture analysis. After calibration, each tube-by-depth time series was visually screened for single-date anomalies, defined as abrupt departures from the surrounding trend followed by immediate recovery. Values identified as anomalous were replaced by linear interpolation between adjacent valid observations.

Storage was computed for the full profile (0 to 3.0 m), the upper profile (0 to 1.2 m), and the lower profile (1.2 to 3.0 m). The upper profile corresponds to the effective root-zone depth often assumed for annual crops (Allen et al., 1998). For treatment-level analysis, the 36 tubes in each treatment were grouped by lateral position relative to the tree row into four position classes (n = 9 per class): Tube 1 at the treeline, Tube 4 at the alleyway center, and Tubes 2 and 3 at intermediate positions (Table 4). Seasonal soil water balance analyses presented here were based on averages from Tubes 1 and 4. Tube 1 served as a within-treatment reference because no cover crop was present in the treeline, whereas Tube 4 represented the center of the alleyway, where treatment differences in orchard floor management were strongest.

Table 4. Tube numbers assigned to each of the four lateral position classes (Tubes 1 through 4) for both the no cover (NC) and cover crop (CC) treatments.

	Averaged Tube Numbers
Tube 1	1, 5, 9, 13, 17, 24, 28, 32, 33
Tube 2	2, 6, 12, 14, 20, 21, 27, 29, 34
Tube 3	3, 7, 11, 15, 19, 22, 26, 30, 35
Tube 4	4, 8, 10, 16, 18, 23, 25, 31, 36

Additional continuous soil moisture observations were collected in each treatment using four TEROS 54 profile probes (METER Group, Inc., Pullman, WA, USA), each installed to 0.6 m depth and co-located with the array experiment along a gradient from the treeline to the alleyway center. These sensors were logged at 15-minute intervals. A cosmic ray neutron sensor (Quaesta Instruments, LLC, Tucson, AZ, USA) with an estimated footprint radius of about 100

m under typical conditions was also installed in each treatment. These continuous measurements were used to corroborate the neutron probe observations, but they were not included in the soil water balance calculations.

2.3 Precipitation and irrigation

Daily precipitation was measured with tipping-bucket rain gauges mounted on both EC flux towers. Daily totals from the two gauges were averaged to obtain a single site precipitation value. These on-site totals were compared with precipitation data from CIMIS Davis Station #006. On days when the on-site gauges recorded zero or near-zero precipitation while CIMIS reported nonzero rainfall, the on-site record was assumed to reflect data loss or instrument malfunction. For these dates, a correction factor (k) was computed as the ratio of cumulative on-site gauge precipitation to cumulative CIMIS precipitation over the nearest three-day window with valid data from both sources (Equation 1). The adjusted daily precipitation was then calculated as the product of k and the CIMIS daily total (Equation 2). On all remaining days, the on-site gauge average was used directly.

$$k = \frac{\sum P_{gauge}}{\sum P_{CIMIS}} \tag{1}$$

$$P_{adj} = k * P_{CIMIS} \tag{2}$$

Irrigation was supplied through a double drip-line system, with each tree serviced by four emitters discharging 2.0 L h^{-1} each. Irrigation scheduling and amounts were determined by the orchard manager using a crop coefficient-based approach. Irrigation amounts were obtained from orchard management records and cross-checked against field observations. Beginning in 2023, flow in the irrigation supply lines of both treatments was monitored with Hortau pressure transducers (Hortau, San Luis Obispo, CA, USA). Irrigation duration on each event was derived

from periods of sustained pressurization. Seasonal irrigation totals were used as direct inputs to the soil water balance.

2.4 Meteorological variables and evapotranspiration

Treatment-level ET_a was estimated using EC flux towers installed near the middle of the northern and southern quadrants of each treatment. Reference evapotranspiration (ET_o) and meteorological data were obtained from CIMIS Davis station. Each tower was equipped with an IRGASON integrated open-path CO_2/H_2O gas analyzer and 3D sonic anemometer (Campbell Scientific, Logan, UT, USA) mounted at 6.5 m height and recording at 20 Hz to resolve turbulent water vapor fluxes. A SN-500 four-component net radiometer (Apogee Instruments, Inc., Logan, UT, USA) measured net radiation. Soil heat flux (G) was estimated from five sensor sets deployed along a diagonal transect spanning the interrow, each consisting of an HFT-3 heat flux plate buried at 8 cm depth (Radiation Energy Balance Systems Inc., Bellevue, WA, USA), Type E thermocouples at 2 and 6 cm depth, and a Hydraprobe soil moisture sensor (Stevens Water Monitoring Systems, Portland, OR, USA) at 5 cm depth. Thermocouple and soil moisture data were used to apply the standard calorimetric correction to measured plate fluxes.

Half-hourly latent heat flux (λE) was calculated from the covariance of vertical wind velocity and water vapor concentration measured by the IRGASON. Raw 20 Hz data were processed following a standard eddy covariance pipeline including spike removal, coordinate rotation, density corrections, and frequency-response adjustments. Density corrections followed Webb et al. (1980), and frequency-response corrections followed Moore (1986) and Massman (2000); the overall processing approach is consistent with that described by Foken et al. (2012). Processed half-hourly fluxes were screened to remove periods with insufficient turbulence, precipitation events, and instrument malfunction. Gaps were filled at the half-hourly resolution

using the Flux Gap Filling Tool (Peddinti, 2026), which implements the marginal distribution sampling (MDS) approach described by Reichstein et al. (2005) and incorporated into the ONEFlux processing pipeline (Pastorello et al., 2020). Gap-filled half-hourly fluxes were aggregated to daily ET_a totals. ET_a from each tower was applied exclusively to the water balance of its corresponding treatment.

2.5 Soil water balance

2.5.1 Neutron probe calibration and measurement

Volumetric water content (VWC) at each access tube and depth was derived from neutron probe count ratios (measured counts divided by standard counts) using a site-specific calibration developed during access tube installation in 2023. The neutron probe was operated at a constant count of 15 seconds per measurement depth. Calibration samples were collected gravimetrically at 72 locations across the study site at 0.3 m depth intervals from 0.3 to 1.5 m, converted to VWC using bulk density data provided by the NCSS, and regressed against neutron count ratios. A single calibration equation was applied to both treatments to avoid introducing between-treatment differences in VWC that would otherwise reflect the separate regressions rather than true differences in soil water content. Because soil texture differed between treatments in the upper profile (silt loam in CC versus silty clay loam in NC; Table 3) and this difference could not be fully separated from the cover crop effect in the unreplicated paired design, texture is treated here as a scope condition rather than as a controlled covariate. The implications of this scope condition for inference are addressed in the Discussion section.

Inter-measurement intervals were typically 10 to 14 days, with maximum gaps of approximately 30 days. The neutron probe method has well-established accuracy for resolving

depth-resolved changes in soil water storage when used with site-specific calibration (Evett and Steiner, 1995; Gaze et al., 2002).

Neutron probe readings at 0.3 m depth intervals from 0.3 to 3.0 m were integrated using a constant-layer-thickness scheme, with each reading representing the 0.3 m layer immediately above the measurement depth (for example, the 0.3 m reading represented the 0 to 0.3 m layer, and the 3.0 m reading represented the 2.7 to 3.0 m layer). Total soil water storage was computed as the sum of VWC at each measurement depth multiplied by 0.3 m, yielding storage in millimeters over the upper profile (0 to 1.2 m) and full profile (0 to 3.0 m) depth ranges. Near-surface water content dynamics were independently verified using the cosmic ray neutron sensor (effective sensing depth approximately 0.3 m) and TEROS 54 profile probes (0.15, 0.30, 0.45, and 0.60 m depths at 15-minute intervals), which provided corroborating evidence for the neutron probe integration in the upper profile. These near-surface measurements were not incorporated into the primary soil water balance calculations.

2.5.2 Water balance framework

A one-dimensional soil water balance was used to assess the effects of winter cover cropping on seasonal water partitioning in each treatment. Calculations were performed separately for two seasonal windows per annual cycle: the winter season (November to March), encompassing the cover crop growing period and pistachio dormancy, and the pistachio growing season (April to October), during which trees are actively transpiring and irrigation is applied. The analysis was conducted for the 2023-2024, 2024-2025, and 2025-26 (winter only) annual cycles, with each seasonal window analyzed independently. For each season and treatment, the water balance was expressed as Equation 3:

$$DP = P + I - ET_a - \Delta S \quad (3)$$

where DP is deep percolation below the measurement depth (mm), P is total precipitation (mm), I is total applied irrigation (mm), ET_a is actual evapotranspiration (mm), and ΔS is the change in soil water storage (mm). Surface runoff and lateral subsurface flow were assumed negligible given the flat topography, the drip irrigation system, and the absence of observed overland flow during the study period. Canopy interception and stemflow were not partitioned explicitly.

DP was estimated as the residual of Equation 3. Negative residuals indicate water balance closure error, most likely arising from underestimation of ET_a or precipitation inputs, or overestimation of ΔS, all within measurement uncertainty. Negative DP values were set to zero to enforce the physical expectation that net vertical flux at the lower measurement boundary is downward during the study period; upward capillary rise from below 3.0 m to the monitored profile was assumed negligible at this site.

2.5.3 Endpoint and interval deep percolation estimation

Two approaches were used to estimate seasonal DP. The endpoint approach (DP_{end}) computed DP from a single ΔS between the start and end dates of each seasonal window. The interval approach (DP_{int}) computed DP between successive measurement dates and summed the non-negative interval estimates across the season. The two approaches were compared to evaluate the sensitivity of seasonal DP estimates to the temporal resolution of storage measurements.

For the endpoint approach, change in soil water storage (ΔS) was calculated from integrated neutron probe readings at the start and end of each seasonal window using Equation 4:

$$\Delta S = S(t_2) - S(t_1) \quad (4)$$

where $S(t_1)$ and $S(t_2)$ are the integrated soil water storage (mm) at the start and end dates of each seasonal window, respectively. When no neutron probe measurement fell exactly on the seasonal

boundary date, the nearest available measurement date was used. ΔS was calculated for the upper profile (0 to 1.2 m) and the full profile (0 to 3.0 m). ΔS for the derived lower layer (1.2 to 3.0 m) was calculated as the difference between full profile and upper profile estimates. The endpoint approach yields a single seasonal ΔS and corresponding DP_{end} for each tube, depth range, treatment, and season.

For the interval approach, DP_{int} was estimated for each interval between successive neutron probe measurement dates using Equation 5:

$$DP_{int} = P_{int} + I_{int} - ET_{a,int} - \Delta S_{int} \quad (5)$$

where P_{int}, I_{int}, $ET_{a,int}$, and ΔS_{int} are the cumulative daily precipitation, irrigation, actual evapotranspiration, and change in integrated soil water storage between successive measurement dates, respectively. On days with missing flux tower data, gap-filled ET_a values were substituted as described in Section 2.4. DP_{int} values were constrained to be non-negative, consistent with the endpoint approach, and summed across each season to obtain seasonal DP_{int} totals for each tube and depth range.

2.5.4 Statistical analysis

Treatment differences in ΔS, DP_{end}, and DP_{int} were assessed using paired t-tests applied independently to each seasonal window and depth range. The experimental design was structured as a blocked comparison, with tree-row-to-interrow position as the blocking factor; each tube position represents an equivalent lateral location relative to the tree row in the CC and NC treatments. Pairing was therefore by position label rather than by geographic proximity, since the two treatments occupy separate quadrants of the orchard and paired tubes are not spatially adjacent. This pairing reduces within-treatment variance attributable to the tree-row-to-interrow

gradient, which is the primary source of spatial heterogeneity in soil water content at this site (n = 36 pairs).

Planned paired t-tests were also conducted within each tube-position group (T1 closest to the tree row through T4 at the interrow center; n = 9 pairs per group; Figure 2) to evaluate the spatial consistency of treatment effects across the tree-row-to-interrow gradient. Normality of within-pair differences was assessed using Shapiro-Wilk tests; where non-normality was indicated ($p < 0.05$), Wilcoxon signed-rank tests were used as a robustness check, and conclusions were consistent with the paired t-test results. All statistical analyses were performed in R version 4.3.3 (R Core Team, 2024), and differences were considered significant at $\alpha = 0.05$.

2.6 Spatiotemporal soil water dynamics

Three-dimensional soil water content distributions around each instrumented tree were characterized using neutron probe data from the 24-tube array in each treatment. VWC profiles from all array tubes, measured at each of the 10 measurement depths from 0.3 to 3.0 m at 0.3 m increments, were spatially interpolated using the Empirical Bayesian Kriging 3D (EBK3D) algorithm in ArcGIS Pro (version 3.1, ESRI, Redlands, CA, USA), following the approach described by Gribov and Krivoruchko (2020). The performance of EBK relative to conventional kriging has been evaluated in detail by Krivoruchko and Gribov (2019). EBK3D was selected because it estimates spatially continuous soil water content volumes with quantified uncertainty from irregular three-dimensional point data and does not require the semivariogram parameters to be specified in advance, making it well suited to the irregular tube spacing of the array. Interpolations were performed separately for each measurement date using consistent algorithm settings across all dates, enabling visualization and quantitative comparison of seasonal changes

in three-dimensional soil water distribution around each instrumented tree across both treatments.

For quantitative analysis, horizontal slices of the three-dimensional interpolated field were extracted at each of the 10 measurement depths (0.3, 0.6, 0.9, 1.2, 1.5, 1.8, 2.1, 2.4, 2.7, and 3.0 m). For each slice, treatment, and measurement date, the arithmetic mean VWC and its spatial standard deviation were computed across the slice area. Depth-slice summaries were used to quantify the vertical distribution of soil water in each treatment and to track treatment differences across the study period. EBK3D uncertainty surfaces were generated for each interpolation but were used only to assess interpolation confidence qualitatively.

Treatment-level vertical redistribution (Figure 5 and Figure 6) was quantified directly from the 36 tube neutron probe dataset rather than from the EBK3D interpolation. For each treatment, depth, and measurement date, mean VWC was computed across the 36 tubes; the CC-minus-NC difference at each 0.3 m depth increment was then averaged over all measurement dates within each seasonal window to yield the per-depth seasonal mean difference. These per-depth differences were summed across three depth zones (0 to 1.2 m, 1.2 to 3.0 m, and 0 to 3.0 m) to obtain the cumulative VWC difference reported in Figures 5 and 6.

3. Results

Results are organized around three questions that follow from the study objectives. The first, addressed in the seasonal water balance subsections, is how winter cover cropping altered the partitioning of ET_a, ΔS, and DP between the CC and NC treatments across three winters and two growing seasons. The second, addressed in the depth-resolved VWC subsections, is whether the apparent treatment effects on ΔS and DP in the conventional 0 to 1.2 m root zone are preserved when the analysis is extended to the full profile. The third, addressed throughout the

seasonal water balance and synthesis subsections, is how the choice of accounting method, endpoint versus interval, affects the magnitude and statistical detection of treatment effects on *DP*.

3.1 Seasonal water balance

3.1.1 Precipitation and irrigation

Precipitation was the only water input during the winter seasons. Total winter precipitation was 334 mm (2023-24), 294 mm (2024-25), and 301 mm (2025-26) (Table 6). No irrigation was applied between November and March in either treatment. During the 2024 growing season, precipitation totaled 23 mm and irrigation totaled 330 mm in CC and 321 mm in NC. In 2025, precipitation totaled 36 mm and irrigation increased to 580 mm in CC and 505 mm in NC. Unless otherwise noted, results are presented as treatment means across all tubes within each profile depth and seasonal window.

3.1.2 Evapotranspiration

Winter ET_a was consistently higher in the CC treatment than in the NC treatment across all three winters. Total winter ET_a was 193 mm (CC) versus 178 mm (NC) in 2023-24, and 201 mm versus 171 mm in 2024-25, and 265 mm versus 203 mm in 2025-26, corresponding to increases of 15, 30, and 62 mm, respectively (Table 5). March was the largest single-month contributor to the winter treatment difference in all three years (18 mm in 2023-24, 17 mm in 2024-25, and 22 mm in 2025-26). In 2023-24 and 2024-25, small CC deficits in the early winter months partially offset the seasonal totals, whereas in 2025-26 CC exceeded NC in every winter month, producing the largest winter difference of the study.

Table 5. Monthly actual evapotranspiration (ET_a, mm) measured by eddy covariance for the cover crop (CC) and no cover (NC) orchards during the 2023-2024, 2024-2025, and 2025-2026 seasons. Diff = CC minus NC. Monthly values are rounded to the nearest mm; seasonal totals are computed from daily sums.

Month	2023-2024			2024-2025			2025-2026		
	CC (mm)	NC (mm)	Diff (mm)	CC (mm)	NC (mm)	Diff (mm)	CC (mm)	NC (mm)	Diff (mm)
November	25	27	-2	32	36	-4	55	37	18
December	23	24	-1	31	33	-2	55	51	4
January	36	37	-1	37	26	11	40	37	3
February	47	45	2	43	36	7	51	36	15
March	63	45	18	58	41	17	64	42	22
Winter Total (Nov-Mar)	193	178	15	201	171	30	265	203	62
April	71	40	31	74	40	34			
May	77	69	8	98	91	7			
June	91	93	-2	110	125	-15			
July	106	115	-9	120	138	-18			
August	86	93	-7	117	139	-22			
September	66	74	-8	86	99	-13			
October	52	59	-7	59	67	-8			
Growing Total (Apr-Oct)	549	543	6	664	700	-36			

Growing season ET_a exhibited the inverse pattern, with CC lower than NC. Total ET_a during April to October was similar between treatments in 2024 (549 mm in CC and 543 mm in NC, a 6 mm difference) but diverged in 2025, when NC totaled 700 mm compared to 664 mm in CC (Table 5). In both years, April showed the largest monthly CC over NC difference (31 mm in 2024 and 34 mm in 2025). CC also exceeded NC in May (8 mm in 2024 and 7 mm in 2025). From June onward, NC exceeded CC in both years, though the magnitude differed considerably: monthly NC minus CC differences ranged from 2 to 9 mm in 2024 and from 13 to 22 mm in 2025 between June and September, with the maximum difference observed in August 2025 (22 mm). The greater NC-CC divergence in 2025 coincided with a 115 mm (CC) and 156 mm (NC) increase in growing season ET_a between years, with the larger absolute increase in NC accounting for the shift from a small CC excess in 2024 to a 36 mm NC-over-CC difference in 2025.

3.1.3 Soil water storage and deep percolation

Deep percolation estimated from the endpoint and interval methods is denoted DP_{end} and DP_{int}, respectively. Treatment differences in ΔS, DP_{end}, and DP_{int} were evaluated using paired t-tests (CC tube *i* vs. NC tube *i*), and depth-resolved comparisons of ΔS between the upper and full profiles were assessed using one-sample t-tests on the within-tube difference. All values reported below are mean ± SD (n = 36 tube pairs); full results are provided in Table 6. One-sample t-tests on the within-tube difference between full-profile and upper-profile ΔS confirmed that the lower profile (1.2 to 3.0 m) carried a storage signal distinct from the upper profile in every season: lower-profile ΔS differed significantly from zero in all three winters (CC 60, 44, and 21 mm; NC 50, 45, and 13 mm; all $p < 0.001$) and in both growing seasons, where it was significantly negative (CC -46 and -55 mm; NC -32 and -29 mm; all $p < 0.001$), indicating that the lower profile gained water each winter and lost water each growing season independently of the upper profile.

In the 2023-2024 winter, ΔS at 0 to 1.2 m was significantly lower in the CC treatment than in the NC treatment (77 ± 20 mm vs. 96 ± 25 mm; $p = 0.001$), whereas ΔS at 0 to 3.0 m did not differ significantly between treatments (138 ± 24 mm vs. 146 ± 33 mm; $p = 0.261$). DP_{end} did not differ significantly between treatments at either depth, while DP_{int} was significantly higher in the CC treatment in the upper profile (0 to 1.2 m) (117 ± 17 mm vs. 109 ± 17 mm; $p = 0.032$) and similar at the full profile (0 to 3.0 m) ($p = 0.187$). Additional *DP* out of the upper profile in CC (evidenced by higher DP_{int} at that depth) was retained within the lower profile rather than passing through the full 3.0 m profile, resulting in lower DP_{int} below 3.0 m in CC. In the 2024 to 2025 winter, ΔS did not differ between treatments at either depth (57 ± 21 mm vs. 57 ± 21 mm at 0 to 1.2 m, $p = 0.988$; 101 ± 27 mm vs. 102 ± 41 mm at 0 to 3.0 m, $p = 0.920$), but DP_{end} and

DP_{int} were both significantly lower in the CC treatment under both calculation methods (all $p \leq 0.010$). At 0 to 1.2 m, DP_{end} CC = 36 ± 21 mm, DP_{end} NC = 66 ± 21 mm; DP_{int} CC = 89 ± 21 mm, DP_{int} NC = 103 ± 12 mm. At 0 to 3.0 m, DP_{end} CC = 7 ± 12 mm, DP_{end} NC = 31 ± 25 mm, DP_{int} CC = 48 ± 15 mm, DP_{int} NC = 62 ± 23 mm. In the 2025 to 2026 winter, ΔS again did not differ between treatments at either depth (15 ± 17 mm vs. 14 ± 10 mm at 0 to 1.2 m, $p = 0.922$; 36 ± 25 mm vs. 27 ± 20 mm at 0 to 3.0 m, $p = 0.138$). DP_{end} was significantly lower in the CC treatment at both depths (23 ± 11 mm vs. 84 ± 10 mm at 0 to 1.2 m, $p < 0.001$; 9 ± 10 mm vs. 71 ± 20 mm at 0 to 3.0 m, $p < 0.001$), whereas DP_{int} did not differ between treatments at either depth (174 ± 9 mm vs. 175 ± 11 mm at 0 to 1.2 m, $p = 0.751$; 184 ± 12 mm vs. 186 ± 24 mm at 0 to 3.0 m, $p = 0.743$). Across all three winters, DP_{end} at 0 to 3.0 m was lower in the CC treatment than in the NC treatment, reaching statistical significance in 2024 to 2025 and 2025 to 2026; DP_{int} at 0 to 3.0 m was lower in CC in the first two winters but did not differ between treatments in 2025 to 2026.

During the 2024 growing season, ΔS at 0 to 1.2 m did not differ between treatments (-58 ± 22 mm vs. -56 ± 23 mm; $p = 0.622$), while ΔS at 0 to 3.0 m was significantly more negative in the CC treatment (-104 ± 30 mm vs. -88 ± 44 mm; $p = 0.048$), indicating greater depletion of deep storage (Table 6). DP_{end} was zero or near-zero across both treatments and depths, with treatment means rounding to 0 mm in all four treatment-by-depth combinations. In contrast, DP_{int} was significantly higher in the CC treatment at both 0 to 1.2 m (57 ± 18 mm vs. 32 ± 13 mm; $p < 0.001$) and 0 to 3.0 m (81 ± 28 mm vs. 53 ± 28 mm; $p < 0.001$). During the 2025 growing season, ΔS again did not differ significantly between treatments at either depth.

Disaggregation by tube position showed that treatment effects on ΔS were spatially consistent but varied in magnitude between treeline and interrow locations (Table 7). In the

upper profile (0 to 1.2 m), ΔS was significantly lower in the CC treatment at both the treeline and interrow positions during the 2023 to 2024 winter ($p = 0.015$ and $p = 0.005$, respectively), at the treeline position during the 2024 to 2025 winter ($p = 0.019$), and again at the treeline position during the 2025 to 2026 winter (7 ± 4 mm vs. 15 ± 9 mm; $p = 0.033$). During the 2024 growing season, treeline tubes in the CC treatment showed less depletion than NC at 0 to 1.2 m ($p = 0.023$), whereas interrow tubes did not differ ($p = 0.692$). At 0 to 3.0 m, treatment differences in ΔS were generally not significant at either position, with the exception of the interrow position in 2023 to 2024 winter ($p = 0.050$). DP_{end} differed significantly between treatments only at the interrow position during the 2024 to 2025 winter, where CC was lower than NC at both 0 to 1.2 m (20 ± 17 vs. 53 ± 23 mm; $p = 0.014$) and 0 to 3.0 m (2 ± 5 vs. 20 ± 18 mm; $p = 0.032$); in the 2025 to 2026 winter, DP_{end} was significantly lower in CC at both positions and depths (treeline 29 ± 4 versus 84 ± 9 mm and 10 ± 9 versus 68 ± 22 mm; interrow 19 ± 14 versus 74 ± 10 mm and 9 ± 12 versus 53 ± 14 mm; all $p < 0.001$). During the 2025 growing season, DP_{end} at 0 to 3.0 m was significantly higher in the CC treatment at both treeline (39 ± 36 vs. 0 mm; $p = 0.012$) and interrow positions (46 ± 42 vs. 4 ± 12 mm; $p = 0.008$). DP_{int} was consistently higher in the CC treatment at interrow positions, reaching significance during both growing seasons at 0 to 1.2 m ($p < 0.001$ in 2024; $p = 0.022$ in 2025) and at 0 to 3.0 m in 2024 ($p = 0.009$). At the treeline position, DP_{int} treatment differences were smaller but still significant during both growing seasons at 0 to 1.2 m ($p = 0.021$ in 2024; $p = 0.002$ in 2025) and in the upper profile during the 2025 to 2026 winter (182 ± 2 vs. 174 ± 8 mm; $p = 0.007$).

Table 6. Seasonal change in soil water storage (*ΔS*, mm) and deep percolation (*DP*, mm) for the cover crop (CC) and no cover (NC) treatments at two profile integration depths (0-1.2 m and 0-3.0 m). *DP* is shown for both the endpoint and interval calculation methods. Values are mean ± SD (n = 36 tubes). Treatment differences were evaluated using paired t-tests (CC tube i vs. NC tube i; df = 35). Significance is indicated on mean ± SD values: *p < 0.05, **p < 0.01, ***p < 0.001. Corresponding p-values are listed in the rightmost columns. N/A indicates cases where all values in both treatments were zero and no test could be performed.

Depth (m)	Season	P (mm)	I CC (mm)	I NC (mm)	ET CC (mm)	ET NC (mm)	ΔS CC (mm)	DP CC end (mm)	DP CC int (mm)	ΔS NC (mm)	DP NC end (mm)	DP NC int (mm)	ΔS p-value	DP end p-value	DP Int p-value
0-1.2 m	2023-24 Winter	334	0	0	193	178	77 ± 20**	63 ± 20	117 ± 17*	96 ± 25**	60 ± 25	109 ± 17*	0.001	0.530	0.032
0-1.2 m	2024 Grow	23	330	321	549	543	-58 ± 22	0 ± 0	57 ± 18***	-56 ± 23	0 ± 0	32 ± 13***	0.622	N/A	<0.001
0-1.2 m	2024-25 Winter	294	0	0	201	171	57 ± 21	36 ± 21***	89 ± 21***	57 ± 21	66 ± 21***	103 ± 12***	0.988	<0.001	<0.001
0-1.2 m	2025 Grow	36	580	505	664	700	-40 ± 35	10 ± 23**	135 ± 35***	-39 ± 29	0 ± 0**	96 ± 24***	0.912	0.009	<0.001
0-1.2 m	2025-26 Winter	301	0	0	265	203	15 ± 17	23 ± 11***	174 ± 9	14 ± 10	84 ± 10***	175 ± 11	0.922	<0.001	0.751
0-3.0 m	2023-24 Winter	334	0	0	193	178	138 ± 24	10 ± 17	80 ± 18	146 ± 33	19 ± 22	86 ± 24	0.261	0.096	0.187
0-3.0 m	2024 Grow	23	330	321	549	543	-104 ± 30*	0 ± 0	81 ± 28***	-88 ± 44*	0 ± 0	53 ± 28***	0.048	0.324	<0.001
0-3.0 m	2024-25 Winter	294	0	0	201	171	101 ± 27	7 ± 12***	48 ± 15**	102 ± 41	31 ± 25***	62 ± 23**	0.920	<0.001	0.010
0-3.0 m	2025 Grow	36	580	505	664	700	-95 ± 70	52 ± 65***	191 ± 65*	-68 ± 61	1 ± 6***	162 ± 51*	0.100	<0.001	0.031
0-3.0 m	2025-26 Winter	301	0	0	265	203	36 ± 25	9 ± 10***	184 ± 12	27 ± 20	71 ± 20***	186 ± 24	0.138	<0.001	0.743

3.1.4 Lower-profile contribution to storage

The change in soil water storage within the lower profile differed significantly from zero in all eight season-treatment combinations ($p < 0.001$ in all cases; Table 6), indicating that this layer contributed substantially to seasonal water dynamics. During the 2023 to 2024 winter, the lower profile contributed 60 ± 14 mm of additional storage in the CC treatment and 50 ± 16 mm in the NC treatment; in the 2024 to 2025 winter, the corresponding values were 44 ± 12 mm and 45 ± 29 mm. During the growing seasons, the same layer showed net depletion: -46 ± 13 mm (CC) and -32 ± 27 mm (NC) in 2024, and -55 ± 43 mm (CC) and -29 ± 36 mm (NC) in 2025. The large within-treatment variability in 2025, where SD exceeded the mean in both treatments, reflects the spatial heterogeneity in deep percolation captured by the tube array and is consistent with the position-dependent patterns described above. These results confirm that integration to 3.0 m captured 44 to 60 mm of winter storage and 29 to 55 mm of growing season depletion that a profile limited to 1.2 m would not have resolved.

Table 7. Seasonal change in soil water storage (*ΔS*, mm) and deep percolation (*DP*, mm) by treeline and interrow position for the cover crop (CC) and no cover (NC) treatments at two profile integration depths (0-1.2 m and 0-3.0 m). DP is shown for both the endpoint and interval calculation methods. Values are mean ± SD (n = 9 tubes per position). Treeline tubes: 1, 5, 9, 13, 17, 24, 28, 32, 33. Interrow tubes: 4, 8, 10, 16, 18, 23, 25, 31, 36. Treatment differences were evaluated using paired t-tests (CC tube i vs. NC tube i; df = 8). Significance is indicated on mean ± SD values: *p < 0.05, **p < 0.01, ***p < 0.001. Corresponding p-values are listed in the rightmost columns. N/A indicates cases where all values in both treatments were zero and no test could be performed.

Depth (m)	Season	Position	ΔS CC (mm)	DP CC endpoint (mm)	DP CC interval (mm)	ΔS NC (mm)	DP NC endpoint (mm)	DP NC interval (mm)	ΔS p-value	DP endpoint p-value	DP interval p-value
0-1.2 m	2023-24 Winter	Treeline	68 ± 15*	73 ± 15	131 ± 18	96 ± 21*	59 ± 21	118 ± 11	0.015	0.191	0.138
0-1.2 m	2023-24 Winter	Interrow	87 ± 20**	54 ± 20	103 ± 12	114 ± 14**	41 ± 14	93 ± 14	0.005	0.127	0.062
0-1.2 m	2024 Grow	Treeline	-36 ± 16*	0 ± 0	43 ± 10*	-56 ± 16*	0 ± 0	31 ± 9*	0.023	N/A	0.021
0-1.2 m	2024 Grow	Interrow	-74 ± 18	0 ± 0	68 ± 7***	-70 ± 23	0 ± 0	43 ± 12***	0.692	N/A	<0.001
0-1.2 m	2024-25 Winter	Treeline	36 ± 14*	57 ± 14	109 ± 16	59 ± 16*	64 ± 16	106 ± 8	0.019	0.411	0.730
0-1.2 m	2024-25 Winter	Interrow	73 ± 17	20 ± 17*	76 ± 20*	70 ± 23	53 ± 23*	96 ± 14*	0.794	0.014	0.025
0-1.2 m	2025 Grow	Treeline	-27 ± 12	0 ± 0	129 ± 21**	-42 ± 26	0 ± 0	98 ± 19**	0.125	N/A	0.002
0-1.2 m	2025 Grow	Interrow	-47 ± 42	16 ± 26	141 ± 38*	-70 ± 18	0 ± 0	103 ± 19*	0.182	0.093	0.022
0-3.0 m	2023-24 Winter	Treeline	141 ± 12	5 ± 7	89 ± 17	149 ± 25	13 ± 19	98 ± 16	0.215	0.095	0.229
0-3.0 m	2023-24 Winter	Interrow	143 ± 27*	8 ± 19	72 ± 19	170 ± 28*	4 ± 8	61 ± 21	0.050	0.560	0.179
0-1.2 m	2025-26 Winter	Treeline	7 ± 4*	29 ± 4***	182 ± 2**	15 ± 9*	84 ± 9***	174 ± 8**	0.033	<0.001	0.007
0-1.2 m	2025-26 Winter	Interrow	18 ± 15	19 ± 14***	168 ± 7	25 ± 10	74 ± 10***	163 ± 7	0.324	<0.001	0.096
0-3.0 m	2024 Grow	Treeline	-81 ± 17	0 ± 0	83 ± 33**	-82 ± 19	0 ± 0	44 ± 22**	0.954	N/A	0.009
0-3.0 m	2024 Grow	Interrow	-123 ± 33	0 ± 0	88 ± 20**	-115 ± 34	0 ± 0	67 ± 16**	0.649	N/A	0.009
0-3.0 m	2024-25 Winter	Treeline	84 ± 21	12 ± 17	51 ± 11	114 ± 52	28 ± 23	53 ± 27	0.254	0.256	0.843
0-3.0 m	2024-25 Winter	Interrow	117 ± 28	2 ± 5*	43 ± 18	110 ± 28	20 ± 18*	58 ± 21	0.595	0.032	0.155
0-3.0 m	2025 Grow	Treeline	-87 ± 37	39 ± 36*	193 ± 32	-69 ± 58	0 ± 0*	157 ± 61	0.461	0.012	0.094
0-3.0 m	2025 Grow	Interrow	-85 ± 56	46 ± 42**	163 ± 42	-131 ± 43	4 ± 12**	181 ± 50	0.073	0.008	0.312
0-3.0 m	2025-26 Winter	Treeline	29 ± 12	10 ± 9***	190 ± 11	30 ± 22	68 ± 22***	180 ± 24	0.862	<0.001	0.266
0-3.0 m	2025-26 Winter	Interrow	34 ± 19	9 ± 12***	178 ± 10*	46 ± 14	53 ± 14***	167 ± 10*	0.201	<0.001	0.012

3.1.5 Sensitivity of DP estimates to calculation method

DP_{int} exceeded DP_{end} in every treatment-season-depth combination (Table 6). Within-tube paired comparisons confirmed that this difference was significant in all cases (Wilcoxon signed-rank, $p < 0.001$ for all 16 treatment-season-depth combinations). During the winter seasons, the ratio of DP_{int} to DP_{end} ranged from 1.3 (NC, 2025 to 2026) to 2.5 (CC, 2024 to 2025) at 0 to 1.2 m and from 1.5 (NC, 2025 to 2026) to 7.7 (CC, 2023 to 2024) at 0 to 3.0 m. The divergence between methods was greater at 0 to 3.0 m than at 0 to 1.2 m in all three winters and the smaller ratios in 2025 to 2026 reflect the unusually large endpoint fluxes that winter, which narrowed the gap between the two accounting methods. During the 2024 growing season, DP_{end} was zero or near-zero for all tubes in both treatments at both depths, while DP_{int} ranged from 32 to 81 mm, making ratios undefined. The largest divergence occurred in the 2025 growing season at 0 to 3.0 m, where DP_{int} reached 191 mm (CC) and 162 mm (NC) compared with DP_{end} values of 52 mm and 1 mm. NC DP_{end} was near zero, precluding a meaningful ratio. The same pattern held at both treeline and interrow positions (Table 7). These comparisons indicate that endpoint accounting systematically muted the magnitude of seasonal deep percolation relative to interval-based accounting. The effect was especially pronounced when the analysis was extended to the full profile.

To understand how these seasonal differences arose within the profile, we next examine depth-resolved volumetric water content and three-dimensional soil water distributions around representative trees.

3.2 Depth-resolved soil water dynamics

3.2.1 Tree-scale three-dimensional soil water distribution

Mean volumetric water content (VWC) from each treatment was computed for each measurement date. Across all dates, VWC in the upper profile (0 to 1.2 m) was lower in the CC treatment than in the NC treatment, whereas VWC within the lower profile was higher in the CC treatment. The CC minus NC sign reversal occurred between the 1.2 m and 1.5 m depth increments on late-winter dates (CC = 36.8 pp versus NC = 35.7 pp at 1.5 m in 2024; CC = 36.5 pp versus NC = 35.7 pp at 1.5 m in 2025), and between 1.5 m and 1.8 m on all other dates. On the late-winter 2024 date (2024-03-11), VWC at 0.3 m was 34.5 pp (CC) versus 37.3 pp (NC), a difference of -2.8 pp, while at 2.1 m it was 37.3 pp (CC) versus 31.3 pp (NC), a difference of +6.2 pp. The same contrast was observed on the late-winter 2025 date (2025-03-03): VWC at 0.3 m was 33.3 pp (CC) versus 36.7 pp (NC), a difference of -3.4 pp, while at 2.1 m it was 35.9 pp (CC) versus 32.0 pp (NC), a difference of +4.0 pp.

During the winter seasons, mean VWC increased across the full profile in both treatments. Upper-profile VWC (0 to 1.2 m) increased by similar amounts in both treatments: 8.9 pp (CC) and 9.2 pp (NC) in the 2023-24 winter, and 5.9 pp (CC) and 5.0 pp (NC) in the 2024-25 winter. In the lower profile (1.2 to 3.0 m), the increase was larger in CC than in NC during 2023-24 (4.7 pp vs. 3.3 pp), while the two treatments were nearly equal in 2024-25 (2.8 pp CC vs. 2.7 pp NC).

During the growing seasons, both treatments showed depletion across the full profile, but the depth distribution differed between years and treatments. In 2024, lower profile VWC (1.2 to 3.0 m) changed by only +0.1 pp in CC and -0.6 pp in NC from midsummer to late summer, indicating negligible net change in deep storage in both treatments. In 2025, the same layer

decreased by 1.6 pp in CC while remaining essentially unchanged (-0.5 pp) in NC from midsummer to late summer, consistent with the greater growing season ΔS at 0 to 3.0 m in the CC treatment (Table 6). By late summer 2025 (2025-10-27), the CC over NC crossover below 1.8 m had converged toward zero: VWC at 2.1 m was 31.9 pp (CC) versus 29.7 pp (NC), and at 3.0 m was 31.8 pp (CC) versus 31.6 pp (NC), compared to differences of +4.0 pp and +2.4 pp at those same depths in late winter 2025.

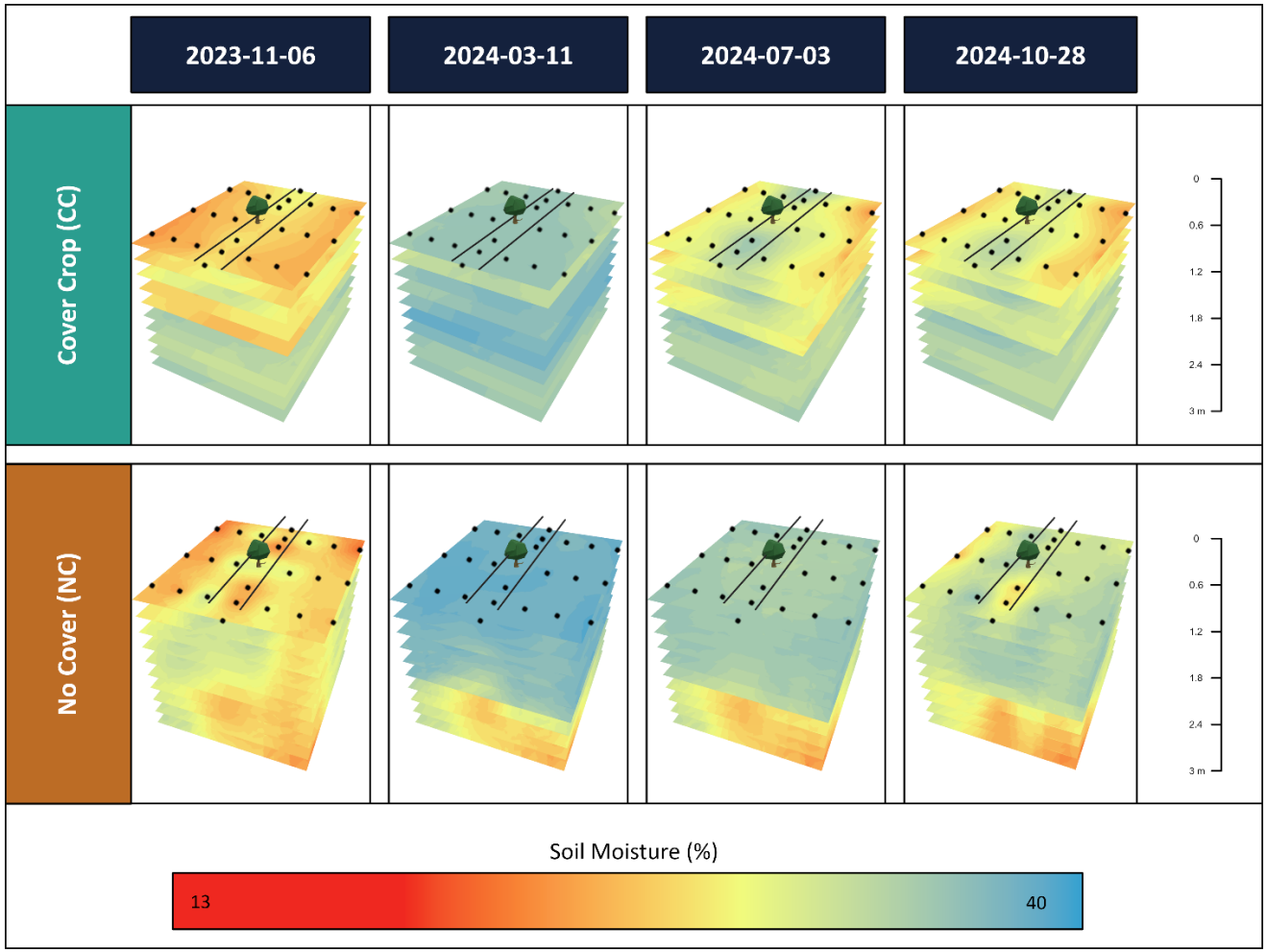


Figure 3. Three-dimensional interpolated soil moisture distributions around a representative tree in the cover crop (CC) and no cover (NC) orchards on four dates during the 2023–2024 season: early winter (2023-11-06), late winter (2024-03-11), midsummer (2024-07-03), and late summer (2024-10-28). For each date and treatment, horizontal slices of volumetric water content are shown at depths 0.3, 0.6, 1.2, 2.1, and 3.0 m, with warmer colors indicating higher soil moisture and cooler colors indicating lower soil moisture.

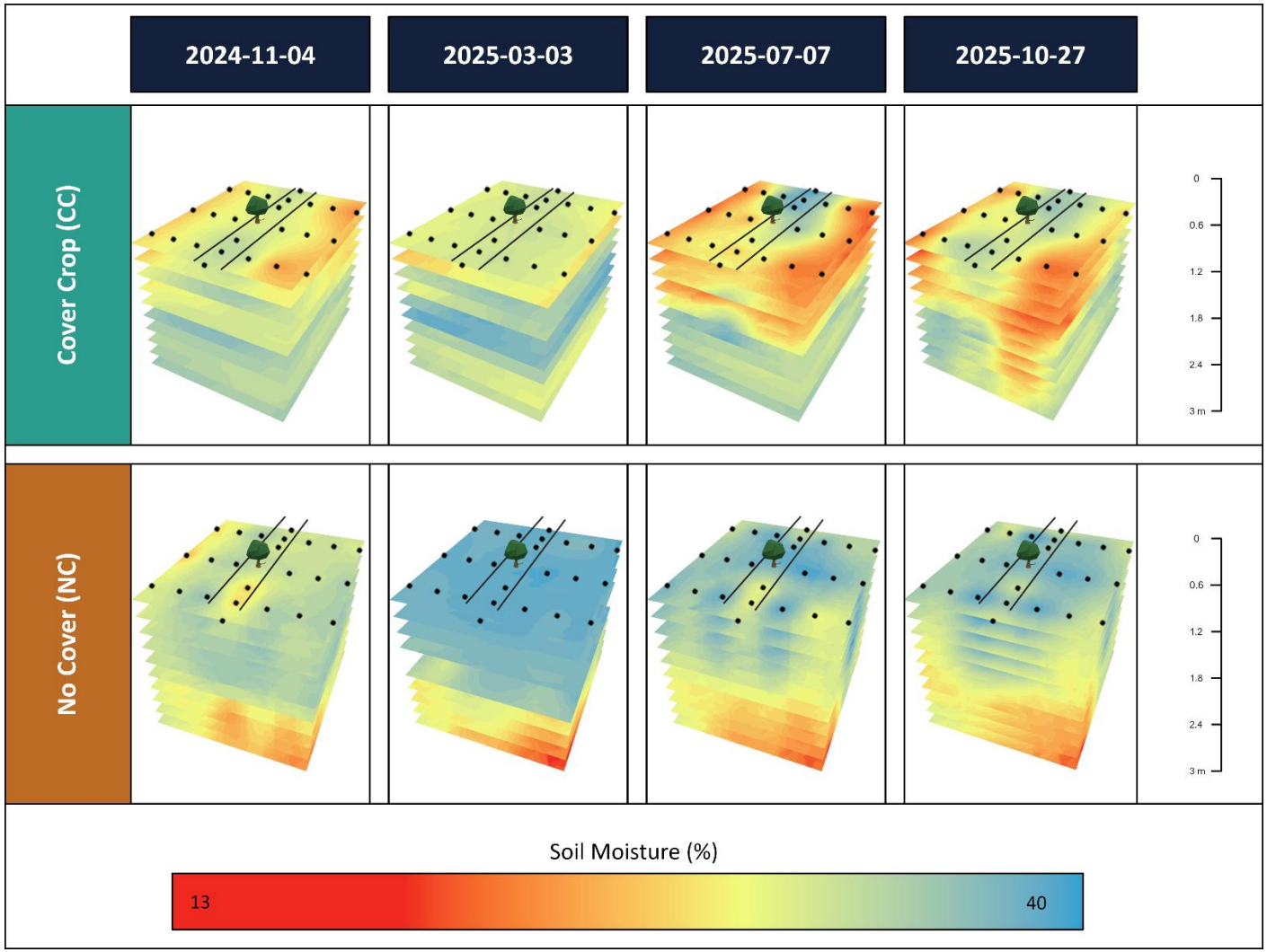


Figure 4. Three-dimensional interpolated soil moisture distributions around a representative tree in the cover crop (CC) and no cover (NC) orchards on four dates during the 2024–2025 season: early winter (2024-11-04), late winter (2025-03-03), midsummer (2025-07-07), and late summer (2025-10-27). For each date and treatment, horizontal slices of volumetric water content are shown at depths 0.3, 0.6, 1.2, 2.1, and 3.0 m, with warmer colors indicating higher soil moisture and cooler colors indicating lower soil moisture.

3.2.2 Treatment-level vertical soil water redistribution

The CC treatment had lower mean VWC than the NC treatment at every depth from 0.3 to 1.5 m in all four seasons, with the largest differences at 0.6 m (ranging from -3.2 pp in 2023-24 winter to -6.3 pp in the 2024 growing season; Figure 5). Below 1.5 m, mean VWC was consistently higher in the CC treatment, with the largest differences at 2.1 m (+3.0 pp in the 2025 growing season to +6.1 pp in 2023-24 winter), and the sign reversal occurred between 1.5 and 1.8 m in every season.

When the per-depth differences were summed across depth zones, the cumulative VWC difference at 0 to 1.2 m was negative in all four seasons, ranging from -8.3 pp in 2023-24 winter to -19.6 pp in the 2025 growing season (Figure 5). The cumulative difference at 1.2 to 3.0 m was positive in all four seasons, ranging from +8.0 pp in the 2025 growing season to +17.4 pp in 2023-24 winter. The full profile cumulative difference (0 to 3.0 m) was positive in 2023-24 winter (+9.1 pp) and near zero in 2024-25 winter (+0.8 pp), and negative in both growing seasons (-5.6 pp in 2024; -11.6 pp in 2025). The full profile net difference shifted from positive in winter to negative in the growing seasons.

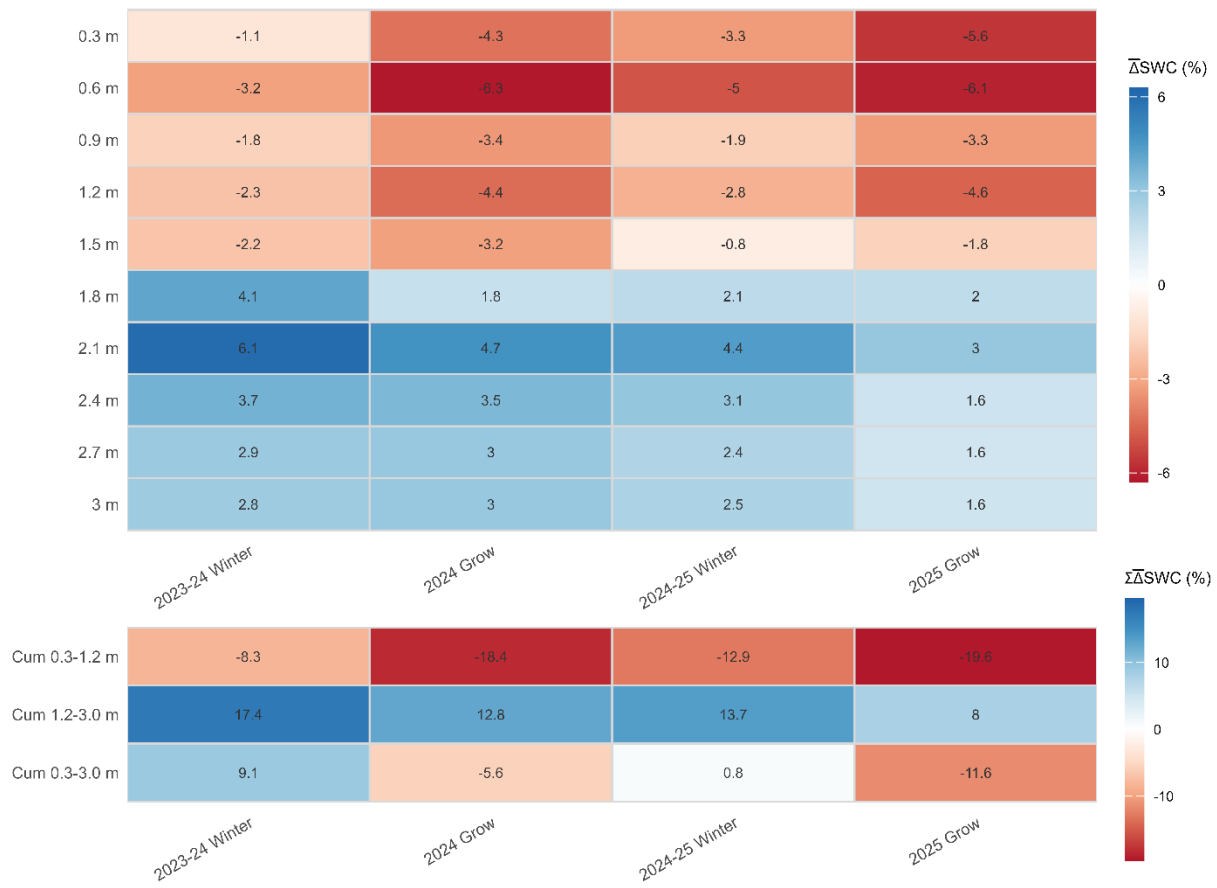


Figure 5. Mean seasonal volumetric water content difference (CC minus NC, percentage points) across all 36 neutron probe tubes. Panel (a): mean difference at each 0.3 m depth increment from 0-3.0 m, computed as the seasonal mean of per-tube, per-date differences. Panel (b): cumulative difference summed across three depth zones (0-1.2 m, 1.2-3.0 m, and 0-3.0 m), derived from the same per-depth values as panel (a). Negative values (red) indicate lower VWC in the CC treatment; positive values (blue) indicate higher VWC in the CC treatment. Color scales are independent between panels.

Disaggregation by tube position showed that the depth-resolved differences were spatially consistent in sign but varied in magnitude (Figure 6). The upper profile (0 to 1.2 m) deficit was largest at the interrow position (T4) in three of four seasons, reaching -30.4 pp during the 2024 growing season compared with -3.4 pp at the treeline (T1). The lower profile (1.2 to 3.0 m) surplus was positive at all positions in all seasons. The full profile cumulative difference (0 to 3.0 m) was positive or near zero at the treeline in three of four seasons (+13.6, +13.2, +2.2, and -

2.8 pp across the four seasons) but negative at the interrow in three of four seasons (+2.0, -22.9, -5.3, and -9.8 pp), consistent with the larger upper profile deficit observed at that position.

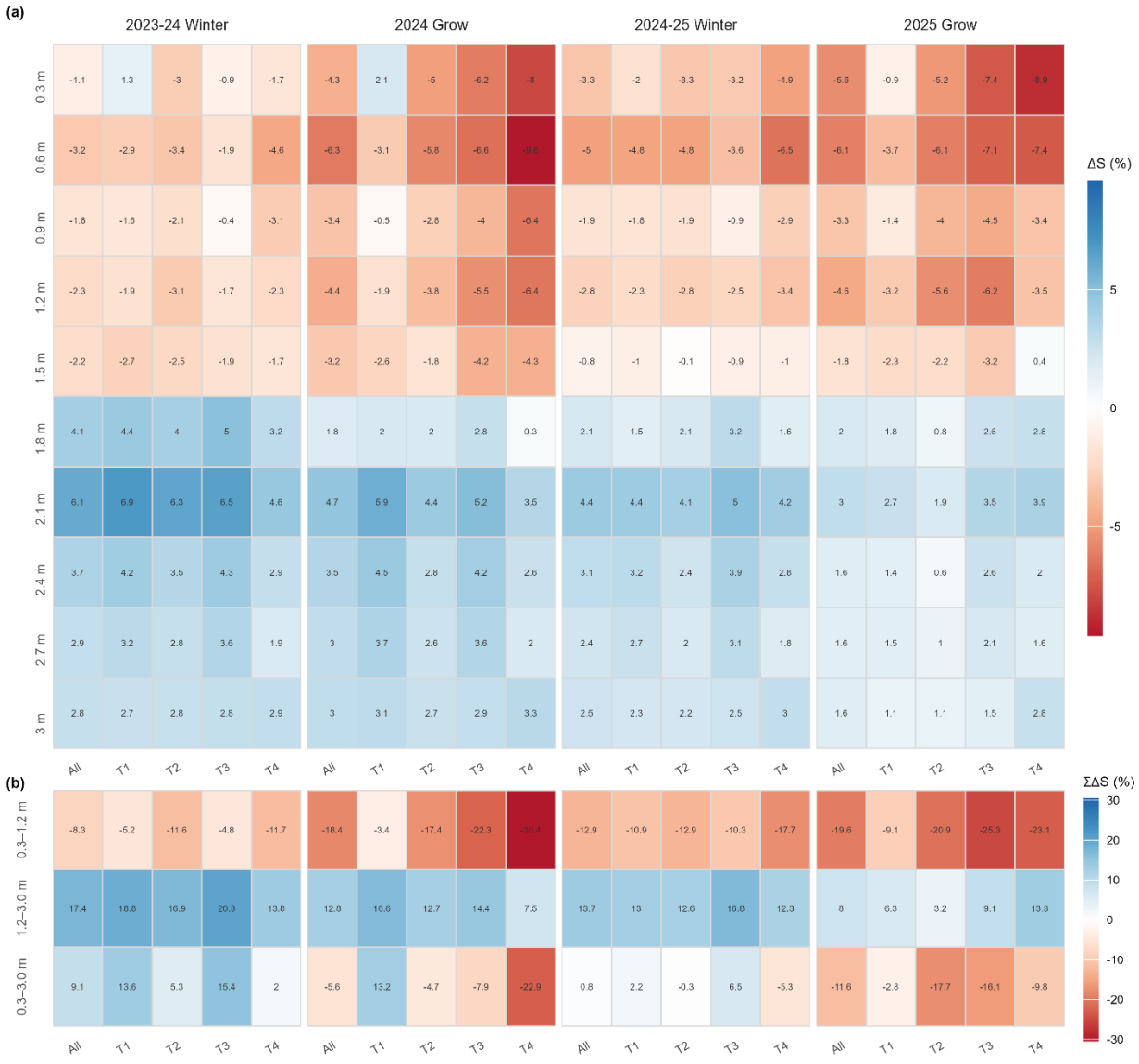


Figure 6. Mean seasonal volumetric water content difference (CC minus NC, percentage points) by tube position for each of the four seasonal periods. Panel (a): mean difference at each 0.3 m depth increment from 0-3.0 m. Panel (b): cumulative difference summed across three depth zones (0-1.2 m, 1.2-3.0 m, and 0-3.0 m). Columns represent the overall mean across all 36 tubes (All) and position-specific means (T1 = treeline center, T2 = near treeline, T3 = near interrow, T4 = interrow center; n = 9 tubes each). Negative values (red) indicate lower VWC in the CC

treatment; positive values (blue) indicate higher VWC in the CC treatment. Color scales are independent between panels and shared across all seasons and positions within each panel.

4. Discussion

4.1 Synthesis of main findings

These results collectively address our three guiding questions about seasonal water partitioning, depth-resolved storage, and the sensitivity of deep percolation estimates to accounting method. This study provides a depth-resolved assessment of how winter cover cropping alters the soil water balance in a young, irrigated pistachio orchard, using paired eddy covariance towers and neutron probe measurements extending to 3.0 m across two consecutive annual cycles. Three principal findings emerge with direct relevance to agricultural water management in deep-rooted perennial systems. First, cover crops increased winter evapotranspiration modestly (15 to 30 mm), but this was partially offset by reduced summer ET_a following termination. Second, cover cropping redistributed soil water downward, with the upper profile becoming drier and the lower profile accumulating additional storage, indicating that water commonly interpreted as lost to deep percolation at shallow measurement depths was largely retained within the full rooting profile. Third, deep percolation estimates were highly sensitive to both calculation method and measurement depth, with the interval-based approach yielding values 1.3 to 7.7 times higher than endpoint calculations. Together, these findings indicate that assessments of cover crop water costs based solely on shallow soil monitoring and seasonal endpoint measurements are likely to overestimate the net water penalty of the practice in deep-rooted perennial systems such as pistachio.

4.2 Evapotranspiration dynamics under winter cover cropping

The modest winter ET_a increases under winter cover cropping (15 mm in 2023-24; 30 mm in 2024-25) are consistent with the expectation that additional transpiring biomass from an

actively growing floor canopy increases total system water use during the winter season. This finding aligns with previous studies in annual and perennial cropping systems that have documented increased winter or early-spring ET_a under cover crops relative to bare ground (DeVincentis et al., 2022). The larger winter ET_a difference in 2024-25 likely reflects the earlier onset of significant precipitation in November 2024 compared with December 2023, which would have enabled earlier cover crop germination and establishment, and a longer period of active transpiration before termination. The monthly ET_a data support this interpretation: in 2023-24, ET_a in the CC treatment did not exceed NC until February, whereas in 2024-25 CC already exceeded NC by January. In both years, most of the winter ET_a difference accrued in February and March.

From an orchard water management perspective, the reversal in monthly ET_a after cover crop termination is particularly important. From June through October, the CC treatment had lower monthly ET_a than the NC treatment in both years (Table 5). At the growing season scale, however, this summer reduction produced a lower CC total only in 2025: totals were 549 mm (CC) versus 543 mm (NC) in 2024 and 664 mm versus 700 mm in 2025, so the treatment difference shifted from CC 6 mm above NC in 2024 to 36 mm below NC in 2025. This shift toward lower CC growing season ET_a coincided with increasing tree canopy development, which likely amplifies the relative importance of soil evaporation suppression beneath the mulch layer. This summer ET_a reduction most likely reflects the insulating and shading effects of CC residue left on the soil surface after termination, which lowers soil surface temperature and suppresses evaporation. Previous work has reported similar ET_a reductions where post-termination residues were left as mulch (Kader et al., 2019; Flynn et al., 2025). An alternative or contributing explanation would be subtle differences in tree canopy development or leaf area index (LAI)

between treatments driving the summer ET_a differences independently of soil evaporation effects.

Daily NDVI values for the CC and NC orchards, shown in Figure S5, diverge between the two treatments in both winter seasons. A divergence also appears in NDVI from the start of the 2025 growing season that was not present in the 2024 growing season. Between August 2024 and November 2024, NDVI was almost identical between treatments, with a small increase in the NC treatment. The NC over CC NDVI gap was larger during the 2025 growing season than in the 2024 growing season, which is consistent with the higher NC ET_a in 2025 and supports a possible difference in tree growth between treatments. The practical consequence is that the winter ET_a cost of cover cropping may be partially or fully offset during the subsequent growing season through this mulch effect, a dynamic that would be missed by studies focused exclusively on the cover crop growing period. For growers, this suggests that any winter ET_a increase under cover crops should be evaluated in the context of potential summer ET_a savings rather than considered in isolation.

4.3 Methodological implications for monitoring depth

The convergence of treatment-level ΔS at 0 to 3.0 m despite clear divergence at 0 to 1.2 m is the most consequential finding of this study. Many studies of cover crop effects on soil water in both annual and perennial cropping systems have confined measurements to the upper 1.2 m of the soil profile (Folorunso et al., 1992; Bodner et al., 2007; Gabriel et al., 2012; Ward et al., 2012; Basche et al., 2016; Sastre et al., 2018; Yang et al., 2020; Cao et al., 2021; Chakraborty et al., 2022; DeVincentis et al., 2022; Haruna et al., 2022; Vanella et al., 2022; Fernando et al., 2024). In shallow-rooted annual systems, this protocol captures most of the relevant soil reservoir. In deep-rooted perennial systems such as pistachio, where roots can access water

below the 1.2 m effective root zone of annual crops, the zone below the conventional measurement depth may function as an additional storage reservoir rather than a loss pathway. Ward et al. (1998) is one of the few studies that examined cover crop effects on the soil water balance in a Mediterranean climate with measurements extending to 3.0 m, though in an annual rotation system. The present study extends this depth-resolved approach to a deep-rooted perennial crop under comparable climatic conditions. In the upper profile (0 to 1.2 m), DP_{int} was significantly higher in the CC treatment in the 2023-24 winter (117 ± 17 mm vs. 109 ± 17 mm; p = 0.032), whereas at the full depth profile (0 to 3.0 m) the treatment difference was not significant (p = 0.187). This depth-dependent reversal in the apparent treatment effect on deep percolation underscores the importance of matching measurement depth to the functional rooting depth of the crop system under study.

The vertical crossover in soil water content between treatments, with CC drier above approximately 1.5 m and wetter below, was observed in every season, at every tube position, and in both the transect and array sampling configurations (Figure 6). The cumulative VWC difference in the upper (0 to 1.2 m) profile was negative in all five seasons (-8.3 to -19.6 pp), while the cumulative difference in the lower (1.2 to 3.0 m) profile was positive in all five seasons (+8.0 to +17.4 pp). The sign reversal between the two conventional integration depths explains why ΔS at 0 to 1.2 m was consistently lower in CC while ΔS at 0 to 3.0 m converged between treatments, and it supports the interpretation that the treatment effect is a redistribution of soil water rather than a net loss from the full profile.

Several complementary mechanisms may account for this redistribution. Cover crop roots may create continuous macropores that persist after root senescence and termination, forming preferential flow pathways that enhance the downward movement of infiltrating water relative to

the undisturbed bare ground (Blanco-Canqui and Ruis, 2020). In addition, organic matter inputs from cover crop root and surface residue decomposition can improve soil aggregate stability and increase saturated hydraulic conductivity in the upper profile, potentially accelerating deep percolation into deeper horizons (Blanco-Canqui et al., 2011; Steele et al., 2012; Blanco-Canqui and Ruis, 2020; Munna and Lal, 2025). Surface crusts observed in the NC treatment, consistent with the TEROS 54 sensor behavior described in the Supplementary Material, may further impede infiltration there, particularly during high-intensity rainfall events. Previous work has shown that cover crops can increase cumulative infiltration by more than 50 percent relative to bare ground, and the redistribution pattern observed here may represent the subsurface expression of that enhanced infiltration capacity (Haruna et al., 2022). Taken together, these mechanisms describe a coherent hydrologic pathway to deep storage. Enhanced infiltration and root-derived preferential flow route a larger fraction of winter precipitation past the upper profile and deliver it to the lower (1.2 to 3.0 m) profile before it can be returned to the atmosphere by evaporation or shallow root uptake (Haruna et al., 2022; Joyce et al., 2002).

Because this depth lies below the zone of strongest winter evaporative demand and root extraction, water arriving there is conserved rather than rapidly lost, accumulating as the deep storage surplus observed under CC. In the NC treatment, surface crusting and lower near-surface hydraulic conductivity instead retain a greater share of infiltrating water in the upper profile, where it remains exposed to evaporation and shallow uptake, and less of it reaches the lower profile (Folorunso et al., 1992). The deep storage gain under cover cropping is best understood not as new water added to the system but as a redistribution of infiltrated precipitation to a lower depth where it is conserved through the wet season until growing season root uptake draws it

down. These mechanisms were not individually tested in this study, and the relative contribution of each to the observed redistribution remains unknown.

The three-dimensional EBK3D interpolations provide corroborating evidence at the individual tree scale. On the late-winter 2024 date (2024-03-11), mean VWC at 0.3 m was 34.4 percent in the CC treatment and 37.6 percent in the NC treatment (difference of -3.2 pp), while at 2.1 m it was 37.1 percent in the CC treatment and 29.3 percent in the NC treatment (+7.8 pp). This within-tree vertical contrast mirrors the treatment-level patterns derived from the 36-tube transect averages, supporting the interpretation that the redistribution signal is not an artifact of between-tree or between-location variability.

Over the study period, the below-root-zone surplus decreased from +17.4 to +8.0 pp, while the root-zone deficit widened from -8.3 to -19.6 pp. During the growing seasons, the 1.5 to 3.0 m profile in the CC treatment showed greater depletion than in the NC treatment (e.g., -2.3 pp vs. +0.1 pp in 2025), and by late summer 2025 the CC minus NC VWC difference below 2.1 m had converged toward zero (31.4 percent CC vs. 32.2 percent NC at 3.0 m). This progressive drawdown is consistent with pistachio roots accessing the redistributed deep storage during the growing season. Direct root measurements would be needed to confirm this mechanism, but if confirmed it would indicate that cover crop enhanced deep storage functions as a supplemental water supply for trees during the irrigation season, with potentially important implications for orchard water management under constrained allocations.

The two treatment blocks also differed in soil texture, which represents the principal confounding variable in this experimental design. The upper profile of the NC block is silty clay loam, whereas the CC block is silt loam (Table 3); the finer-textured NC soil has a higher water-holding capacity and would be expected to retain higher VWC in the upper profile independently

of any CC effect. Three lines of evidence argue against texture as the sole explanation, particularly for the deep-profile signal. First, the textural contrast is largely confined to the upper profile: at and below 1.5 m both treatments classified as silt loam with similar clay contents (Table 3), yet the cover crop treatment was consistently wetter than NC throughout the 1.5 to 3.0 m zone. Second, the vertical crossover appeared at both treeline and interrow positions, even though no cover crops were grown on the treeline. Third, the crossover was consistent in sign across all five seasons, and the deep-profile surplus drew down progressively during the growing seasons, a time-evolving pattern that fixed textural properties cannot generate. Texture likely contributes to the magnitude of the upper profile difference, but the depth reversal and its seasonal dynamics require an active redistribution mechanism that textural differences alone cannot provide. Because the design is unreplicated, this remains an inference rather than a demonstrated causal effect; replicated trials with randomized treatment assignment across matched soils would be required to isolate the CC contribution from inherent soil variability.

4.4 Methodological implications for deep percolation estimation

The systematic divergence between DP_{int} and DP_{end} (ratios of 1.3 to 7.7 across season-depth combinations, computed from treatment means rather than tube-by-tube paired differences) represents an important methodological finding. The interval method, which sums non-negative DP estimates across successive measurement periods, captures transient wetting and drying events that the endpoint method, based on a single ΔS calculation between season start and end dates, cannot resolve. A winter rainfall event may temporarily increase soil water storage and generate deep percolation that the interval method registers as positive DP; if subsequent ET_a or redistribution reduces storage before the next seasonal endpoint, that deep percolation episode is invisible to the endpoint calculation. The magnitude of the observed

difference indicates that DP_{end} estimates could substantially underestimate cumulative deep percolation when measurement intervals span weeks to months. The size of the difference between DP_{end} and DP_{int} estimates also depends on the number of such events during the winter season. A winter with five significant rain events, for example, would result in more unaccounted deep percolation than a winter with only two significant ones.

This sensitivity implies that studies relying on seasonal endpoint water balances may significantly underestimate the volume of water moving through the upper profile, which also has implications for groundwater recharge estimates and for deep percolation below the upper profile (0 to 1.2 m). Ward et al. (1998) demonstrated this directly in a Mediterranean pasture system, where monthly water balance calculations failed to detect a deep percolation episode that was only resolved when calculations were restricted to the days surrounding individual rainfall events. Similar methodological sensitivities have been documented for deep percolation estimates under surface irrigated systems (Bethune et al., 2008) and for full profile soil water and deep percolation monitoring in irrigated potatoes (Yost et al., 2019). The effect was stronger at 0 to 3.0 m than at 0 to 1.2 m, which may reflect the greater capacity of the full profile to buffer transient wetting pulses before they manifest as net positive ΔS at seasonal endpoints in this system.

During the growing seasons, the methodological sensitivity was particularly pronounced at 0 to 3.0 m. The higher DP_{int} values in the CC treatment likely reflect two contributing mechanisms that endpoint calculations cannot resolve. The first is the larger irrigation volumes applied to the CC treatment (9 mm difference in 2024; 74 mm difference in 2025), which may have permitted additional deep percolation. The second is the hypothesized enhanced hydraulic connectivity of the cover cropped soil profile, which may facilitate faster deep percolation

responses to irrigation inputs. Endpoint calculations integrate over full seasonal windows and therefore cannot distinguish these high-frequency responses from slower redistribution, whereas the interval approach captures each deep percolation event and accumulates them over the season. These results emphasize that the choice of temporal aggregation for ΔS is not a minor methodological detail but a primary driver of apparent *DP* magnitude in this system.

4.5 Spatial variability across treeline and interrow positions

Treatment effects on ΔS and *DP* were spatially consistent in direction but varied in magnitude between treeline and interrow positions (Table 7, Figure 5). The upper profile deficit (0 to 1.2 m) was largest at the interrow position (T4), reaching -30.4 pp during the 2024 growing season compared with -3.4 pp at the treeline (T1), consistent with the spatial distribution of cover crop biomass and transpiration. Notably, significant treatment effects on ΔS at 0 to 1.2 m were also detected at treeline positions during both winters ($p = 0.015$ in 2023-24; $p = 0.019$ in 2024-25), despite cover crops being grown only in the interrow.

The significant treatment effects detected at treeline positions, where no CC were planted, warrant careful interpretation. Several processes could account for this observation. Lateral subsurface water movement from the wetter NC interrow toward the tree row could increase treeline VWC in the NC treatment relative to the CC treatment, where the interrow is drier from cover crop water use. Alternatively, trees in the CC treatment may draw upon a larger or deeper portion of the soil reservoir than trees in the NC treatment if preferential flow pathways created by cover crop roots have facilitated deeper root exploration. These mechanisms are not mutually exclusive, and the current dataset cannot distinguish between them. Future studies incorporating measurements of root distribution and lateral flow would help resolve the relative contributions of these processes to the observed spatial patterns.

4.6 Implications for SGMA accounting and orchard management

Under SGMA, groundwater sustainability agencies (GSAs) must quantify the components of the basin water budget, including consumptive use and recharge, to demonstrate progress toward sustainability (Faunt et al., 2016; Borum et al., 2024). Two findings from this study bear directly on how winter cover cropping is represented in that accounting. First, because cover cropping redistributed soil water into the lower profile rather than increasing net losses from the full profile, consumptive use accounting based on shallow soil monitoring would overstate the additional water demand attributable to the practice. A GSA that evaluated only the upper-profile water storage deficit (0 to 1.2 m), for example, would interpret the CC effect as increasing ET_a; however, in this case, it would be misclassifying water stored in the lower profile (1.2 to 3.0 m) as additional ET_a. This would inadvertently penalize growers who adopt winter CC, since the benefits of winter CC are invisible at the conventional root zone measurement depth.

These results suggest two practical adjustments for recharge accounting. Water budgets that seek to credit on-farm practices such as CC for managed aquifer recharge (MAR) should (i) extend soil water monitoring to the functional rooting depth of the perennial crop rather than the 1.2 m depth typical of annual crop systems, and (ii) resolve soil water storage at intervals fine enough to capture individual winter wetting events. Without these adjustments, basin water budgets risk simultaneously overstating the consumptive use penalty of winter CC and understating its potential contribution to *DP* and aquifer recharge, biasing the cost-benefit framing that growers and agencies use when evaluating the practice for SGMA compliance. The magnitude of any net recharge benefit remains site-specific and is not quantified at the basin scale here.

These results have three practical implications for pistachio growers and water managers. First, as the SGMA accounting above implies, adoption decisions should not rest on winter ET_a comparisons or shallow soil moisture monitoring alone, because both overstate the net water cost; accurate accounting of cover crop water use under SGMA-driven allocation constraints requires monitoring the full functional rooting depth of the tree crop. Second, the progressive growing season drawdown of the deep storage surplus is consistent with pistachio roots accessing water that cover crops redistributed into the lower profile; if confirmed by direct root measurements, this would mean cover cropping effectively extends the accessible soil water reservoir for trees, a benefit that may become increasingly valuable as orchards mature and water demand intensifies. Third, the depth-resolved and interval-based monitoring approach demonstrated here provides a methodological template that extends beyond cover cropping: any water balance study in deep-rooted perennial cropping systems should consider whether conventional shallow, endpoint-based protocols are likely to misrepresent the hydrologic processes under investigation.

4.7 Limitations

Several limitations constrain the scope of inference that can be drawn from these results. The study was conducted at a single commercial orchard in the Sacramento Valley, where annual precipitation averages approximately 435 mm, substantially wetter than the primary pistachio production region in the southern San Joaquin Valley (approximately 280 to 330 mm). In drier production regions, cover crop establishment may require supplemental irrigation, which would alter the water balance implications of the practice. The study was also limited to a single cultivar (Golden Hills) during the establishment phase (years 5 to 7 post-planting), when tree water demand was relatively low and the orchard floor accounted for a larger fraction of total

system ET_a than it will in a mature orchard. As canopy closure progresses and root competition for shallow soil moisture intensifies, soil water redistribution under cover crops may shift; in mature orchards with greater alleyway shading, cover crop biomass and transpiration may be lower, reducing both the ET_a cost and hydraulic improvement offered by the practice.

The cover crop mixture employed represents a commercially typical multi-species blend but does not encompass the full range of hydrologic responses possible with alternative species selections. Rooting architecture and depth vary substantially among species, and the soil structural improvements observed here may not be reproducible with shallow-rooted or low-residue covers.

Two field-scale methodological constraints also warrant consideration. Surface runoff was assumed negligible based on the flat topography and drip irrigation system, but field observations revealed more pronounced surface crusting in the NC treatment, particularly during summer. Surface crusts constrain water intake rates, and their formation after prolonged dry periods could influence infiltration during the first significant precipitation events of the following winter. Because runoff was not measured directly, its contribution to the water balance remains unquantified. Any differential runoff between treatments would bias the residual *DP* estimate, potentially inflating *DP* in the NC treatment (where crusting was more pronounced) or deflating it in the CC treatment. In addition, the two-year water balance record, while sufficient to establish consistent seasonal patterns, does not capture the full range of interannual climate variability in the Sacramento Valley, including drought years with insufficient precipitation for winter cover crop establishment without supplemental irrigation and wet years with early-season soil saturation that may limit infiltration enhancement.

Several instrumentation and design constraints also deserve acknowledgment. The neutron probe calibration applied a single pooled regression to both treatments to avoid introducing between-treatment VWC differences from separate calibrations; residual analysis did not reveal systematic bias, but small local biases in VWC estimation remain possible, particularly where treatment soil textures diverge from the pooled calibration mean. Applied irrigation volumes differed between treatments (9 mm in 2024; 74 mm in 2025), reflecting the constraints of a shared commercial irrigation system.

The soil textural differences between treatments represent a potential confounder for the upper profile VWC difference. Laboratory particle-size analysis (Table 3) shows that the two treatment blocks differ in the upper profile: from 0.3 to 1.2 m the NC soil classified as silty clay loam with 28 to 31 percent clay and only 4 to 6 percent sand, whereas the CC soil classified as silt loam with 17 to 20 percent clay and 11 to 21 percent sand. This is consistent with the soil survey mapping, which assigns the NC block almost entirely to Rincon silty clay loam and the CC block to a mix of Sycamore and Yolo silt loams with Rincon silty clay loam. The evidence that this textural contrast is not the sole driver of the observed depth reversal is presented in Section 4.3. Because the two treatments occupy separate, spatially contiguous blocks (CC east, NC west) rather than interspersed replicates, this baseline textural gradient is confounded with treatment and cannot be separated statistically; other inherent block properties that were not characterized, including bulk density, baseline organic matter, and antecedent soil structure, could differ in the same direction (Vanella et al., 2022).

The assumption that net vertical flux at the 3.0 m measurement boundary is downward implies that upward capillary rise from below 3.0 m to the monitored profile is negligible. Site water table information supports this assumption for the study period, but direct measurement of

fluxes at the lower boundary was not performed, and periods of shallow water table rise during wet years could violate this assumption in future monitoring. Finally, because *DP* was calculated as the residual of the water balance, it inherits the cumulative measurement uncertainty of all other components (precipitation, irrigation, ET_a, and ΔS). The magnitude of *DP* should therefore be interpreted with caution, particularly during seasons when its absolute value is small relative to the measurement uncertainty of the input terms.

4.8 Future research

Future research should prioritize multi-site replication across the primary pistachio-producing regions of the San Joaquin Valley, where drier conditions and different soil types may alter the water balance dynamics observed here. Studies spanning orchards at different stages of canopy development are needed to determine whether the redistribution patterns persist as canopy closure and root competition intensify. Long-term monitoring that encompasses years of contrasting precipitation would clarify the interannual variability of these trade-offs. Investigation of alternative cover crop species with different rooting architectures and residue characteristics would help identify which functional traits are most important for promoting the deep soil water redistribution documented in this study. Finally, the depth-resolved monitoring approach employed here could be extended to annual cropping systems, where shallow measurement protocols may similarly underestimate the hydrologic value of cover cropping.

5. Conclusions

The practical message of this study for California pistachio growers and the GSAs that regulate them is that the water cost of winter cover cropping cannot be judged from shallow soil monitoring or seasonal endpoint accounting. Because CC redistributed infiltrated water from the upper profile into the lower (1.2 to 3.0 m) profile rather than driving it out of the rooting profile,

consumptive use accounting confined to the conventional 1.2 m root zone overstates the additional water demand attributed to the practice and understates its potential contribution to deep percolation and managed aquifer recharge. Crediting or debiting growers fairly therefore requires extending monitoring to the functional rooting depth of the perennial crop and resolving soil water storage finely enough to capture individual winter wetting events, since coarser protocols bias the cost-benefit framing against adoption. These implications hold, in the first instance, for a young, establishment phase orchard in the Sacramento Valley, studied under one grower's management with an unreplicated paired design that cannot fully separate the CC effect from inherent soil texture differences. They should be confirmed in mature orchards and in the drier southern San Joaquin Valley before being generalized. More broadly, the depth-resolved, interval-based monitoring framework demonstrated here provides a template for evaluating any orchard floor practice whose hydrologic signal is invisible to conventional shallow, endpoint-based protocols. The unifying lesson is to match the depth and temporal resolution of soil water monitoring to the functional rooting depth of the crop and the event timescale of the process, rather than to protocols inherited from shallow-rooted annual systems.

Acknowledgements

This work was fully funded by USDA NIFA Award #2021-68012-35914. Thank you to Bullseye Farms for allowing us to conduct this research on their private orchard. Special thanks to Aaron Guerra, Ali Ghorbanpour, Anish Sapkota, Benny Briggs, Cassandra Bonfil, Felix Ogunmokun, Floyid Nicolas, Gento Shimamura, Ian Gomez, Isabella Burnett, Krista Blide, Matthew Maciosek, Nicolas Almeida, Sidd Dala, Usama Al-Dughaishi, William Lennon, and Zixuan Gan for assistance with equipment installation and data collection.

References

Abatzoglou, J.T., 2013. Development of gridded surface meteorological data for ecological applications and modelling. Intl Journal of Climatology 33, 121–131. https://doi.org/10.1002/joc.3413.

Adams, C.B., Cosner, J., 2025. Field pea cardinal temperatures, growth and vigor traits of winter- and spring-adapted germplasm at germination and seedling stages. Sci Rep 15, 21759. https://doi.org/10.1038/s41598-025-06342-w.

Alfieri, J.G., Kustas, W.P., Prueger, J.H., McKee, L.G., Hipps, L.E., Gao, F., 2019. A multi-year intercomparison of micrometeorological observations at adjacent vineyards in california's central valley during grapex. Irrig Sci 37, 345–357. https://doi.org/10.1007/s00271-018-0599-3.

Allen, R., Irmak, A., Trezza, R., Hendrickx, J.M.H., Bastiaanssen, W., Kjaersgaard, J., 2011. Satellite-based et estimation in agriculture using sebal and metric. Hydrological Processes 25, 4011–4027. https://doi.org/10.1002/hyp.8408.

Allen, R.G., Burnett, B., Kramber, W., Huntington, J., Kjaersgaard, J., Kilic, A., Kelly, C., Trezza, R., 2013. Automated calibration of the metric-landsat evapotranspiration process. J American Water Resour Assoc 49, 563–576. https://doi.org/10.1111/jawr.12056.

Allen, R.G., Pereira, L.S., 2009. Estimating crop coefficients from fraction of ground cover and height. Irrig Sci 28, 17–34. https://doi.org/10.1007/s00271-009-0182-z.

Allen, R.G., Pereira, L.S., Raes, D., Smith, M., 1998. FAO irrigation and drainage paper no. 56. crop evapotranspiration (guidelines for computing crop water requirements). FAO, Rome.

Allen, R.G., Tasumi, M., Morse, A., Trezza, R., 2005. Satellite-based evapotranspiration by energy balance for western states water management, in: Impacts of Global Climate Change. Presented at the World Water and Environmental Resources Congress 2005, American Society of Civil Engineers, Anchorage, Alaska, United States, pp. 1–18. https://doi.org/10.1061/40792(173)556.

Allen, R.G., Tasumi, M., Trezza, R., 2007. Satellite-based energy balance for mapping evapotranspiration with internalized calibration (metric)—model. J. Irrig. Drain Eng. 133, 380–394. https://doi.org/10.1061/(ASCE)0733-9437(2007)133:4(380).

Anderson, M., Gao, F., Knipper, K., Hain, C., Dulaney, W., Baldocchi, D., Eichelmann, E., Hemes, K., Yang, Y., Medellin-Azuara, J., Kustas, W., 2018. Field-scale assessment of land and water use change over the california delta using remote sensing. Remote Sensing 10, 889. https://doi.org/10.3390/rs10060889.

Anderson, M.C., Norman, J.M., Mecikalski, J.R., Otkin, J.A., Kustas, W.P., 2007. A climatological study of evapotranspiration and moisture stress across the continental united states based on thermal remote sensing: 1. model formulation. J. Geophys. Res. 112, 2006JD007506. https://doi.org/10.1029/2006JD007506.

Baldwin, R., Battany, M., Beede, R., Brar, G.S., Culumber, M., Ferguson, L., Fichtner, E., Gordon, P., Hanson, B., Havliand, D., Hembree, K., Kallsen, C.E., Sanden, B., Michailidas, T.J., Trouillas, F., Zaccaria, D., Harris, L., Stewart, D., 2020. Sample costs to establish and produce pistachios. Technical Report, UCCE ANR Agricultural Issues Center.

Bambach, N., Kustas, W., Alfieri, J., Prueger, J., Hipps, L., McKee, L., Castro, S.J., Volk, J., Alsina, M.M., McElrone, A.J., 2022. Evapotranspiration uncertainty at

micrometeorological scales: the impact of the eddy covariance energy imbalance and correction methods. Irrig Sci 40, 445–461. https://doi.org/10.1007/s00271-022-00783-1.
Basche, A.D., Kaspar, T.C., Archontoulis, S.V., Jaynes, D.B., Sauer, T.J., Parkin, T.B., Miguez, F.E., 2016. Soil water improvements with the long-term use of a winter rye cover crop. Agricultural Water Management 172, 40–50. https://doi.org/10.1016/j.agwat.2016.04.006.
Bastiaanssen, W.G.M., Menenti, M., Feddes, R.A., Holtslag, A.A.M., 1998. A remote sensing surface energy balance algorithm for land (sebal). 1. formulation. Journal of Hydrology 212–213, 198–212. https://doi.org/10.1016/S0022-1694(98)00253-4.
Bellvert, J., Adeline, K., Baram, S., Pierce, L., Sanden, B., Smart, D., 2018. Monitoring crop evapotranspiration and crop coefficients over an almond and pistachio orchard throughout remote sensing. Remote Sensing 10, 2001. https://doi.org/10.3390/rs10122001.
Bergtold, J.S., Ramsey, S., Maddy, L., Williams, J.R., 2019. A review of economic considerations for cover crops as a conservation practice. Renew. Agric. Food Syst. 34, 62–76. https://doi.org/10.1017/S1742170517000278.
Bethune, M.G., Selle, B., Wang, Q.J., 2008. Understanding and predicting deep percolation under surface irrigation. Water Resources Research 44, 2007WR006380. https://doi.org/10.1029/2007WR006380.
Blanco-Canqui, H., Mikha, M.M., Presley, D.R., Claassen, M.M., 2011. Addition of cover crops enhances no-till potential for improving soil physical properties. Soil Science Soc of Amer J 75, 1471–1482. https://doi.org/10.2136/sssaj2010.0430.
Blanco-Canqui, H., Ruis, S.J., 2020. Cover crop impacts on soil physical properties: a review. Soil Science Soc of Amer J 84, 1527–1576. https://doi.org/10.1002/saj2.20129.
Blanco-Canqui, H., Shaver, T.M., Lindquist, J.L., Shapiro, C.A., Elmore, R.W., Francis, C.A., Hergert, G.W., 2015. Cover crops and ecosystem services: insights from studies in temperate soils. Agron. J. 107, 2449–2474. https://doi.org/10.2134/agronj15.0086.
Bodner, G., Loiskandl, W., Kaul, H.-P., 2007. Cover crop evapotranspiration under semi-arid conditions using fao dual crop coefficient method with water stress compensation. Agricultural Water Management 93, 85–98. https://doi.org/10.1016/j.agwat.2007.06.010.
Borum, J., Bruno, E., Castle, S., Chiartas, J., Crowley, R., Decock, C., Delgado, C., DeVincentis, A., Dufour, R., Edwards, A., Flaherty, R., Flynn, M., Grimm, R., Hale, L., Light, S., Little, C., Lowell, K., Minshew, H., Nocco, M., Peterson, C., Roby, M., Roseman, J., Roth, A., Sandoval, S., Silva, S.A., Smet, E., Smither-Kopperl, M., Suvocarev, K., Waterhouse, H., Wauters, V., Williams, S., Zaccaria, D., 2024. Cover cropping in the SGMA era: a comprehensive overview of water impacts, policy implications, and recommendations for California's water managers, The Soil-Water Interface Expert Convening Series: Cover Crop Impacts on Water Budgets. California.
California Department of Food and Agriculture (CDFA), 2025. 2023-2024 California agricultural statistics review.
California Department of Water Resources (DWR), 2025. California's groundwater: bulletin 118 — update 2025. Public Draft, October 2025. California Department of Water Resources, Sacramento, CA.
Cao, Q., Wang, Z., Yang, X., Shen, Y., 2021. The effects of cocksfoot cover crop on soil water balance, evapotranspiration partitioning, and system production in an apple orchard on

the loess plateau of china. Soil and Tillage Research 205, 104788. https://doi.org/10.1016/j.still.2020.104788.
Carlisle, L., 2016. Factors influencing farmer adoption of soil health practices in the United States: a narrative review. Agroecol. Sustain. Food Syst. 40, 583–613. https://doi.org/10.1080/21683565.2016.1156596.
Chakraborty, P., Singh, J., Singh, N., Kumar, S., 2022. Assessing the influence of cover crop on soil water dynamics using soil moisture measurements and hydrus-1d simulations. Soil Science Soc of Amer J 86, 1538–1552. https://doi.org/10.1002/saj2.20477.
DeVincentis, A., Solis, S.S., Rice, S., Zaccaria, D., Snyder, R., Maskey, M., Gomes, A., Gaudin, A., Mitchell, J., 2022. Impacts of winter cover cropping on soil moisture and evapotranspiration in California's specialty crop fields may be minimal during winter months. Calif. Agr. 76, 37–45. https://doi.org/10.3733/ca.2022a0001.
DeVincentis, A.J., Solis, S.S., Bruno, E.M., Leavitt, A., Gomes, A., Rice, S., Zaccaria, D., 2020. Using cost-benefit analysis to understand adoption of winter cover cropping in california's specialty crop systems. Journal of Environmental Management 261, 110205. https://doi.org/10.1016/j.jenvman.2020.110205.
Dhungel, R., Anderson, R.G., French, A.N., Skaggs, T.H., Ajami, H., Wang, D., 2024. Intercomparison of citrus evapotranspiration among eddy covariance, openet ensemble models, and the water and energy balance model (baitsss). Agricultural Water Management 304, 109066. https://doi.org/10.1016/j.agwat.2024.109066.
Diffenbaugh, N.S., Swain, D.L., Touma, D., 2015. Anthropogenic warming has increased drought risk in California. Proc. Natl. Acad. Sci. U.S.A. 112, 3931–3936. https://doi.org/10.1073/pnas.1422385112.
Drechsler, K., Fulton, A., Kisekka, I., 2022. Crop coefficients and water use of young almond orchards. Irrig Sci 40, 379–395. https://doi.org/10.1007/s00271-022-00786-y.
Dunn, M., Ulrich-Schad, J.D., Prokopy, L.S., Myers, R.L., Watts, C.R., Scanlon, K., 2016. Perceptions and use of cover crops among early adopters: findings from a national survey. Journal of Soil and Water Conservation 71, 29–40. https://doi.org/10.2489/jswc.71.1.29.
Evett, S.R., Steiner, J.L., 1995. Precision of neutron scattering and capacitance type soil water content gauges from field calibration. Soil Science Soc of Amer J 59, 961–968. https://doi.org/10.2136/sssaj1995.03615995005900040001x.
Faunt, C.C., Sneed, M., Traum, J., Brandt, J.T., 2016. Water availability and land subsidence in the central valley, california, usa. Hydrogeol J 24, 675–684. https://doi.org/10.1007/s10040-015-1339-x.
Fernando, M., Scott, N., Shrestha, A., Gao, S., Hale, L., 2024. A native plant species cover crop positively impacted vineyard water dynamics, soil health, and vine vigor. Agriculture, Ecosystems & Environment 367, 108972. https://doi.org/10.1016/j.agee.2024.108972.
Firoozi, F., Alavipanah, S.K., Hosseini, S.Z., Asgari, S., Malamiri, H.R.G., Rahimi, K., 2023. Remotely sensed and empirical reference evapotranspiration models to derive crop coefficients for pistachios in the central basin of iran. Iran J Sci Technol Trans Civ Eng 47, 3999–4019. https://doi.org/10.1007/s40996-023-01169-9.
Fisher, J.B., Melton, F., Middleton, E., Hain, C., Anderson, M., Allen, R., McCabe, M.F., Hook, S., Baldocchi, D., Townsend, P.A., Kilic, A., Tu, K., Miralles, D.D., Perret, J., Lagouarde, J.-P., Waliser, D., Purdy, A.J., French, A., Schimel, D., Famiglietti, J.S., Stephens, G., Wood, E.F., 2017. The future of evapotranspiration: global requirements

for ecosystem functioning, carbon and climate feedbacks, agricultural management, and water resources: the future of evapotranspiration. Water Resour. Res. 53, 2618–2626. https://doi.org/10.1002/2016WR020175.
Fisher, J.B., Tu, K.P., Baldocchi, D.D., 2008. Global estimates of the land–atmosphere water flux based on monthly avhrr and islscp-ii data, validated at 16 fluxnet sites. Remote Sensing of Environment 112, 901–919. https://doi.org/10.1016/j.rse.2007.06.025.
Flynn, M.T., Guerrero-Medina, O., McDonald, I.F., Anika, J.T., Ware, E.C., Paw U, K.T., Gaudin, A.C., Fenster, T.L., Lundgren, J.G., Harter, T., Sandoval Solis, S., Suvočarev, K., 2025. A case study of evapotranspiration at five almond orchards on a spectrum of conventional to regenerative management. California Agriculture 79. https://doi.org/10.3733/001c.133243.
Foken, T., Aubinet, M., Leuning, R., 2012. The eddy covariance method, in: Aubinet, M., Vesala, T., Papale, D. (Eds.), Eddy Covariance. Springer Netherlands, Dordrecht, pp. 1–19. https://doi.org/10.1007/978-94-007-2351-1_1.
Folorunso, O.A., Rolston, D.E., Prichard, T., Loui, D.T., 1992. Soil surface strength and infiltration rate as affected by winter cover crops. Soil Technology 5, 189–197. https://doi.org/10.1016/0933-3630(92)90021-R.
Gabriel, J.L., Muñoz-Carpena, R., Quemada, M., 2012. The role of cover crops in irrigated systems: water balance, nitrate leaching and soil mineral nitrogen accumulation. Agriculture, Ecosystems & Environment 155, 50–61. https://doi.org/10.1016/j.agee.2012.03.021.
Garba, I.I., Bell, L.W., Williams, A., 2022. Cover crop legacy impacts on soil water and nitrogen dynamics, and on subsequent crop yields in drylands: a meta-analysis. Agron. Sustain. Dev. 42, 34. https://doi.org/10.1007/s13593-022-00760-0.
Gassman, P.W., Williams, J.R., Wang, X., Saleh, A., Osei, E., Hauck, L.M., Izaurralde, R.C., Flowers, J.D., 2010. Invited review article: the agricultural policy/environmental extender (apex) model: an emerging tool for landscape and watershed environmental analyses. Transactions of the ASABE 53, 711–740. https://doi.org/10.13031/2013.30078.
Gaze, S.R., Stalham, M.A., Allen, E.J., 2002. Accuracy of the neutron probe for measuring changes in soil water storage under potatoes. J. Agric. Sci. 138, 135–152. https://doi.org/10.1017/S0021859601001654.
Goldhamer, D.A., Kjelgren, R.K., Beede, R.H., Williams, L.E., Moore, J.M., Lane, J., Weinberger, G., Menezes, J., Jr., 1985. Water use requirements of pistachio trees and response to water stress. Annual Report of the California Pistachio Commission, Crop Year 1984-1985, 85–92.
Goring, D.G., Nikora, V.I., 2002. Despiking acoustic doppler velocimeter data. J. Hydraul. Eng. 128, 117–126. https://doi.org/10.1061/(ASCE)0733-9429(2002)128:1(117).
Gould, K., Rudnick, J., 2018. Adoption of cover crops in california.
Gribov, A., Krivoruchko, K., 2020. Empirical bayesian kriging implementation and usage. Sci. Total Environ. 722, 137290. https://doi.org/10.1016/j.scitotenv.2020.137290.
Hao, X., Abou Najm, M., Steenwerth, K.L., Nocco, M.A., Basset, C., Daccache, A., 2023. Are there universal soil responses to cover cropping? a systematic review. Science of The Total Environment 861, 160600. https://doi.org/10.1016/j.scitotenv.2022.160600.
Haruna, S.I., Eichas, R.C., Peters, O.M., Farmer, A.C., Lackey, D.Q., Nichols, J.E., Peterson, W.H., Slone, N.A., 2022. In situ water infiltration: influence of cover crops after growth termination. Soil Science Soc of Amer J 86, 769–780. https://doi.org/10.1002/saj2.20390.

Iniesta, F., Testi, L., Goldhamer, D.A., Fereres, E., 2008. Quantifying reductions in consumptive water use under regulated deficit irrigation in pistachio (pistacia vera l.). Agricultural Water Management 95, 877–886. https://doi.org/10.1016/j.agwat.2008.01.013.

Irmak, A., Ratcliffe, I., Ranade, P., Hubbard, K.G., Singh, R.K., Kamble, B., Kjaersgaard, J., 2011. Estimation of land surface evapotranspiration with a satellite remote sensing procedure. Great Plains Research 21, 73–88.

Izaurralde, R.C., Williams, J.R., McGill, W.B., Rosenberg, N.J., Jakas, M.C.Q., 2006. Simulating soil c dynamics with epic: model description and testing against long-term data. Ecological Modelling 192, 362–384. https://doi.org/10.1016/j.ecolmodel.2005.07.010.

Jensen, M.E., Allen, R.G. (Eds.), 2016. Evaporation, evapotranspiration, and irrigation water requirements, Second. ed. American Society of Civil Engineers, Reston, VA. https://doi.org/10.1061/9780784414057.

Jin, Y., He, R., Marino, G., Whiting, M., Kent, E., Sanden, B.L., Culumber, M., Ferguson, L., Little, C., Grattan, S., Paw U, K.T., Lagos, L.O., Snyder, R.L., Zaccaria, D., 2018. Spatially variable evapotranspiration over salt affected pistachio orchards analyzed with satellite remote sensing estimates. Agricultural and Forest Meteorology 262, 178–191. https://doi.org/10.1016/j.agrformet.2018.07.004.

Joyce, B.A., Wallender, W.W., Mitchell, J.P., Huyck, L.M., Temple, S.R., Brostrom, P.N., Hsiao, T.C., 2002. Infiltration and soil water storage under winter cover cropping in span class="nocase">california's span class="nocase">sacramentovalley. Transactions of the ASAE 45. https://doi.org/10.13031/2013.8526.

Kader, M.A., Singha, A., Begum, M.A., Jewel, A., Khan, F.H., Khan, N.I., 2019. Mulching as water-saving technique in dryland agriculture: review article. Bull Natl Res Cent 43, 147. https://doi.org/10.1186/s42269-019-0186-7.

Kaimal, J.C., Finnigan, J.J., 1994. Atmospheric boundary layer flows: their structure and measurement. Oxford University Press, New York.

Kanber, R., Yazar, A., □Nder, S., K□ksal, H., 1993. Irrigation response of pistachio (pistacia vera l.). Irrig Sci 14. https://doi.org/10.1007/BF00195000.

Kandhway, A., Scarpare, F., Liu, M., Nelson, R., Adam, J.C., Anderson, R.G., Conklin, M.H., Safeeq, M., 2025. Water use dynamics of almond and pistachio crops in the mediterranean region amid climate change. Agric. Water Manage. 307, 109219. https://doi.org/10.1016/j.agwat.2024.109219.

Kermani, M.M., Salehi, F., 2006. Determination of pistachio crop evapotranspiration (etc). Acta Hortic. 441–448. https://doi.org/10.17660/ActaHortic.2006.726.71.

Kiniry, J.R., Williams, J.R., Gassman, P.W., Debaeke, P., 1992. A general, process-oriented model for two competing plant species. Transactions of the ASAE 35, 801–810. https://doi.org/10.13031/2013.28665.

Kljun, N., Calanca, P., Rotach, M.W., Schmid, H.P., 2015. A simple two-dimensional parameterisation for flux footprint prediction (ffp). Geosci. Model Dev. 8, 3695–3713. https://doi.org/10.5194/gmd-8-3695-2015.

Knipper, K., Anderson, M., Bambach, N., Kustas, W., Gao, F., Zahn, E., Hain, C., McElrone, A., Belfiore, O.R., Castro, S., Alsina, M.M., Saa, S., 2022. Evaluation of partitioned evaporation and transpiration estimates within the disalexi modeling framework over irrigated crops in california. Remote Sensing 15, 68. https://doi.org/10.3390/rs15010068.

Knipper, K., Anderson, M., Bambach, N., Melton, F., Ellis, Z., Yang, Y., Volk, J., McElrone, A.J., Kustas, W., Roby, M., Carrara, W., Castro, S., Kilic, A., Fisher, J.B., Ruhoff, A., Senay, G.B., Morton, C., Saa, S., Allen, R.G., 2024. A comparative analysis of openet for evaluating evapotranspiration in california almond orchards. Agricultural and Forest Meteorology 355, 110146. https://doi.org/10.1016/j.agrformet.2024.110146.

Koudahe, K., Allen, S.C., Djaman, K., 2022. Critical review of the impact of cover crops on soil properties. International Soil and Water Conservation Research 10, 343–354. https://doi.org/10.1016/j.iswcr.2022.03.003.

Krivoruchko, K., Gribov, A., 2019. Evaluation of empirical bayesian kriging. Spatial Statistics 32, 100368. https://doi.org/10.1016/j.spasta.2019.100368.

Laipelt, L., Henrique Bloedow Kayser, R., Santos Fleischmann, A., Ruhoff, A., Bastiaanssen, W., Erickson, T.A., Melton, F., 2021. Long-term monitoring of evapotranspiration using the sebal algorithm and google earth engine cloud computing. ISPRS Journal of Photogrammetry and Remote Sensing 178, 81–96. https://doi.org/10.1016/j.isprsjprs.2021.05.018.

Leys, C., Ley, C., Klein, O., Bernard, P., Licata, L., 2013. Detecting outliers: do not use standard deviation around the mean, use absolute deviation around the median. Journal of Experimental Social Psychology 49, 764–766. https://doi.org/10.1016/j.jesp.2013.03.013.

Lobell, D.B., Field, C.B., Cahill, K.N., Bonfils, C., 2006. Impacts of future climate change on california perennial crop yields: model projections with climate and crop uncertainties. Agricultural and Forest Meteorology 141, 208–218. https://doi.org/10.1016/j.agrformet.2006.10.006.

Lu, Y.C., Watkins, K.B., Teasdale, J.R., Abdul-Baki, A.A., 2000. Cover crops in sustainable food production. Food Reviews International 16, 121–157. https://doi.org/10.1081/FRI-100100285.

Lubell, M., Blomquist, W., Beutler, L., 2020. Sustainable groundwater management in california: a grand experiment in environmental governance. Society & Natural Resources 33, 1447–1467. https://doi.org/10.1080/08941920.2020.1833617.

Mall, N.K., Herman, J.D., 2019. Water shortage risks from perennial crop expansion in california's central valley. Environ. Res. Lett. 14, 104014. https://doi.org/10.1088/1748-9326/ab4035.

Marino, G., Zaccaria, D., Lagos, L.O., Souto, C., Kent, E.R., Grattan, S.R., Shapiro, K., Sanden, B.L., Snyder, R.L., 2021. Effects of salinity and sodicity on the seasonal dynamics of actual evapotranspiration and surface energy balance components in mature micro-irrigated pistachio orchards. Irrig Sci 39, 23–43. https://doi.org/10.1007/s00271-020-00694-z.

Marino, G., Zaccaria, D., Snyder, R.L., Lagos, O., Lampinen, B.D., Ferguson, L., Grattan, S.R., Little, C., Shapiro, K., Maskey, M.L., Corwin, D.L., Scudiero, E., Sanden, B.L., 2019. Actual evapotranspiration and tree performance of mature micro-irrigated pistachio orchards grown on saline-sodic soils in the san joaquin valley of california. Agriculture 9, 76. https://doi.org/10.3390/agriculture9040076.

Mason, R., Gorres, J., Faulkner, J.W., Doro, L., Merrill, S.C., 2020. Calibrating the apex model for simulations of environmental and agronomic outcomes on dairy farms in the northeast u.s.: a step-by-step example. Applied Engineering in Agriculture 36, 281–301. https://doi.org/10.13031/aea.13679.

Massman, W.J., 2000. A simple method for estimating frequency response corrections for eddy covariance systems. Agricultural and Forest Meteorology 104, 185–198. https://doi.org/10.1016/S0168-1923(00)00164-7.

Melton, F.S., Huntington, J., Grimm, R., Herring, J., Hall, M., Rollison, D., Erickson, T., Allen, R., Anderson, M., Fisher, J.B., Kilic, A., Senay, G.B., Volk, J., Hain, C., Johnson, L., Ruhoff, A., Blankenau, P., Bromley, M., Carrara, W., Daudert, B., Doherty, C., Dunkerly, C., Friedrichs, M., Guzman, A., Halverson, G., Hansen, J., Harding, J., Kang, Y., Ketchum, D., Minor, B., Morton, C., Ortega-Salazar, S., Ott, T., Ozdogan, M., ReVelle, P.M., Schull, M., Wang, C., Yang, Y., Anderson, R.G., 2022. OpenET: filling a critical data gap in water management for the western united states. J American Water Resour Assoc 58, 971–994. https://doi.org/10.1111/1752-1688.12956.

Melton, F.S., Johnson, L.F., Lund, C.P., Pierce, L.L., Michaelis, A.R., Hiatt, S.H., Guzman, A., Adhikari, D.D., Purdy, A.J., Rosevelt, C., Votava, P., Trout, T.J., Temesgen, B., Frame, K., Sheffner, E.J., Nemani, R.R., 2012. Satellite irrigation management support with the terrestrial observation and prediction system: a framework for integration of satellite and surface observations to support improvements in agricultural water resource management. IEEE J. Sel. Top. Appl. Earth Observations Remote Sensing 5, 1709–1721. https://doi.org/10.1109/JSTARS.2012.2214474.

Mitchell, J.P., Peters, D.W., Shennan, C., 1999. Changes in soil water storage in winter fallowed and cover cropped soils. J. Sustain. Agric. 15, 19–31. https://doi.org/10.1300/J064v15n02_04.

Mitchell, J.P., Shrestha, A., Irmak, S., 2015. Trade-offs between winter cover crop production and soil water depletion in the San Joaquin valley, California. J. Soil Water Conserv. 70, 430–440. https://doi.org/10.2489/jswc.70.6.430.

Monteith, J.L., 1965. Evaporation and environment. Symposia of the Society for Experimental Biology 19, 205–234.

Moore, C.J., 1986. Frequency response corrections for eddy correlation systems. Boundary-Layer Meteorol 37, 17–35. https://doi.org/10.1007/BF00122754.

Moore, E.A., Norton, U., 2024. Improving semi-arid agroecosystem services with cover crop mixes. PLoS ONE 19, e0306567. https://doi.org/10.1371/journal.pone.0306567.

Moriasi, D.N., Arnold, J.G., Liew, M.W.V., Bingner, R.L., Harmel, R.D., Veith, T.L., 2007. Model evaluation guidelines for systematic quantification of accuracy in watershed simulations. Transactions of the ASABE 50, 885–900. https://doi.org/10.13031/2013.23153.

Moriasi, D.N., King, K.W., Bosch, D.D., Bjorneberg, D.L., Teet, S., Guzman, J.A., Williams, M.R., 2016. Framework to parameterize and validate apex to support deployment of the nutrient tracking tool. Agric. Water Manage. 177, 146–164. https://doi.org/10.1016/j.agwat.2016.07.009.

Munna, M.N.H., Lal, R., 2025. Impacts of cover cropping and organic amendments on soil physical quality under temperate climate. Cogent Food & Agriculture 11, 2467452. https://doi.org/10.1080/23311932.2025.2467452.

Nash, J.E., Sutcliffe, J.V., 1970. River flow forecasting through conceptual models part i — a discussion of principles. Journal of Hydrology 10, 282–290. https://doi.org/10.1016/0022-1694(70)90255-6.

Nielsen, D.C., Lyon, D.J., Hergert, G.W., Higgins, R.K., Calderón, F.J., Vigil, M.F., 2015. Cover crop mixtures do not use water differently than single-species plantings. Agron. J. 107, 1025–1038. https://doi.org/10.2134/agronj14.0504.

Oregon State University, 2010. Peas - Western Oregon. https://horticulture.oregonstate.edu/oregon-vegetables/peas-western-oregon-0 (accessed 9 May 2026).

Papale, D., Reichstein, M., Aubinet, M., Canfora, E., Bernhofer, C., Kutsch, W., Longdoz, B., Rambal, S., Valentini, R., Vesala, T., Yakir, D., 2006. Towards a standardized processing of net ecosystem exchange measured with eddy covariance technique: algorithms and uncertainty estimation. Biogeosciences 3, 571–583. https://doi.org/10.5194/bg-3-571-2006.

Pastorello, G., Trotta, C., Canfora, E., Chu, H., Christianson, D., Cheah, Y.-W., Poindexter, C., Chen, J., Elbashandy, A., Humphrey, M., Isaac, P., Polidori, D., Reichstein, M., Ribeca, A., Van Ingen, C., Vuichard, N., Zhang, L., Amiro, B., Ammann, C., Arain, M.A., Ardö, J., Arkebauer, T., Arndt, S.K., Arriga, N., Aubinet, M., Aurela, M., Baldocchi, D., Barr, A., Beamesderfer, E., Marchesini, L.B., Bergeron, O., Beringer, J., Bernhofer, C., Berveiller, D., Billesbach, D., Black, T.A., Blanken, P.D., Bohrer, G., Boike, J., Bolstad, P.V., Bonal, D., Bonnefond, J.-M., Bowling, D.R., Bracho, R., Brodeur, J., Brümmer, C., Buchmann, N., Burban, B., Burns, S.P., Buysse, P., Cale, P., Cavagna, M., Cellier, P., Chen, S., Chini, I., Christensen, T.R., Cleverly, J., Collalti, A., Consalvo, C., Cook, B.D., Cook, D., Coursolle, C., Cremonese, E., Curtis, P.S., D'Andrea, E., Da Rocha, H., Dai, X., Davis, K.J., Cinti, B.D., Grandcourt, A.D., Ligne, A.D., De Oliveira, R.C., Delpierre, N., Desai, A.R., Di Bella, C.M., Tommasi, P.D., Dolman, H., Domingo, F., Dong, G., Dore, S., Duce, P., Dufrêne, E., Dunn, A., Dušek, J., Eamus, D., Eichelmann, U., ElKhidir, H.A.M., Eugster, W., Ewenz, C.M., Ewers, B., Famulari, D., Fares, S., Feigenwinter, I., Feitz, A., Fensholt, R., Filippa, G., Fischer, M., Frank, J., Galvagno, M., Gharun, M., Gianelle, D., Gielen, B., Gioli, B., Gitelson, A., Goded, I., Goeckede, M., Goldstein, A.H., Gough, C.M., Goulden, M.L., Graf, A., Griebel, A., Gruening, C., Grünwald, T., Hammerle, A., Han, S., Han, X., Hansen, B.U., Hanson, C., Hatakka, J., He, Y., Hehn, M., Heinesch, B., Hinko-Najera, N., Hörtnagl, L., Hutley, L., Ibrom, A., Ikawa, H., Jackowicz-Korczynski, M., Janouš, D., Jans, W., Jassal, R., Jiang, S., Kato, T., Khomik, M., Klatt, J., Knohl, A., Knox, S., Kobayashi, H., Koerber, G., Kolle, O., Kosugi, Y., Kotani, A., Kowalski, A., Kruijt, B., Kurbatova, J., Kutsch, W.L., Kwon, H., Launiainen, S., Laurila, T., Law, B., Leuning, R., Li, Yingnian, Liddell, M., Limousin, J.-M., Lion, M., Liska, A.J., Lohila, A., López-Ballesteros, A., López-Blanco, E., Loubet, B., Loustau, D., Lucas-Moffat, A., Lüers, J., Ma, S., Macfarlane, C., Magliulo, V., Maier, R., Mammarella, I., Manca, G., Marcolla, B., Margolis, H.A., Marras, S., Massman, W., Mastepanov, M., Matamala, R., Matthes, J.H., Mazzenga, F., McCaughey, H., McHugh, I., McMillan, A.M.S., Merbold, L., Meyer, W., Meyers, T., Miller, S.D., Minerbi, S., Moderow, U., Monson, R.K., Montagnani, L., Moore, C.E., Moors, E., Moreaux, V., Moureaux, C., Munger, J.W., Nakai, T., Neirynck, J., Nesic, Z., Nicolini, G., Noormets, A., Northwood, M., Nosetto, M., Nouvellon, Y., Novick, K., Oechel, W., Olesen, J.E., Ourcival, J.-M., Papuga, S.A., Parmentier, F.-J., Paul-Limoges, E., Pavelka, M., Peichl, M., Pendall, E., Phillips, R.P., Pilegaard, K., Pirk, N., Posse, G., Powell, T., Prasse, H., Prober, S.M., Rambal, S., Rannik, Ü., Raz-Yaseef, N., Rebmann, C., Reed, D., Dios, V.R.D., Restrepo-Coupe, N., Reverter, B.R., Roland, M., Sabbatini, S., Sachs, T.,

Saleska, S.R., Sánchez-Cañete, E.P., Sanchez-Mejia, Z.M., Schmid, H.P., Schmidt, M., Schneider, K., Schrader, F., Schroder, I., Scott, R.L., Sedlák, P., Serrano-Ortíz, P., Shao, C., Shi, P., Shironya, I., Siebicke, L., Šigut, L., Silberstein, R., Sirca, C., Spano, D., Steinbrecher, R., Stevens, R.M., Sturtevant, C., Suyker, A., Tagesson, T., Takanashi, S., Tang, Y., Tapper, N., Thom, J., Tomassucci, M., Tuovinen, J.-P., Urbanski, S., Valentini, R., Van Der Molen, M., Van Gorsel, E., Van Huissteden, K., Varlagin, A., Verfaillie, J., Vesala, T., Vincke, C., Vitale, D., Vygodskaya, N., Walker, J.P., Walter-Shea, E., Wang, H., Weber, R., Westermann, S., Wille, C., Wofsy, S., Wohlfahrt, G., Wolf, S., Woodgate, W., Li, Yuelin, Zampedri, R., Zhang, J., Zhou, G., Zona, D., Agarwal, D., Biraud, S., Torn, M., Papale, D., 2020. The fluxnet2015 dataset and the oneflux processing pipeline for eddy covariance data. Sci Data 7, 225. https://doi.org/10.1038/s41597-020-0534-3.

Pathak, T., Maskey, M., Dahlberg, J., Kearns, F., Bali, K., Zaccaria, D., 2018. Climate change trends and impacts on California agriculture: a detailed review. Agronom. 8, 25. https://doi.org/10.3390/agronomy8030025.

Peddinti, S.R., 2026. Flux gap filling tool: mds and ml gap-filling for micrometeorological data.

Pereira, L.S., Paredes, P., Melton, F., Johnson, L., Wang, T., López-Urrea, R., Cancela, J.J., Allen, R.G., 2020. Prediction of crop coefficients from fraction of ground cover and height. background and validation using ground and remote sensing data. Agricultural Water Management 241, 106197. https://doi.org/10.1016/j.agwat.2020.106197.

Pruitt, W.O., Doorenbos, J., 1977. Empirical calibration, a requisite for evapotranspiration formulae based on daily or longer mean climatic data? Presented at the International Commission on Irrigation and Drainage.

Rahemi, M., Pakkish, Z., 2009. Determination of chilling and heat requirements of pistachio (pistacia vera l.) cultivars. Agricultural Sciences in China 8, 803–807. https://doi.org/10.1016/S1671-2927(08)60281-3.

Rahimzadegan, M., Janani, A., 2019. Estimating evapotranspiration of pistachio crop based on sebal algorithm using landsat 8 satellite imagery. Agric. Water Manag. 217, 383–390. https://doi.org/10.1016/j.agwat.2019.03.018.

Reichstein, M., Falge, E., Baldocchi, D., Papale, D., Aubinet, M., Berbigier, P., Bernhofer, C., Buchmann, N., Gilmanov, T., Granier, A., Grünwald, T., Havránková, K., Ilvesniemi, H., Janous, D., Knohl, A., Laurila, T., Lohila, A., Loustau, D., Matteucci, G., Meyers, T., Miglietta, F., Ourcival, J., Pumpanen, J., Rambal, S., Rotenberg, E., Sanz, M., Tenhunen, J., Seufert, G., Vaccari, F., Vesala, T., Yakir, D., Valentini, R., 2005. On the separation of net ecosystem exchange into assimilation and ecosystem respiration: review and improved algorithm. Global Change Biology 11, 1424–1439. https://doi.org/10.1111/j.1365-2486.2005.001002.x.

Sabiston, L., Sabie, R., Buenemann, M., Stringam, B., Fernald, A., 2024. Comparing field-scale eddy covariance measurements and crop coefficient estimates of alfalfa evapotranspiration to openet model estimates and exploring water budget implications in a dryland environment. Irrig Sci. https://doi.org/10.1007/s00271-024-00941-7.

Sainju, U.M., Singh, B.P., 1997. Winter cover crops for sustainable agricultural systems: influence on soil properties, water quality, and crop yields. HortSci 32, 21–28. https://doi.org/10.21273/HORTSCI.32.1.21.

Saleh, A., Niraula, R., Marek, G.W., Gowda, P.H., Brauer, D.K., Howell, T.A., 2018. Lysimetric evaluation of the apex model to simulate daily et for irrigated crops in the texas high plains. Transactions of the ASABE 61, 65–74. https://doi.org/10.13031/trans.11938.

Sanden, B.L., Ferguson, L., Reyes, H.C., Grattan, S.R., 2004. Effect of salinity on evapotranspiration and yield of san joaquin valley pistachios. Acta Hortic. 583–589. https://doi.org/10.17660/ActaHortic.2004.664.73.

Sastre, B., Marques, M.J., García-Díaz, A., Bienes, R., 2018. Three years of management with cover crops protecting sloping olive groves soils, carbon and water effects on gypsiferous soil. CATENA 171, 115–124. https://doi.org/10.1016/j.catena.2018.07.003.

Schomberg, H.H., White, K.E., Thompson, A.I., Bagley, G.A., Burke, A., Garst, G., Bybee-Finley, K.A., Mirsky, S.B., 2023. Interseeded cover crop mixtures influence soil water storage during the corn phase of corn-soybean-wheat no-till cropping systems. Agricultural Water Management 278, 108167. https://doi.org/10.1016/j.agwat.2023.108167.

Senay, G.B., 2018. Satellite psychrometric formulation of the operational simplified surface energy balance (ssebop) model for quantifying and mapping evapotranspiration. Applied Engineering in Agriculture 34, 555–566. https://doi.org/10.13031/aea.12614.

Senay, G.B., Bohms, S., Singh, R.K., Gowda, P.H., Velpuri, N.M., Alemu, H., Verdin, J.P., 2013. Operational evapotranspiration mapping using remote sensing and weather datasets: a new parameterization for the SSEB approach. J. American Water Resour. Assoc. 49, 577–591. https://doi.org/10.1111/jawr.12057.

Senay, G.B., Parrish, G.E.L., Schauer, M., Friedrichs, M., Khand, K., Boiko, O., Kagone, S., Dittmeier, R., Arab, S., Ji, L., 2023. Improving the operational simplified surface energy balance evapotranspiration model using the forcing and normalizing operation. Remote Sensing 15, 260. https://doi.org/10.3390/rs15010260.

Snapp, S.S., Swinton, S.M., Labarta, R., Mutch, D., Black, J.R., Leep, R., Nyiraneza, J., O'Neil, K., 2005. Evaluating cover crops for benefits, costs and performance within cropping system niches. Agron. J. 97, 322–332. https://doi.org/10.2134/agronj2005.0322a.

Soil Health Institute, 2019. Progress report: adoption of soil health systems based on data from the 2017 U.S. census of agriculture. https://soilhealthinstitute.org/app/uploads/2022/01/Soil-Health-Adoption-Overview_2017-Census-Report_FINAL.pdf (accessed 30 October 2024).

Steele, M.K., Coale, F.J., Hill, R.L., 2012. Winter annual cover crop impacts on no-till soil physical properties and organic matter. Soil Science Soc of Amer J 76, 2164–2173. https://doi.org/10.2136/sssaj2012.0008.

Steglich, E.M., Osorio, J., Doro, L., Jeong, J., Williams, J.R., 2023. Agricultural policy/environmental extender user's manual version 1501.

Tadesse, H.K., Moriasi, D.N., Gowda, P.H., Marek, G., Steiner, J.L., Brauer, D., Talebizadeh, M., Nelson, A., Starks, P., 2018. Evaluating evapotranspiration estimation methods in apex model for dryland cropping systems in a semi-arid region. Agricultural Water Management 206, 217–228. https://doi.org/10.1016/j.agwat.2018.04.007.

Tadesse, H.K., Moriasi, D.N., Gowda, P.H., Steiner, J.L., Talebizadeh, M., Nelson, A.M., Starks, P.J., Marek, G., 2019. Comparison of evapotranspiration simulation performance by apex model in dryland and irrigated cropping systems. J American Water Resour Assoc 55, 1009–1023. https://doi.org/10.1111/1752-1688.12759.

Tadesse, H.K., Moriasi, D.N., Gowda, P.H., Wagle, P., Starks, P.J., Steiner, J.L., Talebizadeh, M., Neel, J.P.S., Nelson, A.M., 2021. Comparison of evapotranspiration and biomass simulation in winter wheat under conventional and conservation tillage systems using

apex model. Ecohydrology & Hydrobiology 21, 55–66. https://doi.org/10.1016/j.ecohyd.2020.08.003.
Talebizadeh, M., Moriasi, D., Gowda, P., Steiner, J.L., Tadesse, H.K., Nelson, A.M., Starks, P., 2018. Simultaneous calibration of evapotranspiration and crop yield in agronomic system modeling using the apex model. Agricultural Water Management 208, 299–306. https://doi.org/10.1016/j.agwat.2018.06.043.
Tawalbeh, Z.M., Bawazir, A.S., Fernald, A., Sabie, R., Heerema, R.J., 2024. Assessing satellite-derived openet platform evapotranspiration of mature pecan orchard in the mesilla valley, new mexico. Remote Sensing 16, 1429. https://doi.org/10.3390/rs16081429.
Teasdale, J.R., Mohler, C.L., 1993. Light transmittance, soil temperature, and soil moisture under residue of hairy vetch and rye. Agronomy Journal 85, 673–680. https://doi.org/10.2134/agronj1993.00021962008500030029x.
Timlin, D., Chun, J.A., Meisinger, J., Kang, K., Fleisher, D., Staver, K., Doherty, C., Russ, A., 2019. Evaluation of the agricultural policy environmental extender (apex) for the chesapeake bay watershed. Agricultural Water Management 221, 477–485. https://doi.org/10.1016/j.agwat.2019.03.046.
Tootelian, D.H., 2023a. Projected pistachio production: 2023 through 2031.
Tootelian, D.H., 2023b. Projected pistachio production: 2023 through 2031.
Unger, P.W., Vigil, M.F., 1998. Cover crop effects on soil water relationships. Journal of Soil and Water Conservation.
United Nations University Institute for Water, Environment and Health (UNU INWEH), Madani, K., 2026. Global water bankruptcy: living beyond our hydrological means in the post crisis era. United Nations University Institute for Water, Environment and Health (UNU INWEH). https://doi.org/10.53328/INR26KAM001.
United States Department of Agriculture (USDA), 2026. Pistachios. https://www.fas.usda.gov/data/production/commodity/0577907 (accessed 13 January 2026).
Vanella, D., Peddinti, S.R., Kisekka, I., 2022. Unravelling soil water dynamics in almond orchards characterized by soil-heterogeneity using electrical resistivity tomography. Agricultural Water Management 269, 107652. https://doi.org/10.1016/j.agwat.2022.107652.
Vendig, I., Guzman, A., De La Cerda, G., Esquivel, K., Mayer, A.C., Ponisio, L., Bowles, T.M., 2023. Quantifying direct yield benefits of soil carbon increases from cover cropping. Nat Sustain 6, 1125–1134. https://doi.org/10.1038/s41893-023-01131-7.
Volk, J.M., Huntington, J.L., Melton, F.S., Allen, R., Anderson, M., Fisher, J.B., Kilic, A., Ruhoff, A., Senay, G.B., Minor, B., Morton, C., Ott, T., Johnson, L., Comini De Andrade, B., Carrara, W., Doherty, C.T., Dunkerly, C., Friedrichs, M., Guzman, A., Hain, C., Halverson, G., Kang, Y., Knipper, K., Laipelt, L., Ortega-Salazar, S., Pearson, C., Parrish, G.E.L., Purdy, A., ReVelle, P., Wang, T., Yang, Y., 2024. Assessing the accuracy of openet satellite-based evapotranspiration data to support water resource and land management applications. Nat Water 2, 193–205. https://doi.org/10.1038/s44221-023-00181-7.
Vukicevich, E., Lowery, T., Bowen, P., Úrbez-Torres, J.R., Hart, M., 2016. Cover crops to increase soil microbial diversity and mitigate decline in perennial agriculture. a review. Agron. Sustain. Dev. 36, 48. https://doi.org/10.1007/s13593-016-0385-7.

Wang, J., Zhang, S., Sainju, U.M., Ghimire, R., Zhao, F., 2021. A meta-analysis on cover crop impact on soil water storage, succeeding crop yield, and water-use efficiency. Agricultural Water Management 256, 107085. https://doi.org/10.1016/j.agwat.2021.107085.

Wang, X., Jeong, J., 2019. APEX-cute 4 user manual.

Wang, X., Williams, J.R., Gassman, P.W., Baffaut, C., Izaurralde, R.C., Jeong, J., Kiniry, J.R., 2012. EPIC and apex: model use, calibration, and validation. Transactions of the ASABE 55, 1447–1462. https://doi.org/10.13031/2013.42253.

Ward, P.R., Dunin, F.X., Micin, S.F., Williamson, D.R., 1998. Evaluating drainage responses in duplex soils in a mediterranean environment. Australian Journal of Soil Research 36, 509–524. https://doi.org/10.1071/S97082.

Ward, P.R., Flower, K.C., Cordingley, N., Weeks, C., Micin, S.F., 2012. Soil water balance with cover crops and conservation agriculture in a mediterranean climate. Field Crops Research 132, 33–39. https://doi.org/10.1016/j.fcr.2011.10.017.

Webb, E.K., Pearman, G.I., Leuning, R., 1980. Correction of flux measurements for density effects due to heat and water vapour transfer. Quart J Royal Meteoro Soc 106, 85–100. https://doi.org/10.1002/qj.49710644707.

Westling, F., Underwood, J., Örn, S., 2018. Light interception modelling using unstructured lidar data in avocado orchards. Computers and Electronics in Agriculture 153, 177–187. https://doi.org/10.1016/j.compag.2018.08.020.

Williams, J.R., Izaurralde, R.C., Williams, C., Steglich, E.M., 2023. Agricultural policy / environmental extender model theoretical documentation version 1501.

Wilson, K., Goldstein, A., Falge, E., Aubinet, M., Baldocchi, D., Berbigier, P., Bernhofer, C., Ceulemans, R., Dolman, H., Field, C., Grelle, A., Ibrom, A., Law, B.E., Kowalski, A., Meyers, T., Moncrieff, J., Monson, R., Oechel, W., Tenhunen, J., Valentini, R., Verma, S., 2002. Energy balance closure at fluxnet sites. Agricultural and Forest Meteorology 113, 223–243. https://doi.org/10.1016/S0168-1923(02)00109-0.

Wutzler, T., Lucas-Moffat, A., Migliavacca, M., Knauer, J., Sickel, K., Šigut, L., Menzer, O., Reichstein, M., 2018. Basic and extensible post-processing of eddy covariance flux data with reddyproc. Biogeosciences 15, 5015–5030. https://doi.org/10.5194/bg-15-5015-2018.

Wyland, L., 1996. Winter cover crops in a vegetable cropping system: impacts on nitrate leaching, soil water, crop yield, pests and management costs. Agriculture, Ecosystems & Environment 59, 1–17. https://doi.org/10.1016/0167-8809(96)01048-1.

Yang, W., Feng, G., Read, J.J., Ouyang, Y., Han, J., Li, P., 2020. Impact of cover crop on corn–soybean productivity and soil water dynamics under different seasonal rainfall patterns. Agronomy Journal 112, 1201–1215. https://doi.org/10.1002/agj2.20110.

Yost, J.L., Huang, J., Hartemink, A.E., 2019. Spatial-temporal analysis of soil water storage and deep drainage under irrigated potatoes in the central sands of wisconsin, usa. Agricultural Water Management 217, 226–235. https://doi.org/10.1016/j.agwat.2019.02.045.

Zaccaria, D., 2023. Updated information on water use and water productivity of pistachio grown on non-saline and salt-affected soils. Statewide Pistachio Day, Visalia Convention Center, Visalia, CA.

Zhang, J., Ranford, T., Taylor, C., 2015. Heat model for pistachio bloom and harvest. Scientia Horticulturae 186, 47–53. https://doi.org/10.1016/j.scienta.2015.02.005.

Zhang, J., Taylor, C., 2011. The dynamic model provides the best description of the chill process on ‘sirora’ pistachio trees in australia. horts 46, 420–425. https://doi.org/10.21273/HORTSCI.46.3.420.

Chapter 2: OpenET Model Performance for Water Accounting and Winter Cover Crop Effect Detection in Young Pistachio Orchards

Charlie Chen[1], Matthew Roby[2], and Isaya Kisekka[1,3]

[1]Hydrologic Science Program, Department of Land, Air, and Water Resources, University of California, Davis, CA 95616, USA
[2]USDA-ARS Sustainable Agricultural Water Systems Research Unit, Davis, CA, 95616, USA
[3]Department of Biological and Agricultural Engineering, University of California, Davis, CA 95616, USA

Corresponding Author: Dr. Isaya Kisekka (email: ikisekka@ucdavis.edu)

This chapter will be submitted for review by the journal Remote Sensing of the Environment. The manuscript, titled *OpenET Model Performance for Water Accounting and Winter Cover Crop Effect Detection in Young Pistachio Orchards*, is prepared by the same co-authors as listed in this chapter.

Highlights

- SIMS led ET_a accuracy and DisALEXI led cover crop signal recovery in young pistachio.
- OpenET Ensemble missed the 2025 cover crop sign reversal that EC measured at -36 mm.
- EC peak K_a rose from 0.57 (year 5) to 0.95 (year 7), 22% below mature-orchard K_c of 1.19.
- CC K_a exceeded NC by +0.10 to +0.26 in April; reversed to -0.17 by late September.
- No OpenET model served both volumetric accounting and cover crop signal detection.
- EC winter CC over NC contrast grew across three winters: +15, +30, +62 mm (2023-24, 2024-25, 2025-26).

Abstract

Remote-sensing evapotranspiration products are widely deployed to map water use in agriculture, but their performance in young orchard systems and their ability to detect actual evapotranspiration (ET_a) differences from orchard floor management practices remain poorly documented. Young orchards have incomplete canopy closure and, relative to mature orchards, a larger contribution of orchard floor evaporation and cover crop transpiration to total ET_a, which can challenge remote sensing model performance. The objectives of this study were to (i) quantify daily-to-seasonal ET_a and actual crop coefficients (K_a) in young pistachio orchards under cover crop (CC) and no cover (NC) management, (ii) evaluate the six OpenET models and the OpenET Ensemble against the eddy covariance (EC) reference for absolute ET_a accuracy, and (iii) determine whether OpenET products can detect the ET_a difference between CC and NC management systems. We deployed paired EC flux towers in adjacent young pistachio orchards in California's Sacramento Valley, one with a winter cover crop planted in alleyways and one left bare, across three growing seasons and three winter seasons spanning years 5 to 7 post-planting (April 2023 to April 2026). Against this reference we evaluated the OpenET models at daily to seasonal scales, testing CC signal recovery with a seasonal difference-of-differences statistic and tracking within-season redistribution through twice-monthly K_a. SIMS achieved the lowest monthly RMSE (19 mm month^{-1}), outperforming the Ensemble (23 mm month^{-1}). DisALEXI recovered the CC signal in 6 of 6 seasons (mean absolute deviation 20 mm), while SIMS recovered 5 of 6. Reported as the CC-minus-NC difference, K_a was higher under CC by +0.10 to +0.26 in April, then turned negative as NC exceeded CC from June onward, reaching its largest magnitude (-0.17) in late September of year 7. EC peak K_a rose from 0.57 (year 5 NC) to 0.95 (year 7 NC). No single OpenET product was best in both use cases. These findings indicate that

OpenET model selection should depend on management objectives, as products optimized for accurate water accounting may not be best suited for detecting treatment-scale management effects.

Keywords: Pistachio; OpenET; Remote sensing evapotranspiration; Eddy covariance; Cover crops; Actual evapotranspiration; Agricultural water management; Irrigation management

1. Introduction

Remote-sensing evapotranspiration (RSET) models are now the de facto basis for groundwater accounting under California's Sustainable Groundwater Management Act (SGMA), but their performance in young perennial orchards and their ability to resolve treatment-scale actual evapotranspiration (ET_a) contrasts between adjacent management systems remain poorly documented. Passed in 2014, SGMA requires groundwater sustainability agencies (GSAs) to bring overdrafted basins into balance, and many GSAs now rely on remotely sensed ET_a estimates to monitor consumptive water use against grower water allocations. The accuracy of RSET models is directly consequential for grower livelihoods and for the success of regional groundwater sustainability plans.

California produces over 400 commodities and supplies roughly three-quarters of the vegetables and one-third of the fruits and nuts in the United States (CDFA, 2025). The management of scarce water supplies, increasingly constrained by extreme droughts (Diffenbaugh et al., 2015), is therefore a problem of national significance. California is one of the world's largest pistachio producers, with bearing acreage growing from 25,440 acres in 1979 to over 450,000 acres in 2023 (Tootelian, 2023). Despite this rapid expansion, published pistachio water use and crop coefficient values come almost exclusively from mature orchards (Table 1). California reference values span a wide range. Goldhamer et al. (1985) reported a peak crop coefficient (K_c) of 1.19 and seasonal crop evapotranspiration (ET_c) of 1019 mm in 10-year-old San Joaquin Valley pistachios using soil water balance with deep percolation correction. Subsequent soil water balance studies in older trees expanded this range, with peak K_c of 1.17 to 1.33 in 11- to 14-year-old non-saline orchards in Kings County (Sanden et al., 2004) and a peak

K_c of 1.36 with seasonal ET_c of 1024 mm under full irrigation in a 12-year-old Madera County regulated deficit irrigation (RDI) experiment (Iniesta et al., 2008).

More recent California measurements based on remote sensing and eddy covariance have produced lower mid-season values. Bellvert et al. (2018) used airborne thermal imagery and a reflectance-based dual K_c approach in a 14-year-old orchard and reported a peak actual crop coefficient (K_a) of 1.10 with seasonal ET_a of 1022 mm. Jin et al. (2018) applied METRIC with Landsat 8 to mature commercial orchards in Kings County and estimated seasonal ET_a of 1064 mm in the non-saline control for the March to October period of 2016, with reductions of 16 to 32 percent in adjacent saline-sodic orchards. Marino et al. (2019) measured ET_a by EC and surface renewal in 31- to 32-year-old saline-sodic orchards in the same Kings County area, and related field measurements at Hanford and Coalinga reported mid-season K_c of 0.91 to 1.05 (Zaccaria, 2023). Outside California, peak K_c of 0.80 in August and seasonal ET_c of 707 to 841 mm have been reported for 35- to 40-year-old pistachios in Turkey (Kanber et al., 1993), and SEBAL- or SEBS-based studies in Iran have been applied at orchards of varying age and with various reference ET formulations (Kermani and Salehi, 2006; Rahimzadegan and Janani, 2019; Firoozi et al., 2023). Studies of young orchard water use are rare, and none of those above addressed orchards with cover crops. Young orchards are a distinct and underexamined case for remote sensing ET. Before canopy closure, a large fraction of total ET_a originates from the orchard floor rather than the tree canopy, so soil evaporation and, where present, cover crop (CC) transpiration contribute disproportionately to field-scale ET_a (Drechsler et al., 2022). Because most satellite RSET models infer ET_a from canopy greenness and temperature, this elevated and spatially heterogeneous floor signal can degrade model performance precisely in establishment-phase orchards. Applying coefficients derived from mature orchards to young, developing trees

generally overestimates water use, misdirects irrigation scheduling, and confounds SGMA compliance accounting. Whether and at what tree age young orchard K_a converges on the mature orchard peak range of 1.10 to 1.36 (spanning reported K_c and K_a) has not been documented in California pistachio at the field scale.

Table 1. Selected published studies of pistachio actual evapotranspiration and peak crop coefficients (K_c or K_a).

Reference	Location	Tree age (years)	Method	Peak K_c or K_a	Seasonal ET_c (mm)
Goldhamer et al. (1985)	Kings County, San Joaquin Valley, USA	10	Soil water balance (neutron probe to 10 ft, deep percolation corrected); Class A pan for reference	1.19 (K_c); 0.96 (K_p)	1019
Kanber et al. (1993)	Birecik, Southeast Anatolia, Turkey	35 to 40	Soil water balance (gravimetric, to 1.8 m); Class A pan ET_o	0.80 (August)	707 to 841 (varies with irrigation interval)
Sanden et al. (2004)	Westside San Joaquin Valley, USA	11 to 14	Soil water balance (neutron probe to 1.7 to 2.0 m); Penman-Monteith ET_o	1.17 (2001); 1.33 (2002)	1221 to 1612 (non-saline 0.5 dS/m)
Kermani and Salehi (2006)	Rafsanjan, Kerman Province, Iran	4 to 10	Drainage lysimeter (9 by 6 by 3.4 m); separate lawn lysimeter for ET_o	0.24 (six-year mean peak)	229 to 562 (Mar to Oct, by tree age)
Iniesta et al. (2008)	Madera County, San Joaquin Valley, USA	12	Soil water balance (neutron probe to 3 m); microsprinkler RDI experiment	1.36 (FI, August)	1024 (FI); 784 (RDI), 18 May to 11 Nov
Bellvert et al. (2018)	San Joaquin Valley, USA	14	Reflectance-based dual K_c with airborne thermal CWSI; validated against EC and SR	1.10 (K_a)	1022 (DOY 61 to 335)
Jin et al. (2018)	Kings County, San Joaquin Valley, USA	~25 to 28	METRIC (Landsat 8); validated against EC and SR	Not reported	725 to 1064 (by salinity, 15 Mar to 15 Oct)
Rahimzadegan and Janani (2019)	Semnan Province, Iran	1 to 15 (mixed)	SEBAL (Landsat 8); validated against FAO-56 dual K_c reference	NA (FAO K_c used as input)	NA (sparse-date imagery)
Marino et al. (2019)[1]	Kings County, San Joaquin Valley, USA	31 to 32	Eddy covariance and surface renewal (residual energy balance)	Not reported	465 to 867 (by salinity, 25 May to 10 Oct)
Firoozi et al. (2023)[2]	Yazd Province, Iran	Not reported	SEBAL and SEBS (Landsat 8); compared against 12 empirical ET_o methods	1.1 to 1.2 (H-S, B-C, Trabert)	Not reported

[1] Marino et al. (2019) measurement window of 25 May to 10 October captures the peak ET_a period but excludes early spring leaf-out and late fall senescence; comparable full-season ET_a would be approximately 20 to 30 percent higher.
[2] Firoozi et al. (2023) reported additional peak K_c values of 1.4 to 1.9 from radiation-based ET_o formulations, which the authors flagged as outside the realistic pistachio K_c range; only the H-S, B-C, and Trabert values are shown.

Winter cover crops are a sustainable conservation practice with documented soil-health benefits (Lu et al., 2000; Blanco-Canqui et al., 2015) but uncertain orchard-scale water costs (DeVincentis et al., 2022; Borum et al., 2024). Cover crops sown in the dormant season can improve soil health (Unger and Vigil, 1998; Blanco-Canqui et al., 2015; Carlisle, 2016), reduce erosion (Joyce et al., 2002), and improve infiltration (Blanco-Canqui and Ruis, 2020), but their transpiration also represents an additional ET_a term that growers must account for under SGMA compliance. Adoption remains low across semi-arid California, where cover crops are planted on less than 5 percent of cropland (Soil Health Institute, 2019). Grower hesitation in orchard systems stems primarily from uncertainty about the water cost (Carlisle, 2016): the concern that winter cover crops, even when sown to coincide with the dormant season, can transpire enough to deplete soil moisture needed by the tree crop in the following growing season, particularly when winter precipitation is insufficient to recharge the soil profile (DeVincentis et al., 2022). Borum et al. (2024) summarized expert consensus that the water impact of cover crops in orchards is best understood not as a single seasonal mean difference but as a structural shift in the timing of ET across the calendar year. The implications differ for winter soil moisture recharge and for spring soil water availability at bud break. Whether satellite RSET models can resolve this temporal structure at the field scale has not been tested. Accurate field-scale ET_a accounting for SGMA compliance and quantitative CC water use estimates for grower decisions converge on a single requirement: RSET models must produce accurate field-scale ET_a in young orchards and resolve the ET_a contrast between CC and NC orchards. Neither has been systematically evaluated.

Field-based ET_a measurement methods such as EC, weighing lysimeters, and Bowen ratio systems are accurate but expensive, require specialized expertise, and cover only the flux footprint of a single tower (Jensen and Allen, 2016). Satellite-based RSET models offer spatially distributed ET_a at field to regional scales and have become widely used by growers, water managers, and regulators (Allen et al., 2005; Fisher et al., 2017). The OpenET platform delivers daily, 30 m resolution ET_a for the western United States by combining six RSET models within Google Earth Engine (Melton et al., 2022). The six models span four architectural families with different physical assumptions about how latent heat flux relates to surface temperature, vegetation indices, and the partitioning of available energy between soil and canopy. The families include a two-source surface energy balance (DisALEXI), three residual single-source surface energy balance models (SSEBop, eeMETRIC, geeSEBAL), a reflectance-based dual-K_c model (SIMS), and a Priestley-Taylor formulation (PT-JPL); details and primary references are summarized in Table 2. The platform also reports an Ensemble mean that has been shown to improve reliability over any single model in continental-scale validation (Volk et al., 2024).

Table 2. Satellite remote-sensing-based evapotranspiration models included in OpenET (adapted from opendata.org/methodologies).

Model	Approach	Primary references
DisALEXI	Two-Source Energy Balance coupled with the continental-scale ALEXI model; Landsat thermal data disaggregates ALEXI's 4 km flux fields to 30 m.	(Anderson et al., 2007, 2018)
eeMETRIC	Google Earth Engine implementation of METRIC; surface energy balance with internalized calibration using reference ET and hot/cold anchor pixels; three-source LST partitioning (sunlit soil, shaded soil, canopy) for tree crops.	(Allen et al., 2007, 2011; Irmak et al., 2011)
geeSEBAL	Google Earth Engine implementation of SEBAL; surface energy-balance residual using hot/cold anchor pixels (CIMEC) to calibrate the near-surface temperature gradient; instantaneous ET scaled to daily via the evaporative fraction.	(Bastiaanssen et al., 1998; Laipelt et al., 2021)
PT-JPL	Priestley-Taylor formulation using net radiation, vegetation indices (NDVI, SAVI), and atmospheric demand (VPD, RH); in OpenET the PT reference is replaced by ASCE grass reference ET.	(Fisher et al., 2008)
SIMS	Reflectance-based dual-crop coefficient (FAO-56) approach; basal crop coefficient derived from NDVI and fractional canopy cover; includes a gridded soil-water-balance module for soil evaporation.	(Melton et al., 2012; Pereira et al., 2020)

SSEBop	Simplified surface energy balance based on satellite psychrometry; applies a correction coefficient to maximum ET using LST, a surface psychrometric constant, and a wet-bulb boundary condition; updated in OpenET using the Forcing and Normalizing Operation technique.	(Senay et al., 2013; Senay, 2018; Senay et al., 2023)
Ensemble	Arithmetic mean of the remaining models at each pixel after up to two outlier values are removed using the median absolute deviation method.	(Leys et al., 2013; Volk et al., 2024)

Volk et al. (2024) validated OpenET across 152 EC sites and reported strong agreement at cropland sites, where the Ensemble achieved a mean absolute error of 15.8 mm month^{-1} (17 percent of mean observed ET) and an R^2 of 0.90, with higher accuracy and stronger multi-model convergence than at shrubland or forested sites. OpenET has not been directly validated in young pistachio orchards, nor has its ability to distinguish ET_a between CC and NC orchard systems been evaluated. These two evaluation use cases depend on different aspects of model performance. Absolute ET_a accuracy depends on overall energy balance closure, while differential accuracy depends on the consistency of bias across treatments. Critically, the model architecture that minimizes error in absolute ET_a may not be the same architecture that best resolves contrasts between adjacent orchard treatments. This dual-use-case structure has not been tested in any operational RSET validation, and the result has direct consequences for SGMA monitoring practice. Resolving it requires a paired-treatment design at the field scale: both treatments share tree age, canopy development, and atmospheric forcing, and differ only in orchard floor management. This study presents the first such design for young California pistachios.

The objectives of this study were to (i) quantify daily-to-seasonal ET_a and K_a in young pistachio orchards under CC and NC management, (ii) evaluate the six OpenET models and the OpenET Ensemble against the EC reference for absolute ET_a accuracy, and (iii) determine whether OpenET models can detect the ET_a difference between CC and NC management systems. We address these objectives through three hypotheses.

First, we estimate daily and seasonal ET_a and K_a in adjacent young pistachio orchards under CC and NC management using EC flux measurements. We expect mean K_a during the winter season in CC to exceed the NC value by at least 10 percent, reflecting additional transpiration from the cover crop canopy in winter and early spring.

Second, we evaluate the six OpenET models and the OpenET Ensemble against EC ET_a across both orchards and across winter and pistachio growing seasons, and, consistent with continental-scale validation, we expect the OpenET Ensemble monthly RMSE to be at least 10 percent lower than the median RMSE of the six individual models.

Third, we hypothesize that no single OpenET model will both minimize absolute ET_a RMSE and best detect the CC treatment signal, since these two evaluation use cases depend on different aspects of model performance.

Section 2 describes the paired EC flux measurements and the OpenET retrieval methods used to test these hypotheses. Section 3 reports validation results across daily, monthly, and seasonal timescales and across both treatments. Section 4 develops the implications for SGMA monitoring practice and for the broader application of RSET models in young orchard systems. These findings bear directly on OpenET deployment in California's young perennial orchard acreage.

2. Materials and Methods

2.1 Study site and treatments

The study was conducted in a 61-hectare commercial pistachio orchard (*Pistacia vera*, cv. Golden Hills) located in the southern Sacramento Valley (38.619° N, 121.725° W), approximately 10 km north of Davis, California (Figure 1). The trees were transplanted in December 2018 (the 2023, 2024, and 2025 growing seasons therefore represent fifth-, sixth-, and

seventh-leaf trees, respectively) with north to south oriented rows spaced 5.8 m apart and trees spaced 5.2 m within rows, resulting in 332 trees ha^{-1}. Irrigation was supplied through a double drip system, with each tree receiving water from four emitters discharging 2.0 L h^{-1} each. Irrigation scheduling and amounts were determined by the orchard manager using a crop coefficient-based approach and applied water totals differed slightly between treatments in each pistachio growing season. No irrigation was applied during either cover crop season (November to March of 2023 to 2024 and 2024 to 2025), reflecting the grower's practice of relying on winter precipitation through cover crop establishment, growth, and termination. During the pistachio growing season, applied water in CC and NC was 136 mm for both treatments in 2023, 330 and 321 mm in 2024 and 580 and 505 mm in 2025, respectively. The lower 2023 total reflects the smaller canopy and water demand of fifth leaf trees. The 2025 difference of 75 mm, with CC receiving approximately 15 percent more applied water than NC, is treated as a potential confounder for ET_a interpretation in Section 4. Key pistachio growth stages include bloom (April), shell split (July to August), harvest (October), and senescence (November).



Figure 1. Study site in the Sacramento Valley, California (inset, blue circle). Two halves of a 61-ha young pistachio orchard (Pistacia vera cv. Golden Hills) are managed under contrasting treatments: a winter cover crop treatment (CC, blue outline) and a no cover crop control (NC, orange outline). Each treatment is instrumented with an open-path eddy covariance flux tower (black triangles). Three nested spatial domains are shown for each treatment: the orchard boundary (NC: orange; CC: blue), the spatial extraction window used to sample OpenET 30-m pixels for comparison against EC ET_a (NC Field: green; CC Field: pink), and a rectangular bounding box around the maximum extent of the multi-year flux footprint (NC: yellow; CC: purple).

The region has a warm summer Mediterranean climate. Over the 30-year record (1996 to 2025), mean daily minimum temperature in December averaged 3.5 °C and mean daily maximum temperature in July averaged 33.0 °C. Mean annual precipitation totals 435 mm and falls predominantly between November and March, with less than 30 mm of cumulative rainfall from June through October, consistent with the reference evapotranspiration (ET_o) climatology summarized in Table 3.

Table 3. Thirty-year mean grass reference evapotranspiration (ETo) and precipitation in Davis, CA (1996-2025).

	Jan	Feb	Mar	Apr	May	Jun	Jul	Aug	Sep	Oct	Nov	Dec
Precipitation (mm)	86.0	87.6	56.7	26.4	14.4	2.5	0.1	1.4	5.4	19.6	45.1	89.9
ET_o (mm)	34.8	54.5	95.1	139	185	208	212	187	146	105	50.5	32.0

The orchard was divided into two halves approximately 30 ha each. The eastern half was assigned to the cover crop (CC) treatment and the western half to the no cover crop (NC) treatment. Winter cover crops were seeded in the CC treatment in November of each year and terminated in late March or April, while the NC alleyways were not seeded with a winter cover crop. Resident winter vegetation that emerged was managed by periodic mowing when needed to maintain bare ground for the study comparison. In-field visits in spring 2023 showed that resident vegetation in the NC treatment was higher than expected, so we worked with the orchard manager to remove it in 2024 and 2025. The CC mixture comprised species drawn from legumes, grains, and brassicas, with composition and seeding rates varying between seasons based on grower preference and seed availability (Table 4). Seeding dates, termination dates, and subsequent mowing schedules are summarized in Table 4. Herbicide was applied in under-tree strips throughout the study and was not directed at alleyway cover crop vegetation in either treatment.

Table 4. Cover crop mixture composition, seeding rate and date, termination date, and subsequent mowing schedule for the 2023-24 and 2024-25 seasons.

Season	Composition	Seeding rate (kg ha^{-1})	Seeding date	Termination date	Post-termination mowings
2023-24	23% grain, 25% bell bean, 25% peas, 15% vetch, 2% brassica	50.4	8 Nov 2023	30 Apr 2024	21 Jun 2024; 16 Oct 2024
2024-25	30% bell bean, 30% peas, 20% vetch, 20% rye	44.8	15 Nov 2024	28 Mar 2025	18 May 2025; 24 Jul 2025
2025-26	30% bell bean, 30% peas, 20% vetch, 20% oats	45.0	24 Oct 2025	3 Mar 2026	7 May 2026

Soils at the study site are mapped by the National Cooperative Soil Survey (NCSS; https://websoilsurvey.nrcs.usda.gov/app/) as silty clay loams. The NC treatment area consists of 98 percent Rincon silty clay loam and 2 percent Capay silty clay by surface area, while the CC treatment footprint consists of 47 percent Sycamore silty clay loam, 34 percent Yolo silt loam, and 19 percent Rincon silty clay loam. Soil particle size distribution was quantified every 0.3 m down to a depth of 3.0 m from samples collected during neutron probe access tube installation in 2023, analyzed with a laser diffraction particle size analyzer (Partica LA-960, HORIBA, Ltd., Kyoto, Japan). One sample per depth was collected from the interrow position at each of four access tube installation locations (n = 4 per depth per treatment). Laboratory-measured particle size distributions at the four sampled CC locations classified all samples as silt loam, which differs from the NRCS surface mosaic and likely reflects the limited spatial coverage of the four sampling locations within a heterogeneous treatment footprint. Laboratory values reported in Table 5 represent the treatment mean at each depth.

Table 5. Laboratory-measured soil particle size distribution (clay, silt, and sand, percent by mass) and USDA textural class by depth for the cover crop (CC) and no cover crop (NC) treatments. Values represent the mean of four samples collected at the interrow position from four access tube installation locations per treatment (n = 4 per depth per treatment).

Depth (m)	CC				NC			
	Clay (%)	Silt (%)	Sand (%)	Soil Type	Clay (%)	Silt (%)	Sand (%)	Soil Type
0.3	17.2	67.8	15.0	Silt Loam	28.0	65.8	6.2	Silty Clay Loam
0.6	19.9	68.8	11.2	Silt Loam	30.9	63.7	5.4	Silty Clay Loam
0.9	20.2	67.8	12.0	Silt Loam	31.3	64.6	4.2	Silty Clay Loam
1.2	19.0	60.3	20.7	Silt Loam	29.5	64.3	6.1	Silty Clay Loam
1.5	21.5	62.5	16.0	Silt Loam	25.5	66.0	8.5	Silt Loam
1.8	22.1	67.8	10.2	Silt Loam	25.1	61.7	13.2	Silt Loam
2.1	22.6	67.3	10.0	Silt Loam	25.7	60.1	14.2	Silt Loam
2.4	22.8	62.3	15.0	Silt Loam	24.2	61.3	14.6	Silt Loam
2.7	21.2	57.6	21.3	Silt Loam	24.8	57.4	17.9	Silt Loam
3.0	21.1	56.5	22.4	Silt Loam	18.7	55.2	26.0	Silt Loam

2.2 Eddy covariance measurements and ET_a derivation

Field-scale energy flux densities were measured at each tower to estimate ET_a. Because the study was conducted in a commercial orchard subject to occasional water stress, ET_a rather than the standard non-stressed FAO crop coefficient (ET_c) was the relevant quantity for SGMA accounting and for OpenET validation.

Latent heat flux (λE) was computed from the surface energy balance equation:

$$\lambda E = R_n - G - H, \quad (1)$$

where R_n is net radiation (W m^{-2}), G is ground heat flux density (W m^{-2}), H is sensible heat flux density (W m^{-2}), λ is the latent heat of vaporization of water MJ kg^{-1}, and λE has units of W m^{-2}. Heat storage in the canopy and surface boundary layer and the energy consumed by photosynthesis each accounted for less than a few percent of the energy balance and were assumed negligible (Jensen and Allen, 2016).

Two EC flux towers were installed, one in each treatment, oriented into the prevailing south-to-north wind direction. Each tower was equipped with an IRGASON integrated CO_2 and H_2O open-path gas analyzer and three-dimensional sonic anemometer (Campbell Scientific, Logan, UT, USA) at a height of 6.5 m, sampling water vapor concentration and three-dimensional wind velocity at 20 Hz. Net radiation was measured with an SN-500 four-component net radiometer (Apogee Instruments, Logan, UT, USA). Soil heat flux was calculated using data from five sensor sets installed along a diagonal transect between adjacent rows to account for radiation variability across the interrow; each set included an HFT-3 heat flux plate (Radiation Energy Balance Systems, Bellevue, WA, USA) buried at 8 cm, Type E thermocouples at 2 cm and 6 cm, and a Hydraprobe volumetric soil moisture sensor at 5 cm

(Stevens Water Monitoring Systems, Portland, OR, USA). Supporting meteorological measurements included air temperature, relative humidity, and precipitation.

Latent heat flux was determined from the 20 Hz data using an established set of EC processing corrections, including spike detection (Goring and Nikora, 2002), two-dimensional coordinate rotation (Kaimal and Finnigan, 1994), and corrections for buoyancy effects (Webb et al., 1980), sensor displacement, and frequency response attenuation (Massman, 2000). A complete description of data collection and processing is given in Alfieri et al. (2019) and Bambach et al. (2022). Flux post-processing was performed using the REddyProc package (Wutzler et al., 2018) in R version 4.3.3 (R Foundation for Statistical Computing, Vienna, Austria). Half-hourly fluxes were quality controlled and screened for periods with undesirable wind direction and insufficient turbulence. The friction velocity (u^*) threshold was determined using the moving point method of Papale et al. (2006) and was [VALUE] m s^{-1} for the CC tower and [VALUE] m s^{-1} for the NC tower. Gaps in λE were filled in two passes. The first pass used the marginal distribution sampling, look up table, and mean diurnal course methods of REddyProc (Reichstein et al., 2005; Wutzler et al., 2018), based on relationships between fluxes and meteorological drivers (incoming shortwave radiation, air temperature, and vapor pressure deficit) within a moving window. Remaining gaps in the half hourly λE record after the REddyProc pass were filled using the same marginal distribution sampling (MDS) algorithm of Reichstein et al. (2005), implemented in the Flux Gap Filling Tool (Peddinti, 2026), which fills missing values from the empirical distribution of fluxes observed under similar incoming shortwave radiation, vapor pressure deficit, and air temperature within a moving window. Daily ET_a was computed by summing the gap filled and closure corrected half hourly λE over each 24

h period and converting from energy to depth units using the latent heat of vaporization at the daily mean air temperature.

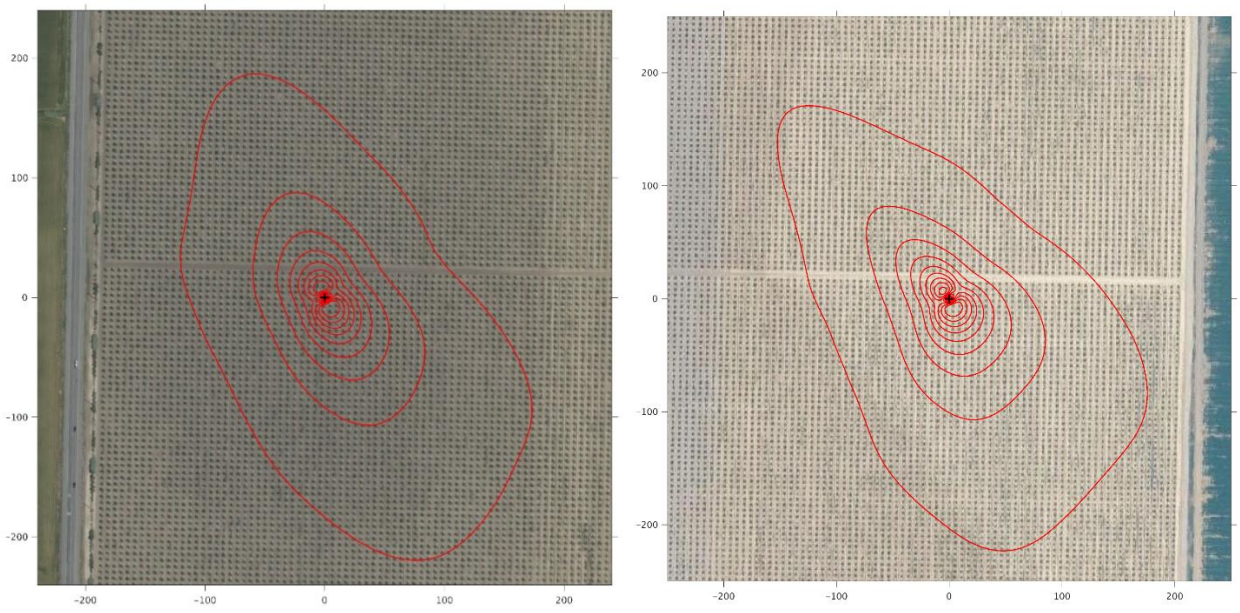


Figure 2. Flux footprints for the eddy covariance (EC) flux tower installed in the cover crop (CC) and no cover crop (NC) orchards.

Flux footprints were modeled using the two-dimensional flux footprint predictor of Kljun et al. (2015), implemented in the online Flux Footprint Prediction (FFP) calculator (https://ffp2d.kljun.net/). Footprint dimensions were calculated for each 30-minute averaging period from the measured friction velocity, mean wind speed, wind direction, atmospheric stability (Obukhov length), boundary-layer height, and the standard deviation of lateral wind velocity, with a measurement height of 6.5 m and aerodynamic roughness lengths of 0.03 m for the NC tower and 0.21 m for the CC tower, with corresponding zero-plane displacement heights of 0.34 m and 2.35 m, respectively.

Energy balance closure was assessed at each tower using the slope of the linear regression of available energy ($R_n - G$) against the turbulent flux sum ($H + \lambda E$) over the full 30-

minute record (Wilson et al., 2002). The regression slope is reported as the energy balance closure ratio (EBR). As is characteristic of EC sites, closure was incomplete at both towers, commonly attributed to low-frequency flux loss, a mismatch between the turbulent flux source area and the footprint sampled by the soil heat flux sensors, and unmeasured energy storage between the measurement height and the surface (Wilson et al., 2002). To preserve the measured Bowen ratio ($\beta = H / \lambda E$) while forcing closure, half-hourly λE was corrected using the Bowen-ratio-preserving residual approach, in which H and λE are scaled proportionally so that $H + \lambda E = R_n - G$. Daily ET_a was then computed from the corrected half-hourly λE following Equation 1. Reference evapotranspiration (ET_o) and meteorological data were obtained from CIMIS Davis Station (#006).

2.3 OpenET

OpenET is a web-based platform (www.openetdata.org) that integrates six widely used RSET models with the Google Earth Engine framework to deliver daily ET_a data at 30 m spatial resolution for the contiguous United States (Melton et al., 2022). OpenET also reports an Ensemble mean computed after excluding up to two outlier model values per pixel using the median absolute deviation method (Leys et al., 2013; Volk et al., 2024). The platform uses Landsat as its primary data source and supplements with data from GOES, Sentinel-2, Suomi NPP, MODIS, and ECOSTRESS to improve temporal coverage. Because satellite overpasses occur every 8 to 16 days, depending on cloud cover, OpenET interpolates daily ET_a between clear-sky overpass dates by computing the fraction of reference ET ($ET_of = ET_a / ET_o$ at the time of overpass) at each overpass, linearly interpolating ET_of between dates, and multiplying by daily ET_o. For this study, OpenET was queried with CIMIS specified as the ET_o source (see retrieval details below). The platform also supports gridMET (Abatzoglou, 2013) as an alternative.

For this study, daily ET_a, ET_o, and the normalized difference vegetation index (NDVI) values were retrieved for each of the six OpenET models and the OpenET Ensemble for the 1 January 2023 to 31 December 2025 period via the OpenET API on 24 April 2026, using OpenET platform version v2.1 (Melton et al., 2022). Retrieval requests specified daily temporal interval, CIMIS as the ET_o source, output units of mm, and the spatial reducer set to the unweighted mean of all 30 m pixels intersecting each retrieval polygon. Because the OpenET multi polygon raster timeseries endpoint limits each request to a single calendar year, the retrieval script was executed once per year for 2023, 2024, and 2025 with identical parameters except for the date range. Brief descriptions of each model are given in Table 2; readers are referred to the listed primary references and the OpenET documentation (www.openetdata.org/methodologies) for full model details.

Each treatment was retrieved at two spatial scales using two distinct polygons. The Field subset polygons (CC: 10.1 ha; NC: 10.6 ha) were defined within the southern half of each orchard's interior and provide the spatial average over that area, matching the operational use case for water budget accounting in Chen et al. (in preparation). The Flux subset polygons (CC: 15.5 ha; NC: 14.0 ha) were defined as rectangular bounding boxes around the maximum extent of the multi-year EC flux footprint (Figure 2) and provide a more direct comparison to the EC measurement, although the sub pixel mismatch between the EC footprint and the 30 m Landsat grid means that even Flux subset comparisons retain some spatial aggregation error. Reporting both subsets serves as an extraction area sensitivity test.

2.4 Reference evapotranspiration and actual crop coefficient calculation

Actual crop coefficients (K_a) were computed as the ratio of measured or modeled ET_a to grass reference evapotranspiration (ET_o), the inverse of the FAO 56 single crop coefficient

equation (Allen et al., 1998). K_a is distinguished from the FAO 56 crop coefficient K_c, which is the tabulated coefficient defined for a well maintained and stress-free crop under standard reference conditions. K_a values reported here may be reduced below K_c by water stress, partial canopy development in young trees, or interrow management practices. K_a was computed as the ratio of ET_a to grass reference evapotranspiration (ET_o):

$$K_a = \frac{ET_a}{ET_o} \tag{2}$$

where ET_a is the actual evapotranspiration (mm day^{-1}), ET_o is the grass reference evapotranspiration (mm day^{-1}), and K_a is dimensionless. Both eddy covariance derived ET (ECET) and the OpenET model ET estimates (RSET) were used in the numerator to produce two parallel K_a time series that could be compared directly.

Daily K_a was computed by applying Equation 2 to each daily ET_a-ET_o pair, producing time series at the same temporal resolution as the EC and RSET measurements. The ECET K_a time series serves as the reference for K_a analysis, while the RSET K_a time series are reported alongside for direct comparison.

Daily reference evapotranspiration (ET_o) values for the Bullseye orchard were obtained from the California Irrigation Management Information System (CIMIS) Davis Station (ID 006; 38.536° N, 121.776° W), located approximately 10 km from the field site. Hourly ET_o was computed using the CIMIS Penman equation, a modified Penman formulation (Pruitt and Doorenbos, 1977) parameterized with a wind function and station specific cloud factors developed at the University of California, Davis. Hourly values were summed over 24-hour periods to produce daily totals, which were further aggregated to monthly sums.

During an initial pass of the dataset, we identified a cluster of 47 days in the 2025-26 winter for which Davis ET_o fell below 1.0 mm/d, with 27 days below 0.3 mm/d. Because such low daily values appeared inconsistent with our preliminary cover crop and no cover crop ET_a estimates from the eddy covariance towers, these values were provisionally flagged and replaced with a seasonal climatology. Subsequent diagnostic work attributed the inconsistency to extended CC tower outages and an associated gap fill artifact in the ET_a record, not to any defect in the ET_o series.

Two independent lines of evidence supported retaining the original CIMIS Davis values. First, the nearby CIMIS Woodland station (#125), located approximately 10 km to the west, reported very low daily ET_o on the same days: 26 of the 27 days with Davis ET_o below 0.3 mm/d also had Woodland ET_o below 0.3 mm/d, and the two stations agree closely across the full record ($r = 0.99$, mean Davis minus Woodland = 0.14 mm/d). Second, 14 of these 27 days had measurable precipitation at the Davis CIMIS rain gauge, with 7 days exceeding 5 mm and a maximum of 35.3 mm on 2025-11-13. The low daily ET_o values are therefore consistent with the persistent cloud cover, low net radiation, and near saturation atmospheric conditions characteristic of Sacramento Valley winter storm days, and we treat them as physically plausible measurements rather than instrument artifacts.

The decision to retain the unadjusted CIMIS Davis series has two implications for the analysis that deserve to be stated explicitly. First, the seasonal cumulative ET_o for the 2025-2026 winter (254.5 mm) is lower than the corresponding totals for the 2023-2024 (261.1 mm) and 2024-2025 (287.1 mm) winters, reflecting the unusual frequency of low ET_o storm days in this season rather than a method change. Second, daily crop coefficient (K_a) values computed as ET_a ET_o are sensitive to the very low ET_o denominator on storm days. We therefore restrict daily K_a

calculations to days with Davis ET_o > 0.5 mm/d (and compute season level K_a summaries from cumulative ET_a and cumulative ET_o to avoid the small denominator problem).

In addition to daily K_a values, cumulative K_a was computed at the bi-monthly scale by integrating ET_a and ET_o separately over each of 15 bi-monthly windows spanning April 1 to November 15, then taking the ratio of the cumulative ET_a to the cumulative ET_o. This bi-monthly aggregation reduces day-to-day noise while preserving the within-season phenological structure. The November 1 to 15 window falls outside the pistachio growing season as defined here but is reported to maintain comparability with the K_c curve of Goldhamer et al. (1985), which was reported on a similar bi-monthly basis.

2.5 Statistical evaluation

Seven statistical metrics were used to evaluate the agreement between modeled (RSET) and observed (EC) ET_a: the slope of a linear regression forced through the origin (Slope), mean bias error (MBE), percent bias (PBIAS), mean absolute error (MAE), root mean square error (RMSE), coefficient of determination (r^2), and the Nash-Sutcliffe efficiency (NSE). Formulas are given in Table 6. Observed ET_a was used as the independent variable and the modeled ET_a as the dependent variable. This convention follows Volk et al. (2024) and treats the EC observation as the reference input and the model output as the response, so that slope < 1 indicates model underestimation and slope > 1 indicates overestimation. The same metrics were applied to the six OpenET models and the OpenET Ensemble allowing direct comparison of all products on a common footing.

Table 6. Statistical metrics used to compare remote sensing-based evapotranspiration (RSET) model output with eddy covariance ET_a. P_i are predicted ET values, $\bar{O}$ is the mean of observed values across the n paired observations, and O_i are observed ET values.

Name	Equation
Linear regression slope forced through the origin (Slope)	$y = bx + a;\ a = 0$

Mean bias error (MBE)	$MBE = \frac{1}{n}\sum_{i=1}^{n}(P_i - O_i)$
Mean absolute error (MAE)	$MAE = \frac{1}{n}\sum_{i=1}^{n}\lvert P_i - O_i\rvert$
Root mean square error (RMSE)	$RMSE = \sqrt{\sum_{i=1}^{n}\frac{(P_i - O_i)^2}{n}}$
Coefficient of determination (r^2)	$r^2 = \frac{n(\sum xy) - (\sum x)(\sum y)}{\sqrt{[n\sum x^2 - (\sum x)^2][n\sum y^2 - (\sum y)^2]}}$
Nash-Sutcliffe Efficiency (NSE)	$NSE = 1 - \frac{\sum_{i=1}^{n}(O_i - P_i)^2}{\sum_{i=1}^{n}(O_i - \bar{O})^2}$
Percent Bias (PBIAS)	$PBIAS = \left[\frac{\sum_{i=1}^{n}(S_i - O_i)}{\sum_{i=1}^{n}O_i}\right] \times 100$

Model performance was evaluated against two criteria, each corresponding to a distinct application. The first criterion is absolute ET_a accuracy, which serves volumetric water accounting. The second criterion is differential accuracy, or cover crop signal detection, which serves the treatment signal detection use case.

Treatment signal detection accuracy was quantified at the seasonal scale across six seasons spanning the study period: three pistachio growing seasons (April to October of 2023, 2024, and 2025) and three intervening cover crop winter seasons (November to March of 2023-24, 2024-25, and 2025-26). For each season, the EC-observed CC-minus-NC ET_a difference (in mm, summed over the season) was computed as the ground-truth signal. The same difference was computed for each of the six OpenET models and the OpenET Ensemble. Two signal detection metrics were calculated: (1) sign recovery count, the number of seasons (out of six) in which the modeled CC minus NC ET_a had the same sign as the EC-observed CC minus NC ET_a, and (2) mean absolute difference-of-differences (mean |DOD|), the mean absolute deviation between modeled and EC-observed CC minus NC ET_a across the six seasons. Sign recovery count is sensitive to whether a model correctly identifies the direction of the cover crop effect

(CC ET_a greater than NC, or NC ET_a greater than CC); mean |DOD| is sensitive to how accurately the model captures the size of the effect.

Daily ET_a was retained for analysis only when both EC and RSET values were available on the same day after the gap-filling and footprint-exclusion procedures described in Section 2.2. Seasonal CC minus NC contrasts and difference-of-differences values are reported as integer-rounded mm and are computed from the rounded CC and NC seasonal totals.

3. Results

3.1 Climate and atmospheric demand context

The 2023 to 2025 study period spanned a transition from above-normal to below-normal precipitation in the Sacramento Valley while atmospheric demand and mean air temperature varied within 8 percent and 1.5 °C of their respective long-term mean across all three years. Annual precipitation totaled 626, 488, and 390 mm at the Davis CIMIS station in 2023, 2024, and 2025, respectively, corresponding to 144, 112, and 90 percent of the 1996 to 2025 long-term mean of 435 mm. Pistachio growing season precipitation (April to October) totaled 17, 28, and 48 mm in 2023, 2024, and 2025, against a 30-year mean of 70 mm. Cover crop season precipitation (November to March) totaled 381 mm in 2023 to 2024 and 369 mm in 2024 to 2025, both within 5 percent of the 365 mm long-term mean (Table 7).

Growing season mean T_a was 19.6, 21.1, and 20.3 °C in 2023, 2024, and 2025, respectively, against the long-term mean of 19.9 °C, with 2024 the warmest year (+1.3 °C above the long-term mean) and 2023 and 2025 within 0.4 °C of the long-term mean (Table 7). Cover crop season mean T_a was 11.0 °C in 2023 to 2024 and 10.5 °C in 2024 to 2025, both within 1 °C of the 10.0 °C long-term mean.

Atmospheric demand was likewise consistent across the three growing seasons (Table 7). Growing season ET_o totaled 1122, 1209, and 1143 mm in 2023, 2024, and 2025, varying within an 87 mm range, equivalent to approximately 7 percent of the 30-year growing season ET_o normal of 1182 mm; all three annual totals were within 5 percent of that normal. Cover crop season ET_o totaled 261, 287, and 248 mm in 2023-24, 2024-25, and 2025-26 respectively, 98, 107, and 93 percent of the 267 mm long-term normal. The narrow range of precipitation, temperature, and ET_o across the three study years means that interannual differences in measured ET_a and actual crop coefficients reported below cannot be primarily attributed to differences in atmospheric demand or background climate.

Table 7. Monthly average solar radiation (R_s, W m^{-2}), mean air temperature (T_a, °C), relative humidity (RH_{avg}, %), wind speed at 2 m above the grass surface at the CIMIS Davis station (u, m s^{-1}), minimum relative humidity (RH_{min}, %), vapor pressure (e, kPa), monthly cumulative precipitation (mm), and monthly cumulative grass reference evapotranspiration (ET_o, mm) at the young pistachio orchard near Davis, CA for 2023 to 2025.

	R_s (W m^{-2})	T_a (ºC)	RH_{avg} (%)	u (m s^{-1})	RH_{min} (%)	e (kPa)	Precipitation (mm)	ET_o (mm)
2023								
January	94	9.0	76	3.3	58	0.9	247.4	45.4
February	132	8.0	70	2.7	49	0.7	65.1	54.0
March	166	9.6	74	2.8	55	0.9	187.3	70.8
April	278	14.8	58	2.4	34	1.0	4.4	146.1
May	287	17.0	66	2.3	44	1.3	12.1	158.5
June	319	19.8	60	2.4	38	1.4	0.0	186.9
July	328	23.6	54	2.1	30	1.6	0.1	211.6
August	281	24.0	55	2.3	32	1.6	0.2	186.8
September	229	20.3	60	2.1	36	1.4	0	130.8
October	168	17.7	56	2.1	33	1.2	0	100.9
November	117	12.5	62	2.3	41	0.9	21.9	61.7
December	77	10.0	80	1.8	62	1.0	87.3	30.7
2024								
January	79	10.0	85	2.1	69	1.1	91.7	28.8
February	133	10.5	81	2.3	61	1.0	138.5	49.9
March	184	12.2	72	2.7	51	1.0	40.7	90.1
April	254	15.1	64	2.1	42	1.1	16.4	130.5
May	312	19.4	50	2.9	30	1.1	10.9	204.7
June	326	23.2	49	2.5	29	1.4	0.3	215.6
July	314	25.8	50	2.3	26	1.6	0	219.6
August	281	23.2	52	2.1	29	1.5	0	182.3
September	231	21.9	51	1.9	27	1.3	0	142.3
October	170	19.4	49	2.2	29	1.1	0	114.4
November	104	11.0	68	2.4	47	0.9	101.8	54.0
December	75	9.6	85	2.2	68	1.0	86.9	29.3

2025								
January	114	8.9	66	2.6	46	0.8	11.2	63.4
February	133	10.8	74	2.6	55	1.0	142	52.4
March	185	12.0	72	2.6	49	1.0	26.6	88.1
April	250	15.5	62	2.4	38	1.1	3.6	134.4
May	318	19.6	53	2.8	32	1.2	1.5	201.8
June	341	21.3	56	2.3	34	1.4	0.1	203.3
July	327	21.7	60	2.4	35	1.6	0	204.2
August	288	23.9	54	1.9	30	1.6	0	186.3
September	205	22.8	58	2.2	36	1.6	0	127.6
October	159	17.0	68	2.1	45	1.3	42.4	85.6
November	87	12.6	86	1.8	70	1.3	81.3	33.2
December	49	8.5	93	2.2	84	1.1	80.8	14.3

3.2 Eddy covariance ET_a and the cover crop ET signal

The CC minus NC growing season ET_a contrast declined monotonically across the three pistachio growing seasons, from +36 mm in 2023 to +6 mm in 2024 to -36 mm in 2025. Daily, cumulative, and monthly ET_a for both treatments are shown in Figure 3 and Figure 4 and Table 8.

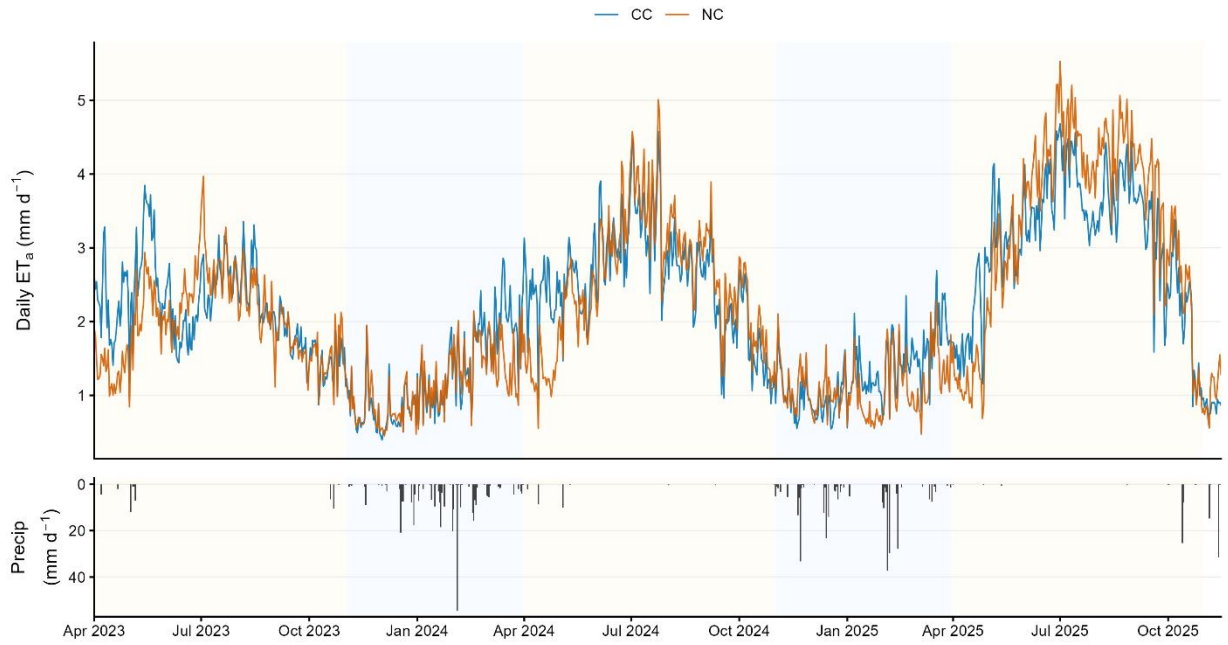


Figure 3. Daily eddy covariance ET_a for the cover crop (CC, blue) and no cover crop (NC, orange) treatments at the orchard from April 2023 through November 2025. Daily precipitation at the orchard tower is shown as the lower

panel. Background bands distinguish growing seasons (light yellow) from cover crop winter seasons (light blue) and delimit the season boundaries used in the analysis.

Across the three growing seasons, the CC minus NC contrast declined monotonically from +36 mm in 2023 to +6 mm in 2024 and then reversed to -36 mm in 2025 (Table 8). In 2023 the positive contrast was concentrated in April and May, the period immediately following cover crop termination. By 2024, the positive April contribution (+31 mm) was offset almost entirely by negative July through October values. In 2025 the reversal was driven by June to October NC ET_a exceeding CC by 8 to 22 mm per month. The +6 mm 2024 contrast is well within the typical 5 to 10 percent uncertainty range for EC seasonal totals at this site type (Bambach et al., 2022) and should not be interpreted as a meaningful treatment difference; the +36 mm 2023 and -36 mm 2025 contrasts are larger than this uncertainty band.

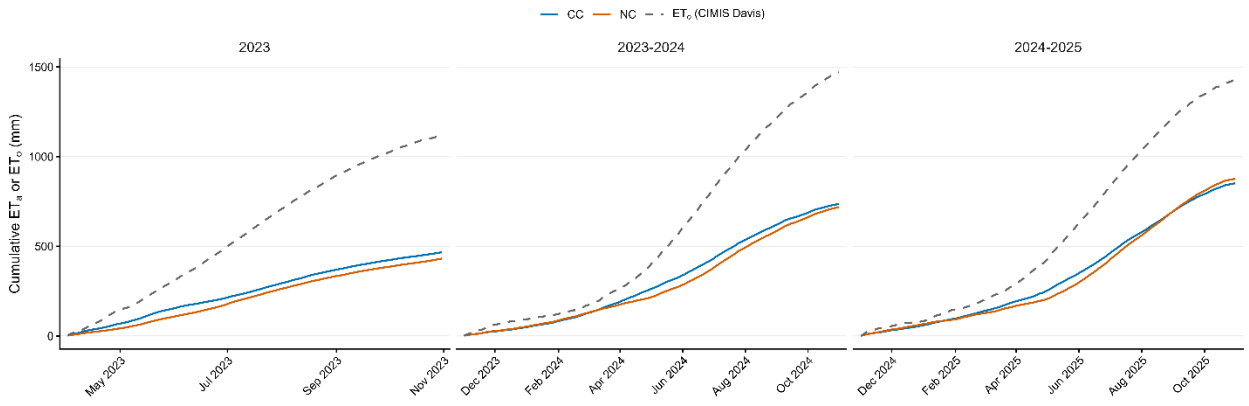


Figure 4. Cumulative eddy covariance ET_a for the cover crop (CC, blue) and no cover crop (NC, orange) treatments, with cumulative grass reference evapotranspiration from the CIMIS Davis station (ET_o, gray dashed) shown as an atmospheric demand benchmark. Panels show cumulative traces from a baseline of zero for three windows: the 2023 pistachio growing season (April to October 2023), the 2023-24 cover crop season followed by the 2024 pistachio growing season (November 2023 to October 2024), and the 2024-25 cover crop season followed by the 2025 pistachio growing season (November 2024 to October 2025).

Winter ET_a was higher in CC than in NC in all three winters, with CC totals exceeding NC by +15 mm in 2023-24, +30 mm in 2024-25, and +62 mm in 2025-26 (Table 8). The contrast was driven primarily by greater March ET_a in CC, consistent with cover crop biomass

accumulation and increased transpiration ahead of termination. In all three winters CC trailed NC through November and December, then exceeded NC by larger margins from late winter onward (Figure 3). March alone contributed +18 mm in 2023-24, +17 mm in 2024-25, and +22 mm in 2025-26, accounting for more than the entire 2023-24 contrast, over half of the 2024-25 contrast, and about a third of the 2025-26 contrast.

The 2025 reversal occurred during the peak summer months. June through October all showed NC ET_a exceeding CC by 7 to 19 mm per month, producing a steady divergence of the cumulative traces from June onward (Figure 4) and a -76 mm negative contrast over those five months that more than offset the +20 mm positive April and May contribution. Pooled across all three growing seasons, mean April-to-October ET_a was 554 mm in CC and 558 mm in NC, a contrast of -4 mm, or less than 1 percent of either treatment total.

Table 8. Monthly actual evapotranspiration (ET_a, mm) measured by eddy covariance for the cover crop (CC) and no cover crop (NC) orchards across the six study seasons spanning 2023 to 2025. Diff = CC minus NC. Monthly values and seasonal totals are computed from daily sums and rounded to the nearest mm. Diff is computed from the rounded seasonal totals. Negative Diff values indicate NC ET_a exceeded CC; positive values indicate CC ET_a exceeded NC.

Month	**CC ET_a (mm)**	**NC ET_a (mm)**	**Diff (mm)**
2023 growing season (April to October)			
April	68	41	+27
May	85	68	+17
June	59	68	-9
July	81	87	-6
August	77	72	+5
September	53	51	+2
October	46	47	-1
Seasonal total	**469**	**433**	**+36**
2023-24 winter (November to March)			
November	25	27	-2
December	23	24	-1
January	36	37	-1
February	47	45	+2
March	63	45	+18
Seasonal Total	**193**	**178**	**+15**

2024 growing season (April to October)			
April	71	40	+31
May	77	69	+8
June	91	93	-2
July	106	115	-9
August	86	93	-7
September	66	74	-8
October	52	59	-7
Seasonal Total	**549**	**543**	**+6**
2024-25 winter (November to March)			
November	32	36	-4
December	31	33	-2
January	37	26	+11
February	43	36	+7
March	58	41	+17
Seasonal Total	**201**	**171**	**+30**
2025 growing season (April to October)			
April	74	40	+34
May	98	91	+7
June	110	125	-15
July	120	138	-18
August	117	139	-22
September	86	100	-14
October	59	67	-8
Seasonal Total	**664**	**700**	**-36**
2025-26 winter (November to March)			
November	55	37	+18
December	55	50	+5
January	40	37	+3
February	51	36	+15
March	64	42	+22
Seasonal Total	**265**	**203**	**+62**

3.3 EC-derived actual crop coefficients in young pistachio

Actual crop coefficients (K_a) were computed at two temporal resolutions: daily K_a as the ratio of daily ET_a to daily ET_o (Figure 5), and bi-monthly K_a as the ratio of summed ET_a to summed ET_o over each of 15 bi-monthly windows (April 1-15 through November 1-15), with the maximum of the 15 window values reported as the year's peak.

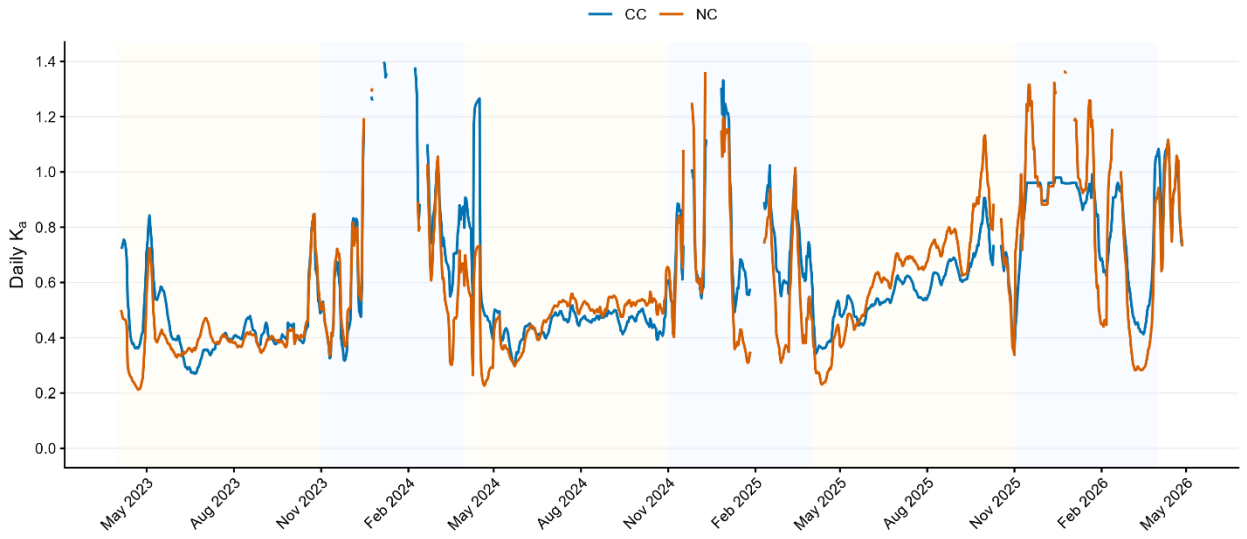


Figure 5. Daily actual crop coefficient (K_a) for the cover crop (CC, blue) and no cover crop (NC, orange) treatments at the orchard from April 2023 through October 2025, computed as the ratio of daily eddy covariance ET_a to CIMIS Davis ET_o. A 7-day moving-average smoother is applied. Background bands distinguish growing seasons (light yellow) from cover crop winter seasons (light blue).

EC peak K_a remained between 0.53 and 0.63 in years 5 and 6 in both treatments, well below Goldhamer et al.'s (1985) mature-orchard peak K_c of 1.19 and Bellvert et al.'s (2018) mature-orchard peak K_a of 1.10. By year 7, peak K_a jumped to 0.95 in NC at the October 1-15 window. CC peak K_a reached 0.82 at October 1-15. The year 7 NC value was 20 percent below the Goldhamer benchmark and 14 percent below the Bellvert benchmark; the year 7 CC value was 31 percent below the Goldhamer benchmark (Table 9, Figure 6).

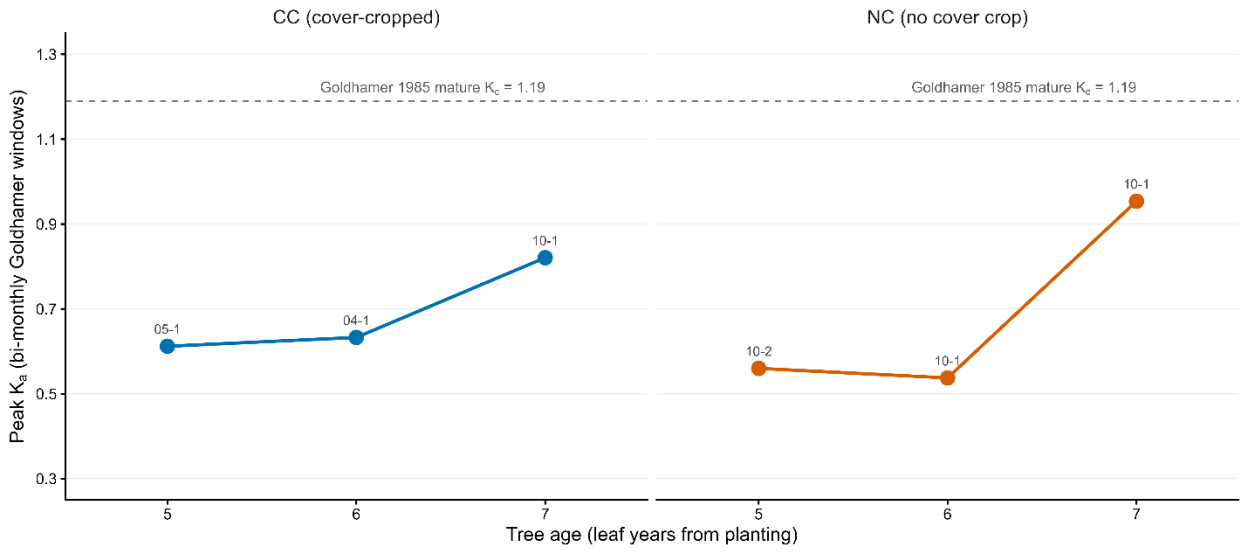


Figure 6. Peak EC-derived actual crop coefficient (K_a) by tree age for the cover crop (CC, blue, left panel) and no cover crop (NC, orange, right panel) treatments. Peak K_a is the maximum across 15 bi-monthly windows from April 1-15 through November 1-15, where each window K_a is computed as the ratio of summed daily ET_a to summed daily ET_o. The peak bi-monthly window for each year is annotated above each point. The dashed gray line indicates the mature-orchard peak K_c of 1.19 from Goldhamer et al. (1985).

The peak K_a window shifted from early in the growing season to mid-fall across the three years. In years 5 and 6 the CC peak occurred early in the growing season (May 1-15 in 2023, April 1-15 in 2024), while the NC peak occurred in October. By year 7 both treatments peaked in the October 1-15 window.

Table 9. Peak actual crop coefficient (K_a) by year, treatment, and ET_a source, Field subset. Peak is the maximum across 15 bi-monthly windows from April 1-15 through November 1-15, where each window-K_a is computed as the ratio of summed daily ET_a to summed daily ET_o (CIMIS Davis Station 006). EC values are the ground reference.

Source	2023 CC	2023 NC	2024 CC	2024 NC	2025 CC	2025 NC
EC	0.62	0.57	0.63	0.53	0.96	0.95
DisALEXI	0.74	0.57	0.58	0.41	0.61	0.69
Ensemble	0.54	0.38	0.50	0.35	0.64	0.74
PT-JPL	0.96	0.91	0.90	0.77	0.97	0.97
SIMS	0.59	0.52	0.67	0.41	0.72	0.65
SSEBop	0.48	0.31	0.49	0.19	0.61	0.80
eeMETRIC	0.36	0.38	0.32	0.40	0.59	0.82
geeSEBAL	0.41	0.30	0.37	0.31	0.68	0.61

3.4 OpenET model performance against EC: validation metrics and bias structure

This section evaluates the first of the two evaluation criteria defined in Section 2.5, absolute ET_a accuracy, by comparing each OpenET product against EC ET_a at daily and monthly resolution across both orchards. Daily 1:1 scatter for the seven OpenET products is shown in Figure 8, and daily MBE by model and season is shown in Figure 9. Monthly 1:1 scatter (Figure S1), monthly EC ET_a with CIMIS Davis ET_o overlay (Figure S4, and inter-model spread of monthly ET_a across the six OpenET products; Figure S2) are presented in the supplementary materials. The corresponding pooled validation metrics are reported in Table 10 and Figure 7 (daily) and Table 11 (monthly); the seasonal decomposition and extraction subset sensitivity are reported in Table S2 and Table S4, respectively. Signal-detection accuracy, the second use case, is taken up separately in Section 3.5 and requires CC and NC paired contrasts.

Table 10. Daily ET_a validation metrics, Field subset, 2023 to 2025 (n = 945 except eeMETRIC, n = 930-945; and geeSEBAL, n = 913-928). Models ordered by daily RMSE within the CC treatment.

Model	Treatment	Slope	MBE (mm/d)	MAE (mm/d)	RMSE (mm/d)	r^2	NSE	% Bias
SIMS	CC	0.94	-0.15	0.59	0.75	0.61	+0.35	-7.0
Ensemble	CC	0.78	-0.51	0.77	0.89	0.55	+0.10	-23.8
DisALEXI	CC	0.80	-0.45	0.76	0.92	0.52	+0.04	-20.9
SSEBop	CC	0.71	-0.67	0.81	0.95	0.56	-0.03	-31.0
PT-JPL	CC	1.12	+0.35	0.83	1.15	0.38	-0.51	+16.1
eeMETRIC	CC	0.46	-1.22	1.23	1.38	0.52	-1.17	-56.2
geeSEBAL	CC	0.51	-1.09	1.24	1.45	0.28	-1.36	-50.6
SIMS	NC	0.81	-0.41	0.63	0.77	0.69	+0.52	-20.2
DisALEXI	NC	0.75	-0.49	0.75	0.90	0.58	+0.36	-24.2
Ensemble	NC	0.67	-0.70	0.81	0.96	0.66	+0.27	-34.4
PT-JPL	NC	0.55	-0.96	0.97	1.15	0.67	-0.06	-47.1
eeMETRIC	NC	1.10	+0.46	0.91	1.24	0.34	-0.24	+22.4
SSEBop	NC	0.47	-1.15	1.18	1.39	0.53	-0.54	-56.5
geeSEBAL	NC	0.45	-1.14	1.27	1.50	0.33	-0.76	-56.1

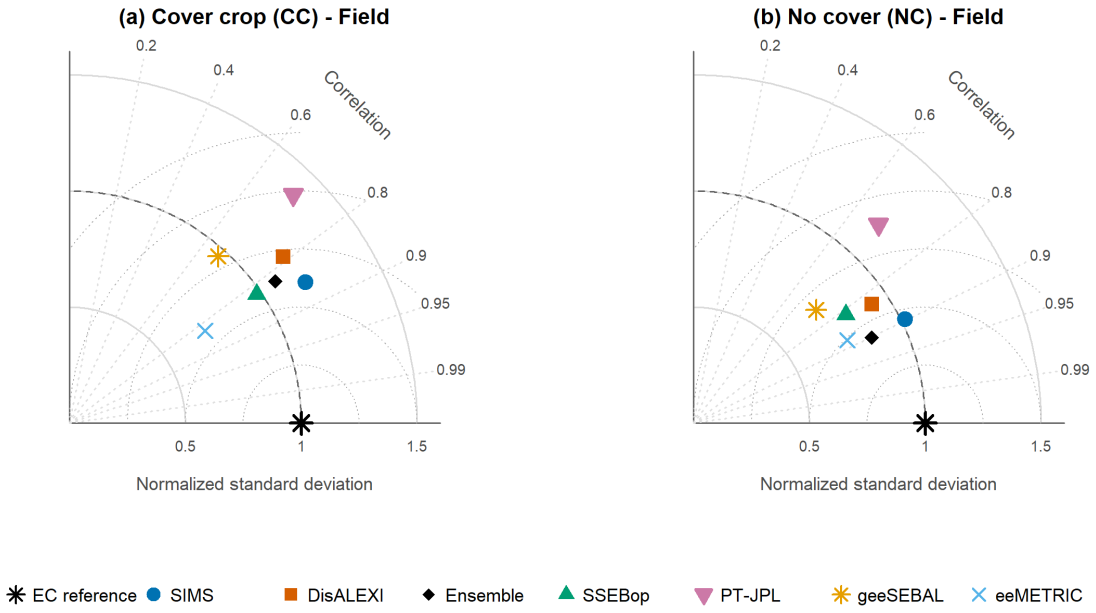


Figure 7 Taylor diagram comparing seven OpenET products against eddy covariance monthly ET_a for the (a) cover crop (CC) and (b) no cover (NC) Field subsets, 2023–2025. Radial distance is the model standard deviation normalized by the EC reference standard deviation; azimuthal position is the Pearson correlation with EC; dotted arcs centered on the reference are normalized centered-RMS difference. Products closest to the reference point have both realistic variance and high correlation.

In CC, daily RMSE ranged from 0.75 mm per day (SIMS) to 1.45 mm per day (geeSEBAL), a factor-of-two spread across the seven products (Table 10). The same ranking persisted at monthly resolution, where SIMS achieved 19.0 mm per month against the Ensemble's 22.7 mm per month (Table 11). NC results followed similar ordering, with SIMS again leading at 0.77 mm per day and 20.5 mm per month.

PT-JPL was the only product to overestimate daily ET_a in both treatments (+16.1 percent CC, -47.1 percent NC). The remaining six products underestimated EC in both treatments, with the largest negative biases from SSEBop (-31.0 percent CC, -56.5 percent NC), eeMETRIC (-56.2 percent CC, with eeMETRIC overestimating NC at +22.4 percent), and geeSEBAL (-50.6 percent CC, -56.1 percent NC). SIMS, the absolute accuracy leader, was also the smallest bias

product in CC (-7 percent) and a moderately negative bias product in NC (-20 percent), confirming that its low RMSE reflects a small mean error rather than canceling deviations. The Ensemble inherited the negative tendency of its majority negative constituents (-24 percent CC, -34 percent NC).

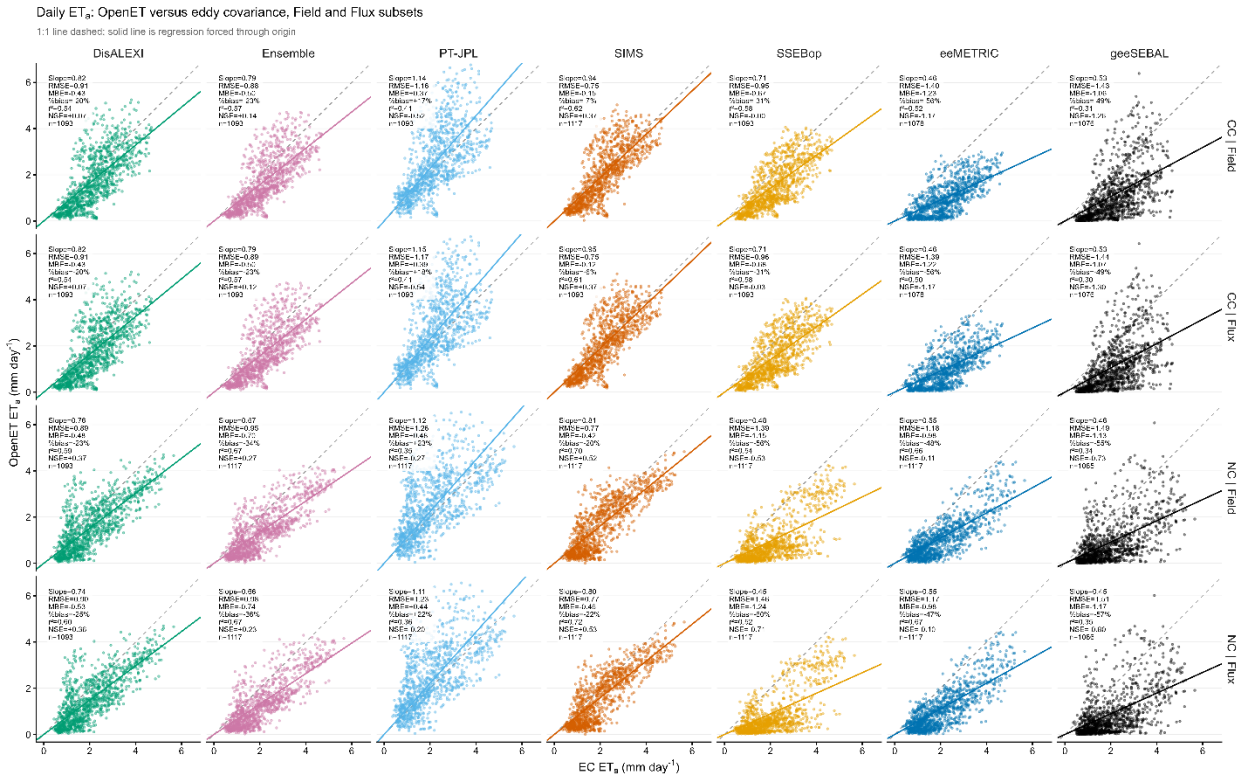


Figure 8. Daily ET_a from the seven OpenET products versus eddy covariance ET_a across the cover crop (CC) and no cover crop (NC) treatments and the Field and Flux subsets at the orchard. Each panel shows the seven products in columns (DisALEXI, OpenET Ensemble, PT-JPL, SIMS, SSEBop, eeMETRIC, geeSEBAL) and the four region-by-subset combinations in rows (CC Field, CC Flux, NC Field, NC Flux). The dashed line is the 1:1 reference; the solid line is the regression forced through the origin. Per-panel statistics report the slope of the regression forced through the origin (Slope), root mean square error (RMSE), mean bias error (MBE), percent bias, the coefficient of determination (r^2), Nash-Sutcliffe efficiency (NSE), and the number of paired daily observations.

A separation between absolute accuracy and temporal-pattern fidelity emerged in the NC monthly statistics. The Ensemble's higher monthly r^2 in NC (0.86 versus 0.69 for SIMS) indicates higher temporal correlation with EC; the lower SIMS RMSE reflects its smaller mean bias rather than higher temporal correlation. The corresponding signal-detection performance, which depends on differential bias rather than absolute accuracy, is reported in Section 3.5.

Having established absolute ET_a accuracy for each product, we next examine how well they recover the CC versus NC treatment difference at the seasonal scale.

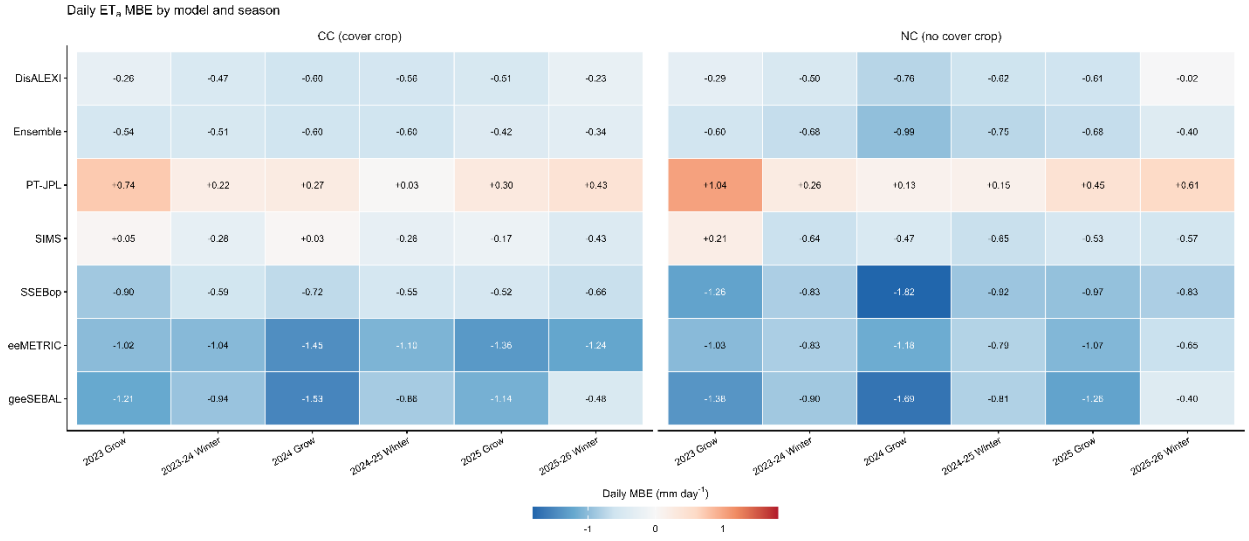


Figure 9. Daily ET_a mean bias error (MBE) by OpenET product and season, presented as a heatmap with seasons on the x-axis (2023 Grow, 2023-24 Winter, 2024 Grow, 2024-25 Winter, 2025 Grow) and products on the y-axis. The two panels show the cover cropped (CC) and no cover crop (NC) treatments. Cell color encodes daily MBE in mm per day, with red indicating positive bias (model overestimates EC ET_a) and blue indicating negative bias.

Seasonal decomposition of daily RMSE (Table S2) is discussed in Section 3.4. CC daily RMSE in the 2024 and 2025 grow seasons exceeded the 2023-24 and 2024-25 winter values for every product, with the ratio reaching three-fold in some cases (geeSEBAL CC: 1.80 mm per day in 2024 Grow versus 0.89 in 2024-25 Winter). Daily RMSE roughly tracked the magnitude of mean observed ET_a in each season, scaling from 0.43 to 2.04 mm per day across the model-by-season combinations. The 2024 Grow season produced the worst daily RMSE for every model in NC and for five of seven models in CC, coinciding with the highest atmospheric demand of the three growing seasons (ET_o of 1209 mm) and with the canopy-development transition documented in Section 3.3. The seasonal MBE structure shown in Figure 9 follows the same pattern: PT-JPL's positive bias was largest in the 2023 Grow season, while the negative biases of geeSEBAL, eeMETRIC, and SSEBop deepened in the 2024 Grow season. The cover

crop winter seasons, by contrast, produced narrower model spread, with daily RMSE bunched between 0.43 and 1.22 mm per day in 2023-24 Winter and between 0.43 and 1.14 in 2024-25 Winter.

Table 11. Monthly ETa validation metrics, Field subset (n = 32 monthly values per model and treatment). Models ordered by monthly RMSE within the CC treatment.

Model	Treatment	Slope	MBE (mm/mo)	MAE (mm/mo)	RMSE (mm/mo)	r^2	NSE	% Bias
SIMS	CC	0.95	-5.0	15.9	19.0	0.71	+0.44	-7.6
Ensemble	CC	0.79	-15.5	20.8	22.7	0.69	+0.21	-23.8
DisALEXI	CC	0.82	-13.6	21.1	23.9	0.63	+0.13	-20.8
SSEBop	CC	0.72	-20.2	21.9	25.3	0.70	+0.02	-30.9
PT-JPL	CC	1.14	+10.6	21.5	29.6	0.48	-0.34	+16.1
eeMETRIC	CC	0.51	-33.6	35.9	39.5	0.45	-1.38	-51.4
geeSEBAL	CC	0.47	-36.7	36.8	39.5	0.68	-1.35	-55.8
SIMS	NC	0.82	-12.8	17.6	20.5	0.78	+0.57	-20.8
DisALEXI	NC	0.76	-15.0	21.1	23.8	0.68	+0.44	-24.1
Ensemble	NC	0.68	-21.5	23.3	25.8	0.79	+0.33	-34.8
PT-JPL	NC	0.56	-29.4	29.4	32.7	0.80	-0.08	-47.5
eeMETRIC	NC	1.12	+13.4	23.8	33.0	0.40	-0.10	+21.6
SSEBop	NC	0.48	-35.2	35.2	39.7	0.66	-0.59	-56.8
geeSEBAL	NC	0.45	-35.7	36.9	41.8	0.53	-0.76	-57.7

Inter-model spread, illustrated in Table 11, was larger than the spread between treatments for any single model. The seven products differed in monthly RMSE by 21 mm per month (range 17.2 to 38.4) within the CC orchard alone, while the same product evaluated in CC versus NC differed in monthly RMSE by less than 7 mm per month for all products except SSEBop. The structural choice of model architecture therefore mattered more for absolute accuracy than the choice of orchard treatment. Of the seven products, six had negative MBE. The Ensemble's bias of -0.51 mm per day in CC and -0.70 mm per day in NC tracked this majority sign (Table 10).

The choice of pixel-extraction subset had a small effect on validation metrics relative to the choice of model (Table S4). Daily RMSE differed between the field subset and flux footprint extractions by 1 to 5 percent for all model-treatment combinations except SSEBop in NC (+5.8

percent for the flux subset) and PT-JPL in NC (-4.8 percent), neither of which changed the overall model ranking. The 1 to 5 percent extraction sensitivity is small relative to the factor-of-two range across models and supports the use of the field subset polygon extraction as the primary basis for the validation metrics reported throughout this study, with the flux footprint subset retained as a sensitivity test. Field subset and flux footprint MBE values agreed to within 0.1 mm per day for all products in CC and within 0.13 mm per day for all products in NC.

Taken together, SIMS led or tied for lead in nine of ten season-by-treatment combinations in daily RMSE. The OpenET Ensemble was the second-best product at the monthly scale and outperformed the median individual model by 18 percent (CC) and 21 percent (NC), comfortably exceeding the 10 percent threshold specified in H2, but was systematically less accurate than SIMS in absolute ET_a terms. Whether the same ranking holds for the second use case, recovery of the CC versus NC ET_a contrast, is the subject of Section 3.5.

3.5 Detection of the cover crop ET signal by RSET

This section evaluates the second of the two evaluation criteria defined in Section 2.5, recovery of the CC minus NC ET_a contrast at the seasonal scale. Section 3.4 identified SIMS as the absolute ET_a accuracy leader. The question for this section is whether SIMS also leads on signal detection, or whether a different model architecture is required to recover the small differential between adjacent treatments. The seasonal CC minus NC ET_a, by model and by season, is shown in Figure 10 and reported in Table 12; the difference-of-differences (DOD) between modeled and EC-observed CC minus NC contrasts is reported in Table 13; and a model-by-model summary of sign-recovery count and mean absolute DOD is reported in Table 14.

Table 12. Seasonal CC minus NC ETa by model and season (mm/season, Field subset). CC and NC seasonal totals are rounded to the nearest mm; differences are computed by subtracting the rounded CC and NC totals.

Model/source	2023 Grow	2023-24 Winter	2024 Grow	2024-25 Winter	2025 Grow	2025-26 Winter

Eddy covariance (EC)	+36	+15	+6	+30	-36	+62
DisALEXI	+41	+19	+40	+38	-13	+32
Ensemble	+47	+42	+89	+52	+19	+42
PT-JPL	-29	+9	+35	+11	-68	-10
SIMS	+2	+72	+114	+89	+40	+80
SSEBop	+115	+52	+241	+86	+58	+67
eeMETRIC	+38	-20	-51	-17	-98	-30
geeSEBAL	+78	+8	+41	+26	-8	+26

Eddy covariance measured six seasonal CC minus NC contrasts (Table 12) spanning -36 mm to +36 mm, with the 2025 Grow sign reversal as the most discriminating test because it requires a model to detect a sign change against the conventional cover crop ET cost prior assumption. A model that simply assumes CC always evaporates more than NC, or that responds to interrow vegetation but not to differential canopy maturation, will get five of six seasons in the right direction but miss 2025 Grow.

Table 13. Difference of differences: (RSET CC-NC) minus (EC CC-NC) (mm/season, Field subset, integer-rounded). Mean |DOD| is the average absolute deviation across all six seasons.

Model	**2023 Grow**	**2023-24 Winter**	**2024 Grow**	**2024-25 Winter**	**2025 Grow**	**Mean |DOD|**	**2025-26 Winter**	**Mean |DOD|**
DisALEXI	-1	+6	+30	+16	+35	-30	-30	20
Ensemble	+5	+19	+64	+25	+58	-20	-20	32
PT-JPL	-65	-5	+27	-14	-27	-72	-72	35
SIMS	-37	+21	+87	+36	+74	+18	+18	46
SSEBop	+86	+49	+240	+72	+97	+5	+5	92
eeMETRIC	-2	-31	-50	-52	-36	-92	-92	44
geeSEBAL	+37	+1	+34	-6	+45	-36	-36	27

Two of the seven OpenET products recovered the EC sign in all six seasons (Table 13). DisALEXI led the panel with a mean |DOD| of 20 mm. geeSEBAL was second at 27 mm, despite producing the largest absolute ET_a underestimate of any product (-58 percent in NC). Three products achieved 5 of 6 sign matches: Ensemble (mean |DOD| 32 mm), SSEBop (mean |DOD| 92 mm), and SIMS (mean |DOD| 46 mm, inverting the 2023 Grow sign). PT-JPL

achieved 4 of 6 (mean |DOD| 35 mm). SSEBop's elevated |DOD| reflects a single 240 mm catastrophic miss in 2024 Grow. eeMETRIC achieved only 2 of 6.

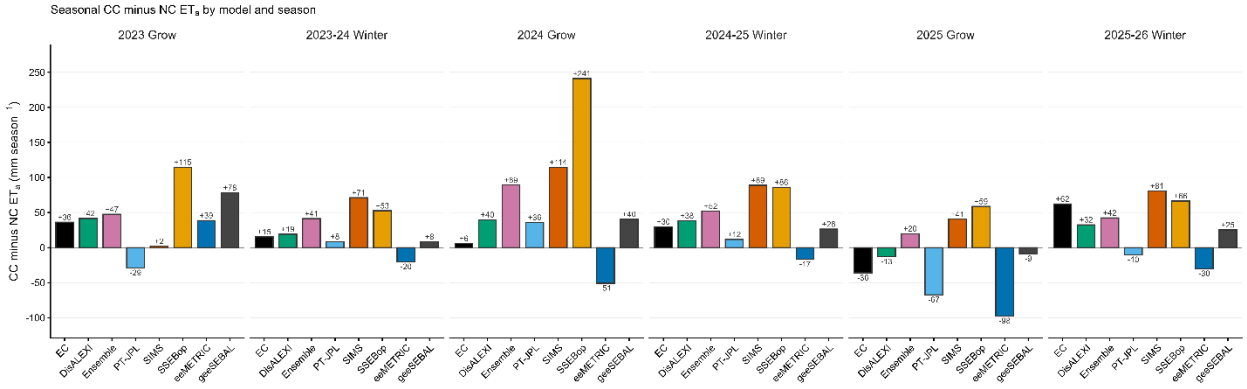


Figure 10. Seasonal CC minus NC ET_a contrast across the six study seasons (2023 Grow, 2023-24 Winter, 2024 Grow, 2024-25 Winter, 2025 Grow, 2025-26 Winter), Field subset, monthly source. EC (black) is the ground reference. Bar height is the seasonal sum of CC ET_a minus NC ET_a in mm. Positive values indicate CC exceeds NC; negative values indicate NC exceeds CC. Numerical labels are integer-rounded seasonal contrasts.

The geeSEBAL result demonstrates a divergence between absolute and signal-detection accuracy: the largest absolute bias coexists with 6 of 6 sign recovery. geeSEBAL's daily MBE was -1.13 mm per day in CC and -1.25 mm per day in NC, the two largest negative biases in Table 10, but its proportional underestimate was nearly identical between the two treatments (-52.7 percent and -58.6 percent). When the seasonal sums are differenced, the bulk of the negative bias cancels and the modeled CC minus NC contrast preserves the sign of the EC observation in all six seasons. DisALEXI's smaller bias in both treatments (-20.9 percent CC, -25.9 percent NC) follows the same proportional pattern and produces the lowest mean |DOD|.

The opposite pattern explains why SIMS, the absolute-accuracy leader, ranks sixth of seven on signal detection. SIMS daily MBE was -0.15 mm per day in CC and -0.41 mm per day in NC, a roughly five-fold treatment-dependent difference in bias even though both biases are small in absolute terms. The CC minus NC differential therefore inherits a 0.26 mm per day

systematic offset that propagates to the seasonal totals and inverts the small-magnitude EC signals in 2023 Grow and 2025 Grow.

The OpenET Ensemble's failure to recover the 2025 sign reversal carries policy implications discussed in Section 4.5. The Ensemble reported a CC minus NC contrast of +19 mm in 2025 Grow against the EC value of -36 mm, a 75 mm DOD that places the modeled and observed differentials on opposite sides of zero (Table 12). The Ensemble's mean |DOD| of 32 mm placed it fourth in the seven-product panel (Table 13). The accuracy advantage that gave the Ensemble second place on monthly RMSE did not carry over to the seasonal differential.

Table 14. Signal-detection summary by model. Models ranked by sign-recovery count (descending) and then by mean |DOD| (ascending). The 'Largest single-season |DOD|' column gives the season with each model's largest absolute deviation from the EC contrast.

Model	Sign matches (out of 6)	Mean |DOD| (mm)	Largest single-season |DOD|	Failure mode
DisALEXI	6/6	20	2024 Grow (30)	Mild miss; preserves sign in all six seasons. Best overall.
geeSEBAL	6/6	27	2023 Grow (42)	Sign correct in all six seasons; magnitude understated in 2025 Grow (-8 vs EC -36) and 2025-26 Winter (+26 vs EC +62).
Ensemble	5/6	32	2024 Grow (64)	Misses the 2025 Grow sign reversal (+19 vs EC -36); pulled high in 2024 Grow by SSEBop's extreme overestimate.
SIMS	5/6	46	2024 Grow (87)	Inverts sign in 2025 Grow; large positive bias in 2024 and 2025 Grow.
SSEBop	5/6	92	2024 Grow (240)	Extreme overestimation in 2024 Grow (+241 vs EC +6); the largest |DOD| of any model in any season.
PT-JPL	4/6	35	2025-26 Winter (72)	Inverts sign in 2023 Grow and 2025-26 Winter; misses the 2025-26 cover crop signal entirely.
eeMETRIC	2/6	44	2025-26 Winter (92)	Inverts sign in four of six seasons; the 2025 Grow reversal is registered but the 2025-26 Winter signal is missed.

The signal-detection results support hypothesis H3, that no single OpenET product would achieve both the lowest absolute ET_a RMSE and the highest signal-detection accuracy. SIMS led on absolute accuracy; two products achieved 6 of 6 sign matches; DisALEXI led on signal

detection by the secondary metric of mean |DOD| (20 mm vs geeSEBAL's 27 mm). The absolute-accuracy leader (SIMS) and the signal-detection leader (DisALEXI) are different products. Of the seven products, only DisALEXI ranked top three on both use cases (top three on monthly RMSE in both treatments, first on mean |DOD|). geeSEBAL was second on signal detection but worst on absolute accuracy. The OpenET Ensemble was second on absolute accuracy but fourth on signal detection. The implication is that the choice of OpenET product depends on which evaluation criterion is most relevant for the intended application.

The six season EC contrasts shown in Table 12 also reveal that the cover crop ET signal is small at the seasonal-mean scale and reverses sign between 2024 and 2025 Grow. The pooled three-year mean April-to-October CC minus NC contrast in EC is -4 mm, less than 1 percent of seasonal ET_a; the within-season temporal structure underlying this near-zero mean is reported in Section 3.6.

3.6 Bi-monthly Ka structure: temporal redistribution between treatments

The peak K_a analysis and the seasonal CC minus NC contrasts collapse the within-season K_a profile to single-number summaries. The bi-monthly K_a structure, computed as the ratio of summed ET_a to summed ET_o within each of the 15 windows from April 1-15 through November 1-15, preserves the within-season phenological profile and reveals a temporal redistribution between treatments that is invisible in the seasonal-mean K_a. Per-year EC bi-monthly K_a by window and treatment is reported in Table 15, three-year-mean bi-monthly profiles for the top OpenET performers identified in Sections 3.4 and 3.5 are reported in Table 16, the full per-year panel for all eight sources is reported in Table S3, and the visual bi-monthly profile is shown Figure S3.

Table 15. EC bi-monthly K_a by window, year, and treatment (Field subset, 2023 to 2025). Each window-K_a is the ratio of summed daily ET_a to summed daily ET_o (CIMIS Davis Station 006). Tree ages are 5, 6, and 7 in 2023, 2024, and 2025 respectively.

Window	2023 CC	2024 CC	2025 CC	Mean CC	2023 NC	2024 NC	2025 NC	Mean NC
Apr 1-15	0.56	0.63	0.35	0.51	0.34	0.37	0.26	0.32
Apr 16-30	0.39	0.48	0.51	0.46	0.23	0.26	0.31	0.27
May 1-15	0.61	0.41	0.50	0.49	0.46	0.36	0.42	0.41
May 16-31	0.48	0.35	0.46	0.43	0.39	0.32	0.48	0.39
Jun 1-15	0.34	0.44	0.52	0.44	0.34	0.42	0.61	0.46
Jun 16-30	0.30	0.41	0.55	0.42	0.38	0.44	0.62	0.48
Jul 1-15	0.36	0.48	0.61	0.48	0.42	0.52	0.68	0.54
Jul 16-31	0.40	0.47	0.55	0.48	0.40	0.53	0.66	0.53
Aug 1-15	0.42	0.46	0.60	0.49	0.38	0.52	0.72	0.54
Aug 16-31	0.39	0.48	0.65	0.51	0.38	0.51	0.75	0.55
Sep 1-15	0.41	0.47	0.75	0.54	0.40	0.53	0.87	0.59
Sep 16-30	0.41	0.46	0.74	0.54	0.39	0.53	0.91	0.61
Oct 1-15	0.39	0.48	0.82	0.54	0.39	0.54	0.95	0.63
Oct 16-31	0.53	0.41	0.63	0.51	0.56	0.49	0.64	0.56
Nov 1-15	0.40	0.49	0.53	0.47	0.41	0.52	0.65	0.52

The CC profile shape inverted across the three study years (Table 15). In year 5, CC K_a peaked in May 1-15 (0.62) and declined to a Jun 16-30 minimum of 0.30, with a modest October recovery. In year 6, the peak shifted earlier to Apr 1-15 (0.63), then declined through the season. In year 7, the profile reversed: CC K_a was lowest in April (0.37) and rose to a peak of 0.82 at Oct 1-15. The peak window shifted from cover crop-dominated early spring in years 5 and 6 to canopy-dominated late fall in year 7 and into the early cover crop season, an inversion that the three-year-mean column buries by averaging early-year and late-year peaks at 0.42 to 0.64 across April through November.

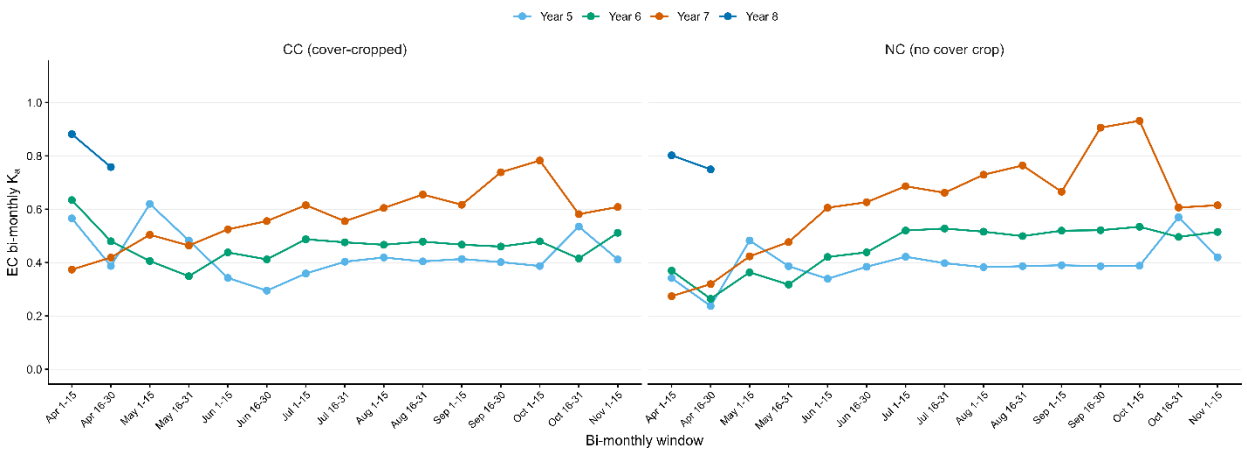


Figure 11. Bi-monthly EC-derived actual crop coefficient (K_a) for the cover cropped (CC, left panel) and no cover crop (NC, right panel) treatments across three leaf years: year 5 (2023, blue), year 6 (2024, green), and year 7 (2025, orange). Each window K_a is computed as the ratio of summed daily ET_a to summed daily ET_o over each of 15 bi-monthly windows from April 1-15 through November 1-15.

The NC profile retained a similar shape across all three years but expanded sharply in magnitude in year 7 (Table 15). NC peaked in October in all three years, with year-5 and year-6 maximum at 0.53 to 0.57 and the year-7 maximum at 0.95, exceeding earlier years by 63 to 75 percent. The year-7 expansion was not confined to the late-season peak window: Jun 16-30 NC K_a rose from 0.38 to 0.44 in years 5 and 6 to 0.63 in year 7.

The CC minus NC bi-monthly differential evolved across years in a structured way. April differentials were positive in all three years, ranging from +0.10 to +0.26. The largest single April differential was Apr 1-15 in year 6 (+0.26). The Apr 1-15 differential ranged across years (+0.23 in year 5, +0.26 in year 6, +0.10 in year 7), reflecting year-7 late-spring cover crop persistence under high atmospheric demand. From Jun 1-15 onward, the differential turned negative in all three years, but the magnitudes evolved sharply: late-season differentials (Sep through Oct 1-15) were near zero in year 5 (0 to +0.02), small negative in year 6 (-0.05 to -0.06), and substantially negative in year 7 (-0.05 to -0.17, with the Sep 16-30 differential of -0.17 the largest single-window negative across the three-year panel). The year-7 late-season widening of

the negative CC minus NC differential is the within-season concentration of the seasonal sign reversal of -36 mm.

The Apr 16-30 window holds an asymmetrical role between treatments. For NC, it was the lowest K_a window in years 5 and 6 (0.23 and 0.26 in Apr 16-30) and the second lowest in year 7 (0.31, with Apr 1-15 at 0.26), reflecting bare-ground evaporation under high atmospheric demand and dry surface soil. For CC, the lowest K_a window varied by year: Jun 16-30 in year 5 (0.30), May 16-31 in year 6 (0.35), and Apr 1-15 in year 7 (0.35), and Apr 1-15 in year 7 (0.37). The asymmetry produced an annual positive Apr 16-30 CC minus NC differential of +0.15 in year 5, +0.22 in year 6, and +0.10 in year 7, the second largest such window in years 5 and 6 and the largest in year 7. April is therefore the policy-relevant target window for cover crop termination-timing decisions.

Six of the seven OpenET products underestimated EC peak K_a in year 7 NC (Table 9). PT-JPL was the only product to overestimate (+4 percent of EC). The six underestimating products spanned -12 percent (eeMETRIC) to -34 percent (geeSEBAL), with the OpenET Ensemble at -20 percent. The architectural and operational implications of these model differences are discussed in Section 4.4.

Table 16. Three-year mean bi-monthly K_a by source and treatment for top performers identified in Sections 3.4 and 3.5 (Field subset, 2023 to 2025). Each window-K_a is the ratio of summed daily ET_a to summed daily ET_o (CIMIS Davis Station 006) across the three growing seasons. Per-year values for all eight sources, including PT-JPL, SSEBop, and eeMETRIC, are reported in Supplementary Material.

Source	Treat.	Apr 1-15	Apr 16-30	May 1-15	May 16-31	Jun 1-15	Jun 16-30	Jul 1-15	Jul 16-31	Aug 1-15	Aug 16-31	Sep 1-15	Sep 16-30	Oct 1-15	Oct 16-31	Nov 1-15
EC	CC	0.51	0.46	0.49	0.43	0.44	0.42	0.48	0.48	0.49	0.51	0.54	0.54	0.54	0.51	0.47
EC	NC	0.32	0.27	0.41	0.39	0.46	0.48	0.54	0.53	0.54	0.55	0.59	0.61	0.60	0.56	0.52
Ensemble	CC	0.54	0.52	0.48	0.47	0.44	0.39	0.34	0.31	0.32	0.34	0.32	0.34	0.28	0.30	0.31
Ensemble	NC	0.29	0.31	0.31	0.35	0.36	0.33	0.33	0.32	0.35	0.41	0.38	0.42	0.30	0.33	0.32
SIMS	CC	0.64	0.62	0.55	0.54	0.55	0.50	0.45	0.42	0.42	0.43	0.41	0.42	0.34	0.35	0.37
SIMS	NC	0.36	0.41	0.38	0.42	0.49	0.48	0.46	0.45	0.45	0.46	0.45	0.45	0.35	0.36	0.36
DisALEXI	CC	0.62	0.60	0.51	0.47	0.46	0.43	0.40	0.31	0.31	0.34	0.31	0.28	0.21	0.25	0.28
DisALEXI	NC	0.44	0.44	0.38	0.37	0.41	0.40	0.42	0.35	0.35	0.40	0.37	0.37	0.26	0.29	0.29
geeSEBAL	CC	0.37	0.29	0.38	0.40	0.30	0.16	0.19	0.14	0.26	0.20	0.17	0.19	0.20	0.18	0.17
geeSEBAL	NC	0.18	0.16	0.25	0.28	0.21	0.16	0.18	0.18	0.28	0.25	0.21	0.28	0.21	0.21	0.18

OpenET bi-monthly profiles diverged from EC most strongly in April, with the divergence concentrated in two opposite directions. PT-JPL produced the largest early-season overestimate of any product, with three-year-mean CC April K_a of 0.84 to 0.88 against EC CC of 0.50 to 0.55, and NC April K_a of 0.76 to 0.77 against EC NC of 0.27 to 0.33 (Table S3). PT-JPL's profile remained near 0.38 to 0.88 throughout the growing season in both treatments, with little phenological structure, consistent with the positive bias documented in Section 3.4. eeMETRIC produced the opposite April failure, with three-year-mean CC Apr 1-15 K_a of 0.15 against EC CC of 0.55, an underestimate of 0.40 in CC; NC K_a was uniformly low (0.14 to 0.47 across the season), missing the differential between treatments (Table S3). geeSEBAL produced a similar CC April underestimate (0.29 to 0.35 versus EC 0.50 to 0.55; Table 16) and continued to underestimate through most of the season. The April underestimates of eeMETRIC and geeSEBAL coincide with elevated CC monthly mean NDVI (0.51 in April, peaking at 0.55 in February), so the failure is not explained by undetected cover crop greenness in the satellite signal.

The OpenET Ensemble at three-year mean tracked the EC profile shape reasonably well in the April-to-June windows of the panel (within 0.07 in CC; Table 16) but underestimated EC K_a substantially from July onward, with three-year-mean CC Ensemble K_a of 0.29 to 0.34 from Jul 1-15 through Oct 1-15 against EC of 0.48 to 0.55. The three-year mean understates the year-by-year structure of this miss.

The systematic late-season miss is concentrated in year 7 (Table S3). At the EC year-7 NC peak window (Oct 1-15), the Ensemble K_a was 0.43 against EC 0.95, an underestimate of 0.50 at the single window of greatest interest. At Sep 16-30, year-7 Ensemble NC K_a was 0.74 against EC 0.91, an underestimate of 0.17. The Ensemble registered some of the year-7 NC late-

season rise but capped at roughly 0.7 to 0.75 while EC reached above 0.9. A similar but less dramatic year-7 miss appears in CC, with year-7 Ensemble Oct 1-15 K_a of 0.39 against EC 0.82. The year-7 Ensemble miss in the late-season windows quantitatively explains the 2025 sign reversal miss.

DisALEXI and SIMS produced bi-monthly profiles intermediate between the Ensemble and EC at the three-year mean (Table 16). DisALEXI CC tracked the EC profile within 0.03 in April and within 0.04 from May 1-15 through Jun 16-30, and then declined through the rest of the growing season to 0.22 in Oct 1-15 against EC 0.55, the largest late-season CC underestimate among the products in Table 16. SIMS CC produced the steepest April-to-October decline of any product retained in the main-text panel (0.64 in Apr 1-15 to 0.34 in Oct 1-15). SSEBop CC produced a profile broadly similar in magnitude to the Ensemble (Table 16). Most products tracked EC within 0.10 K_a during mid-summer windows but diverged in April and during the late-season fall recovery. The full per-source profile structure is shown in Table 16 and Table S3.

The bi-monthly profile patterns documented above are mirrored in the seasonal results of Sections 3.4 and 3.5, with the cover crop ET signal showing structured time-of-year evolution rather than uniform behavior, the year 6 to year 7 maturation transition manifesting in both peak windows and within-season profile shape, and OpenET products consistently missing the year-7 late-season K_a recovery. Implications for window-resolved practice attribution and for product selection are developed in Section 4.

3.7 NDVI verification of cover crop greenness and canopy maturation

The April K_a underestimates from eeMETRIC, geeSEBAL, and SSEBop admit two competing explanations: a model-physics failure (the satellite sees the cover crop but the model architecture mis-attributes the latent heat flux) or a satellite-retrieval failure (the cover crop is too

sparse, too small in scale, or too closely co-located with bare soil for the satellite to see it). NDVI computed from the same Landsat retrievals that drive the OpenET model panel provides a direct test of which explanation holds. If NDVI shows a clear CC-versus-NC greenness contrast in the windows where eeMETRIC and geeSEBAL underestimate K_a, the satellite sees the cover crop and the model failure is structural rather than observational. Daily NDVI time series for both treatments are shown in Figure 12, and three-year mean NDVI by treatment is reported in Table 17.

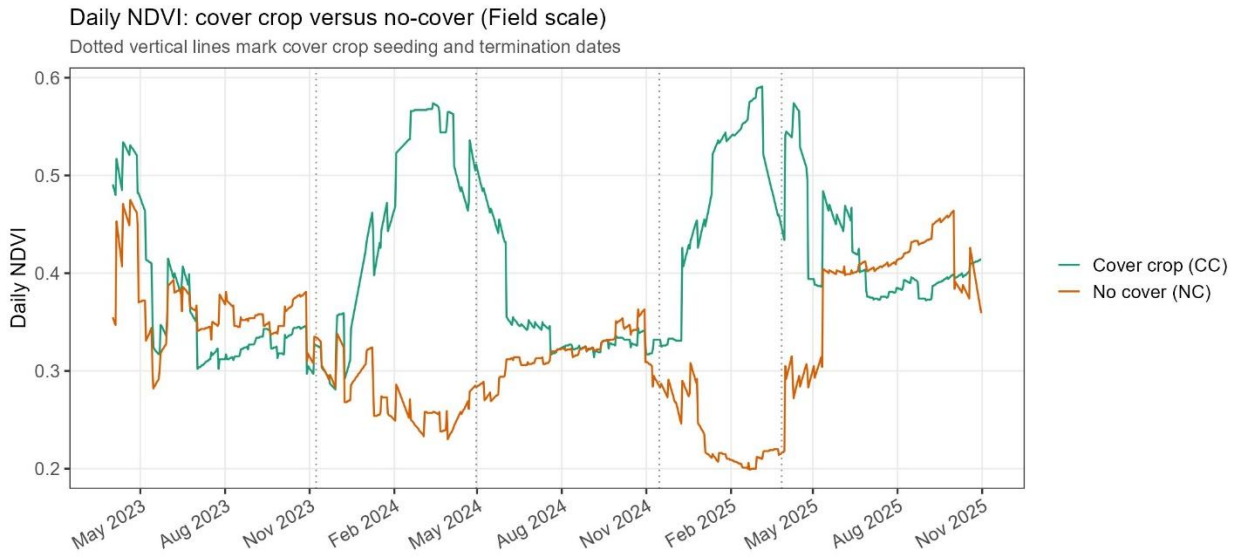


Figure 12. Daily NDVI for the cover cropped (CC) and no cover cropped (NC) treatments from April 2023 through November 2025. NDVI was extracted from the same Landsat retrievals used by the OpenET model panel and aggregated to the Field subset. Vertical gray bands indicate cover crop windows.

NDVI showed a clear and persistent CC-versus-NC greenness contrast across both cover crop seasons. The contrast was largest in February and March, when cover crop biomass and transpiration peaked ahead of termination. The three-year-mean CC-minus-NC NDVI contrast was +0.30 to +0.32 in February and March (CC 0.53 to 0.55 against NC 0.23; Table 17), with the contrast extending from January through April in both cover crop cycles.

The April K_a underestimates of eeMETRIC and geeSEBAL therefore cannot be attributed to satellite blindness. eeMETRIC reported three-year-mean CC Apr 1-15 K_a of 0.15 against EC 0.51 at a CC NDVI of 0.51; geeSEBAL reported CC Apr 1-15 K_a of 0.37 against the same EC value at the same CC NDVI; SSEBop's CC Apr 1-15 K_a of 0.50 nearly matches EC's 0.51, but at a CC NDVI of 0.51 the FAO-56 dual-K_c construction would predict an even higher K_a, indicating that SSEBop's apparent agreement is incidental rather than driven by the observed greenness. The mismatch between observed greenness and modeled latent heat flux indicates a model-physics failure rather than a sensor-side limitation. The architectural interpretation, including the role of hot/cold endmember calibration in residual SEB models, is developed in Section 4.2.

The 2023 NC April NDVI of 0.30 was modestly elevated above the 2024 (0.26) and 2025 (0.28) values, reflecting resident winter vegetation in the NC treatment before the cover crop trial began (Table 4). The CC-versus-NC contrast in April 2023 (+0.13) is smaller than in 2024 to 2025 but consistent in sign. The 2023 NC treatment can still be characterized as bare ground for the purposes of the cover crop signal-detection analysis, since the resident-vegetation effect on subsequent ET_a was minimal.

A second observation worth noting is the late-season convergence and inversion of the NDVI signal. From July through October, three-year-mean NDVI was slightly higher in NC than in CC (0.36 to 0.38 in NC versus 0.34 to 0.36 in CC; CC-NC contrast of -0.01 to -0.03), a small but persistent reversal that coincides with the late-season K_a inversion. The NC pistachio canopy was a brighter target than the CC pistachio canopy in the second half of the growing season. The late-season NDVI signal alone does not separate this canopy-density mechanism from a soil-darkness mechanism (NC bare soil under irrigation may retain different albedo and surface

moisture than CC residue), but Figure 12 shows that the NC late-season NDVI rise tracked the trajectory of the year-7 NC late-season K_a rise.

The seasonal NDVI structure verifies that the satellite saw the cover crop and saw the canopy expansion. The OpenET model failures documented in Sections 3.4, 3.5, and 3.6 are therefore not retrieval failures. They are model-physics failures, which Section 4.2 interprets in light of each model's architectural assumptions about how latent heat flux relates to surface temperature, vegetation indices, and the partitioning of available energy.

Table 17. Per-year and three-year-mean monthly NDVI by treatment (Field subset, 2023 to 2025). Per-year columns are monthly arithmetic means of daily NDVI within each year-month; the Mean columns are daily-pooled three-year means within each calendar month. Mean CC-NC is the difference between Mean CC and Mean NC. n/a indicates months without observations (January to March 2023 and November to December 2025). Daily pooling weights each day equally and may produce a Mean different from the simple average of the per-year columns when monthly day counts differ across years. n/a for November to December 2025 reflects the end of the analysis retrieval window on October 31, 2025.

Month	2023 CC	2024 CC	2025 CC	Mean CC	2023 NC	2024 NC	2025 NC	Mean NC	Mean CC-NC
Jan	n/a	0.48	0.52	0.48	n/a	0.31	0.21	0.25	+0.23
Feb	n/a	0.56	0.58	0.55	n/a	0.26	0.21	0.23	+0.32
Mar	n/a	0.56	0.57	0.53	n/a	0.22	0.20	0.23	+0.30
Apr	0.43	0.55	0.45	0.51	0.30	0.26	0.28	0.33	+0.18
May	0.45	0.40	0.46	0.43	0.37	0.31	0.40	0.33	+0.10
Jun	0.32	0.36	0.38	0.39	0.36	0.31	0.39	0.36	+0.03
Jul	0.31	0.31	0.40	0.34	0.37	0.31	0.41	0.36	-0.02
Aug	0.33	0.33	0.37	0.34	0.34	0.32	0.43	0.37	-0.03
Sep	0.33	0.33	0.38	0.35	0.35	0.33	0.44	0.38	-0.03
Oct	0.33	0.32	0.41	0.36	0.36	0.34	0.43	0.37	-0.01
Nov	0.31	0.33	n/a	0.32	0.33	0.36	n/a	0.30	+0.02
Dec	0.30	0.37	n/a	0.38	0.27	0.25	n/a	0.29	+0.09

4. Discussion

The narrow range of growing season ET_o across the three study years means that interannual differences in measured ET_a or actual crop coefficients (K_a) reported in subsequent sections are not attributable to differences in atmospheric demand. The year-to-year ET_a pattern that emerges, therefore, mostly reflects changes in orchard development and cover crop management, not weather variability. This climate stable framing supports interpreting the year-to-year cover crop ET_a signal reported below as a treatment-and-maturity effect rather than a climate driven one.

4.1 Cover crop ET in young pistachio: magnitude and timing

The eddy covariance record across three growing seasons reframes what "cover crop ET cost" means in young pistachio orchards. A reading focused on annual or seasonal means alone would conclude that the cost was small and inconsistent: the three-year growing season range was -36 to +36 mm, the pooled mean was -5 mm or approximately 1 percent of seasonal ET_a, and all three winter contrasts were positive at +15 to +62 mm. The +6 mm 2024 contrast in particular sits within the typical 5 to 10 percent uncertainty range for EC seasonal totals at this site type (Bambach et al., 2022) and should not be interpreted as a meaningful treatment difference. From these numbers alone, a grower deciding whether to adopt a winter cover crop would conclude that the long-run ET cost is essentially zero, and a SGMA water manager would treat cover cropped and bare orchards as effectively interchangeable for seasonal-mean ET_a accounting. The bi-monthly K_a analysis demonstrates that this reading is incomplete.

The cover crop ET signal in this orchard is structural in time rather than uniform across the growing season. CC K_a exceeded NC by +0.10 to +0.26 across April bi-monthly windows, when cover crop transpiration peaked before termination, declined to near zero by late May, and

turned negative from June onward as pistachio canopy demand exceeded the residue evaporation that remained in the cover cropped interrow. Prior cover crop ET_a work in California has framed the cost primarily as a winter or early spring quantity that competes with soil water recharge ahead of the growing season (DeVincentis et al., 2022; Borum et al., 2024). The young pistachio data here show that this winter framing accounts for only part of the cost: a positive April CC ET_a signal of this magnitude can be offset by a negative summer signal that arises from a different mechanism, namely differential canopy expansion between treatments rather than residue evaporation differences.

The 2025 sign reversal at the seasonal scale is the within-season concentration of this same mechanism, taken to the limit. In year 7, the late-season CC-NC differential widened to -0.05 to -0.17 across September through Oct 1-15, with the Sep 16-30 differential of -0.17 the steepest CC shortfall observed across the three growing seasons. The integrated -36 mm seasonal signal arose from a -76 mm June through October NC advantage that was only partially offset by a +20 mm April-May CC advantage. Year 7 NC bi-monthly peak K_a of 0.95 sits at the lower end of the published mature pistachio peak K_c range, which spans 0.80 (Kanber et al., 1993) through 1.10 (Bellvert et al., 2018) to 1.19 (Goldhamer et al., 1985) and 1.36 (Iniesta et al., 2008) across irrigation system and management contexts. At the seasonal mean scale the gap is more pronounced: year 7 NC seasonal mean K_a of approximately 0.60 (April through October) falls well below the seasonal mean K_a of 0.81 to 0.93 reported by Marino et al. (2019) for non-saline mature pistachio in the southern San Joaquin Valley over a comparable 4.5 month window; however, that study was conducted in a mature orchard with much older trees (~27-31 years old). The peak window of the young orchard reaches the seasonal mean of a mature orchard, but the seasonal aggregate has not yet converged. Comparable mid-development plateaus before mature

peak K_c values are achieved have been reported for young California almond orchards by Drechsler et al. (2022). The conventional "cover crop ET cost" prior, in which CC always utilizes more water than NC, is not a reliable expectation in young orchard systems transitioning to mature canopy: the sign of the seasonal signal can flip when the pistachio canopy has grown enough that NC trees transpire more aggressively than CC trees in the canopy dominated months.

Three mechanistic explanations are consistent with the year-by-year evolution. The first mechanism is direct soil water competition: CC trees may have entered June with lower soil water reserves than NC trees because cover crop transpiration drew down soil water near the end of the winter season, and the deficit propagated into reduced summer transpiration capacity. This soil water depletion mechanism is well documented in California cover crop systems, where Mitchell et al. (2015) reported substantial trade-offs between winter cover crop biomass production and soil water depletion in the Central Valley, with summer season carry-over effects on subsequent crops. The second mechanism is canopy size: NC trees may have expanded canopy more aggressively over years 5 to 7 because the absence of interrow competition allowed greater belowground resource capture, translating into a larger effective root zone and supporting more aggressive mid-season transpiration. The year-7 NC peak K_a of 0.95 versus CC peak K_a of 0.82, combined with September NC NDVI of approximately 0.38 versus CC 0.35 (Figure 12) is consistent with a canopy size component. The third mechanism is soil temperature. Cover crop residues and the standing canopy reduce solar radiation reaching the soil surface and dampen soil heat flux, lowering summer soil temperatures relative to bare ground (Teasdale and Mohler, 1993; Blanco-Canqui et al., 2011). TEROS soil temperature sensors at this site recorded CC temperatures averaging 1 to 2 °C cooler than NC at 30 to 60 cm depths during the 2025 growing

season (Figure S5), with the contrast most pronounced at depth where active roots are concentrated. Cooler root zone temperatures reduce root hydraulic conductance through both water viscosity effects in the warm temperature range and aquaporin regulation, which lowers root water uptake capacity and the transpiration that the canopy can sustain (Cochard et al., 2000; Aroca et al., 2012). The viscosity-driven component is small in absolute terms (roughly 2 to 3 percent per °C in the 15 to 35°C range), so the soil temperature mechanism is unlikely to be the dominant driver of the 2025 reversal but is consistent with a contributing role. The data here cannot definitively partition the seasonal signal among the three mechanisms.

Two confounders should be kept in mind when interpreting these mechanisms. First, the 2025 growing season CC orchard received 75 mm more applied water than NC (Table 6). As a result, some of the year-7 negative summer differential could be attributable to the irrigation difference rather than to canopy or soil water competition alone. Had CC and NC been irrigated identically in 2025, the seasonal signal would likely have been less negative than the measured -36 mm, although the sign of the contrast (NC > CC in summer months) is not expected to reverse because the canopy and NDVI evidence is independent of applied water. Second, the CC and NC treatment footprints differ in surface soil texture, with CC silt loam and NC silty clay loam in the upper 1.2 m (Table 5). The lighter CC texture would be expected to drain more rapidly under unsaturated conditions and could contribute to a difference in soil water availability between treatments that compounds the cover crop transpiration effect. The cover crop mixture also varied between the 2023-24 and 2024-25 seasons, but Nielsen et al. (2015) reported that single species and mixed species cover crop plantings did not differ in water use under irrigated conditions, suggesting that the mixture variation between cycles is unlikely to explain the year-to-year ET_a differences observed here. Multi-site replication with matched soil texture and

irrigation regimes would be required to disentangle the canopy, soil water, and management contributions to the seasonal signal.

The implication for the cover crop water use literature is that single year differencing in young orchard systems is not a reliable estimator of the long-run ET cost. The three-year growing season record produced contrasts ranging from +36 mm to -36 mm across years 5 to 7, a 72 mm spread that exceeds the absolute magnitude of any individual seasonal contrast. A study that sampled only year 5 would report a +36 mm cover crop ET cost; a study that sampled only year 7 would report a -36 mm cover crop benefit. Neither characterization holds across the full record. Hypothesis H1, which predicted that mean K_a during the cover crop season in CC would exceed the NC value by at least 10 percent, is supported on the cover crop active windows: the April CC versus NC K_a differential of +0.10 to +0.26 against an NC April K_a baseline of approximately 0.27 to 0.33 corresponds to a 27 to 96 percent CC excess across all three study years, and all three winter ET_a contrasts (+15, +30, and +62 mm) confirmed CC > NC during the active cover crop window. The hypothesis is silent on the post-termination canopy dominated windows from June onward, in which the sign of the contrast can reverse, as documented above. These findings build on the SGMA cover crop overview by Borum et al. (2024) by demonstrating that the cover crop ET signal in young perennial orchards is not adequately characterized at the seasonal mean scale, and they extend the soil water trade-off framework of Mitchell et al. (2015) into the orchard system context.

All three winters showed CC > NC contrasts (+15, +30, and +62 mm for 2023-24, 2024-25, and 2025-26 respectively), concentrated in late winter (February to March) when cover crop transpiration peaked ahead of termination. The cover crop did not change winter ET_a in November or December, when the cover crop was establishing under low atmospheric demand,

but raised ET_a in late winter by an amount comparable to half the growing season contrast. The cover crop ET cost, taken across an entire calendar year, is therefore the sum of a positive winter contribution, a positive early-spring contribution, and a year-dependent summer-fall contribution that can be near zero or sharply negative. Cover crop adoption in young California pistachio orchards does not have a single ET cost: the cost is structural in time, and its sign at the seasonal scale depends on the orchard's stage of canopy development. The April differential of +0.10 to +0.26 K_a, by contrast, was positive in all three years and is the single window that retains a robust grower relevant interpretation across the canopy development trajectory; the corresponding monitoring recommendation for SGMA practice attribution is developed in Section 4.5.

4.2 Why OpenET models disagree: model-physics interpretation

The four model families represented in the OpenET platform produced systematically different errors against EC ET_a, and the pattern of those errors is interpretable in light of each family's architectural assumptions about how latent heat flux relates to surface temperature, vegetation indices, and the partitioning of available energy between soil and canopy. The NDVI evidence confirms that the failures are not satellite retrieval failures. The cover crop was visible in February-March (CC versus NC NDVI contrast of +0.30 to +0.32) and in April (+0.18), the same windows in which the bi-monthly K_a divergence between OpenET products was largest. NDVI is a useful but not exhaustive indicator of satellite vegetation visibility; saturation at high cover and sensitivity to soil background may produce mismatches between greenness signals and latent heat fluxes that the four model architectures resolve in different ways. The model failures are nonetheless architectural rather than observational, and the four families fail in different ways consistent with their respective formulations.

PT-JPL was positive in both treatments; eeMETRIC was positive in NC only. Each of these two products underestimated in the other treatment (PT-JPL NC: -47.1 percent; eeMETRIC CC: -56.2 percent). The remaining five products underestimated EC ET_a in both treatments, with the largest negative biases from geeSEBAL (-50.6 percent CC, -56.1 percent NC) and SSEBop (-31.0 percent CC, -56.5 percent NC; Table 10). The bi-monthly K_a structure shows where this overestimate is concentrated: PT-JPL three-year-mean CC April K_a exceeding EC by 0.30 to 0.45 in both treatments and remained near 0.46 to 0.88 throughout the growing season with little phenological structure (Table S3). The mechanism is consistent with the Priestley-Taylor basis of PT-JPL: the model scales radiation-driven equilibrium evaporation by eco-physiological constraint functions derived from vegetation indices and atmospheric demand, rather than by an explicit canopy resistance term (Fisher et al., 2008). Because the constraints are keyed to greenness, a sparse young orchard with green interrow vegetation supplies a high VI signal while the formulation lacks a soil water constraint strong enough to damp transpiration, so PT-JPL attributes ET_a to greenness even when soil water and energy availability would limit actual transpiration.

The three residual single-source SEB models, eeMETRIC, geeSEBAL, and SSEBop, produced the largest absolute ET_a underestimates with monthly biases ranging from -28 to -54 percent in CC and -47 to -56 percent in NC (Table 11). This family of models calibrates the near-surface temperature gradient by selecting hot and cold endmembers within each scene, and the latent heat flux is computed as the residual of the surface energy balance after sensible heat is determined from the temperature gradient (Bastiaanssen et al., 1998; Allen et al., 2007; Senay et al., 2013). The endmember selection step is sensitive to landscape heterogeneity and is a known challenge in automated SEB calibration (Allen et al., 2013). In a sparse young orchard, a

substantial fraction of each Landsat pixel is bare or sparsely vegetated soil under high atmospheric demand, which raises pixel mean surface temperatures toward values typical of fully senescent or dry surfaces. When the algorithm selects hot endmembers from the scene's overall temperature distribution, the young pistachio orchard pixels themselves can occupy an intermediate position rather than being clearly identified as the cool end target. The resulting near surface temperature gradient is steeper than physically appropriate for the orchard pixel, allocating a larger share of available energy to sensible heat and leaving an underestimated residual for latent heat. The bi-monthly K_a structure documents the consequence directly at the April window: eeMETRIC reported three-year-mean CC Apr 1-15 K_a of 0.15 against EC 0.51 at a CC NDVI of 0.51; geeSEBAL reported CC Apr 1-15 K_a of 0.37 against the same EC value at the same CC NDVI; SSEBop's CC Apr 1-15 K_a of 0.50 nearly matches EC's 0.51, but at a CC NDVI of 0.53 the FAO-56 dual-Kc construction would predict an even higher K_a (Allen et al., 1998), indicating that SSEBop's agreement is incidental rather than driven by the observed greenness.

The three residual SEB models differ in the magnitude of their April underestimate, in ways consistent with their respective hot endmember selection algorithms. eeMETRIC produced the most extreme suppression of latent heat in April (CC Apr 1-15 K_a 0.15) but recovered some structure later in the growing season (CC Sep 16-30 K_a 0.32 at three-year mean). geeSEBAL produced a more uniform underestimate across the growing season (CC Apr 1-15 K_a 0.37, declining further to 0.14 to 0.26 in mid summer). SSEBop produced an intermediate pattern, with CC profile broadly similar to the OpenET Ensemble in magnitude (Table S3). The common architectural feature across all three is that the interrow in a sparse young orchard sits between

the model's hot and cold reference temperatures rather than at either extreme, and the latent heat residual computed from the resulting gradient does not respond to the observed greenness signal.

SIMS, the reflectance-based dual-K_c model, achieved the lowest absolute ET_a errors of any product. SIMS infers the basal crop coefficient from NDVI and fractional canopy cover, includes a gridded soil water balance module for soil evaporation, and does not require thermal data (Melton et al., 2012; Pereira et al., 2020). The dual-K_c formulation is the closest of the four families to the FAO-56 approach (Allen et al., 1998; Allen and Pereira, 2009), which has been calibrated against decades of agricultural water use measurements. It is well matched to the young drip irrigated system in which transpiration is approximately proportional to canopy cover and irrigation supplies the soil evaporation component. SIMS achieved daily MBE of -0.15 mm per day in CC and -0.41 mm per day in NC, the smallest absolute biases. The finding that SIMS minimizes RMSE in both treatments is therefore consistent with its architectural alignment with the orchard system. SIMS's bi-monthly profile shows the limit of this alignment for differential signal detection. The CC treatment K_a falls from about 0.64 in Apr 1-15 to about 0.34 by Oct 1-15, whereas the NC treatment stays nearly flat (about 0.36 to 0.35). SIMS, therefore, resolves a clear CC-minus-NC difference of roughly 0.28 in early spring, when CC greenness is highest, but that difference collapses toward zero by late summer as pistachio NDVI comes to dominate the VI signal in both treatments. Because the same NDVI-to-K_c mapping then drives both treatments, SIMS captures absolute ET_a accurately in each treatment individually yet underestimates the seasonal persistence of the treatment contrast, which is what the difference-of-differences signal-detection metric penalizes.

DisALEXI, the two-source SEB model, performed second best on absolute accuracy and best on signal detection. The two-source architecture partitions sensible and latent heat between

soil and canopy components separately (Anderson et al., 2007, 2018), which means that the soil and canopy components can scale independently with treatment specific surface conditions. In a CC orchard, the interrow soil component sees an active winter cover crop with elevated NDVI and lower surface temperature, while in a NC orchard the same component sees bare or near-bare soil with higher surface temperature; the two-source partitioning preserves this distinction even when the canopy components are similar. The bi-monthly K_a structure shows that DisALEXI tracks the EC profile shape closely from May 1-15 through Jun 16-30 in CC (within 0.04 of EC at three-year mean) before diverging in late summer, and the per-year DOD analysis shows that DisALEXI recovered the EC sign of the CC-NC contrast in all six seasons with the smallest mean |DOD| (20 mm). The two-source advantage for signal detection is mechanistic. When the differential between treatments arises mostly from interrow soil conditions rather than from canopy differences, the two-source partitioning attributes the differential to the soil component and preserves it in the modeled CC-NC difference. This soil canopy partitioning skill has been documented in vineyard contexts where soil and canopy components have markedly different surface temperatures (Knipper et al., 2022), and the present results extend that evidence into a young orchard system with active interrow vegetation. Single-source residual-SEB models and reflectance-based dual-K_c models both collapse soil and canopy contributions into a single per-pixel ET_a estimate and lose this resolution.

The OpenET Ensemble inherits the failure modes of its constituents in proportion to their majority sign pattern in this orchard system. Five of the six constituents underestimated EC ET_a (PT-JPL is the lone overestimator in both treatments), and the median-based outlier removal that the Ensemble employs (Volk et al., 2024) cannot rescue the underlying ET_a estimate when the majority of constituents are biased in the same direction. The Ensemble's daily MBE of -0.51

mm per day in CC and -0.70 mm per day in NC tracks the median negative signal across the constituent models, and the resulting monthly RMSE of 21.8 mm per month in CC sits between SIMS (best, 17.2) and DisALEXI (third, 23.0). Volk et al. (2024) report that the OpenET Ensemble achieves small mean bias against EC at the continental scale, an ensemble property that does not extend to young pistachio in this study where the constituent models share a sign of bias. The Ensemble's structural reliance on majority sign neutralization breaks down in systems where canopy sparseness biases the residual-SEB models in a common direction. The signal-detection performance of the Ensemble inherits a similar structural compromise: the Ensemble's mean |DOD| of 32 mm placed it third behind DisALEXI and geeSEBAL. The 2025 Grow sign reversal that the Ensemble missed (modeled +19 mm against EC -36 mm) is the within season concentration of the year-7 NC late-season K_a recovery that none of the seven products tracked at the level EC measured. The Ensemble averaging step does not impart skill that none of the constituent models possess; in this orchard system, all seven products underestimate the year-7 NC late-season demand, and the Ensemble inherits that limitation.

The architectural patterns documented here parallel findings in other recent OpenET evaluations against EC ground truth in California tree and forage crops. Knipper et al. (2024) reported model specific biases in California almond orchards; Tawalbeh et al. (2024) found residual-SEB underestimates in mature pecan; Dhungel et al. (2024) and Sabiston et al. (2024) documented OpenET biases in citrus and alfalfa systems, respectively. The young pistachio case extends this evidence into a sparse canopy young orchard system where the architectural fit principle has not previously been tested with a paired treatment contrast. A useful complementary comparison comes from Marino et al. (2019, 2021), whose mature non-saline pistachio EC measurements in the southern San Joaquin Valley represent the operational target

system that OpenET was designed to validate against. The underperformance in our young orchard relative to expected mature orchard performance is consistent with the architectural fit thesis that sparse canopy systems pose challenges that mature orchard validation does not surface.

Two implications follow from the architectural diagnosis. First, the choice of OpenET product for a young orchard application should be informed by the architectural fit between the model and the system being measured. The reflectance-based dual-K_c approach matches young drip irrigated orchards best for absolute ET_a accuracy but cannot resolve treatment differences when the canopy NDVI dominates the vegetation index input. The two-source SEB approach trades some absolute accuracy for the ability to resolve interrow treatment effects when the differential arises from soil component differences. Residual single-source SEB models systematically underestimate ET_a in sparse young orchard systems via hot endmember misallocation, and the OpenET Ensemble inherits this underestimate when single-source SEB models make up the majority. Second, the bi-monthly K_a structure provides a diagnostic test that distinguishes architectural failure modes more sharply than seasonal mean RMSE alone. PT-JPL's near-flat profile, eeMETRIC's April underestimate at high observed greenness, geeSEBAL's uniform underestimate, and SIMS's similar CC and NC profile shapes are all visible in the bi-monthly structure but invisible in the seasonal-mean monthly RMSE. A model evaluation that reports only seasonal mean RMSE will miss the diagnostic features that distinguish architectural fit from architectural mismatch.

These architectural inferences rest on six seasons at a single instrumented orchard, and the DisALEXI signal-detection advantage in particular requires multi-site replication before being treated as a generalizable architectural property. The young pistachio results documented

here provide a starting point for testing the architectural fit framework against other young California orchards. Section 4.5 develops the corresponding monitoring recommendation that practical OpenET use under SGMA should consider both the absolute-accuracy ranking and the architectural fit, and that the Ensemble should not be used as-is for either question in young pistachio.

4.3 Two evaluation skills, two different best models

The two use cases reward different aspects of model behavior, which is why no single product ranks first on both. Volumetric water accounting is a level problem: it depends on how closely a model reproduces the absolute magnitude of ET_a, so it rewards low bias and low RMSE against the EC reference. Treatment-signal detection is a difference problem: it depends on whether a model reproduces the sign and relative magnitude of the CC minus NC contrast, evaluated here as a difference-of-differences. A model can carry a large but consistent absolute bias in both treatments and still recover the treatment signal accurately, because that shared bias cancels in the difference. Conversely, a model can track the absolute ET_a magnitude well but miss the signal if it maps both treatments through the same vegetation index (VI) relationship and therefore returns nearly identical values for CC and NC. SIMS illustrates the first use case and DisALEXI the second: SIMS minimizes absolute error but compresses the treatment contrast, whereas DisALEXI is less accurate in absolute terms but preserves the CC minus NC difference across seasons. Accuracy and signal detection are thus partly decoupled skills, and ranking models on one does not predict their ranking on the other.

The validation results establish that no single OpenET product performed best on both absolute ET_a accuracy and cover crop signal detection. SIMS achieved the lowest monthly RMSE in every treatment-by-season but recovered the EC sign in only 5 of 6 seasons.

DisALEXI achieved 6 of 6 sign recovery and the lowest mean |DOD| in the panel but ranked third on monthly RMSE (Table 11 and Table 14). The two products are not the same, and the dual use case divergence between them is not a coincidence: SIMS' absolute-accuracy advantage and DisALEXI's signal-detection advantage arise from different architectural choices, and the divergence is structural rather than incidental.

The implication for OpenET users is that the right product depends on the question being asked. Two use cases draw on the platform with different requirements.

The first use case is volumetric water accounting, in which the goal is to estimate total ET_a over a defined area and time period as accurately as possible. Volumetric water accounting under SGMA (Lubell et al., 2020) requires ET_a estimates that match water deliveries within tolerable error margins for groundwater pumping allocations and water rights documentation. For this use case, absolute ET_a accuracy is the limiting metric and the appropriate product is the one that minimizes RMSE against ground truth data. SIMS is the absolute-accuracy leader in this study and is the appropriate choice for young pistachio orchards. The OpenET Ensemble ranks second on absolute accuracy (CC 21.8, NC 24.8 mm per month) and produces a systematic ET_a underestimate of approximately 13 to 20 mm per month relative to EC across both treatments. For volumetric accounting in this young pistachio orchard, the Ensemble would credit growers with less ET_a than they consume, an error of approximately 100 to 140 mm per growing season at the orchard level. Whether this magnitude generalizes to other young California pistachio orchards depends on whether the Ensemble's negative bias is stable across sites; majority sign driven Ensemble biases have been observed in other tree crop OpenET validation studies (Knipper et al., 2024; Tawalbeh et al., 2024) suggesting the structural pattern is not specific to

young pistachio, but multi-site replication in pistachio specifically is needed to confirm the bias magnitude.

The second use case is signal-detection accuracy of management practices, in which the goal is to detect or quantify the ET_a difference between two orchards that differ in their floor management practices. Cover crop incentive programs under SGMA (Borum et al., 2024) require defensible practice based ET_a attribution to credit or debit growers for management interventions, and similar paired treatment comparisons arise in regulated deficit irrigation evaluations and in before-and-after assessment of irrigation system upgrades. For this use case, the limiting metric is differential accuracy: the model must produce a CC-minus-NC contrast that recovers the sign and magnitude of the underlying treatment effect. DisALEXI achieved 6 of 6 sign matches with mean |DOD| of 20 mm in this study and is the appropriate choice. SIMS, the absolute-accuracy leader, ranks fourth of seven on signal detection and would invert the sign of the small magnitude EC signal in two of the three growing seasons. For signal-detection accuracy, SIMS' low absolute error in both treatments individually does not translate into a useful differential, because the bias is treatment-dependent. The Ensemble's mean |DOD| of 32 mm placed it third in the panel and missed the 2025 sign reversal that EC measured at -36 mm; for signal-detection accuracy under SGMA that credits growers for cover crop adoption, the Ensemble would assign a positive ET_a cost in 2025 that was not present in the EC data.

The dual use case structure also defines a category of OpenET products that are poorly suited for either application in this orchard system. geeSEBAL and SSEBop produced large absolute ET_a underestimates in NC (-55 to -56 percent at the monthly mean), and although geeSEBAL achieved 6 of 6 sign matches and SSEBop 5 of 6, their mean |DOD| values (27 and 92 mm, respectively) reflect that the signal recovery comes through bias cancellation rather than

genuine differential resolution. PT-JPL produced 4 of 6 sign matches with mean |DOD| of 35 mm but inverted the 2023 Grow sign and showed a treatment-dependent bias pattern (CC +21.4 percent, NC +25.6 percent) that compounds the signal-detection error. eeMETRIC produced 2 of 6 sign matches with mean |DOD| of 44 mm and a similarly treatment-dependent bias pattern in the opposite direction (CC -54.6 percent, NC -46.8 percent). None of these four products is the best choice for either volumetric water accounting or signal-detection accuracy in young pistachio. A user selecting an OpenET product for a young orchard application should therefore not default to the Ensemble, which inherits the biases of these constituents in proportion to their majority sign pattern. These avoidance recommendations are scoped to the young pistachio system tested here; the same products may have applications in mature crops or other system contexts where their architectural limitations matter less.

The dual use case divergence between SIMS and DisALEXI also has implications for how new RSET models should be benchmarked. The OpenET continental-scale validation effort (Volk et al., 2024) reports model performance against EC ground truth using pooled RMSE metrics that aggregate across crop types, climate regimes, and orchard ages. Volk et al. (2024) report Ensemble accuracy that supports its role as the recommended platform default at the continental scale, and our SIMS absolute-accuracy ranking in young pistachio is broadly consistent with the magnitude of pooled RMSE values that Volk reports for SIMS at the continental aggregate. However, pooled RMSE does not test signal-detection accuracy, because pooled metrics combine paired observations from many sites without preserving the within-site treatment contrasts that drive practice attribution. A signal-detection benchmark requires within-site paired differences of the kind this study provides: two adjacent treatments, identical climate forcing, identical canopy biology, and a measurable treatment-induced difference in ET_a. Paired-

treatment site designs are uncommon in the OpenET validation literature; the GRAPEX vineyard intercomparisons (Alfieri et al., 2019; Knipper et al., 2022) provide adjacent EC tower comparisons but not always with controlled treatment differences. The field-scale CC versus NC paired tower design used here is among the relatively rare designs that allow the dual use case question to be tested directly. Future RSET validation studies that aim to support both volumetric water accounting and signal-detection accuracy applications should include paired treatment site designs alongside the conventional pooled validation approach.

Our finding that the Ensemble is suboptimal for both volumetric accounting (where SIMS leads) and signal-detection accuracy (where DisALEXI leads) in young pistachio runs counter to the implicit platform default in OpenET (Volk et al., 2024). The discrepancy reflects a system-specific limitation in young sparse canopy orchards rather than a critique of the Ensemble approach in mature crops. The cost of the dual use case divergence is borne by the user. A user who selects the OpenET Ensemble because it is the platform default and applies it indiscriminately to both volumetric water accounting and signal-detection questions will receive answers that are systematically biased on both fronts: the Ensemble's absolute ET_a is approximately 5 mm per month in CC and 6 mm per month in NC worse than SIMS, and the Ensemble's signal-detection accuracy is approximately twice the mean |DOD| of DisALEXI in this study. The solution is to select among the OpenET constituents based on the application's measurement target: SIMS for volumetric water accounting, DisALEXI for signal-detection accuracy of management interventions. These product-selection recommendations are based on six seasons at a single instrumented orchard, and should be tested in additional paired-treatment site designs before being adopted as universal guidance for young California pistachio. The

Section 4.5 recommendations translate this principle into specific monitoring guidance for SGMA practice.

4.4 Comparison with mature and young orchard Kc curves

The EC peak K_a trajectory across years 5 to 7 anchors the young orchard K_a curve to the published pistachio K_c benchmarks established in mature orchards. The published mature pistachio peak K_c range is wider than is sometimes recognized: Kanber et al. (1993) reported peak K_c of 0.80 in surface-irrigated pistachio in Turkey, Goldhamer et al. (1985) reported peak K_c of 1.19 in 10-year-old San Joaquin Valley orchards under soil water balance methodology with deep percolation correction, Bellvert et al. (2018) reported peak K_a of 1.10 in a 14-year-old California orchard using airborne thermal imagery and a reflectance-based dual-K_c approach, and Iniesta et al. (2008) reported peak K_c of 1.36 under regulated deficit irrigation in Spain. The wide range across these studies reflects substantial variability in irrigation system, soil, climate regime, alternate-bearing cycle, and methodology. The year-7 NC peak K_a of 0.95 measured in this study sits at the lower end of this published range, 19 percent above Kanber's value, 14 percent below Bellvert's, and 20 percent below Goldhamer's, indicating that a seventh-leaf orchard approaches but does not reach the mature California pistachio peak benchmarks. At the seasonal mean scale, Marino et al. (2019, 2021) reported K_a of 0.81 to 0.93 over a 4.5 month window (May to October) in mature non-saline pistachio in the southern San Joaquin Valley. The year-7 NC seasonal mean K_a at our site was approximately 0.60 (April through October), well below Marino's mature seasonal mean, even as the bi-monthly peak approached the lower end of mature peak benchmarks. The peak window of the young orchard reaches the seasonal mean of a mature orchard, but the seasonal aggregate has not yet converged.

The year-by-year trajectory of EC peak K_a provides quantitative information about the canopy development curve. Peak K_a in year 5 and year 6 sat at approximately half the mature orchard reference (0.54 to 0.63 across both treatments and both years; Table 9), then jumped sharply in year 7 to 0.82 in CC (Oct 1-15) and 0.95 in NC, with the year-6 to year-7 NC increase of +0.42 representing a 79 percent magnitude increase in a single year. The non-linearity of this trajectory is the substantive finding for young orchard water budget planning. A linear interpolation between leaf-year 5 and the Goldhamer peak K_a of 1.19 would predict peak K_a of approximately 0.75 in year 7, well below the observed 0.95 in NC; a linear interpolation against the Bellvert plateau of 1.10 would predict approximately 0.71. The non-linearity holds against these mid-range mature K_c benchmarks, though linear interpolation against the highest published peak K_c (Iniesta et al., 2008) would predict a year-7 value closer to the observed 0.95. Comparable non-linear canopy maturation trajectories have been documented in young almond orchards in California, where Drechsler et al. (2022) reported year-by-year K_c development that included rapid expansion phases between specific leaf years rather than smooth linear progression. The actual pistachio trajectory observed here is closer to a step transition between years 6 and 7, in which the orchard moves from a low demand canopy state to within 14 to 20 percent of the Goldhamer-Bellvert mature range in a single year. The "step transition" framing is based on three consecutive leaf years (5, 6, 7) at one orchard, and the transition could reflect canopy area expansion, root system development, alternate-bearing cycle phasing, or a combination of these effects. Multi-year EC observations at additional sites with different alternate-bearing phases and management regimes are needed to establish whether the step transition is a generalizable canopy maturation feature or a specific outcome of this orchard's biology and management.

The mature orchard K_c benchmarks themselves were derived under different methodological conventions, which warrants a brief reconciliation against the FAO-56 framework (Allen et al., 1998) from which both pistachio peak K_c values originate. Goldhamer et al. (1985) used soil water balance with weekly to bi-weekly resolution and Class A pan reference evaporation, with peak K_c reported at the bi-monthly maximum across the growing season. Bellvert et al. (2018) used a reflectance-based dual-K_c approach driven by daily ET_o, with peak K_a reported as a single day or short window maximum during peak vegetation. The bi-monthly Goldhamer convention used in this study (15 windows from April 1-15 through November 1-15, with within-window K_a defined as the ratio of summed daily ET_a to summed daily ET_o) matches the Goldhamer methodology more directly than the Bellvert methodology, and the comparison against Goldhamer 1.19 is therefore the more appropriate reference. Under a daily ET_a to daily ET_o computation rather than the bi-monthly aggregation, the year-7 NC peak K_a would shift modestly (typically upward by 0.05 to 0.10 in pistachio orchards, based on Bellvert et al. 2018), but the qualitative finding that year 7 approaches but does not reach the mature plateau holds across both conventions.

The OpenET model panel did not track the year-6 to year-7 canopy maturation transition that EC measured. Year-7 NC peak K_a deviations from EC ranged from -14 to -36 percent across the six non-PT-JPL products, with the Ensemble at -22 percent (0.74 against EC 0.95). PT-JPL was closest at +2 percent (0.97), but its proximity reflects the vegetation index driven ET attribution that produces overestimation in sparse young orchard systems rather than genuine tracking of the canopy maturation signal. None of the seven products reached the EC year-7 NC peak K_a within plus or minus 5 percent. This is the same panel that achieved 18 to 21 percent monthly RMSE reduction relative to the median individual model, demonstrating that absolute-

accuracy validation at the seasonal mean scale does not guarantee accuracy at peak windows where canopy demand is highest.

The structural reason for the OpenET panel's failure to track the year-7 canopy-maturation transition is documented in Section 3.6: the year-7 underestimate is concentrated in late season windows (Sep 16-30 through Oct 16-31) where the EC NC profile rose to a 0.91 to 0.95 plateau but the OpenET panel uniformly underestimated. The Ensemble's NC peak K_a rose from 0.35 in year 6 to 0.74 in year 7, an increase of 0.39 that nearly matched the EC increase of 0.42 in magnitude but at a level approximately 0.20 below EC throughout. Several other products showed similar patterns of magnitude tracking with level offset (Table S3). The architectural mechanisms explain why this offset arises: residual single-source SEB models suppress latent heat in sparse young orchard systems via hot endmember misallocation, and reflectance-based dual-K_c models do not respond differentially to canopy density beyond the saturated NDVI range that mature pistachio reaches by year 7. The two-source DisALEXI architecture preserves more of the late-season structure but its peak K_a of 0.69 still falls 27 percent below EC. Architectural patterns documented for young pistachio here parallel canopy development tracking limitations recently reported for OpenET in California almond orchards (Knipper et al., 2024), suggesting that the failure to track canopy maturation transitions is a generalizable property of the OpenET models in young California tree crop systems rather than a feature specific to pistachio.

The implications for the young orchard K_c literature, currently dominated by mature orchard benchmarks (Goldhamer et al., 1985; Bellvert et al., 2018; Marino et al., 2019, 2021) with limited young orchard documentation in pistachio specifically and a more extensive almond young orchard literature exemplified by Drechsler et al. (2022), are twofold. First, the year-by-

year trajectory documented here suggests that pistachio canopy maturation in young orchard systems is non-linear, with a step-like transition between years 6 and 7, and that simple linear scaling of mature orchard K_c with tree age is unreliable. Second, the year-7 NC peak of 0.95 is an empirical anchor for the young orchard K_a curve in Sacramento Valley pistachio under drip irrigation. Site-specific factors including soil texture, irrigation system, alternate-bearing phase, and microclimate may shift this value in other young pistachio orchards; multi-site replication is needed to establish the variance in the trajectory. Future studies of young California pistachio water use that need a K_a benchmark for seventh-leaf trees can reference 0.95 (NC) and 0.82 (CC) at the peak window conditioned on the management regime and climate of the Sacramento Valley study site. Until a multi-site, multi-year network of young orchard EC measurements is available to establish the variance in the year-by-year trajectory, the OpenET Ensemble should not be used as the primary source of young orchard K_a given the documented 22 percent underestimate at the year-7 peak window, and SIMS (year-7 NC peak 0.65, deviation -32 percent) and DisALEXI (year-7 NC peak 0.69, deviation -27 percent) are no better. The most defensible approach for young California pistachio K_a benchmarks is therefore to use the EC values documented here as point estimates. The implications for SGMA accounting under the canopy maturation transition are developed in Section 4.5.

4.5 Practical recommendations for SGMA compliance monitoring

The validation results in Sections 3.4 and 3.5, the bi-monthly K_a diagnostics in Section 3.6, and the dual use case framework developed in Section 4.3 translate into specific guidance for SGMA compliance monitoring of young pistachio orchards. SGMA places groundwater extraction reporting and basin balance accountability on local Groundwater Sustainability Agencies (GSAs), with remote-sensing-derived ET_a increasingly relied upon as the primary

measurement of agricultural water consumption (Lubell et al., 2020; Melton et al., 2022). The recommendations below are framed around two distinct use cases (volumetric water accounting and signal-detection accuracy of management interventions) and a practical irrigation scheduling resource (the bi-monthly K_a curve).

For volumetric water accounting, the appropriate OpenET product is the one that minimizes RMSE against ground truth. SIMS achieved the lowest monthly RMSE and smallest CC bias in this study (Table 10 and Table 11) and is the recommended product for groundwater-allocation accounting under SGMA in young pistachio orchards. The OpenET Ensemble underestimated absolute ET_a by approximately 17 mm per month in CC and 22 mm per month in NC, which propagates to an approximately 150 mm shortfall over a seven month growing season at the orchard level. SIMS reduces this error to approximately 20 mm per growing season (0.16 acre-feet per hectare) at the pooled mean, a seven-fold improvement. The 150 mm per season magnitude is based on the bias measured at our single instrumented site and may differ at other young California pistachio orchards depending on canopy structure and management; multi-site replication is needed to confirm the magnitude before basin-scale extrapolation.

For signal-detection accuracy, in which the goal is to detect or quantify the ET_a difference between two management treatments, the appropriate OpenET product is DisALEXI. DisALEXI achieved 6 of 6 sign matches with the lowest mean |DOD| (Table 14) and is the appropriate choice. Examples of signal-detection accuracy applications under SGMA include crediting growers for cover crop adoption (DeVincentis et al., 2022; Borum et al., 2024), evaluating the ET_a impact of regulated deficit irrigation, and benchmarking ET_a changes following irrigation system upgrades. The OpenET Ensemble produced a mean |DOD| of 32 mm and missed the 2025 sign reversal that EC measured at -36 mm. SIMS, the absolute-accuracy leader, ranked

sixth of seven on signal detection (mean |DOD| 46 mm) and is not appropriate for signal-detection accuracy despite its volumetric water accounting performance.

The magnitude of the model choice penalty in young pistachio is substantial. eeMETRIC reported 2024 Grow CC ET_a of 255 mm against the EC value of 548 mm, a 293 mm shortfall at a single orchard in a single season. This shortfall is large enough that it would substantially affect a grower's groundwater allocation under per-acre basin pumping budgets. SSEBop reported 2024 Grow CC-NC contrast of +241 mm against the EC value of +6 mm, an overstatement of the cover crop effect by approximately 235 mm. For a grower seeking credit under a cover crop incentive program, the SSEBop attribution would substantially overstate the ET_a added by cover crop adoption. eeMETRIC, geeSEBAL, SSEBop, and PT-JPL are not recommended for either volumetric accounting or signal-detection accuracy in young pistachio orchards under SGMA.

The OpenET Ensemble's role under SGMA needs to be reconsidered for young orchard applications specifically. The Ensemble was designed as a conservative aggregation that limits the influence of any single deviating product (Volk et al., 2024). In mature orchards and well-validated crop climate combinations, this design is appropriate. In young pistachio, however, the Ensemble inherits the systematic negative bias of the residual single-source SEB models, produces an absolute ET_a that is approximately 5 mm per month worse than SIMS in CC and 7 mm per month worse in NC, and recovers the cover crop signal in 5 of 6 seasons but misses the 2025 signal reversal. The Ensemble's underperformance in young pistachio is consistent with cross crop OpenET evaluations in California tree systems (Knipper et al., 2024) where constituent models share a sign of bias and the majority sign neutralization assumption breaks down. The equal weight Ensemble masks the architectural diagnostic information that distinguishes good products from bad in this orchard system. SGMA monitoring agencies that

adopt Ensemble-based accounting as a default may produce systematically biased ET_a estimates, with bias magnitude that depends on orchard age and canopy structure. Our recommendation that GSAs select among OpenET constituents based on the application's measurement target, rather than defaulting to the Ensemble, runs counter to current platform guidance (Volk et al., 2024) and to the implicit standard practice in California GSAs. The discrepancy is scoped to young sparse canopy orchards where the architectural fit principle departs from the well-validated crop climate combinations on which the Ensemble was originally tested.

The bi-monthly K_a curves in Table 15 and Table 16 provide a directly usable irrigation scheduling resource for young California pistachio orchards. EC peak K_a rose from 0.57 in year 5 NC to 0.95 in year 7 NC, with the year-by-year trajectory documented per bi-monthly window. Growers and irrigation managers can use the Table 15 EC values directly: for a seventh-leaf orchard, expect peak K_a of 0.95 in October at NC and 0.82 in October at CC, with the within season profile rising monotonically from approximately 0.26 in early April to the late-season peak. Year-by-year peak values for years 5 and 6 are documented in Table 15 for orchards at earlier stages of canopy development. Growers currently using mature orchard K_c benchmarks (e.g., Goldhamer's peak K_c of 1.19) for seventh-leaf orchards would over apply by roughly 25 percent above the measured requirement. Adjusting irrigation schedules to the year-by-year benchmarks documented here would reduce this over application during the canopy development years when mature K_c values do not yet apply.

The April differential is the most informative window for evaluating cover crop termination timing decisions in this orchard system: CC NDVI peaks in February-March (CC 0.55 versus NC 0.23 at three-year mean) and CC ET_a peaks in early April, with a CC-NC advantage of +0.10 to +0.26 across April bi-monthly windows in 2023 to 2025. Termination too

early eliminates the cover crop biomass before it has accumulated nitrogen and soil organic matter benefits (Mitchell et al., 2015; DeVincentis et al., 2022); termination too late shifts the cover crop ET_a peak into the period when the pistachio canopy is breaking dormancy and competing for soil water. The bi-monthly K_a curves identify the Apr 1-15 window as the maximum positive CC-NC differential window in years 5 and 6 and the Apr 16-30 window as the comparable maximum in year 7, suggesting that grower termination timing in mid-April aligns the cover crop *ET* peak with the end of the cover crop growing window and minimizes carry over into pistachio bud break. These termination timing recommendations are specific to the mixed species cover crops planted in November and the climate of the Sacramento Valley study site; cover crop species composition, planting density, and overwinter precipitation patterns will shift the optimal termination timing in other orchard systems.

The recommendations above are conditional on the orchard system tested in this study. The dual use case framework (SIMS for volumetric water accounting, DisALEXI for signal-detection accuracy) is expected to generalize to other young California pistachio orchards under similar management. The specific peak K_a and bi-monthly K_a values are site-specific and require validation in other orchard systems. Section 4.6 develops the limitations of single-site documentation in more detail and identifies the multi-site network design that would establish whether the year-by-year K_a trajectory documented here is universal or specific to this site.

These results translate into objective-specific guidance. When the goal is field- to basin-scale volumetric water accounting for SGMA, agencies should prioritize the product with the lowest validated absolute error in the relevant crop and growth stage, which, for young pistachios, is SIMS. The OpenET Ensemble, although robust at continental scale, underperformed both leading individual models in this young orchard setting and is not the

default choice for absolute accounting here. Where the goal is attributing an ET_a effect to a management practice, for example crediting or incentivizing winter cover cropping, the product that reliably recovers the treatment signal should be used even at some cost in absolute accuracy, which here is DisALEXI. For programs that must serve both purposes, the two functions should be assigned to different products rather than expecting one product to satisfy both. Because the best product is crop- and stage-specific, agencies should also favor products whose errors have been characterized against local reference data for the system being monitored rather than assuming continental validation transfers to young perennial orchards.

4.6 Limitations

The findings of this study are subject to constraints that future work should address. The validation rests on a single instrumented orchard system with two paired treatments (CC and NC) over three growing seasons and three cover crop winter seasons, corresponding to six seasons from one site. Both orchards are managed by the same grower under similar irrigation scheduling and similar interrow management within their respective treatments. The dual use case framework, the canopy maturation trajectory, and the bi-monthly K_a curves are documented at this single site and should be tested against young pistachio orchards in other Sacramento Valley locations and in San Joaquin Valley locations before being treated as universal. The specific peak K_a values (year-7 NC 0.95, CC 0.82) are field-scale measurements and may vary across sites with different soil texture, irrigation system, alternate-bearing cycle, and cover crop species composition. Even within a single orchard, the EC tower footprints sample a subset of the orchard area; spatial heterogeneity of ET_a within young pistachio orchards has not been quantified here and may add another scale of uncertainty to the bi-monthly K_a values. A multi-site network of three to five young pistachio orchards instrumented with EC towers, paired by

management treatment where possible, would establish the variance in the year-by-year K_a trajectory and refine the young-orchard K_c benchmarks. The GRAPEX vineyard intercomparison (Alfieri et al., 2019) provides a precedent for paired-site EC validation of remote sensing *ET* in California tree crop systems.

Irrigation in both orchards was managed by the grower under commercial constraints rather than by the research team. The CC and NC treatments received nominally the same irrigation schedule based on grower observations, but small differences in actual irrigation supply between treatments are possible. Specifically, the 2025 growing season CC orchard received approximately 75 mm more applied water than NC, which could explain some of the year-7 negative summer differential. Any irrigation differential between treatments would propagate to the EC ET_a difference in ways that the analysis here cannot fully separate from the cover crop or canopy maturation effects. The 2025 sign reversal of -36 mm is large enough that an irrigation supply explanation alone is unlikely to account for it, but smaller magnitude contrasts (+6 mm in 2024 Grow) may be partly attributable to irrigation differences. Future work that includes applying the same amount of irrigation per treatment would tighten the attribution.

The cover crop mixture varied between the two cover crop seasons. The 2023-24 season and the 2024-25 season used different seed mixes, and the two seasons also differed in seeding density and in the November planting window. The bi-monthly NDVI peaks (CC 0.55 to 0.58 across the two seasons; Table 17) and seasonal mean greenness contrasts (+0.30 to +0.32 in February-March, three-year mean) were broadly consistent across the two seasons, suggesting that the cover crop water use signal is robust to the specific mixture used here, but a controlled comparison across mixtures would refine this generalization.

The year-7 NC catch up to and overtake of CC complicates clean treatment effect inference. The 2025 sign reversal arose because the canopy maturation signal in NC outpaced the canopy maturation in CC, and Section 4.1 identified two candidate mechanisms (direct competition for soil water, canopy size differences) that the data here cannot fully separate. A study with paired EC towers running through full pistachio canopy maturation (years 8 to 12) would establish whether the NC catch up persists, plateaus, or reverses, and would establish the long run difference in mature orchard K_a between cover cropped and bare orchard systems.

CIMIS Davis Station 006 ET_o was applied uniformly to both treatments. This assumes that the local atmospheric demand at the orchard (approximately 10 km from the Davis station) is well represented by the Davis ET_o measurement. Local microclimate effects from the cover crop canopy in CC versus the bare ground in NC may produce small differences in within orchard atmospheric demand that the uniform Davis ET_o cannot resolve. The bi-monthly K_a values reported here would be modestly affected by use of an in orchard ET_o measurement; the qualitative findings (year-by-year K_a trajectory, dual use case framework, OpenET architecture diagnoses) are not expected to change with a more local ET_o source. A future installation of a small weather station at the orchard would test this assumption directly.

Three additional limitations are worth noting. First, the OpenET retrieval extended through November 15, 2025, and does not include the 2025-26 cover crop winter cycle. The third complete winter cycle would extend the cover crop signal-detection record by approximately one season-pair, and a future revision of this analysis after the 2025-26 cycle is complete would test whether the year-7 to year-8 transition continues the canopy-maturation trajectory or stabilizes near the year-7 plateau. Second, the EC measurements at both towers underwent quality control screening that excluded periods with insufficient turbulence, sensor malfunction, or footprint

contamination by adjacent fields, and gap-filling was applied for short missing periods using temperature, vapor pressure deficit, and incoming radiation as predictors (Wutzler et al., 2018). The resulting daily ET_a series have residual gap-filling uncertainty that propagates to the seasonal totals reported here. Third, the analysis treats the EC measurements as the ground truth, but EC has its own known errors including energy balance closure failure (typically 10 to 30 percent under closure; Wilson et al., 2002; Bambach et al., 2022) and footprint heterogeneity at the field scale (Kljun et al., 2015). The EC values reported here have undergone footprint correction and energy balance ratio screening, but residual EC uncertainty remains a component of the apparent OpenET model errors. Independent validation using lysimeter measurements or surface renewal techniques would partially decouple the OpenET model errors from the EC measurement uncertainty.

The OpenET architectural diagnoses are based on the model's behavior in this single young pistachio orchard. The Ensemble underperformance documented here is consistent with the architectural fit thesis but does not generalize a critique of the Ensemble approach beyond young sparse canopy systems; the Volk et al. (2024) continental-scale Ensemble validation supports the platform default for the broader crop climate combinations on which it was originally tested. The qualitative findings of this study (the dual use case framework, the OpenET architectural diagnoses, the structural temporal redistribution of the cover crop signal, and the non-linear canopy maturation trajectory) are robust against the documented uncertainties because their qualitative direction holds across plausible perturbations. The specific magnitudes (the 150 mm growing season ET_a shortfall, the year-7 NC peak K_a of 0.95, the +0.10 to +0.26 April CC-NC differential) are field-scale point estimates that combine genuine treatment effects with EC measurement uncertainty (5 to 10 percent typical for seasonal totals; Bambach et al.,

2022), gap-filling uncertainty, and remaining model bias. The point estimate magnitudes should be interpreted within these uncertainty bounds and should be quantified through multi-site replication in future work.

5. Conclusions

This study evaluated the six OpenET models and the OpenET Ensemble against EC ET_a measurements in adjacent young pistachio orchards under winter cover crop (CC) and bare (NC) management in California's Sacramento Valley over three growing seasons and three cover crop winter seasons (April 2023 to April 2026; tree ages 5 to 7). The validation evaluated each product on two distinct skills: absolute ET_a accuracy and recovery of the CC-versus-NC differential. Five conclusions follow from the validation results.

First, two distinct OpenET products emerge as best on two distinct use cases. SIMS achieved the lowest monthly RMSE (19.0 mm per month in CC, 20.5 in NC) for absolute ET_a accuracy and the smallest CC bias (-0.05 mm per day) of any product. DisALEXI achieved the lowest mean |DOD| (20 mm) and recovered the EC sign of the cover crop ET_a contrast in 6 of 6 seasons. No single product was best on both use cases. The divergence is structural: SIMS' reflectance-based dual-K_c architecture matches the young drip-irrigated orchard for absolute ET_a but does not respond differentially to interrow cover crop versus bare soil when pistachio NDVI dominates the vegetation index input. DisALEXI's two-source surface energy balance partitions soil and canopy components separately and preserves the interrow treatment difference.

Second, the OpenET Ensemble underperforms both leading individual models. Ensemble monthly RMSE exceeded SIMS by approximately 4 mm per month in CC and 6 mm per month in NC, and the Ensemble missed the 2025 cover crop signal reversal that EC measured at -36 mm. The Ensemble's equal-weight aggregation inherits the systematic negative bias of its

residual surface energy balance constituents in this orchard system, producing a structural ET_a underestimate of approximately 100 to 140 mm per growing season at the orchard level. The Ensemble should not be used as the default product for either volumetric water accounting or signal-detection accuracy under SGMA in young pistachio. This finding is scoped to young sparse-canopy orchards; the Volk et al. (2024) continental-scale Ensemble validation supports the platform default for the broader crop-climate combinations on which it was originally tested.

Third, EC peak K_a rose from 0.57 in year 5 to 0.95 in year 7 NC, approaching but not reaching Goldhamer 1985's mature orchard peak K_c of 1.19 (20 percent shortfall) and Bellvert et al.'s 2018 mature orchard peak K_a of 1.10 (14 percent shortfall). None of the seven OpenET products tracked this canopy maturation trajectory: deviations at the year-7 NC peak window ranged from -12 to -34 percent across the six non-PT-JPL products, with the OpenET Ensemble underestimating year-7 NC peak K_a by 22 percent. The young orchard K_a curve documented here under the bi-monthly convention provides a quantitative anchor for sixth- and seventh-leaf pistachio that has not previously been available at field scale in California.

Fourth, the EC-measured cover crop ET_a signal evolved structurally across the three growing seasons, ranging from +36 mm (year 5) to +6 mm (year 6) to -36 mm (year 7). The 2025 sign reversal arose because the canopy maturation signal in NC outpaced the canopy maturation in CC, with the year-7 NC peak K_a of 0.95 versus CC peak K_a of 0.82 (Oct 1-15 window for both treatments) indicates that NC trees expanded canopy more aggressively than CC trees in the canopy dominated months. Two candidate mechanisms (direct competition for early spring soil water and canopy size differences) are consistent with this pattern, but the data here cannot fully separate them. Single year differencing is therefore not a reliable estimator of the long run cover crop ET_a cost in young orchard systems. The pooled three-year-mean April-

to-October contrast was -5 mm, less than 1 percent of seasonal ET_a, which obscures the within season redistribution.

Fifth, the bi-monthly K_a structure shows that the cover crop ET_a signal is structural in time rather than uniform across the growing season. CC K_a exceeded NC by +0.10 to +0.26 in April, when cover crop transpiration peaked before termination; was near zero by late May; and turned negative from June onward as pistachio canopy demand exceeded the residue evaporation that remained in the cover cropped interrow. The within season redistribution is invisible in seasonal mean K_a. Practice based ET_a attribution under SGMA monitoring would benefit from window resolved rather than seasonally aggregated comparison, particularly during April when CC and NC profiles diverge most.

The validation results support hypothesis H3 (no single OpenET product leads on both absolute accuracy and signal detection) and exceed the H2 threshold (Ensemble beats median individual model by 18 percent in CC and 21 percent in NC, both above the 10 percent specification). Hypothesis H1, which predicted that mean Ka during the cover crop season in CC would exceed the NC value by at least 10 percent, is partially supported: the April CC versus NC Ka differential of +0.10 to +0.26 against an NC April Ka baseline of approximately 0.27 to 0.33 corresponds to a 45 to 115 percent CC excess in the cover crop active windows, far exceeding the 10 percent threshold; however, the pooled three-year-mean April-to-October contrast was only +2 mm or less than 0.5 percent of seasonal ETa, which falls below the 10 percent threshold at the seasonal scale.

The implications for OpenET use in young California pistachio are direct. Volumetric water accounting under SGMA is best served by SIMS. Signal-detection accuracy of management interventions is best served by DisALEXI. The equal-weight Ensemble is

suboptimal for either application in young orchard systems. The bi-monthly K_a curves reported here provide a directly usable irrigation scheduling and grower attribution resource, with the caveat that single-site documentation requires multi-site validation before being treated as a universal benchmark for young California pistachio. A multi-site network of three to five young pistachio orchards instrumented with EC towers, paired by management treatment where possible, would establish the variance in the year-by-year K_a trajectory and refine the young-orchard K_c benchmarks proposed here.

These findings demonstrate that OpenET product selection should be governed by the management objective rather than by a single accuracy ranking, because products optimized for accurate absolute water accounting are not necessarily best suited for detecting treatment-scale management effects, and vice versa. In these young pistachio orchards, the two objectives separated cleanly: SIMS provided the most accurate absolute ET_a for SGMA volumetric accounting, whereas DisALEXI most reliably detected the CC ET_a signal for management attribution. More broadly, as satellite ET products are increasingly used both to account for consumptive use and to credit on-farm practices, validation and product choice should be reported against the specific use case, and a single product should not be assumed to serve both. This distinction is likely to matter most in sparse-canopy, establishment-phase orchards and other heterogeneous systems where absolute accuracy and differential sensitivity are most likely to diverge.

Acknowledgements

This work was fully funded by USDA NIFA Award #2021-68012-35914. Thank you to Bullseye Farms for allowing us to conduct this research on their private orchard. Special thanks to Aaron Guerra, Ali Ghorbanpour, Anish Sapkota, Benny Briggs, Cassandra Bonfil, Felix Ogunmokun, Floyid Nicolas, Gento Shimamura, Ian Gomez, Isabella Burnett, Krista Blide, Matthew Maciosek, Nicolas Almeida, Sidd Dala, Usama Al-Dughaishi, William Lennon, and Zixuan Gan for assistance with equipment installation and data collection.

References

Abatzoglou, J.T., 2013. Development of gridded surface meteorological data for ecological applications and modelling. Intl Journal of Climatology 33, 121–131. https://doi.org/10.1002/joc.3413.

Adams, C.B., Cosner, J., 2025. Field pea cardinal temperatures, growth and vigor traits of winter- and spring-adapted germplasm at germination and seedling stages. Sci Rep 15, 21759. https://doi.org/10.1038/s41598-025-06342-w.

Alfieri, J.G., Kustas, W.P., Prueger, J.H., McKee, L.G., Hipps, L.E., Gao, F., 2019. A multi-year intercomparison of micrometeorological observations at adjacent vineyards in california's central valley during grapex. Irrig Sci 37, 345–357. https://doi.org/10.1007/s00271-018-0599-3.

Allen, R., Irmak, A., Trezza, R., Hendrickx, J.M.H., Bastiaanssen, W., Kjaersgaard, J., 2011. Satellite-based et estimation in agriculture using sebal and metric. Hydrological Processes 25, 4011–4027. https://doi.org/10.1002/hyp.8408.

Allen, R.G., Burnett, B., Kramber, W., Huntington, J., Kjaersgaard, J., Kilic, A., Kelly, C., Trezza, R., 2013. Automated calibration of the metric-landsat evapotranspiration process. J American Water Resour Assoc 49, 563–576. https://doi.org/10.1111/jawr.12056.

Allen, R.G., Pereira, L.S., 2009. Estimating crop coefficients from fraction of ground cover and height. Irrig Sci 28, 17–34. https://doi.org/10.1007/s00271-009-0182-z.

Allen, R.G., Pereira, L.S., Raes, D., Smith, M., 1998. FAO irrigation and drainage paper no. 56. crop evapotranspiration (guidelines for computing crop water requirements). FAO, Rome.

Allen, R.G., Tasumi, M., Morse, A., Trezza, R., 2005. Satellite-based evapotranspiration by energy balance for western states water management, in: Impacts of Global Climate Change. Presented at the World Water and Environmental Resources Congress 2005, American Society of Civil Engineers, Anchorage, Alaska, United States, pp. 1–18. https://doi.org/10.1061/40792(173)556.

Allen, R.G., Tasumi, M., Trezza, R., 2007. Satellite-based energy balance for mapping evapotranspiration with internalized calibration (metric)—model. J. Irrig. Drain Eng. 133, 380–394. https://doi.org/10.1061/(ASCE)0733-9437(2007)133:4(380).

Anderson, M., Gao, F., Knipper, K., Hain, C., Dulaney, W., Baldocchi, D., Eichelmann, E., Hemes, K., Yang, Y., Medellin-Azuara, J., Kustas, W., 2018. Field-scale assessment of land and water use change over the california delta using remote sensing. Remote Sensing 10, 889. https://doi.org/10.3390/rs10060889.

Anderson, M.C., Norman, J.M., Mecikalski, J.R., Otkin, J.A., Kustas, W.P., 2007. A climatological study of evapotranspiration and moisture stress across the continental united states based on thermal remote sensing: 1. model formulation. J. Geophys. Res. 112, 2006JD007506. https://doi.org/10.1029/2006JD007506.

Baldwin, R., Battany, M., Beede, R., Brar, G.S., Culumber, M., Ferguson, L., Fichtner, E., Gordon, P., Hanson, B., Havliand, D., Hembree, K., Kallsen, C.E., Sanden, B., Michailidas, T.J., Trouillas, F., Zaccaria, D., Harris, L., Stewart, D., 2020. Sample costs to establish and produce pistachios. Technical Report, UCCE ANR Agricultural Issues Center.

Bambach, N., Kustas, W., Alfieri, J., Prueger, J., Hipps, L., McKee, L., Castro, S.J., Volk, J., Alsina, M.M., McElrone, A.J., 2022. Evapotranspiration uncertainty at

micrometeorological scales: the impact of the eddy covariance energy imbalance and correction methods. Irrig Sci 40, 445–461. https://doi.org/10.1007/s00271-022-00783-1.
Basche, A.D., Kaspar, T.C., Archontoulis, S.V., Jaynes, D.B., Sauer, T.J., Parkin, T.B., Miguez, F.E., 2016. Soil water improvements with the long-term use of a winter rye cover crop. Agricultural Water Management 172, 40–50. https://doi.org/10.1016/j.agwat.2016.04.006.
Bastiaanssen, W.G.M., Menenti, M., Feddes, R.A., Holtslag, A.A.M., 1998. A remote sensing surface energy balance algorithm for land (sebal). 1. formulation. Journal of Hydrology 212–213, 198–212. https://doi.org/10.1016/S0022-1694(98)00253-4.
Bellvert, J., Adeline, K., Baram, S., Pierce, L., Sanden, B., Smart, D., 2018. Monitoring crop evapotranspiration and crop coefficients over an almond and pistachio orchard throughout remote sensing. Remote Sensing 10, 2001. https://doi.org/10.3390/rs10122001.
Bergtold, J.S., Ramsey, S., Maddy, L., Williams, J.R., 2019. A review of economic considerations for cover crops as a conservation practice. Renew. Agric. Food Syst. 34, 62–76. https://doi.org/10.1017/S1742170517000278.
Bethune, M.G., Selle, B., Wang, Q.J., 2008. Understanding and predicting deep percolation under surface irrigation. Water Resources Research 44, 2007WR006380. https://doi.org/10.1029/2007WR006380.
Blanco-Canqui, H., Mikha, M.M., Presley, D.R., Claassen, M.M., 2011. Addition of cover crops enhances no-till potential for improving soil physical properties. Soil Science Soc of Amer J 75, 1471–1482. https://doi.org/10.2136/sssaj2010.0430.
Blanco-Canqui, H., Ruis, S.J., 2020. Cover crop impacts on soil physical properties: a review. Soil Science Soc of Amer J 84, 1527–1576. https://doi.org/10.1002/saj2.20129.
Blanco-Canqui, H., Shaver, T.M., Lindquist, J.L., Shapiro, C.A., Elmore, R.W., Francis, C.A., Hergert, G.W., 2015. Cover crops and ecosystem services: insights from studies in temperate soils. Agron. J. 107, 2449–2474. https://doi.org/10.2134/agronj15.0086.
Bodner, G., Loiskandl, W., Kaul, H.-P., 2007. Cover crop evapotranspiration under semi-arid conditions using fao dual crop coefficient method with water stress compensation. Agricultural Water Management 93, 85–98. https://doi.org/10.1016/j.agwat.2007.06.010.
Borum, J., Bruno, E., Castle, S., Chiartas, J., Crowley, R., Decock, C., Delgado, C., DeVincentis, A., Dufour, R., Edwards, A., Flaherty, R., Flynn, M., Grimm, R., Hale, L., Light, S., Little, C., Lowell, K., Minshew, H., Nocco, M., Peterson, C., Roby, M., Roseman, J., Roth, A., Sandoval, S., Silva, S.A., Smet, E., Smither-Kopperl, M., Suvocarev, K., Waterhouse, H., Wauters, V., Williams, S., Zaccaria, D., 2024. Cover cropping in the SGMA era: a comprehensive overview of water impacts, policy implications, and recommendations for California's water managers, The Soil-Water Interface Expert Convening Series: Cover Crop Impacts on Water Budgets. California.
California Department of Food and Agriculture (CDFA), 2025. 2023-2024 California agricultural statistics review.
California Department of Water Resources (DWR), 2025. California's groundwater: bulletin 118 — update 2025. Public Draft, October 2025. California Department of Water Resources, Sacramento, CA.
Cao, Q., Wang, Z., Yang, X., Shen, Y., 2021. The effects of cocksfoot cover crop on soil water balance, evapotranspiration partitioning, and system production in an apple orchard on

the loess plateau of china. Soil and Tillage Research 205, 104788. https://doi.org/10.1016/j.still.2020.104788.
Carlisle, L., 2016. Factors influencing farmer adoption of soil health practices in the United States: a narrative review. Agroecol. Sustain. Food Syst. 40, 583–613. https://doi.org/10.1080/21683565.2016.1156596.
Chakraborty, P., Singh, J., Singh, N., Kumar, S., 2022. Assessing the influence of cover crop on soil water dynamics using soil moisture measurements and hydrus-1d simulations. Soil Science Soc of Amer J 86, 1538–1552. https://doi.org/10.1002/saj2.20477.
DeVincentis, A., Solis, S.S., Rice, S., Zaccaria, D., Snyder, R., Maskey, M., Gomes, A., Gaudin, A., Mitchell, J., 2022. Impacts of winter cover cropping on soil moisture and evapotranspiration in California's specialty crop fields may be minimal during winter months. Calif. Agr. 76, 37–45. https://doi.org/10.3733/ca.2022a0001.
DeVincentis, A.J., Solis, S.S., Bruno, E.M., Leavitt, A., Gomes, A., Rice, S., Zaccaria, D., 2020. Using cost-benefit analysis to understand adoption of winter cover cropping in california's specialty crop systems. Journal of Environmental Management 261, 110205. https://doi.org/10.1016/j.jenvman.2020.110205.
Dhungel, R., Anderson, R.G., French, A.N., Skaggs, T.H., Ajami, H., Wang, D., 2024. Intercomparison of citrus evapotranspiration among eddy covariance, openet ensemble models, and the water and energy balance model (baitsss). Agricultural Water Management 304, 109066. https://doi.org/10.1016/j.agwat.2024.109066.
Diffenbaugh, N.S., Swain, D.L., Touma, D., 2015. Anthropogenic warming has increased drought risk in California. Proc. Natl. Acad. Sci. U.S.A. 112, 3931–3936. https://doi.org/10.1073/pnas.1422385112.
Drechsler, K., Fulton, A., Kisekka, I., 2022. Crop coefficients and water use of young almond orchards. Irrig Sci 40, 379–395. https://doi.org/10.1007/s00271-022-00786-y.
Dunn, M., Ulrich-Schad, J.D., Prokopy, L.S., Myers, R.L., Watts, C.R., Scanlon, K., 2016. Perceptions and use of cover crops among early adopters: findings from a national survey. Journal of Soil and Water Conservation 71, 29–40. https://doi.org/10.2489/jswc.71.1.29.
Evett, S.R., Steiner, J.L., 1995. Precision of neutron scattering and capacitance type soil water content gauges from field calibration. Soil Science Soc of Amer J 59, 961–968. https://doi.org/10.2136/sssaj1995.03615995005900040001x.
Faunt, C.C., Sneed, M., Traum, J., Brandt, J.T., 2016. Water availability and land subsidence in the central valley, california, usa. Hydrogeol J 24, 675–684. https://doi.org/10.1007/s10040-015-1339-x.
Fernando, M., Scott, N., Shrestha, A., Gao, S., Hale, L., 2024. A native plant species cover crop positively impacted vineyard water dynamics, soil health, and vine vigor. Agriculture, Ecosystems & Environment 367, 108972. https://doi.org/10.1016/j.agee.2024.108972.
Firoozi, F., Alavipanah, S.K., Hosseini, S.Z., Asgari, S., Malamiri, H.R.G., Rahimi, K., 2023. Remotely sensed and empirical reference evapotranspiration models to derive crop coefficients for pistachios in the central basin of iran. Iran J Sci Technol Trans Civ Eng 47, 3999–4019. https://doi.org/10.1007/s40996-023-01169-9.
Fisher, J.B., Melton, F., Middleton, E., Hain, C., Anderson, M., Allen, R., McCabe, M.F., Hook, S., Baldocchi, D., Townsend, P.A., Kilic, A., Tu, K., Miralles, D.D., Perret, J., Lagouarde, J.-P., Waliser, D., Purdy, A.J., French, A., Schimel, D., Famiglietti, J.S., Stephens, G., Wood, E.F., 2017. The future of evapotranspiration: global requirements

for ecosystem functioning, carbon and climate feedbacks, agricultural management, and water resources: the future of evapotranspiration. Water Resour. Res. 53, 2618–2626. https://doi.org/10.1002/2016WR020175.
Fisher, J.B., Tu, K.P., Baldocchi, D.D., 2008. Global estimates of the land–atmosphere water flux based on monthly avhrr and islscp-ii data, validated at 16 fluxnet sites. Remote Sensing of Environment 112, 901–919. https://doi.org/10.1016/j.rse.2007.06.025.
Flynn, M.T., Guerrero-Medina, O., McDonald, I.F., Anika, J.T., Ware, E.C., Paw U, K.T., Gaudin, A.C., Fenster, T.L., Lundgren, J.G., Harter, T., Sandoval Solis, S., Suvočarev, K., 2025. A case study of evapotranspiration at five almond orchards on a spectrum of conventional to regenerative management. California Agriculture 79. https://doi.org/10.3733/001c.133243.
Foken, T., Aubinet, M., Leuning, R., 2012. The eddy covariance method, in: Aubinet, M., Vesala, T., Papale, D. (Eds.), Eddy Covariance. Springer Netherlands, Dordrecht, pp. 1–19. https://doi.org/10.1007/978-94-007-2351-1_1.
Folorunso, O.A., Rolston, D.E., Prichard, T., Loui, D.T., 1992. Soil surface strength and infiltration rate as affected by winter cover crops. Soil Technology 5, 189–197. https://doi.org/10.1016/0933-3630(92)90021-R.
Gabriel, J.L., Muñoz-Carpena, R., Quemada, M., 2012. The role of cover crops in irrigated systems: water balance, nitrate leaching and soil mineral nitrogen accumulation. Agriculture, Ecosystems & Environment 155, 50–61. https://doi.org/10.1016/j.agee.2012.03.021.
Garba, I.I., Bell, L.W., Williams, A., 2022. Cover crop legacy impacts on soil water and nitrogen dynamics, and on subsequent crop yields in drylands: a meta-analysis. Agron. Sustain. Dev. 42, 34. https://doi.org/10.1007/s13593-022-00760-0.
Gassman, P.W., Williams, J.R., Wang, X., Saleh, A., Osei, E., Hauck, L.M., Izaurralde, R.C., Flowers, J.D., 2010. Invited review article: the agricultural policy/environmental extender (apex) model: an emerging tool for landscape and watershed environmental analyses. Transactions of the ASABE 53, 711–740. https://doi.org/10.13031/2013.30078.
Gaze, S.R., Stalham, M.A., Allen, E.J., 2002. Accuracy of the neutron probe for measuring changes in soil water storage under potatoes. J. Agric. Sci. 138, 135–152. https://doi.org/10.1017/S0021859601001654.
Goldhamer, D.A., Kjelgren, R.K., Beede, R.H., Williams, L.E., Moore, J.M., Lane, J., Weinberger, G., Menezes, J., Jr., 1985. Water use requirements of pistachio trees and response to water stress. Annual Report of the California Pistachio Commission, Crop Year 1984-1985, 85–92.
Goring, D.G., Nikora, V.I., 2002. Despiking acoustic doppler velocimeter data. J. Hydraul. Eng. 128, 117–126. https://doi.org/10.1061/(ASCE)0733-9429(2002)128:1(117).
Gould, K., Rudnick, J., 2018. Adoption of cover crops in california.
Gribov, A., Krivoruchko, K., 2020. Empirical bayesian kriging implementation and usage. Sci. Total Environ. 722, 137290. https://doi.org/10.1016/j.scitotenv.2020.137290.
Hao, X., Abou Najm, M., Steenwerth, K.L., Nocco, M.A., Basset, C., Daccache, A., 2023. Are there universal soil responses to cover cropping? a systematic review. Science of The Total Environment 861, 160600. https://doi.org/10.1016/j.scitotenv.2022.160600.
Haruna, S.I., Eichas, R.C., Peters, O.M., Farmer, A.C., Lackey, D.Q., Nichols, J.E., Peterson, W.H., Slone, N.A., 2022. In situ water infiltration: influence of cover crops after growth termination. Soil Science Soc of Amer J 86, 769–780. https://doi.org/10.1002/saj2.20390.

Iniesta, F., Testi, L., Goldhamer, D.A., Fereres, E., 2008. Quantifying reductions in consumptive water use under regulated deficit irrigation in pistachio (pistacia vera l.). Agricultural Water Management 95, 877–886. https://doi.org/10.1016/j.agwat.2008.01.013.

Irmak, A., Ratcliffe, I., Ranade, P., Hubbard, K.G., Singh, R.K., Kamble, B., Kjaersgaard, J., 2011. Estimation of land surface evapotranspiration with a satellite remote sensing procedure. Great Plains Research 21, 73–88.

Izaurralde, R.C., Williams, J.R., McGill, W.B., Rosenberg, N.J., Jakas, M.C.Q., 2006. Simulating soil c dynamics with epic: model description and testing against long-term data. Ecological Modelling 192, 362–384. https://doi.org/10.1016/j.ecolmodel.2005.07.010.

Jensen, M.E., Allen, R.G. (Eds.), 2016. Evaporation, evapotranspiration, and irrigation water requirements, Second. ed. American Society of Civil Engineers, Reston, VA. https://doi.org/10.1061/9780784414057.

Jin, Y., He, R., Marino, G., Whiting, M., Kent, E., Sanden, B.L., Culumber, M., Ferguson, L., Little, C., Grattan, S., Paw U, K.T., Lagos, L.O., Snyder, R.L., Zaccaria, D., 2018. Spatially variable evapotranspiration over salt affected pistachio orchards analyzed with satellite remote sensing estimates. Agricultural and Forest Meteorology 262, 178–191. https://doi.org/10.1016/j.agrformet.2018.07.004.

Joyce, B.A., Wallender, W.W., Mitchell, J.P., Huyck, L.M., Temple, S.R., Brostrom, P.N., Hsiao, T.C., 2002. Infiltration and soil water storage under winter cover cropping in span class="nocase">california's span class="nocase">sacramentovalley. Transactions of the ASAE 45. https://doi.org/10.13031/2013.8526.

Kader, M.A., Singha, A., Begum, M.A., Jewel, A., Khan, F.H., Khan, N.I., 2019. Mulching as water-saving technique in dryland agriculture: review article. Bull Natl Res Cent 43, 147. https://doi.org/10.1186/s42269-019-0186-7.

Kaimal, J.C., Finnigan, J.J., 1994. Atmospheric boundary layer flows: their structure and measurement. Oxford University Press, New York.

Kanber, R., Yazar, A., □Nder, S., K□ksal, H., 1993. Irrigation response of pistachio (pistacia vera l.). Irrig Sci 14. https://doi.org/10.1007/BF00195000.

Kandhway, A., Scarpare, F., Liu, M., Nelson, R., Adam, J.C., Anderson, R.G., Conklin, M.H., Safeeq, M., 2025. Water use dynamics of almond and pistachio crops in the mediterranean region amid climate change. Agric. Water Manage. 307, 109219. https://doi.org/10.1016/j.agwat.2024.109219.

Kermani, M.M., Salehi, F., 2006. Determination of pistachio crop evapotranspiration (etc). Acta Hortic. 441–448. https://doi.org/10.17660/ActaHortic.2006.726.71.

Kiniry, J.R., Williams, J.R., Gassman, P.W., Debaeke, P., 1992. A general, process-oriented model for two competing plant species. Transactions of the ASAE 35, 801–810. https://doi.org/10.13031/2013.28665.

Kljun, N., Calanca, P., Rotach, M.W., Schmid, H.P., 2015. A simple two-dimensional parameterisation for flux footprint prediction (ffp). Geosci. Model Dev. 8, 3695–3713. https://doi.org/10.5194/gmd-8-3695-2015.

Knipper, K., Anderson, M., Bambach, N., Kustas, W., Gao, F., Zahn, E., Hain, C., McElrone, A., Belfiore, O.R., Castro, S., Alsina, M.M., Saa, S., 2022. Evaluation of partitioned evaporation and transpiration estimates within the disalexi modeling framework over irrigated crops in california. Remote Sensing 15, 68. https://doi.org/10.3390/rs15010068.

Knipper, K., Anderson, M., Bambach, N., Melton, F., Ellis, Z., Yang, Y., Volk, J., McElrone, A.J., Kustas, W., Roby, M., Carrara, W., Castro, S., Kilic, A., Fisher, J.B., Ruhoff, A., Senay, G.B., Morton, C., Saa, S., Allen, R.G., 2024. A comparative analysis of openet for evaluating evapotranspiration in california almond orchards. Agricultural and Forest Meteorology 355, 110146. https://doi.org/10.1016/j.agrformet.2024.110146.

Koudahe, K., Allen, S.C., Djaman, K., 2022. Critical review of the impact of cover crops on soil properties. International Soil and Water Conservation Research 10, 343–354. https://doi.org/10.1016/j.iswcr.2022.03.003.

Krivoruchko, K., Gribov, A., 2019. Evaluation of empirical bayesian kriging. Spatial Statistics 32, 100368. https://doi.org/10.1016/j.spasta.2019.100368.

Laipelt, L., Henrique Bloedow Kayser, R., Santos Fleischmann, A., Ruhoff, A., Bastiaanssen, W., Erickson, T.A., Melton, F., 2021. Long-term monitoring of evapotranspiration using the sebal algorithm and google earth engine cloud computing. ISPRS Journal of Photogrammetry and Remote Sensing 178, 81–96. https://doi.org/10.1016/j.isprsjprs.2021.05.018.

Leys, C., Ley, C., Klein, O., Bernard, P., Licata, L., 2013. Detecting outliers: do not use standard deviation around the mean, use absolute deviation around the median. Journal of Experimental Social Psychology 49, 764–766. https://doi.org/10.1016/j.jesp.2013.03.013.

Lobell, D.B., Field, C.B., Cahill, K.N., Bonfils, C., 2006. Impacts of future climate change on california perennial crop yields: model projections with climate and crop uncertainties. Agricultural and Forest Meteorology 141, 208–218. https://doi.org/10.1016/j.agrformet.2006.10.006.

Lu, Y.C., Watkins, K.B., Teasdale, J.R., Abdul-Baki, A.A., 2000. Cover crops in sustainable food production. Food Reviews International 16, 121–157. https://doi.org/10.1081/FRI-100100285.

Lubell, M., Blomquist, W., Beutler, L., 2020. Sustainable groundwater management in california: a grand experiment in environmental governance. Society & Natural Resources 33, 1447–1467. https://doi.org/10.1080/08941920.2020.1833617.

Mall, N.K., Herman, J.D., 2019. Water shortage risks from perennial crop expansion in california's central valley. Environ. Res. Lett. 14, 104014. https://doi.org/10.1088/1748-9326/ab4035.

Marino, G., Zaccaria, D., Lagos, L.O., Souto, C., Kent, E.R., Grattan, S.R., Shapiro, K., Sanden, B.L., Snyder, R.L., 2021. Effects of salinity and sodicity on the seasonal dynamics of actual evapotranspiration and surface energy balance components in mature micro-irrigated pistachio orchards. Irrig Sci 39, 23–43. https://doi.org/10.1007/s00271-020-00694-z.

Marino, G., Zaccaria, D., Snyder, R.L., Lagos, O., Lampinen, B.D., Ferguson, L., Grattan, S.R., Little, C., Shapiro, K., Maskey, M.L., Corwin, D.L., Scudiero, E., Sanden, B.L., 2019. Actual evapotranspiration and tree performance of mature micro-irrigated pistachio orchards grown on saline-sodic soils in the san joaquin valley of california. Agriculture 9, 76. https://doi.org/10.3390/agriculture9040076.

Mason, R., Gorres, J., Faulkner, J.W., Doro, L., Merrill, S.C., 2020. Calibrating the apex model for simulations of environmental and agronomic outcomes on dairy farms in the northeast u.s.: a step-by-step example. Applied Engineering in Agriculture 36, 281–301. https://doi.org/10.13031/aea.13679.

Massman, W.J., 2000. A simple method for estimating frequency response corrections for eddy covariance systems. Agricultural and Forest Meteorology 104, 185–198. https://doi.org/10.1016/S0168-1923(00)00164-7.

Melton, F.S., Huntington, J., Grimm, R., Herring, J., Hall, M., Rollison, D., Erickson, T., Allen, R., Anderson, M., Fisher, J.B., Kilic, A., Senay, G.B., Volk, J., Hain, C., Johnson, L., Ruhoff, A., Blankenau, P., Bromley, M., Carrara, W., Daudert, B., Doherty, C., Dunkerly, C., Friedrichs, M., Guzman, A., Halverson, G., Hansen, J., Harding, J., Kang, Y., Ketchum, D., Minor, B., Morton, C., Ortega-Salazar, S., Ott, T., Ozdogan, M., ReVelle, P.M., Schull, M., Wang, C., Yang, Y., Anderson, R.G., 2022. OpenET: filling a critical data gap in water management for the western united states. J American Water Resour Assoc 58, 971–994. https://doi.org/10.1111/1752-1688.12956.

Melton, F.S., Johnson, L.F., Lund, C.P., Pierce, L.L., Michaelis, A.R., Hiatt, S.H., Guzman, A., Adhikari, D.D., Purdy, A.J., Rosevelt, C., Votava, P., Trout, T.J., Temesgen, B., Frame, K., Sheffner, E.J., Nemani, R.R., 2012. Satellite irrigation management support with the terrestrial observation and prediction system: a framework for integration of satellite and surface observations to support improvements in agricultural water resource management. IEEE J. Sel. Top. Appl. Earth Observations Remote Sensing 5, 1709–1721. https://doi.org/10.1109/JSTARS.2012.2214474.

Mitchell, J.P., Peters, D.W., Shennan, C., 1999. Changes in soil water storage in winter fallowed and cover cropped soils. J. Sustain. Agric. 15, 19–31. https://doi.org/10.1300/J064v15n02_04.

Mitchell, J.P., Shrestha, A., Irmak, S., 2015. Trade-offs between winter cover crop production and soil water depletion in the San Joaquin valley, California. J. Soil Water Conserv. 70, 430–440. https://doi.org/10.2489/jswc.70.6.430.

Monteith, J.L., 1965. Evaporation and environment. Symposia of the Society for Experimental Biology 19, 205–234.

Moore, C.J., 1986. Frequency response corrections for eddy correlation systems. Boundary-Layer Meteorol 37, 17–35. https://doi.org/10.1007/BF00122754.

Moore, E.A., Norton, U., 2024. Improving semi-arid agroecosystem services with cover crop mixes. PLoS ONE 19, e0306567. https://doi.org/10.1371/journal.pone.0306567.

Moriasi, D.N., Arnold, J.G., Liew, M.W.V., Bingner, R.L., Harmel, R.D., Veith, T.L., 2007. Model evaluation guidelines for systematic quantification of accuracy in watershed simulations. Transactions of the ASABE 50, 885–900. https://doi.org/10.13031/2013.23153.

Moriasi, D.N., King, K.W., Bosch, D.D., Bjorneberg, D.L., Teet, S., Guzman, J.A., Williams, M.R., 2016. Framework to parameterize and validate apex to support deployment of the nutrient tracking tool. Agric. Water Manage. 177, 146–164. https://doi.org/10.1016/j.agwat.2016.07.009.

Munna, M.N.H., Lal, R., 2025. Impacts of cover cropping and organic amendments on soil physical quality under temperate climate. Cogent Food & Agriculture 11, 2467452. https://doi.org/10.1080/23311932.2025.2467452.

Nash, J.E., Sutcliffe, J.V., 1970. River flow forecasting through conceptual models part i — a discussion of principles. Journal of Hydrology 10, 282–290. https://doi.org/10.1016/0022-1694(70)90255-6.

Nielsen, D.C., Lyon, D.J., Hergert, G.W., Higgins, R.K., Calderón, F.J., Vigil, M.F., 2015. Cover crop mixtures do not use water differently than single-species plantings. Agron. J. 107, 1025–1038. https://doi.org/10.2134/agronj14.0504.

Oregon State University, 2010. Peas - Western Oregon. https://horticulture.oregonstate.edu/oregon-vegetables/peas-western-oregon-0 (accessed 9 May 2026).

Papale, D., Reichstein, M., Aubinet, M., Canfora, E., Bernhofer, C., Kutsch, W., Longdoz, B., Rambal, S., Valentini, R., Vesala, T., Yakir, D., 2006. Towards a standardized processing of net ecosystem exchange measured with eddy covariance technique: algorithms and uncertainty estimation. Biogeosciences 3, 571–583. https://doi.org/10.5194/bg-3-571-2006.

Pastorello, G., Trotta, C., Canfora, E., Chu, H., Christianson, D., Cheah, Y.-W., Poindexter, C., Chen, J., Elbashandy, A., Humphrey, M., Isaac, P., Polidori, D., Reichstein, M., Ribeca, A., Van Ingen, C., Vuichard, N., Zhang, L., Amiro, B., Ammann, C., Arain, M.A., Ardö, J., Arkebauer, T., Arndt, S.K., Arriga, N., Aubinet, M., Aurela, M., Baldocchi, D., Barr, A., Beamesderfer, E., Marchesini, L.B., Bergeron, O., Beringer, J., Bernhofer, C., Berveiller, D., Billesbach, D., Black, T.A., Blanken, P.D., Bohrer, G., Boike, J., Bolstad, P.V., Bonal, D., Bonnefond, J.-M., Bowling, D.R., Bracho, R., Brodeur, J., Brümmer, C., Buchmann, N., Burban, B., Burns, S.P., Buysse, P., Cale, P., Cavagna, M., Cellier, P., Chen, S., Chini, I., Christensen, T.R., Cleverly, J., Collalti, A., Consalvo, C., Cook, B.D., Cook, D., Coursolle, C., Cremonese, E., Curtis, P.S., D'Andrea, E., Da Rocha, H., Dai, X., Davis, K.J., Cinti, B.D., Grandcourt, A.D., Ligne, A.D., De Oliveira, R.C., Delpierre, N., Desai, A.R., Di Bella, C.M., Tommasi, P.D., Dolman, H., Domingo, F., Dong, G., Dore, S., Duce, P., Dufrêne, E., Dunn, A., Dušek, J., Eamus, D., Eichelmann, U., ElKhidir, H.A.M., Eugster, W., Ewenz, C.M., Ewers, B., Famulari, D., Fares, S., Feigenwinter, I., Feitz, A., Fensholt, R., Filippa, G., Fischer, M., Frank, J., Galvagno, M., Gharun, M., Gianelle, D., Gielen, B., Gioli, B., Gitelson, A., Goded, I., Goeckede, M., Goldstein, A.H., Gough, C.M., Goulden, M.L., Graf, A., Griebel, A., Gruening, C., Grünwald, T., Hammerle, A., Han, S., Han, X., Hansen, B.U., Hanson, C., Hatakka, J., He, Y., Hehn, M., Heinesch, B., Hinko-Najera, N., Hörtnagl, L., Hutley, L., Ibrom, A., Ikawa, H., Jackowicz-Korczynski, M., Janouš, D., Jans, W., Jassal, R., Jiang, S., Kato, T., Khomik, M., Klatt, J., Knohl, A., Knox, S., Kobayashi, H., Koerber, G., Kolle, O., Kosugi, Y., Kotani, A., Kowalski, A., Kruijt, B., Kurbatova, J., Kutsch, W.L., Kwon, H., Launiainen, S., Laurila, T., Law, B., Leuning, R., Li, Yingnian, Liddell, M., Limousin, J.-M., Lion, M., Liska, A.J., Lohila, A., López-Ballesteros, A., López-Blanco, E., Loubet, B., Loustau, D., Lucas-Moffat, A., Lüers, J., Ma, S., Macfarlane, C., Magliulo, V., Maier, R., Mammarella, I., Manca, G., Marcolla, B., Margolis, H.A., Marras, S., Massman, W., Mastepanov, M., Matamala, R., Matthes, J.H., Mazzenga, F., McCaughey, H., McHugh, I., McMillan, A.M.S., Merbold, L., Meyer, W., Meyers, T., Miller, S.D., Minerbi, S., Moderow, U., Monson, R.K., Montagnani, L., Moore, C.E., Moors, E., Moreaux, V., Moureaux, C., Munger, J.W., Nakai, T., Neirynck, J., Nesic, Z., Nicolini, G., Noormets, A., Northwood, M., Nosetto, M., Nouvellon, Y., Novick, K., Oechel, W., Olesen, J.E., Ourcival, J.-M., Papuga, S.A., Parmentier, F.-J., Paul-Limoges, E., Pavelka, M., Peichl, M., Pendall, E., Phillips, R.P., Pilegaard, K., Pirk, N., Posse, G., Powell, T., Prasse, H., Prober, S.M., Rambal, S., Rannik, Ü., Raz-Yaseef, N., Rebmann, C., Reed, D., Dios, V.R.D., Restrepo-Coupe, N., Reverter, B.R., Roland, M., Sabbatini, S., Sachs, T.,

Saleska, S.R., Sánchez-Cañete, E.P., Sanchez-Mejia, Z.M., Schmid, H.P., Schmidt, M., Schneider, K., Schrader, F., Schroder, I., Scott, R.L., Sedlák, P., Serrano-Ortíz, P., Shao, C., Shi, P., Shironya, I., Siebicke, L., Šigut, L., Silberstein, R., Sirca, C., Spano, D., Steinbrecher, R., Stevens, R.M., Sturtevant, C., Suyker, A., Tagesson, T., Takanashi, S., Tang, Y., Tapper, N., Thom, J., Tomassucci, M., Tuovinen, J.-P., Urbanski, S., Valentini, R., Van Der Molen, M., Van Gorsel, E., Van Huissteden, K., Varlagin, A., Verfaillie, J., Vesala, T., Vincke, C., Vitale, D., Vygodskaya, N., Walker, J.P., Walter-Shea, E., Wang, H., Weber, R., Westermann, S., Wille, C., Wofsy, S., Wohlfahrt, G., Wolf, S., Woodgate, W., Li, Yuelin, Zampedri, R., Zhang, J., Zhou, G., Zona, D., Agarwal, D., Biraud, S., Torn, M., Papale, D., 2020. The fluxnet2015 dataset and the oneflux processing pipeline for eddy covariance data. Sci Data 7, 225. https://doi.org/10.1038/s41597-020-0534-3.

Pathak, T., Maskey, M., Dahlberg, J., Kearns, F., Bali, K., Zaccaria, D., 2018. Climate change trends and impacts on California agriculture: a detailed review. Agronom. 8, 25. https://doi.org/10.3390/agronomy8030025.

Peddinti, S.R., 2026. Flux gap filling tool: mds and ml gap-filling for micrometeorological data.

Pereira, L.S., Paredes, P., Melton, F., Johnson, L., Wang, T., López-Urrea, R., Cancela, J.J., Allen, R.G., 2020. Prediction of crop coefficients from fraction of ground cover and height. background and validation using ground and remote sensing data. Agricultural Water Management 241, 106197. https://doi.org/10.1016/j.agwat.2020.106197.

Pruitt, W.O., Doorenbos, J., 1977. Empirical calibration, a requisite for evapotranspiration formulae based on daily or longer mean climatic data? Presented at the International Commission on Irrigation and Drainage.

Rahemi, M., Pakkish, Z., 2009. Determination of chilling and heat requirements of pistachio (pistacia vera l.) cultivars. Agricultural Sciences in China 8, 803–807. https://doi.org/10.1016/S1671-2927(08)60281-3.

Rahimzadegan, M., Janani, A., 2019. Estimating evapotranspiration of pistachio crop based on sebal algorithm using landsat 8 satellite imagery. Agric. Water Manag. 217, 383–390. https://doi.org/10.1016/j.agwat.2019.03.018.

Reichstein, M., Falge, E., Baldocchi, D., Papale, D., Aubinet, M., Berbigier, P., Bernhofer, C., Buchmann, N., Gilmanov, T., Granier, A., Grünwald, T., Havránková, K., Ilvesniemi, H., Janous, D., Knohl, A., Laurila, T., Lohila, A., Loustau, D., Matteucci, G., Meyers, T., Miglietta, F., Ourcival, J., Pumpanen, J., Rambal, S., Rotenberg, E., Sanz, M., Tenhunen, J., Seufert, G., Vaccari, F., Vesala, T., Yakir, D., Valentini, R., 2005. On the separation of net ecosystem exchange into assimilation and ecosystem respiration: review and improved algorithm. Global Change Biology 11, 1424–1439. https://doi.org/10.1111/j.1365-2486.2005.001002.x.

Sabiston, L., Sabie, R., Buenemann, M., Stringam, B., Fernald, A., 2024. Comparing field-scale eddy covariance measurements and crop coefficient estimates of alfalfa evapotranspiration to openet model estimates and exploring water budget implications in a dryland environment. Irrig Sci. https://doi.org/10.1007/s00271-024-00941-7.

Sainju, U.M., Singh, B.P., 1997. Winter cover crops for sustainable agricultural systems: influence on soil properties, water quality, and crop yields. HortSci 32, 21–28. https://doi.org/10.21273/HORTSCI.32.1.21.

Saleh, A., Niraula, R., Marek, G.W., Gowda, P.H., Brauer, D.K., Howell, T.A., 2018. Lysimetric evaluation of the apex model to simulate daily et for irrigated crops in the texas high plains. Transactions of the ASABE 61, 65–74. https://doi.org/10.13031/trans.11938.

Sanden, B.L., Ferguson, L., Reyes, H.C., Grattan, S.R., 2004. Effect of salinity on evapotranspiration and yield of san joaquin valley pistachios. Acta Hortic. 583–589. https://doi.org/10.17660/ActaHortic.2004.664.73.

Sastre, B., Marques, M.J., García-Díaz, A., Bienes, R., 2018. Three years of management with cover crops protecting sloping olive groves soils, carbon and water effects on gypsiferous soil. CATENA 171, 115–124. https://doi.org/10.1016/j.catena.2018.07.003.

Schomberg, H.H., White, K.E., Thompson, A.I., Bagley, G.A., Burke, A., Garst, G., Bybee-Finley, K.A., Mirsky, S.B., 2023. Interseeded cover crop mixtures influence soil water storage during the corn phase of corn-soybean-wheat no-till cropping systems. Agricultural Water Management 278, 108167. https://doi.org/10.1016/j.agwat.2023.108167.

Senay, G.B., 2018. Satellite psychrometric formulation of the operational simplified surface energy balance (ssebop) model for quantifying and mapping evapotranspiration. Applied Engineering in Agriculture 34, 555–566. https://doi.org/10.13031/aea.12614.

Senay, G.B., Bohms, S., Singh, R.K., Gowda, P.H., Velpuri, N.M., Alemu, H., Verdin, J.P., 2013. Operational evapotranspiration mapping using remote sensing and weather datasets: a new parameterization for the SSEB approach. J. American Water Resour. Assoc. 49, 577–591. https://doi.org/10.1111/jawr.12057.

Senay, G.B., Parrish, G.E.L., Schauer, M., Friedrichs, M., Khand, K., Boiko, O., Kagone, S., Dittmeier, R., Arab, S., Ji, L., 2023. Improving the operational simplified surface energy balance evapotranspiration model using the forcing and normalizing operation. Remote Sensing 15, 260. https://doi.org/10.3390/rs15010260.

Snapp, S.S., Swinton, S.M., Labarta, R., Mutch, D., Black, J.R., Leep, R., Nyiraneza, J., O'Neil, K., 2005. Evaluating cover crops for benefits, costs and performance within cropping system niches. Agron. J. 97, 322–332. https://doi.org/10.2134/agronj2005.0322a.

Soil Health Institute, 2019. Progress report: adoption of soil health systems based on data from the 2017 U.S. census of agriculture. https://soilhealthinstitute.org/app/uploads/2022/01/Soil-Health-Adoption-Overview_2017-Census-Report_FINAL.pdf (accessed 30 October 2024).

Steele, M.K., Coale, F.J., Hill, R.L., 2012. Winter annual cover crop impacts on no-till soil physical properties and organic matter. Soil Science Soc of Amer J 76, 2164–2173. https://doi.org/10.2136/sssaj2012.0008.

Steglich, E.M., Osorio, J., Doro, L., Jeong, J., Williams, J.R., 2023. Agricultural policy/environmental extender user's manual version 1501.

Tadesse, H.K., Moriasi, D.N., Gowda, P.H., Marek, G., Steiner, J.L., Brauer, D., Talebizadeh, M., Nelson, A., Starks, P., 2018. Evaluating evapotranspiration estimation methods in apex model for dryland cropping systems in a semi-arid region. Agricultural Water Management 206, 217–228. https://doi.org/10.1016/j.agwat.2018.04.007.

Tadesse, H.K., Moriasi, D.N., Gowda, P.H., Steiner, J.L., Talebizadeh, M., Nelson, A.M., Starks, P.J., Marek, G., 2019. Comparison of evapotranspiration simulation performance by apex model in dryland and irrigated cropping systems. J American Water Resour Assoc 55, 1009–1023. https://doi.org/10.1111/1752-1688.12759.

Tadesse, H.K., Moriasi, D.N., Gowda, P.H., Wagle, P., Starks, P.J., Steiner, J.L., Talebizadeh, M., Neel, J.P.S., Nelson, A.M., 2021. Comparison of evapotranspiration and biomass simulation in winter wheat under conventional and conservation tillage systems using

apex model. Ecohydrology & Hydrobiology 21, 55–66. https://doi.org/10.1016/j.ecohyd.2020.08.003.
Talebizadeh, M., Moriasi, D., Gowda, P., Steiner, J.L., Tadesse, H.K., Nelson, A.M., Starks, P., 2018. Simultaneous calibration of evapotranspiration and crop yield in agronomic system modeling using the apex model. Agricultural Water Management 208, 299–306. https://doi.org/10.1016/j.agwat.2018.06.043.
Tawalbeh, Z.M., Bawazir, A.S., Fernald, A., Sabie, R., Heerema, R.J., 2024. Assessing satellite-derived openet platform evapotranspiration of mature pecan orchard in the mesilla valley, new mexico. Remote Sensing 16, 1429. https://doi.org/10.3390/rs16081429.
Teasdale, J.R., Mohler, C.L., 1993. Light transmittance, soil temperature, and soil moisture under residue of hairy vetch and rye. Agronomy Journal 85, 673–680. https://doi.org/10.2134/agronj1993.00021962008500030029x.
Timlin, D., Chun, J.A., Meisinger, J., Kang, K., Fleisher, D., Staver, K., Doherty, C., Russ, A., 2019. Evaluation of the agricultural policy environmental extender (apex) for the chesapeake bay watershed. Agricultural Water Management 221, 477–485. https://doi.org/10.1016/j.agwat.2019.03.046.
Tootelian, D.H., 2023a. Projected pistachio production: 2023 through 2031.
Tootelian, D.H., 2023b. Projected pistachio production: 2023 through 2031.
Unger, P.W., Vigil, M.F., 1998. Cover crop effects on soil water relationships. Journal of Soil and Water Conservation.
United Nations University Institute for Water, Environment and Health (UNU INWEH), Madani, K., 2026. Global water bankruptcy: living beyond our hydrological means in the post crisis era. United Nations University Institute for Water, Environment and Health (UNU INWEH). https://doi.org/10.53328/INR26KAM001.
United States Department of Agriculture (USDA), 2026. Pistachios. https://www.fas.usda.gov/data/production/commodity/0577907 (accessed 13 January 2026).
Vanella, D., Peddinti, S.R., Kisekka, I., 2022. Unravelling soil water dynamics in almond orchards characterized by soil-heterogeneity using electrical resistivity tomography. Agricultural Water Management 269, 107652. https://doi.org/10.1016/j.agwat.2022.107652.
Vendig, I., Guzman, A., De La Cerda, G., Esquivel, K., Mayer, A.C., Ponisio, L., Bowles, T.M., 2023. Quantifying direct yield benefits of soil carbon increases from cover cropping. Nat Sustain 6, 1125–1134. https://doi.org/10.1038/s41893-023-01131-7.
Volk, J.M., Huntington, J.L., Melton, F.S., Allen, R., Anderson, M., Fisher, J.B., Kilic, A., Ruhoff, A., Senay, G.B., Minor, B., Morton, C., Ott, T., Johnson, L., Comini De Andrade, B., Carrara, W., Doherty, C.T., Dunkerly, C., Friedrichs, M., Guzman, A., Hain, C., Halverson, G., Kang, Y., Knipper, K., Laipelt, L., Ortega-Salazar, S., Pearson, C., Parrish, G.E.L., Purdy, A., ReVelle, P., Wang, T., Yang, Y., 2024. Assessing the accuracy of openet satellite-based evapotranspiration data to support water resource and land management applications. Nat Water 2, 193–205. https://doi.org/10.1038/s44221-023-00181-7.
Vukicevich, E., Lowery, T., Bowen, P., Úrbez-Torres, J.R., Hart, M., 2016. Cover crops to increase soil microbial diversity and mitigate decline in perennial agriculture. a review. Agron. Sustain. Dev. 36, 48. https://doi.org/10.1007/s13593-016-0385-7.

Wang, J., Zhang, S., Sainju, U.M., Ghimire, R., Zhao, F., 2021. A meta-analysis on cover crop impact on soil water storage, succeeding crop yield, and water-use efficiency. Agricultural Water Management 256, 107085. https://doi.org/10.1016/j.agwat.2021.107085.

Wang, X., Jeong, J., 2019. APEX-cute 4 user manual.

Wang, X., Williams, J.R., Gassman, P.W., Baffaut, C., Izaurralde, R.C., Jeong, J., Kiniry, J.R., 2012. EPIC and apex: model use, calibration, and validation. Transactions of the ASABE 55, 1447–1462. https://doi.org/10.13031/2013.42253.

Ward, P.R., Dunin, F.X., Micin, S.F., Williamson, D.R., 1998. Evaluating drainage responses in duplex soils in a mediterranean environment. Australian Journal of Soil Research 36, 509–524. https://doi.org/10.1071/S97082.

Ward, P.R., Flower, K.C., Cordingley, N., Weeks, C., Micin, S.F., 2012. Soil water balance with cover crops and conservation agriculture in a mediterranean climate. Field Crops Research 132, 33–39. https://doi.org/10.1016/j.fcr.2011.10.017.

Webb, E.K., Pearman, G.I., Leuning, R., 1980. Correction of flux measurements for density effects due to heat and water vapour transfer. Quart J Royal Meteoro Soc 106, 85–100. https://doi.org/10.1002/qj.49710644707.

Westling, F., Underwood, J., Örn, S., 2018. Light interception modelling using unstructured lidar data in avocado orchards. Computers and Electronics in Agriculture 153, 177–187. https://doi.org/10.1016/j.compag.2018.08.020.

Williams, J.R., Izaurralde, R.C., Williams, C., Steglich, E.M., 2023. Agricultural policy / environmental extender model theoretical documentation version 1501.

Wilson, K., Goldstein, A., Falge, E., Aubinet, M., Baldocchi, D., Berbigier, P., Bernhofer, C., Ceulemans, R., Dolman, H., Field, C., Grelle, A., Ibrom, A., Law, B.E., Kowalski, A., Meyers, T., Moncrieff, J., Monson, R., Oechel, W., Tenhunen, J., Valentini, R., Verma, S., 2002. Energy balance closure at fluxnet sites. Agricultural and Forest Meteorology 113, 223–243. https://doi.org/10.1016/S0168-1923(02)00109-0.

Wutzler, T., Lucas-Moffat, A., Migliavacca, M., Knauer, J., Sickel, K., Šigut, L., Menzer, O., Reichstein, M., 2018. Basic and extensible post-processing of eddy covariance flux data with reddyproc. Biogeosciences 15, 5015–5030. https://doi.org/10.5194/bg-15-5015-2018.

Wyland, L., 1996. Winter cover crops in a vegetable cropping system: impacts on nitrate leaching, soil water, crop yield, pests and management costs. Agriculture, Ecosystems & Environment 59, 1–17. https://doi.org/10.1016/0167-8809(96)01048-1.

Yang, W., Feng, G., Read, J.J., Ouyang, Y., Han, J., Li, P., 2020. Impact of cover crop on corn–soybean productivity and soil water dynamics under different seasonal rainfall patterns. Agronomy Journal 112, 1201–1215. https://doi.org/10.1002/agj2.20110.

Yost, J.L., Huang, J., Hartemink, A.E., 2019. Spatial-temporal analysis of soil water storage and deep drainage under irrigated potatoes in the central sands of wisconsin, usa. Agricultural Water Management 217, 226–235. https://doi.org/10.1016/j.agwat.2019.02.045.

Zaccaria, D., 2023. Updated information on water use and water productivity of pistachio grown on non-saline and salt-affected soils. Statewide Pistachio Day, Visalia Convention Center, Visalia, CA.

Zhang, J., Ranford, T., Taylor, C., 2015. Heat model for pistachio bloom and harvest. Scientia Horticulturae 186, 47–53. https://doi.org/10.1016/j.scienta.2015.02.005.

Zhang, J., Taylor, C., 2011. The dynamic model provides the best description of the chill process on ‘sirora’ pistachio trees in australia. horts 46, 420–425. https://doi.org/10.21273/HORTSCI.46.3.420.

Chapter 3: APEX simulation of cover cropping in a California pistachio orchard under future climate scenarios

Charlie Chen[1], Matthew Roby[2], and Isaya Kisekka[1,3]

[1]Hydrologic Science Program, Department of Land, Air, and Water Resources, University of California, Davis, CA 95616, USA
[2]USDA-ARS Sustainable Agricultural Water Systems Research Unit, Davis, CA, 95616, USA
[3]Department of Biological and Agricultural Engineering, University of California, Davis, CA 95616, USA

This chapter will be submitted for review by the journal Agricultural Water Management. The manuscript, titled *APEX simulation of cover cropping in a California pistachio orchard under future climate scenarios,* is prepared by the same co-authors as listed in this chapter.

Highlights

- Survey identifies five core grower concerns about pistachio winter cover cropping.
- Paired orchard APEX is calibrated to monthly ET, with soil water, LAI, biomass, and yield evaluated as diagnostic checks.
- Sensitivity analysis identifies root growth and soil strength (PARM2) as the dominant parameter for monthly ET_a in both orchards, with soil evaporation and plant cover factor (PARM17) nearly co-dominant in the cover cropped orchard.
- LOCA2 CMIP6 scenarios project rising water stress under SSP5-8.5 end of century.

Abstract

California pistachio acreage has expanded faster than groundwater supply under SGMA, leaving open whether winter cover cropping is a viable agronomic and water management practice in this system. We integrate two complementary studies to address this gap: an IRB approved online survey of California pistachio growers, farm managers, and agronomic advisors (n = 18 completing, 17 reporting on a cover crop orchard, 9 on a no cover orchard, 8 on both), and a paired orchard APEX simulation for a commercial 61-ha pistachio orchard near Davis, CA, calibrated to eddy covariance monthly evapotranspiration, with neutron probe soil water content, leaf area index, cover crop biomass, and pistachio yield evaluated as diagnostic checks. Across these targets, only monthly evapotranspiration met standard performance thresholds. Key grower concerns identified by the survey focus on agronomic (water competition between cover crop and trees) and economic (SGMA water costs, uncertain economic returns) concerns. Sensitivity analysis identified PARM2 (root growth and soil strength) as the dominant parameter in both orchards, followed by PARM17 (soil evaporation and plant cover factor) and PARM1 (Penman-Monteith canopy PET factor). The calibrated model was projected across seven climate scenarios combining three CMIP6 pathways (SSP2-4.5, SSP3-7.0, SSP5-8.5) with mid-century (2035 to 2065) and end of century (2070 to 2099) windows from the LOCA2 hybrid downscaled ensemble, plus a 1996 to 2025 observed baseline, to quantify cover crop water tradeoffs and inform SGMA era irrigation management.

Keywords: pistachio, cover crop, APEX model, climate scenarios, grower survey

1. Introduction

This study examines winter cover crop practices in California pistachio orchards using two complementary methods: an IRB-approved online survey of growers, farm managers, and agronomic advisors, and a process-based Agricultural Policy/Environmental eXtender (APEX) model simulation of a paired orchard study site in the Sacramento Valley. Together the methods address two linked questions: what concerns shape grower decisions about winter cover cropping in pistachio orchards under current conditions, and how do cover crop water balance and yield outcomes shift under projected climates?

Pistachios are California's seventh largest crop by agricultural value (CDFA, 2025), with bearing acreage having grown from roughly 25,000 acres in 1979 to over 450,000 acres in 2023 (Tootelian, 2023b). This rapid expansion has occurred against intensifying water scarcity and the regulatory constraints of California's Sustainable Groundwater Management Act (SGMA). Despite the scale of the industry, the orchard cover crop literature in California is dominated by almond (DeVincentis et al., 2020, 2022), with comparatively little quantitative work in pistachio. Pistachio differs from almonds in key ways that influence cover crop performance: a deeper rooting profile, later spring leaf out that lengthens the cover crop competition window, alternate bearing that complicates yield interpretation, and higher salinity tolerance that broadens the irrigation water options. Cover cropping is widely promoted for soil health and erosion control (Lu et al., 2000; Blanco-Canqui et al., 2015), but adoption in California remains low (Soil Health Institute, 2019), in part because grower relevant evidence on agronomic, hydrologic, and economic outcomes in pistachio systems is limited. To our knowledge, no published study has quantified winter cover crop water effects in California pistachio under projected climate,

leaving growers and water managers without a defensible basis for evaluating the practice under SGMA.

Closing this evidence gap requires both descriptive and projective information. Grower surveys describe what pistachio growers currently value and worry about, capturing the operational, agronomic, and economic constraints that shape adoption decisions (Carlisle, 2016; Dunn et al., 2016). Surveys, however, are inherently retrospective and cannot indicate how current practices will perform under climates that have not yet occurred. This matters because California's Mediterranean climate is projected to become warmer and more variable in winter precipitation (Diffenbaugh et al., 2015; Pathak et al., 2018), and perennial crop yields are sensitive to such shifts (Lobell et al., 2006; Kandhway et al., 2025).

Process-based biophysical models address the projective side of the question. APEX and comparable models simulate coupled water, nutrient, and biomass dynamics in cropping systems and have been applied to orchards and perennial crops (Talebizadeh et al., 2018; Mason et al., 2020) but applications to California pistachio with a winter cover crop component are rare. Models alone, however, can simulate scenarios that have little bearing on the decisions growers face. Pairing the two methods addresses this asymmetry. The survey identifies the management concerns most salient to current pistachio growers, which in turn frame the management questions these scenarios are designed to inform. In this study, the simulated scenarios vary climate under a single fixed management, with cover crop species, termination timing, and irrigation allocation identified as priorities for future scenario work. The model then quantifies how cover crop performance shifts under those grower relevant management options across baseline and future climates.

Within this integrated survey to modeling design, this study pursues three objectives: (i) to characterize current winter cover crop practices, perceived benefits, and primary concerns among California pistachio growers, farm managers, and agronomic advisors through an IRB-approved online survey, providing management context for the simulation scenarios; (ii) to calibrate and validate APEX for a paired pistachio orchard with and without a winter cover crop near Davis, California, using a multi-year record of evapotranspiration, soil water content, leaf area index, cover crop biomass, and pistachio yield; and (iii) to apply the calibrated model to project winter cover crop effects under climate scenarios drawn from the LOCA2 downscaled CMIP6 ensemble.

The remainder of this paper is organized as follows. Section 3.1 presents the survey results, covering sample composition, reported management practices, concerns and benefits, information sources, and the linkage between survey findings and the modeling scenario design. Section 3.2 reports a unified Sobol sensitivity analysis across the model's primary output targets. Section 3.3 reports the uncalibrated baseline model outputs for the CC and NC orchards. Section 3.4 reports the performance of the calibrated APEX model against field observation data. Section 3.5 reports the climate scenario outcomes. Section 4 closes with a discussion of limitations and implications for grower communication under SGMA.

2. Methods

2.1 Online survey

2.1.1 IRB approval and survey development

The survey was reviewed and approved by the University of California, Davis Institutional Review Board (IRB) prior to deployment (IRB ID 2160522-1, approved 24 November 2025, and determined to qualify for exempt review). The first page of the survey

presented an electronic informed-consent statement that described the purpose of the study, the voluntary nature of participation, the approximate time required to complete the survey, the procedures used to protect respondent confidentiality, and contact information for the principal investigator and the IRB. Respondents were required to confirm that they were at least 18 years of age and to indicate consent before being presented with substantive questions.

The survey was developed iteratively in consultation with a group of ~30 stakeholders from across the California pistachio sector, including University of California Cooperative Extension agronomic advisors, UC ANR specialists, academic researchers, county Groundwater Sustainability Agency (GSA) officials, industry organizations (California Pistachio Research Board, American Pistachio Growers, California Farm Bureau), state regulatory agencies (CDFA), conservation NGOs (Sustainable Conservation), and graduate and undergraduate students. The same group provided initial feedback to shape the scope, terminology, and branching structure of the instrument and then pilot-tested the updated draft prior to public deployment. Feedback from both rounds was used to refine question wording, response options, branching logic, and overall length, with the goal of minimizing respondent burden while preserving the level of detail needed for quantitative aggregation. The final survey was implemented on the Qualtrics platform (Qualtrics, Provo, UT).

2.1.2 Survey design

The survey was structured into three branches reflecting the different respondent types in the California pistachio industry. Branch 1 collected information on a cover crop (CC) orchard (Q8–Q43). Branch 2 collected the same operational details for a no cover (NC) orchard (Q45–Q65). Branch 3 covered consultant-specific questions on client base, advisory topics, and observed barriers (Q67–Q79). All completing respondents were also asked about agronomic,

operational, and economic concerns regarding cover cropping (Q83–Q85), the value placed on potential benefits (Q86), and the priority of identified knowledge gaps (Q87–Q88). All completing respondents were also asked to rank seven information sources for CC decision-making (Q81) and three broad categories of CC benefits (Q82).

2.1.3 Distribution and recruitment

The survey was distributed through several channels intended to reach a broad cross-section of California pistachio professionals. An article on CC research in pistachios was featured in the January 2026 issue of West Coast Nut and the January-February 2026 issue of Progressive Crop Consultant; each article included a QR code linking to the survey. The survey link was also included in one issue of the Madera County Groundwater Sustainability Agency monthly newsletter. Additional dissemination occurred through email circulation by the California Pistachio Research Board, the California Farm Bureau, UC Cooperative Extension, Sustainable Conservation, the American Pistachio Growers, and faculty networks at UC Davis.

Eligibility was limited to individuals at least 18 years of age with a current professional involvement in the California pistachio industry as a grower, farm manager, agronomic advisor, or researcher. The active data collection window ran from December 2025 to May 2026.

2.1.4 Survey Analysis

Given the obtained sample sizes (n = 18 completing, n = 17 CC, n = 9 NC), all analyses were descriptive; no inferential statistical tests were applied, because the sample sizes do not support them. Responses were analyzed using R version 4.3.3 (R Foundation for Statistical Computing, Vienna, Austria). The data collection window yielded 29 raw responses, of which 18 met the completion criteria. Of those 18 finished respondents, 9 reported on a CC orchard only, 8 reported on both a CC and an NC orchard, and 1 reported on an NC orchard only.

2.2 APEX Model

2.2.1 Study site and experimental design

The study was conducted in a 61-hectare commercial pistachio orchard (*Pistacia vera*, cv. Golden Hills) located in the southern Sacramento Valley (38.619 °N, 121.725 °W), approximately 10 km north of Davis, California (Figure 1). Trees were transplanted in December 2018, so the 2023, 2024, and 2025 growing seasons correspond to fifth-, sixth-, and seventh-leaf trees, respectively, with north-south rows spaced 5.8 m apart and trees spaced 5.2 m within rows, for a planting density of 332 trees ha^{-1}. Irrigation was supplied through a double drip system, with four emitters per tree discharging 2.0 L h^{-1}. Timing and volumes were set by the orchard manager using a crop coefficient-based approach. No irrigation was applied during either winter season (November to March of 2023-24 and 2024-25); the CC relied on winter precipitation for establishment and growth. Applied irrigation during the pistachio growing season totaled 136 mm in both treatments in 2023, 330 mm (CC) and 321 mm (NC) in 2024, and 580 mm (CC) and 505 mm (NC) in 2025.



Figure 1. Map of the Bullseye pistachio orchard showing the treatment quadrant layout (cover crop, CC; no cover crop, NC), the location of the eddy covariance towers in each treatment, the neutron probe access tube installation locations for the transect and array experiments, and the location of additional soil moisture sensors (cosmic ray neutron sensor and TEROS 54 profile probes) installed in each treatment.

The region has a warm-summer Mediterranean climate. Over the 1996 to 2025 baseline period, mean daily minimum temperature in December was 3.5 °C and mean daily maximum temperature in July was 33.0 °C, with mean annual precipitation of 435 mm falling mainly between November and March and less than 30 mm of cumulative rainfall from June through October (Table 1).

Table 1. Thirty-year mean grass reference evapotranspiration (ETo) and precipitation in Davis, CA (1996-2025).

	Jan	Feb	Mar	Apr	May	Jun	Jul	Aug	Sep	Oct	Nov	Dec

Precipitation (mm)	86.0	87.6	56.7	26.4	14.4	2.5	0.1	1.4	5.4	19.6	45.1	89.9
ET_o (mm)	34.8	54.5	95.1	139	185	208	212	187	146	105	50.5	32.0

The orchard was divided into four quadrants of approximately 15 ha each, with the two eastern quadrants assigned to the cover crop (CC) treatment and the two western quadrants to the no cover (NC) treatment. Winter cover crops were seeded in the CC treatments in late October or November and terminated in late March or April, while NC treatments were maintained as bare ground with periodic mowing of resident vegetation. The CC mixture included legumes, grains, and brassicas, with composition and seeding rates varying between seasons according to grower preference, and herbicide was applied in under-tree strips only, not to alleyway vegetation. Seeding dates, termination dates, and post-termination mowing schedules are summarized in Table 2.

Table 2. Winter cover crop mixture, seeding rate and date, termination date, and post-termination mowing schedule for the 2023-24, 2024-25, and 2025-26 seasons.

Season	Composition	Seeding rate (kg ha^{-1})	Seeding date	Termination date	Post-termination mowings
2023-24	23% grain, 35% bell bean, 25% peas, 15% vetch, 2% brassica	50	8 Nov 2023	30 Apr 2024	21 Jun 2024; 16 Oct 2024
2024-25	30% bell bean, 30% peas, 20% vetch, 20% rye	45	15 Nov 2024	28 Mar 2025	18 May 2025; 24 Jul 2025
2025-26	30% bell bean, 30% peas, 20% vetch, 20% oats	45	24 Oct 2025	5 Mar 2026	7 May 2026

2.2.2 Weather data

The APEX weather input set comprised daily precipitation (mm), maximum and minimum air temperature (°C), mean daily wind speed at 2 m (m s^{-1}), mean daily relative humidity (percent), and total daily solar radiation (MJ m^{-2} day^{-1}), corresponding to the NGN = 2345 option in which all six variables are read directly from the user weather file rather than generating any of them stochastically. Daily weather data from 2007 to 2026 was collected from

the California Irrigation Management Information System (CIMIS) Davis Station #006. Days with missing or quality-flagged CIMIS observations were filled using data from the nearest neighboring CIMIS station, Woodland #226. Figure 2 summarizes annual precipitation, mean daily maximum and minimum air temperature, and total annual ET_o across 2007-2025 and provides visual context for the interannual variability imposed on the model.

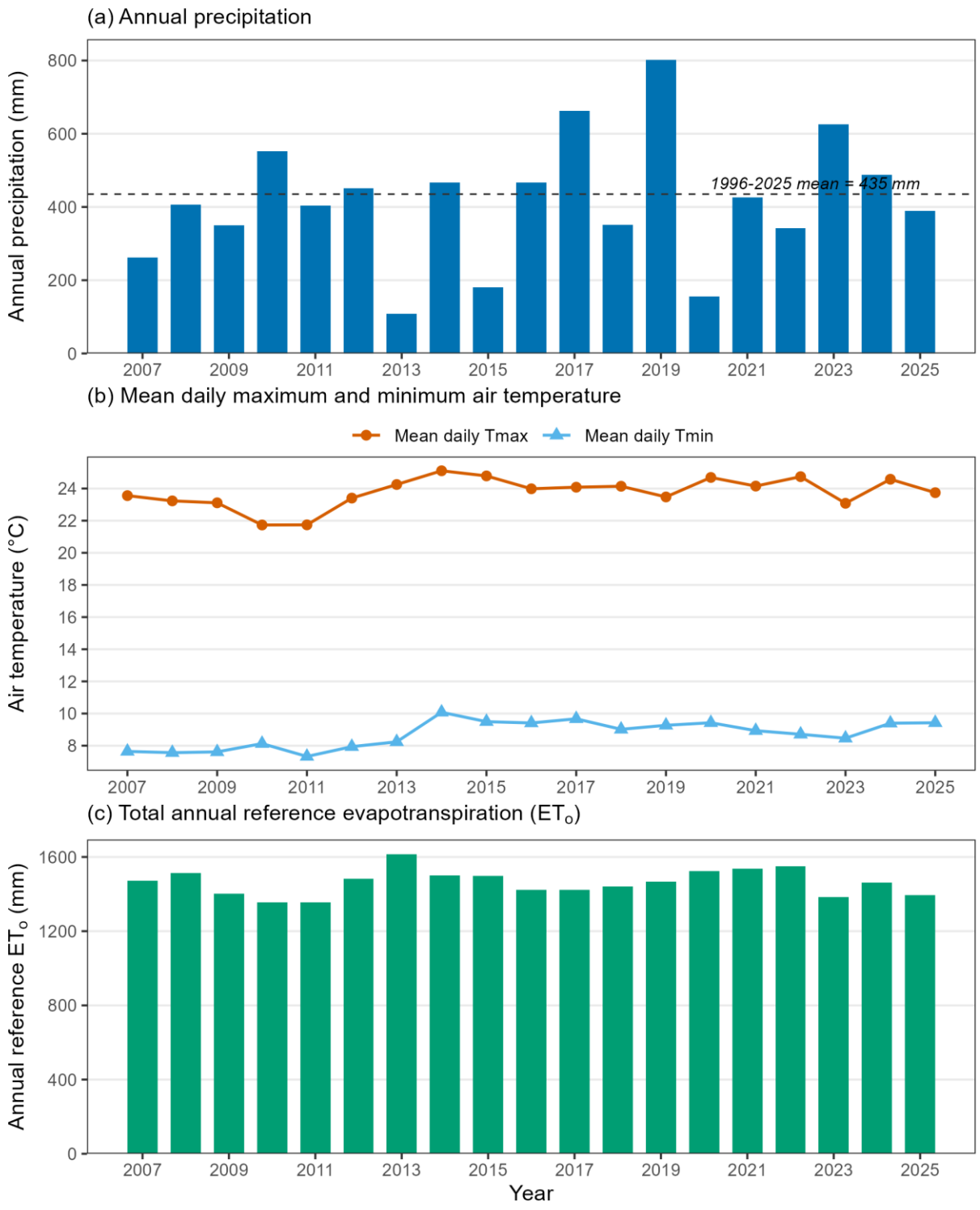


Figure 2. Annual weather summary at CIMIS Davis station #006 for the 2007 to 2025 simulation period. (a) Annual precipitation totals (mm), with the 30-year mean (1996 to 2025) of 435 mm shown for reference. (b) Mean daily

maximum (red) and minimum (blue) air temperature by year. (c) Total annual reference evapotranspiration (ET_o, mm) computed by the Penman-Monteith method.

2.2.3 Measured calibration and validation data

Energy flux densities at field scale were measured in each treatment using the eddy covariance (EC) method to quantify actual evapotranspiration (ET_a). Each flux station was equipped with an IRGASON integrated open-path CO_2/H_2O gas analyzer and 3D sonic anemometer (Campbell Scientific, Logan, UT, USA) mounted at 6.5 m height and recording at 20 Hz, together with an SN-500 four-component net radiometer (Apogee Instruments, Inc., Logan, UT, USA). Soil heat flux (G) was estimated from five sensor sets deployed along a diagonal transect spanning the interrow, each consisting of an HFT-3 heat flux plate buried at 8 cm (Radiation Energy Balance Systems Inc., Bellevue, WA, USA), Type E thermocouples at 2 and 6 cm depth, and Hydraprobe soil moisture sensors (Stevens Water Monitoring Systems, Portland, OR, USA) at 5 cm, with thermocouple and soil moisture data used to apply the standard calorimetric correction to plate fluxes.

Half-hourly latent heat flux (λE) was calculated from the covariance of vertical wind velocity and water vapor concentration measured by the IRGASON. The 20 Hz raw data were processed following a standard EC pipeline including spike removal, coordinate rotation, density corrections, and frequency response adjustments; processed fluxes were screened to remove periods with insufficient turbulence, precipitation events, and instrument malfunction. Gaps were filled at the half-hourly resolution using the Flux Gap Filling Tool (Peddinti, 2026), which implements the marginal distribution sampling (MDS) approach of Reichstein et al. (2005), and gap-filled fluxes were aggregated to daily ET_a totals. ET_a from each tower was applied only to the water balance of its corresponding treatment, and auxiliary measurements included air temperature and relative humidity.

Volumetric soil water content (θ, $m^3\ m^{-3}$) was measured with a neutron probe (CPN 503 Elite Hydroprobe, InstroTek, Inc., Raleigh, NC, USA) at 72 access tube locations. Four sampling locations were established in each treatment. At three of these, four access tubes were arranged as a transect running from the middle of a tree row to the middle of the adjacent alleyway. At the fourth location, 24 tubes were arranged as an array centered on a single tree. Readings were collected at 0.3 m depth intervals from 0.3 to 3.0 m per tube, yielding ten depths per tube. Measurements were conducted on 13 dates in 2023, 29 dates in 2024, and 26 dates in 2025, with campaigns scheduled to bracket major precipitation events, cover crop growth and termination periods, and peak pistachio water use.

During access tube installation in 2023, soil samples were collected at each 0.3 m interval for gravimetric water content determination and soil texture analysis. A site-specific calibration equation was developed from paired neutron count ratios and gravimetric water contents and applied to convert raw counts to θ. After calibration, θ time series for each tube and depth were visually inspected for single-date anomalies, defined as abrupt deviations followed by immediate recovery to the prior trend, and identified values were replaced by linear interpolation between adjacent valid measurements.

Pistachio canopy and cover crop leaf area index (LAI) were measured during the same field visits using a LI-2200C Plant Canopy Analyzer (LI-COR, Lincoln, NE, USA) following the protocol of Westling et al. (2018). Measurements were taken within two hours after sunrise on clear days. At each transect point, an above-canopy handheld reading obtained from a ladder was paired with a below canopy reading taken above any CC and below the tree canopy to estimate pistachio LAI. In the CC treatment during the winter season (November to March), a second below canopy reading was taken at ground level beneath the CC canopy at the same point;

pairing this with the above CC reading allowed CC LAI to be separated from pistachio LAI. Each transect spanned an alleyway between two adjacent tree rows. Three to five transects were laid out per treatment, with start points co-located with neutron probe access tubes so that LAI and soil water content could be paired. Field campaigns were conducted at approximately monthly intervals from November 2023 through September 2025, yielding 28 measurement dates. Cover crop LAI was recorded only when a living CC canopy was present in the alleyway, limiting that calibration target to February to June 2024 and February to April 2025.

Cover crop standing biomass and canopy height were measured by destructive sampling at near-monthly intervals through each winter season and into the post-termination period. On each sampling date, aboveground biomass samples were collected from four to five randomly selected points within the flux footprint of the CC treatment. At each point, all aboveground cover crop biomass within a quadrat was clipped at ground level. The clipped vegetation was oven-dried to constant mass and weighed to determine total aboveground dry biomass. Canopy height was determined by measuring the height of the standing cover crop biomass at three sub-points within each of the four to five biomass sampling locations. Aboveground dry biomass and canopy height were averaged from four to five samples per date to obtain treatment-level means, expressed in t ha^{-1} and cm, respectively. Sampling was conducted on 19 dates from February 2024 through April 2025, capturing active growth and termination for both winter seasons (2023-2024 and 2024-2025).

Pistachio yield for 2024 and 2025, the first and second harvest years for the orchard, was obtained from orchard manager records. Yields were reported on a kernel pounds-per-acre basis by treatment and converted to t ha^{-1} for analysis.

Soil particle size distribution was quantified at 0.3 m increments to 3.0 m using samples collected during neutron probe access tube installation in 2023 and analyzed with a laser diffraction particle size analyzer (Partica LA-960, HORIBA, Ltd., Kyoto, Japan). One sample per depth was collected from the interrow position at each of four installation locations (n = 4 per depth per treatment). Additional soil physical and chemical properties were obtained from the National Cooperative Soil Survey (NCSS; https://websoilsurvey.nrcs.usda.gov/app/), and records of irrigation, fertilization, harvesting, and cover crop operations were supplied by the orchard manager.

Table 3. Summary of measured calibration and validation data, with measurement instrument, sampling frequency, replication, period of record, and observed range for each APEX calibration target.

Target	Instrument	Sampling frequency	Replication	Period of record	Observed range
Actual ET (ET_a)	Eddy covariance (IRGASON open-path gas analyzer and 3D sonic anemometer)	30 min, aggregated to daily	1 tower per treatment	Mar 2023 to Dec 2025	0.4 to 5.5 mm d^{-1}
Soil water content (SWC)	Neutron probe (0.3 m increments to 3.0 m)	Approximately bi-weekly	36 access tubes per southern treatment quadrant (72 total)	Sep 2023 to Dec 2025	0.2 to 0.4 m^3 m^{-3}
Pistachio leaf area index (LAI)	LI-2200 Plant Canopy Analyzer	Approximately monthly	3 to 5 transects per treatment, 5 points per transect	Feb 2024 to Sep 2025	0.04 to 1.3
Cover crop LAI	LI-2200 Plant Canopy Analyzer	Approximately monthly	3 to 5 transects, 5 points per treatment	Feb to Jun 2024 and Feb to Apr 2025 (active windows)	0.75 to 8.4
Cover crop standing biomass	Destructive clip and dry sampling	Approximately monthly	4 to 5 measurements	Feb 2024 to Apr 2025	2.3 to 12.4 t ha^{-1}
Cover crop canopy height	Direct height measurement	Approximately monthly	4 to 5 measurements	Feb 2024 to Apr 2025	12 to 75 cm
Pistachio yield	Harvest records	Annual	2 treatments (NC, CC)	2024 to 2025 (year-6, year-7)	0.2 to 1.1 t ha^{-1}

2.2.4 APEX model description, setup, and baseline parameters

The Agricultural Policy/Environmental eXtender (APEX) model (v1501) is a process-based biophysical model developed by USDA-ARS and Texas A&M AgriLife Research as a

multi-field extension of the Environmental Policy Integrated Climate (EPIC) model, designed to simulate the effects of agricultural management practices on hydrology, crop growth, nutrient cycling, and erosion at field to small watershed scales (Gassman et al., 2010; Williams et al., 2023). The model operates on a daily time step, organizes the simulated landscape into homogeneous subareas (each with its own combination of soil, slope, vegetation, and management), and integrates twelve components covering climate, hydrology, crop growth, nutrient and pesticide cycling, erosion sedimentation, soil temperature, management, and economics. The unified crop growth module simulates more than 100 plant species, supports up to ten species growing simultaneously with daily competition for light, water, and nutrients (Kiniry et al., 1992; Williams et al., 2023), and represents perennial tree crops with year-round root systems and base-temperature-driven dormancy, making APEX well suited to evaluate pistachio orchards with a winter cover crop.

Potential evapotranspiration was calculated using the Penman-Monteith method (Monteith, 1965; Allen et al., 1998), implemented in APEX as:

$$E_o = \frac{R_n \times \Delta + 86.66 \times \rho_a \times \delta \times \frac{\mu_{10}}{r_a}}{\lambda \times (\Delta + \gamma) \times (1 + \frac{r_c}{r_a})} \quad (1)$$

$$r_c = \frac{p_1}{LAI_s \times r_{cr} \times f(\delta)} \times \exp\,(330 - CO_2) \quad (2)$$

where E_o is potential evapotranspiration (mm d^{-1}), R_n is net radiation (MJ m^{-2} d^{-1}), Δ is the slope of saturation vapor pressure curve (kPa $^oC^{-1}$), λ is the latent heat of vaporization (MJ kg^{-1}), γ is the psychrometric constant (kPa $^oC^{-1}$), δ is the vapor pressure deficit (kPa), ρ_a is air density (kg m^{-3}), μ_{10} is mean wind speed at 10 m height (m s^{-1}), r_a is aerodynamic resistance for heat and vapor transfer (s m^{-1}), and r_c is canopy resistance for vapor transfer (s m^{-1}). The calibration parameter p1 (PARM1 in APEX) ranges from 1 to 2 and scales canopy resistance; LAIs is the

summed leaf area index of all crops growing at the time, r_{cr} is crop leaf resistance (s m^{-1}), and CO2 is atmospheric CO_2 concentration (g m^{-3}) (Steglich et al., 2023). PARM17, the soil evaporation plant cover factor, partitions evaporative demand between canopy transpiration and bare soil evaporation as a function of LAI and ground cover.

Surface runoff was estimated by the NRCS curve number method with the daily curve number updated as a function of the soil moisture index (the NVCN = 4 option in APEX), which couples runoff partitioning to antecedent soil water content. Vertical soil water redistribution was simulated by the storage routing method, with deep percolation governed by saturated hydraulic conductivity and the 4 mm slug exponent of PARM82 (Williams et al., 2023). Soil temperature was simulated by a daily heat transport model driven by air temperature and soil moisture, with phase lag through depth. Soil organic carbon and nitrogen were tracked through the Century pool structure as implemented in APEX (Izaurralde et al., 2006; Williams et al., 2023), with five pools per soil layer for each element: structural litter, metabolic litter, microbial biomass, slow humus, and passive humus. The full set of governing equations for biomass accumulation, heat unit accumulation, leaf area development, crop stress factors, and process coupling is documented in Williams et al. (2023) and is not reproduced here.

The model was configured using APEX Editor v.2203. The CC and NC treatments were each represented as an independent subarea with no routing connection between them, so the only on-field water input was precipitation, supplemented with irrigation on the orchard manager's schedule. The configuration used Penman Monteith ET_o, the NRCS curve number runoff method modified by a soil moisture index, and the APEX default equations for soil water redistribution and percolation. Site, subarea, soil, operations, control file, and parameter file inputs are summarized in Tables 4 to 8. The full set of governing equations for biomass

accumulation, heat unit accumulation, leaf area development, and crop stress is documented in Williams et al. (2023) and is not reproduced here. These choices follow two precedents. Saleh et al. (2018) found that Penman Monteith outperformed alternative PET options against weighing lysimeter data in a semi-arid irrigated system. Timlin et al. (2019) reported that a variable daily curve number linked to a soil moisture index produced robust water balance simulations across a range of soils and management systems.

Table 4. Physical characteristics of the NC and CC orchard baseline models, including key site, soil, and subarea parameters used in APEX.

APEX Param.	**Description**	**Value**	**Comments**
Site file			
YLAT	Latitude	38.62	Bullseye orchard centroid
XLOG	Longitude	-121.72	Bullseye orchard centroid
ELEV	Elevation	13	Used in Penman-Monteith PET calculation
CO2X	CO_2 concentration in the atmosphere (ppm)	409	Mean for the simulation period; held constant
Soil file			
SALB	Soil albedo	0.06	Bare soil reflectance
HSG	Soil hydrologic group	3	From NCSS Web Soil Survey
TSLA	Maximum number of soil layers after splitting	10	10 layers: 0.3 to 3.0 at 0.3 m increments
RTN1	Number of years of cultivation at start of simulation	50.0	
XIDK	Soil grouping	2.00	Mixed soil group
FHP	Fraction of Org C in passive pool	0.70	
Subarea file			
LUNS	Land use number (range 1 to 35)	21	Tree crop with cover
FL	Field length (km)	0.387	Quadrant-scale; identical for NC and CC
FW	Field width (km)	0.374	Quadrant-scale; identical for NC and CC
WSA	Watershed area (ha)	14.41	Approximately 15 ha per quadrant
NIRR	Irrigation application rigidity	1	Fixed: user-scheduled volumes applied as written
IRR	Irrigation type code	5	Drip irrigation
VIMX	Maximum annual application volume (mm)	800	Encompasses observed orchard practice
ARMX	Maximum single application volume (mm)	40	Encompasses observed orchard practice
SLP	Slope (m m^{-1})	0	Orchard had flat topography
NVCN	CN-CN2 code	4	Daily CN updated via NVCN = 4 (soil moisture index)

Table 5. Soil properties used in the simulation of the CC and NC orchards. Bulk density from NCSS; sand, silt, and clay from particle-size analyzer (HORIBA Partica LA-960). Wilting point (WP), Field capacity (FC), Saturated hydraulic conductivity (SC), organic carbon (OC), and pH to be filled from NCSS Web Soil Survey.

Depth (m)	BD (Mg m^{-3})	Sand (%)	Silt (%)	Clay (%)	WP (m^3 m^{-3})	FC (m3 m-3)	SC (mm h^{-1})	OC (%)	pH
Cover crop (CC) orchard									
0.3	1.36	24.01	66.28	9.71	0.20	0.33	2.17	2.07	6.80
0.6	1.37	9.56	73.94	16.50	0.18	0.32	2.40	1.28	7.40
0.9	1.39	5.60	74.91	19.49	0.17	0.31	3.86	0.72	7.90
1.2	1.41	23.15	60.45	16.40	0.15	0.30	4.41	0.59	8.00
1.5	1.48	18.59	66.18	15.23	0.13	0.28	5.00	0.50	8.00
1.8	1.48	12.40	69.29	18.31	0.13	0.28	5.00	0.50	8.00
2.1	1.48	12.55	68.96	18.49	0.13	0.28	5.00	0.00	8.00
2.4	1.48	20.49	60.27	19.24	0.13	0.28	5.00	0.00	8.00
2.7	1.48	25.29	57.01	17.70	0.13	0.28	5.00	0.00	8.00
3.0	1.48	25.83	58.58	15.59	0.13	0.28	5.00	0.00	8.00
No cover crop (NC) orchard									
0.3	1.45	5.04	68.11	26.85	0.20	0.33	2.70	2.00	7.90
0.6	1.41	4.25	60.35	35.40	0.22	0.34	1.39	1.08	8.10
0.9	1.40	3.41	64.78	31.81	0.22	0.34	0.91	0.75	8.20
1.2	1.40	3.61	67.29	29.10	0.22	0.34	0.91	0.75	8.20
1.5	1.41	2.61	71.09	26.30	0.21	0.33	1.39	0.55	8.20
1.8	1.43	24.63	51.37	24.00	0.18	0.31	2.70	0.00	8.20
2.1	1.42	30.75	48.57	20.68	0.18	0.31	2.70	0.00	8.20
2.4	1.42	25.27	53.99	20.74	0.18	0.31	2.70	0.00	8.20
2.7	1.42	23.64	55.23	21.13	0.18	0.31	2.70	0.00	8.20
3.0	1.42	22.33	57.76	19.91	0.18	0.31	2.70	0.00	8.20

Note: NCSS Web Soil Survey only provides data up to 1.5 m. Values from 1.5 m were applied for all layers below it.

Before formal calibration, several APEX inputs were configured to reflect site management practices and to produce a numerically stable baseline simulation. The orchard uses drip irrigation, represented by IRR = 5 and NIRR = 1 so that user specified irrigation volumes are applied; ARMX = 40 mm and VIMX = 800 mm were chosen to encompass the full range of observed practice. For 2019 to 2022, when management records were less detailed than for 2023 to 2025, an auto-irrigation supplement was included to maintain plausible summer pistachio water status: the water-stress trigger BIR was set to 0.80 on 1 May and reset to −1000 on 31 October, restricting auto-triggered irrigation to the active growing season and preventing

unintended events during dormancy or winter seasons. Outside this window, irrigation was manual only, following recorded dates and volumes, and from 2023 onward all irrigation events in both orchards were manually specified. In all years, no irrigation was applied to the CC during the winter season; the winter cover crop relied entirely on winter precipitation, consistent with reported practice.

The pistachio entry in CROPCOM.DAT was parameterized from species-specific literature rather than generic deciduous tree defaults. The base temperature for growth, TBS, was retained at its default value of 10 °C. The APEX TBS parameter governs the lower temperature bound for biomass accumulation across all phenological stages and differs from the cardinal temperatures used in chilling-hour or growing-degree-hour phenological models. For context, the 4.4 °C base reported by Zhang and Taylor (2011) applies to growing-degree-hour accumulation from chill fulfilment to bloom in 'Sirora' pistachio in Australia, and the 4.5 °C base reported by Rahemi and Pakkish (2009) applies to chilling and heat requirements of Iranian pistachio cultivars; neither reference prescribes the APEX biomass accumulation base temperature. The optimum temperature for plant growth, TOP, was retained at its default of 30 °C, the upper end of the 25 to 30 °C range identified by Zhang et al. (2015) and below the 32 °C upper threshold identified for post-bloom heat accumulation. A higher TOP within the bloom phase range was preferred because TOP in the APEX temperature-stress function governs biomass accumulation across all phenological stages, not only bloom. Both TBS and TOP are treated as stable within species in the APEX documentation (Steglich et al., 2023) and were retained at their defaults throughout calibration.

Table 6. Sample years from the APEX operation schedules. One representative winter and pistachio season is shown for CC and NC treatments.

Operation	TID	Date	Rate	Other
NC orchard, 2024 pistachio season				

Drip irrigation	530 (IHC = 8)	Apr to Oct 2024	321 mm (season total)	Summarized as season total
Fertilizer application	580 (IHC = 9)	Apr to Oct 2024	KTS: 94 kg/ha 8-4-8: 552 kg/ha UN-32: 168 kg/ha	Manager record
Pistachio harvest	626 (IHC = 2)	15 Oct 2024	0.20 t ha^{-1}	First harvest
CC orchard, 2023 to 2024 cover crop season				
Cover crop seeding	139 (IHC = 5)	8 Nov 2023	50.4 kg ha^{-1}	23% grain, 35% bell bean, 25% peas, 15% vetch, 2% brassica
Cover Crop Mowing	675 (IHC = 2)	30 Apr 2024	Once before termination in April	Mow only; no soil disturbance
Cover crop termination	451 (IHC = 1)	30 Apr 2024	Once at end of winter season	Kill operation
CC orchard, 2024 pistachio season				
Drip irrigation	530 (IHC = 8)	Apr to Oct 2024	330 mm (season total)	Summarized as season total
Fertilizer application	580 (IHC = 9)	Apr to Oct 2024	KTS: 94 kg/ha 8-4-8: 552 kg/ha UN-32: 168 kg/ha	Manager record
Pistachio harvest	626 (IHC = 2)	15 Oct 2024	0.20 t ha^{-1}	First harvest

The deterministic curve number option (ISCN = 1) was selected over the APEX default stochastic option (ISCN = 0). The stochastic option superimposes a ±5 unit triangular perturbation on the calculated daily curve number, which adds run to run noise.

Table 7. Key APEX control file (APEXCONT.DAT) settings used for both NC and CC orchards.

Parameter	Description	Default	Baseline	Comments
NBYR	Simulation duration (years)	40	19	Run from 2007 to 2025; 2007 to 2018 used as warm-up
IYR0	Beginning year	1960	2007	Eleven years prior to tree transplanting
IPD	Print code	2	6	Daily output
NGN	Weather input code	2345	2345	Read precipitation, T, wind, RH, solar from weather file
IGN	Number of random number cycles	0	0	Same seed used for all simulations
IET	Potential ET equation	4	1	Penman-Monteith
ISCN	Stochastic CN estimation	1	1	Deterministic CN
ITYP	Peak rainfall rate code	1	1	SCS TR55 Type I rainfall pattern (Pacific maritime climate, appropriate for Davis)
ISTA	Soil profile code	0	1	Static profile
IHUS	Auto heat unit scheduling	0	0	Operations scheduled by date, not heat units
NVCN0	Daily CN calculation method	4	4	Variable daily CN linked to soil moisture index
INFL0	Runoff estimation methodology	0	0	Curve number (not Green-Ampt)
IERT	Enrichment ratio method code	0	0	EPIC method
LBP	Soluble P runoff method	0	0	GLEAMS method (not modified nonlinear)
NUPC	N and P plant uptake code	1	1	S-curve uptake
ISLF	Slope length and steepness factor	0	0	RUSLE slope factor
ICO2	Atmospheric CO_2 mode	0	0	Constant CO_2 over the simulation

ISW	Soil water calculation code	0	2	Rawls method, static (short simulation period; Wang et al. (2012) uses same option)
RFN0	N in rainfall (ppm)	0.8	0.8	Default retained
CO20	Atmospheric CO_2 (ppm)	330	409	Period mean; matches CO2X in Table 4
DRV	Equation for water erosion	3	3	MUSS (small-watershed MUSLE)

Table 8. APEX default versus adjusted crop parameter values used in the baseline simulation for pistachio (PIST) and the winter pea cover crop proxy (WPEA). References for non-default values are given in the Comments column.

Parameter	Description	APEX default	Adjusted value	Comments / reference
Pistachio (PIST)				
TBS	Minimum temperature for plant growth (°C)	10	10	Rahemi and Pakkish (2009); Zhang et al. (2015)
TOP	Optimum temperature for plant growth (°C)	30	30	Default retained; consistent with Zhang et al. (2015)
DMLA	Maximum potential leaf area index	5	3	Iteratively fit to LAI data
DLAI	Fraction of growing season at LAI decline onset	0.99	0.99	Default retained
DLAP1	First point on optimal LAI curve	5.05	5.05	Default retained
DLAP2	Second point on optimal LAI curve	40.95	40.95	Default retained
HI	Harvest index	0.75	0.75	Default retained
PPLP1	Population to LAI scaling, first point	1000.95	1000.95	Default retained
PPLP2	Population to LAI scaling, second point	100.05	100.05	Default retained
IDC	Crop category number	8 (deciduous)	8 (deciduous)	Default retained; Pistachio is a deciduous nut tree
Winter pea cover crop proxy (WPEA)				
TBS	Minimum temperature for plant growth (°C)	1	1	Default retained; consistent with Adams and Cosner (2025)
TOP	Optimum temperature for plant growth (°C)	14	14	Default retained
DMLA	Maximum potential leaf area index	4	8	LI-2200 cover crop LAI data
DLAI	Fraction of growing season when leaf area declines	0.90	0.95	LI-2200 cover crop LAI data
DLAP1	First point on optimal LAI curve	15.02	15.02	Default retained
DLAP2	Second point on optimal LAI curve	50.95	50.95	Default retained
HI	Harvest index	0.55	0.55	Default retained
PHU	Potential heat units to maturity (°C-days)	n/a	1600	Bracketed by 1200 to 1800 from Oregon State University (2010)
PPLP1	Population to LAI scaling, first point	20.20	20.20	Default retained
PPLP2	Population to LAI scaling, second point	100.90	100.90	Default retained
IDC	Crop category number	2	2	Default retained

2.2.5 Sensitivity analysis

A global sensitivity analysis was performed for each of three APEX output categories using the Sobol variance decomposition method as implemented in APEX-CUTE 4.6 (Wang and Jeong, 2019). The three categories were water balance, crop yield, and soil nitrogen, with monthly ET_a used as the target variable for all three categories because it had the longest observational record. The approach follows the multi-objective approach of Tadesse et al. (2018) for simultaneous ET_a and yield calibration. While separate analyses were conducted for each category, the water balance was the primary analysis. Results of the sensitivity analysis for the other categories are provided in the Supplementary Materials.

For each output category, the parameter set was drawn from the process grouped APEX-CUTE 4.6 parameter list: water balance (27 parameters), crop yield (17 parameters) and soil nitrogen (25 parameters).

The Sobol method produces first-order sensitivity indices (SI_First), which capture main effects on output variance, and total-order indices (SI_Total), which capture main effects plus all interactions; parameters with high SI_Total were treated as interaction-dominated and flagged for adjustment during calibration. The total iteration count for each Sobol analysis was calculated as:

$$N = 2I(P + 1) \tag{3}$$

where I is the sampling interval and P is the number of parameters in the test set; I was set to 6000 for all parameter groups. Following Tadesse et al. (2018), parameters with SI_Total of at least 0.05 were classified as sensitive for the corresponding output category, and the sensitive parameter set identified by each category was carried into the corresponding step of the calibration procedure.

2.2.6 Model evaluation criteria

Model performance against each calibration target was assessed using five complementary statistics: the Nash-Sutcliffe efficiency (NSE; Nash and Sutcliffe, 1970), percent bias (PBIAS; Moriasi et al., 2007), the coefficient of determination (R^2), the root mean square error (RMSE), and the RMSE-observed standard deviation ratio (RSR) (Table 9).

Table 9. Statistical metrics used to evaluate the performance, with equations for NSE, PBIAS, R^2, RMSE, and RSR.

Name	Equation
Nash-Sutcliffe Efficiency (NSE)	$NSE = 1 - \frac{\sum_{i=1}^{n}(O_i - P_i)^2}{\sum_{i=1}^{n}(O_i - \bar{O})^2}$
Percent Bias (PBIAS)	$PBIAS = \left[\frac{\sum_{i=1}^{n}(O_i - S_i)}{\sum_{i=1}^{n} O_i}\right] \times 100$
Coefficient of determination (R^2)	$R^2 = \frac{n(\sum xy) - (\sum x)(\sum y)}{\sqrt{[n\sum x^2 - (\sum x)^2][n\sum y^2 - (\sum y)^2]}}$
Root mean square error (RMSE)	$RSME = \sqrt{\sum_{i=1}^{n}\frac{(P_i - O_i)^2}{n}}$
RMSE-observations standard deviation ratio (RSR)	$RSR = \frac{RMSE}{STDEV_{obs}} = \frac{\sqrt{\sum_{i=1}^{n}(Y_i^{obs} - Y_i^{sim})^2}}{\sqrt{(Y_i^{obs} - Y^{mean})^2}}$

where O_i and S_i are the i-th observed and simulated values, $\bar{O}$ and $\bar{S}$ are the means of the observed and simulated series, and n is the number of paired observations. NSE ranges from minus infinity to 1 and measures how well simulations match observations relative to the observed variance, with NSE = 1 indicating a perfect match, NSE = 0 indicating skill equal to using the observed mean, and NSE < 0 indicating worse-than-mean performance. PBIAS is expressed as a percentage, with positive values indicating model underestimation and negative values indicating overestimation. R^2 measures the proportion of observed variance explained by the linear regression of simulated on observed values, with values closer to 1 indicating stronger linear association, RMSE has the same units as the variable and is interpreted relative to the

observed mean and measurement uncertainty, and RSR is RMSE normalized by the standard deviation of the observations, producing a dimensionless measure that ranges from 0 (perfect simulation) upward; lower values indicate better performance, with RSR less than or equal to 0.50 commonly classified as very good, 0.50 to 0.60 as good, 0.60 to 0.70 as satisfactory, and greater than 0.70 as unsatisfactory at the monthly time step (Moriasi et al., 2007).

Calibration performance was judged satisfactory by the Moriasi et al. (2016) thresholds for monthly scale water quality and crop system modeling, requiring NSE > 0.50, R^2 > 0.60, and PBIAS within ±15 percent for streamflow equivalent processes (including ET and soil water content). For crop yield, the relaxed PBIAS threshold of PBIAS ± 25 percent recommended by Wang et al. (2012) was adopted to reflect higher uncertainty in field scale yield measurement, and these thresholds were applied to each calibration target as summarized in Table 9.

2.2.7 Calibration and validation

The model was run from 2007 through 2025, with a 10-year warm-up period (2007-2017) preceding tree establishment in 2018 and a calibration window of 2023 to 2024, with 2025 used for independent validation. Calibration used the Dynamically Dimensioned Search (DDS) algorithm as implemented in APEX-CUTE (Wang and Jeong, 2019), evaluated against monthly ET_a over the parameters identified as most sensitive: PARM1 (Penman-Monteith canopy PET factor), PARM2 (root growth-soil strength), PARM12 (soil evaporation coefficient), and PARM17 (soil evaporation-plant cover factor). The calibration strategy was to retain APEX default values whenever site-specific justification was lacking and to constrain all adjustments to literature supported ranges.

Calibration proceeded in three steps. First, monthly ET_a was matched to EC-derived ET_a by adjusting the sensitive parameters: PARM1 (Penman-Monteith canopy PET factor), PARM2

(root growth and soil strength), PARM12 (soil evaporation coefficient), and PARM17 (soil evaporation and plant cover factor). This four-parameter ET_a calibration is consistent with prior APEX calibration in irrigated and dryland systems, which have likewise identified canopy PET, soil evaporation, and root-zone strength parameters as the dominant controls on ET_a (Tadesse et al., 2019).

Second, leaf area index (LAI) was matched to LI-2200 measurements by adjusting the maximum LAI (DMLA) and the heat unit accumulation parameters in the pistachio and CC (WPEA) entries of CROP.DAT, which control phenological progression. The pistachio base and optimum temperature parameters (TBS = 10 °C, TOP = 30 °C), set from species-specific literature, were held fixed throughout calibration. For the CC, no published APEX-specific PHU value exists for winter pea (*Pisum sativum*), so PHU was derived using the approach of Mason et al. (2020) for corn and Tadesse et al. (2019) for winter wheat: published cardinal temperatures for Austrian winter pea (T_b = −0.98 °C; Adams and Cosner, 2025) were used to confirm consistency with the WPEA base temperature (TBS = 1 °C), and published growing-degree-days to maturity ranges for processing peas (1200-1700 heat units above a 4.4 °C base; Oregon State University, 2010) were used to bracket the physiological range. Under the Davis CIMIS record, a winter pea CC planted in November and allowed to reach physiological maturity in late spring would accumulate approximately 1500-1800 GDD above TBS = 1 °C. Because the CC is terminated by mowing prior to maturity, PHU was set somewhat above the GDD-to-maturity range to keep simulated heat unit index (HUI) below 1 throughout the pre-mow window, then refined by iterative fitting to the LI-2200 LAI series data.

Third, pistachio yield was evaluated against the 2025 harvest record; the 2024 first-commercial-harvest value (0.2 t/ha) was excluded as anomalously low for the year-6 stage,

against the UC ANR Sample Costs template expected year-6 yield of 0.74 t ha^{-1} (Baldwin et al., 2020). With parameters retained at APEX defaults, including the standard nut tree harvest index HI = 0.75, simulated orchard mean yield was evaluated using a ±25 percent PBIAS threshold for crop yield recommended by Wang et al. (2012).

2.2.8 Climate scenario design

The calibrated orchard system was exposed to a structured set of future climates derived from LOCA2-downscaled CMIP6 projections to evaluate how management and parameter choices perform under changing conditions. To align the analysis with survey findings and keep the focus on grower relevant outcomes, scenarios were analyzed in terms of water balance, pistachio yield, and cover crop biomass at termination, which directly reflect respondent concerns. Throughout, scenarios are denoted Historical, SSP245_Mid, SSP245_End, SSP370_Mid, SSP370_End, SSP585_Mid, and SSP585_End for consistency across text, tables, and figures.

The scenario matrix combined three emissions pathways with two future time periods. Three Shared Socioeconomic Pathways from the sixth Coupled Model Intercomparison Project (CMIP6) frame the emissions axis: SSP2-4.5 (middle of the road, moderate mitigation), SSP3-7.0 (regional rivalry, mid high emissions without mitigation), and SSP5-8.5 (fossil fueled development, very high emissions). Two thirty-year time periods frame the time horizon axis: mid-century (2035 to 2065), and end of century (2070 to 2099). The scenario matrix yields six future scenarios, which together with a single historical baseline form the seven scenario set. The historical baseline was taken as the observed 1996 to 2025 period. Scenario results are reported as change relative to this observed baseline, ensuring internal consistency because the calibration and scenario comparison share the same reference period.

For each scenario, the five-model California “priority subset” was used: ACCESS-CM2, MPI-ESM1-2-HR, EC-Earth3, FGOALS-g3, CNRM-ESM2-1. These models were selected by Cal Adapt for the Fifth Climate Change Assessment on the basis of their performance in simulating historical California climate variables and their availability for the LOCA2 hybrid downscaling effort. For each scenario, the APEX weather program WXPM3020 was run on each GCM’s daily output to generate monthly statistics, which were then averaged across the five GCMs to produce a single ensemble-mean WP1 monthly statistics file. The averaged WP1 file comprises monthly maximum and minimum air temperature (OBMX, OBMN), the monthly standard deviations of those temperatures (SDTMX, SDTMN), monthly precipitation total (RMO), monthly standard deviation and skew of daily precipitation (RST2, RST3), monthly wet day after dry day and wet day after wet day probabilities (PRW1, PRW2), monthly mean number of rain days (UAVM), monthly mean half hour rainfall (WI), monthly solar radiation (OBSL), monthly relative humidity (RH), and monthly mean wind speed (UAV0). Across GCM spread for each monthly statistic is reported in Supplementary Table S2 as a measure of GCM uncertainty.

APEX was run with NGN set to -1 in APEXCONT.DAT, which instructs the model to generate daily weather internally from the WP1 monthly statistics file using the skewed normal precipitation distribution and the temperature variance terms (Williams et al., 2023). For each scenario, one thousand stochastic realizations were run by incrementing the IGN random number generator seed between runs, with each realization covering the full thirty-year scenario period. Annual ACY and SAD output files were collected for each realization and pooled into per scenario distributions. The calibrated APEX parameter set was held constant across all scenarios so that differences in outcome reflect only the climate forcing rather than configuration changes.

To isolate the CC treatment effect from stochastic weather noise, the CC and NC treatments were run in a paired design. For each scenario, the same sequence of IGN random number generator seeds was applied to both treatments, so that each CC realization is matched to a NC realization with identical internally generated daily weather. Paired differencing of annual and monthly outputs then attributes output differences to the CC treatment rather than to weather realization. One thousand stochastic realizations were generated per scenario per treatment by incrementing the IGN seed between runs, yielding 1000 paired CC-NC members per scenario for the water balance comparison. Ensemble medians and 10th-to-90th percentile ranges are reported throughout.

Not all simulated years were used in the scenario comparison. Because the Bullseye orchard was transplanted in December 2018, the first several simulated years of each scenario capture establishment and canopy development rather than mature orchard conditions. The analysis was therefore restricted to the eight calendar years within each scenario period that best correspond to the observed field data window (2018 to 2025).

Post-processing and figure generation were performed in R version 4.3.3. Annual ACY output files were parsed for pistachio yield (YLDG), annual evapotranspiration (ET), and annual deep percolation (PRK) for each scenario, treatment, and realization. For monthly analyses, the SAD output files were parsed to extract monthly ET_a and monthly precipitation totals. Per-scenario distributions were assembled by pooling the observed field data records across all 1000 realizations, producing a distribution of 8000 annual or monthly values per scenario and treatment. Three complementary figure types are used to present the climate scenario results. Absolute seasonal cycle figures show the ensemble mean monthly ET_a or precipitation under each scenario, with the 10th-to-90th percentile band as a ribbon, faceted by scenario so that

within-scenario variability is visible. Scenario minus baseline difference figures subtract the baseline monthly mean from each future scenario's monthly mean for the same variable, isolating the climate signal from the background seasonal cycle and making modest but systematic shifts legible against the large seasonal amplitude at this site.

The link to the survey findings enters at the interpretation step. Each of the five grower concerns identified in the survey is examined across the seven-scenario set using the axes of the scenario matrix most informative for that concern.

3. Results

3.1 Survey Results

The online survey was designed to do two things in support of the modeling work that follows. First, it characterizes current cover crop practices, perceived challenges, and information priorities among California pistachio operators, providing practitioner context for an evaluation that would otherwise rest on a single instrumented orchard. Second, it identifies which climate sensitivities matter most to growers, so that the scenarios simulated in APEX address concrete operational questions rather than generic future climate projections. The remainder of Section 3.1 reports the composition of the respondent sample, summarizes responses on cover crop challenges, concerns, benefits, knowledge gaps, and observed outcomes, and makes the linkage from survey findings to scenario design explicit. Results are reported descriptively. The completing sample (n = 18) and the smaller subsample for the NC treatment (n = 9) do not support inferential statistics, and the sample is biased toward experienced cover crop adopters rather than representing a random draw from California pistachio operations. Findings should therefore be read as characterizing what concerns and priorities arise among practitioners

who have already engaged with the practice, not as estimates of the prevalence of those concerns across the industry.

3.1.1 Sample composition

Sample composition by orchard treatment (CC = cover crop, NC = no cover), respondent role (grower, farm manager, agronomic advisor), and recruitment branch is summarized below. Of the 18 respondents who completed the survey, 17 reported cover cropping on at least one orchard block (CC) and 9 reported no cover on at least one orchard block (NC); eight respondents reported both treatments across different blocks, so the CC and NC sample sizes are not mutually exclusive. The denominators for figures and tables that follow exclude Unsure and Prefer not to answer responses unless otherwise stated in the figure caption.

The survey received 28 responses, of which 18 met the completion criteria (Figure 3). Among the 18 completing respondents, 16 (89 percent) were growers or farm managers, with two respondents identifying as a CCA, PCA, or independent consultant (including one who selected "Other" and wrote in "consultant") (Figure 4a). The 18 orchards described by these respondents were concentrated in the major California pistachio counties, with Fresno (n = 8) and Kern (n = 7) accounting for 65 percent of the orchards, and the southern San Joaquin Valley counties of Kern, Fresno, Tulare, and Madera together accounting for 91 percent (Figure 4b). This distribution mirrors statewide production, in which the same group of counties contributes more than 90 percent of California pistachio output (CDFA, 2025). Winter CC usage among the represented orchards was generally well established. Of the 17 orchards with CC history reported, 8 (47 percent) reported 6 to 10 years of experience, 5 (29 percent) reported 2 to 5 years, 3 (18 percent) reported more than 15 years, and 1 (6 percent) reported 11 to 15 years (Figure 4d).

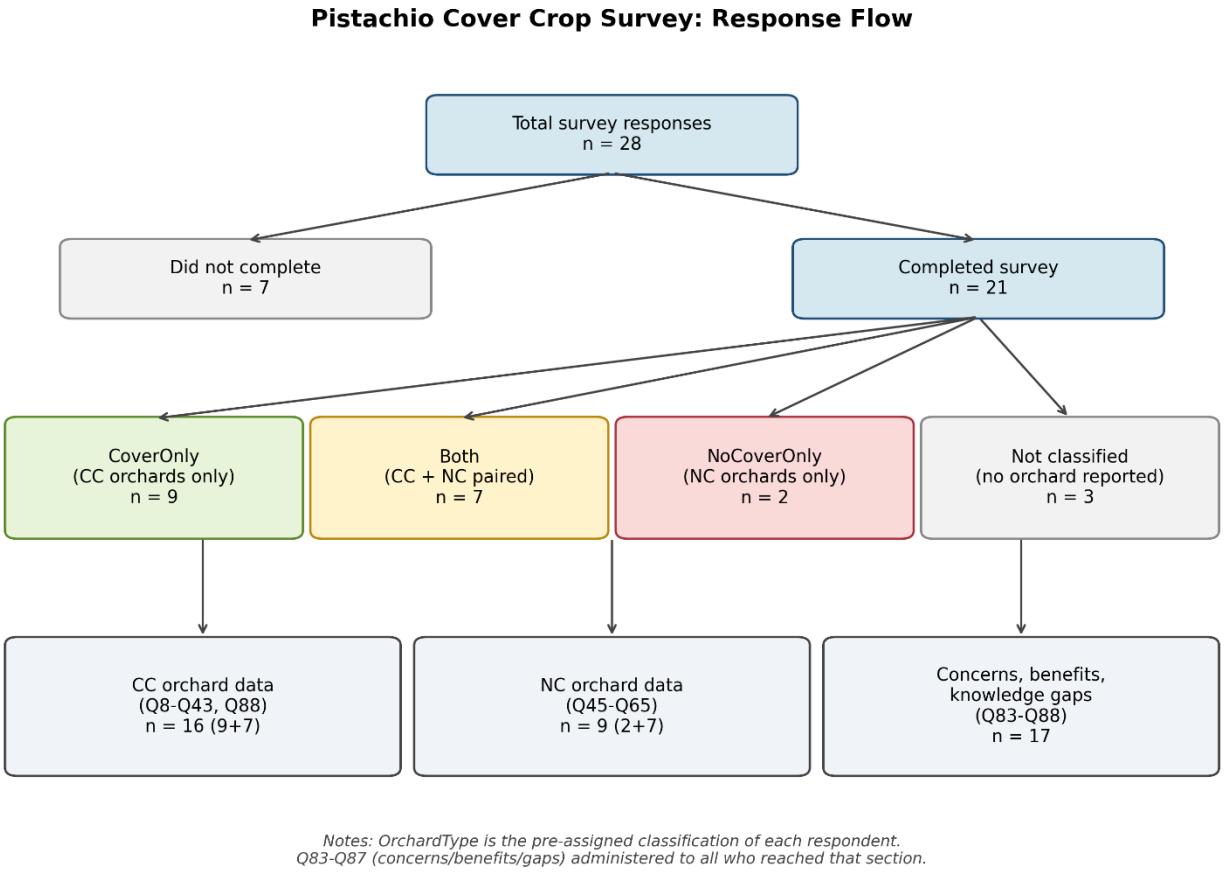


Figure 3. Flow of respondents through the pistachio cover crop survey. Of 28 total survey responses, 18 met the completion criteria. Completing respondents were classified by OrchardType (cover crop (CC), no cover crop (NC), or both). Three downstream analysis populations are used in subsequent figures: CC data, n = 17; NC data, n = 9; and the common blocks, n = 18. All completing respondents were classified by OrchardType.

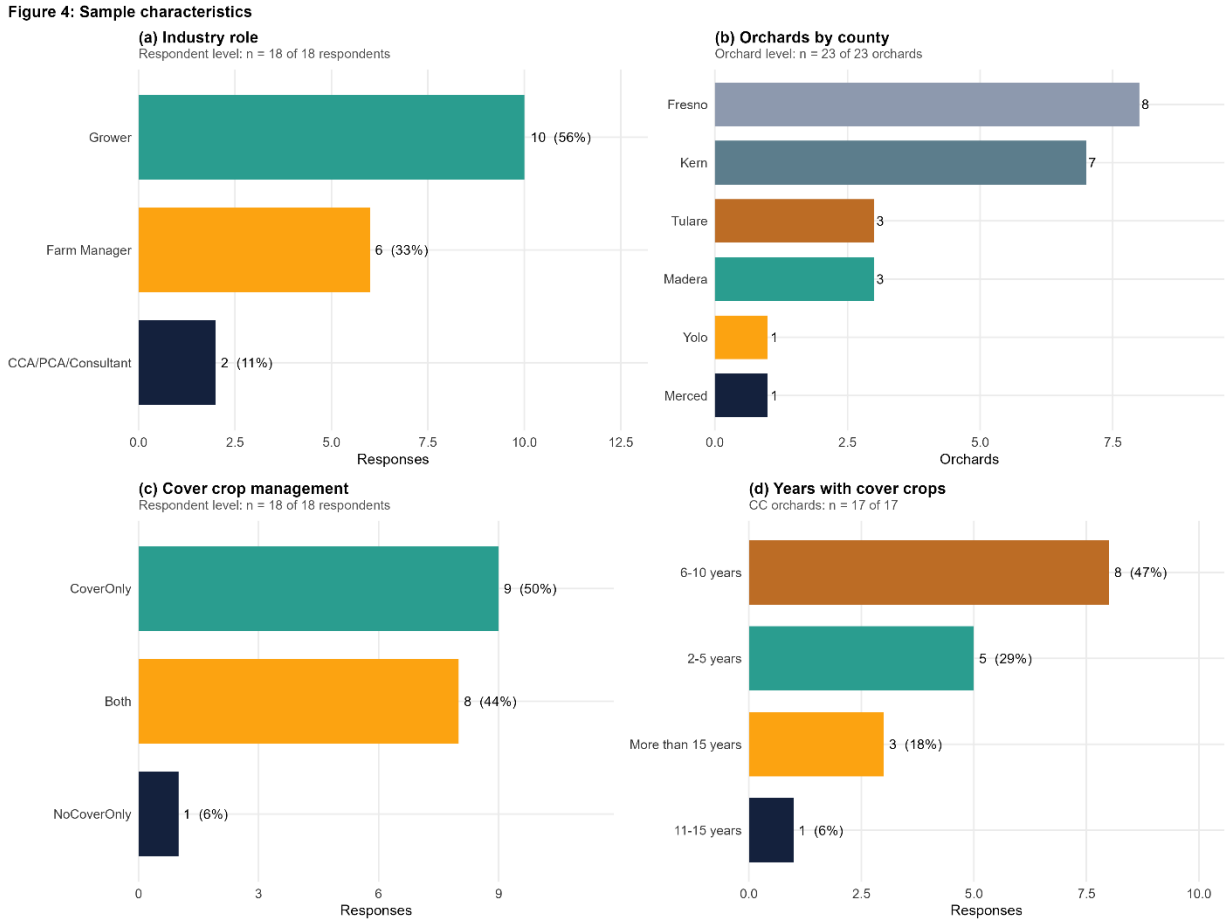


Figure 4. Sample characteristics of the 18 respondents who completed the survey. (a) Respondent role; the majority were growers (n = 10) or farm managers (n = 6), with two respondents identifying as a CCA, PCA, or consultant (including one who selected "Other" and wrote in "consultant"). (b) County of the orchard described in each response; a single respondent contributing both a CC and an NC orchard appears in this panel twice. The 18 orchards shown represent the subset of CC and NC orchards for which a county was reported, so respondents in the Both category appear in this panel one or two times depending on whether they provided county information for one or both of their orchards. (c) Cover crop management mix as classified by OrchardType: CoverOnly = manages only cover cropped orchards; Both = manages both CC and NC orchards (paired observations); NoCoverOnly = manages only orchards without cover crops. (d) Years of cover crop usage reported among orchards using cover crops; the largest group reported 6 to 10 years of experience, indicating a sample biased toward established adopters rather than recent or prospective adopters.

3.1.2 Orchard characteristics

The 18 orchards described in the survey spanned a broad range of operation sizes, tree ages, soil textures, and reported yields (Figure 5). Reported acreage was concentrated in the 1,001 to 5,000 acre range (7 of 17 orchards, 41 percent), with 4 (24 percent) under 100 acres and the remaining 6 distributed across the 101 to 500, 501 to 1,000, and more than 5,000 acre ranges.

Tree age was distributed across all life stages: 7 of 18 orchards (39 percent) reported trees more than 20 years old and 4 (22 percent) reported trees 6 to 10 years old, with the remaining 7 distributed across the 5 years or less, 11 to 15 years, and 16 to 20 years categories. Self-reported yields clustered at the upper end of the typical pistachio range: 10 of 18 orchards (56 percent) reported more than 3,000 lb ac^{-1}, 5 (28 percent) reported 2,501 to 3,000 lb ac^{-1}, and 3 (17 percent) reported less than 1,000 lb ac^{-1}, the last category capturing several young orchards in establishment. Soil textures were dominated by clay loam (8 of 18) and sandy loam (5 of 18), with the remaining 5 distributed across clay, silty clay loam, sandy, and one Unsure response.

This characterization situates the modeled Bullseye orchard against the sample. Bullseye is a 61-ha operation in its sixth and seventh leaf during the field data window, with a Rincon silty clay loam soil texture and a first (low) commercial yield of 0.20 t ha^{-1} in 2024 and approximately 1.07 t ha^{-1} in 2025. The modeled orchard is therefore smaller than the median surveyed operation, younger than most, and yields lower than the bulk of the sample, but its soil texture and management profile fall within the range described by the survey respondents.

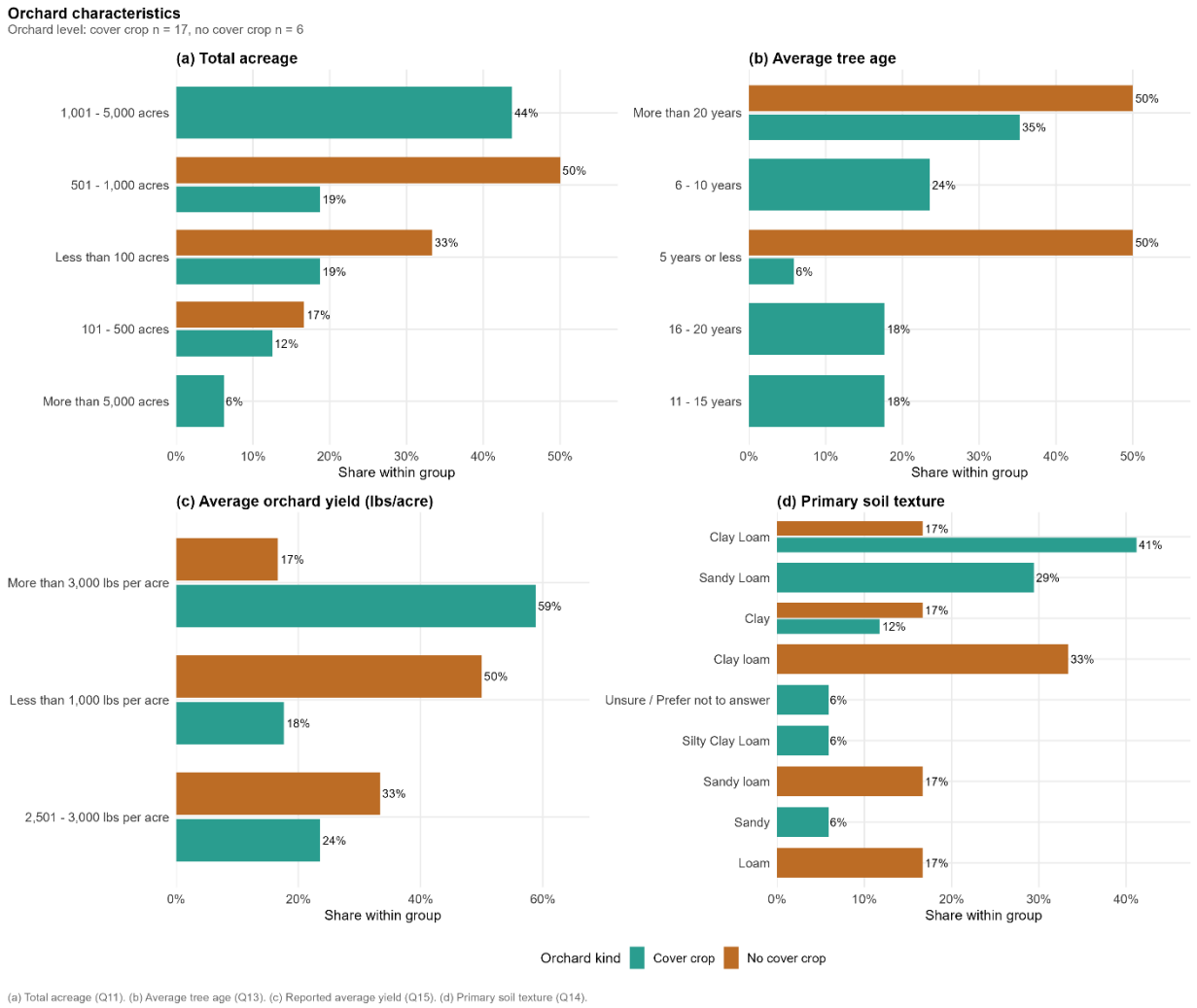


Figure 5. Orchard characteristics of the 18 orchards described by completing respondents. (a) Reported total acreage in 2025 (Q11, n = 17 with 1 NaN). (b) Average tree age in 2025 (Q13, n = 18). (c) Reported average yield in 2025 (Q15, n = 18). (d) Primary soil texture in 2025 (Q14, n = 18, including 1 Unsure response).

3.1.3 Reported management practices

Among orchards using cover crops in the sample (n = 16 to 17, varying by question), management practices were broadly consistent with low input, rainfed cover cropping (Figure 6). The most commonly reported species type was native or volunteer vegetation (47 percent), followed by cereal grasses (41 percent) and legumes and brassicas (29 percent). Among the 12 respondents who reported a specific species count for a seeded mix, 4 reported a single species, 3 reported 2 to 3 species, 2 reported 4 to 5 species, and 3 reported 6 or more species (Figure 7a).

Among the 8 respondents who reported a seeding method, 7 used a drill and 1 broadcast by ground (Figure 7b). Results showed a concentrated CC planting window of October through December and a wider termination window spanning February through July (Figure 7c).

The prominence of native or volunteer vegetation reflects a substantial subset of respondents who do not seed a cover crop mix at all but instead manage the resident understory through mowing alone, an approach intermediate between bare ground and seeded cover cropping that is not always captured in surveys structured around a binary cover or no cover question. Among respondents who provided a termination method, the dominant approaches were natural termination (50 percent) and mowing (44 percent), with herbicide application and disking each used by only 12 percent of respondents. After termination, 88 percent of respondents reported leaving residue on top of the soil as mulch rather than incorporating it. Mowing was the dominant practice for alleyway weed control (86 percent), with herbicide application (43 percent), CC competition (33 percent), and natural termination (33 percent) reported as additional practices (Figure 6d).

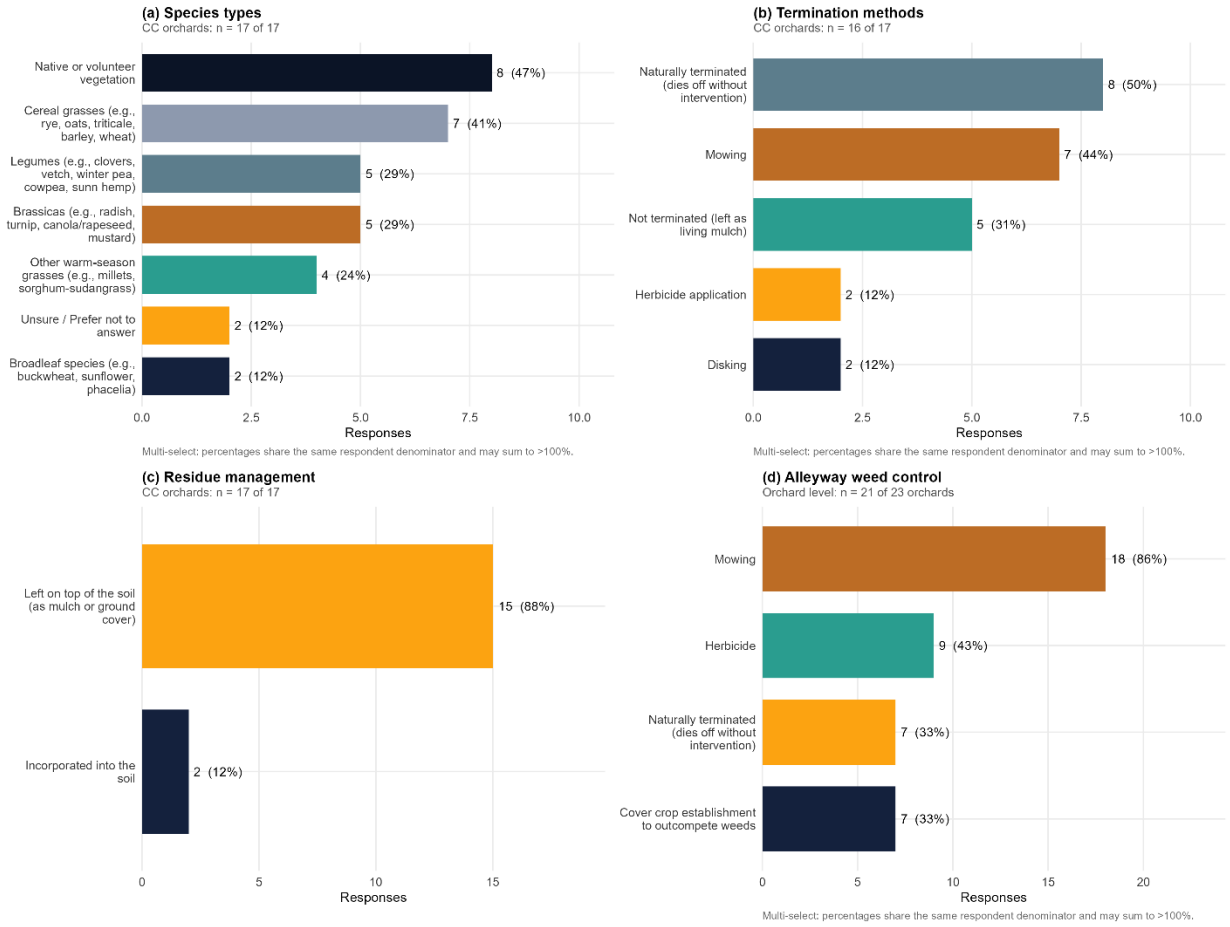


Figure 6. Cover crop management practices reported by respondents managing a cover crop (CC) orchard. (a) Species included in the CC mix (Q31); (b) Termination method (Q38); (c) Residue management after termination (Q39); (d) Weed control practice in the alleyways (Q26).

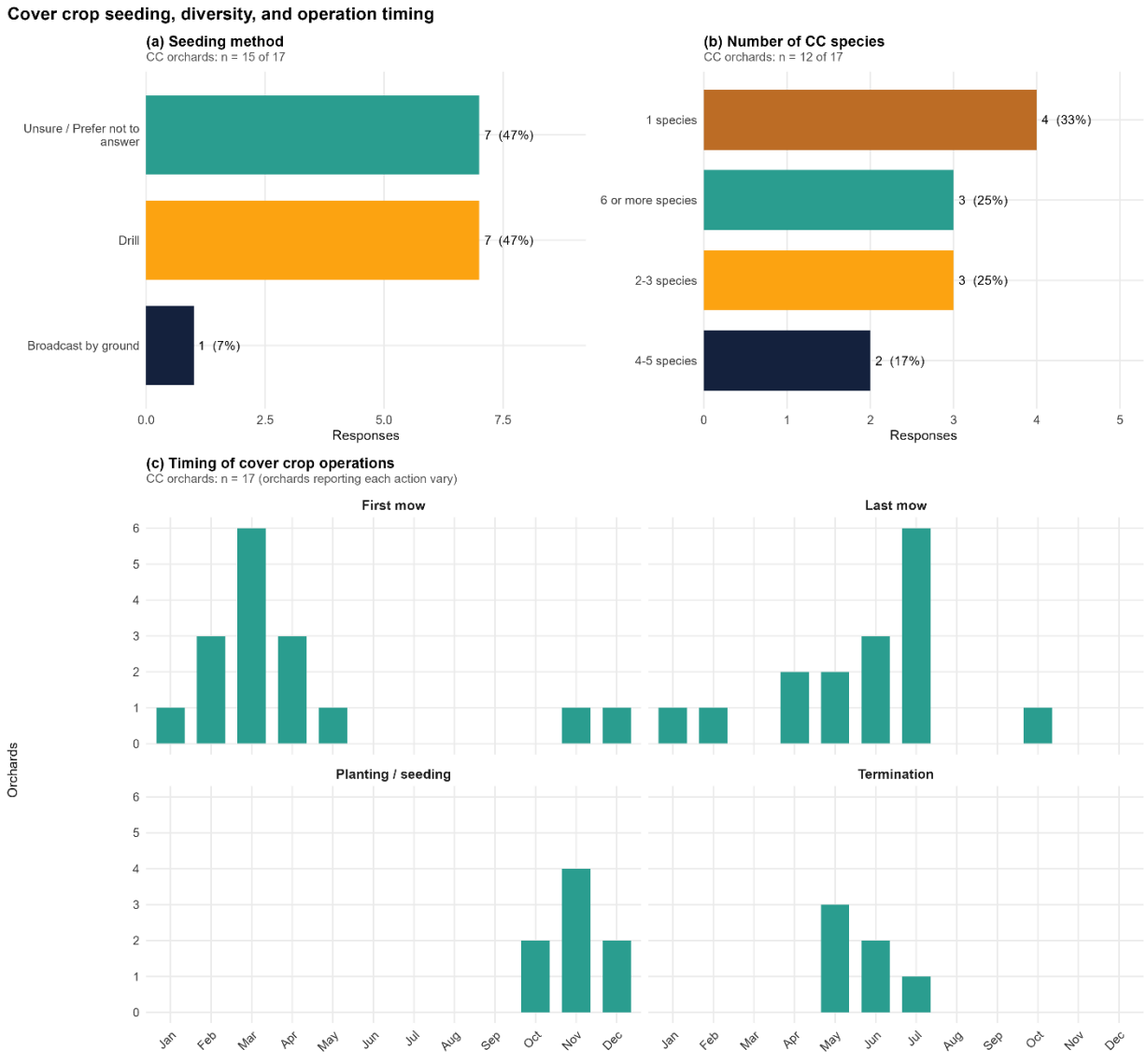


Figure 7. Cover crop seeding and timing practices reported by CC orchard respondents. (a) Number of species included in the cover crop mix (Q30, n = 12 respondents who reported a specific species count). (b) Seeding method (Q32, n = 8 reporting respondents, plus 7 Unsure / Prefer not to answer responses). (c) Calendar timing of cover crop seeding, first mow, last mow, and termination events (Q34_1 to Q34_4, n = 8 to 14 per event).

3.1.4 Report challenges

Among 16 respondents who completed the cover crop challenges section (Q43; Figure 6), the three challenges most frequently rated as "very important" were pest, disease, or weed complications (38 percent); uncertain economic return or yield impacts (33 percent); and high

establishment or input costs (27 percent). The items most frequently dismissed as "not important" were poor germination or stand establishment (80 percent) and lack of information or technical guidance (69 percent).

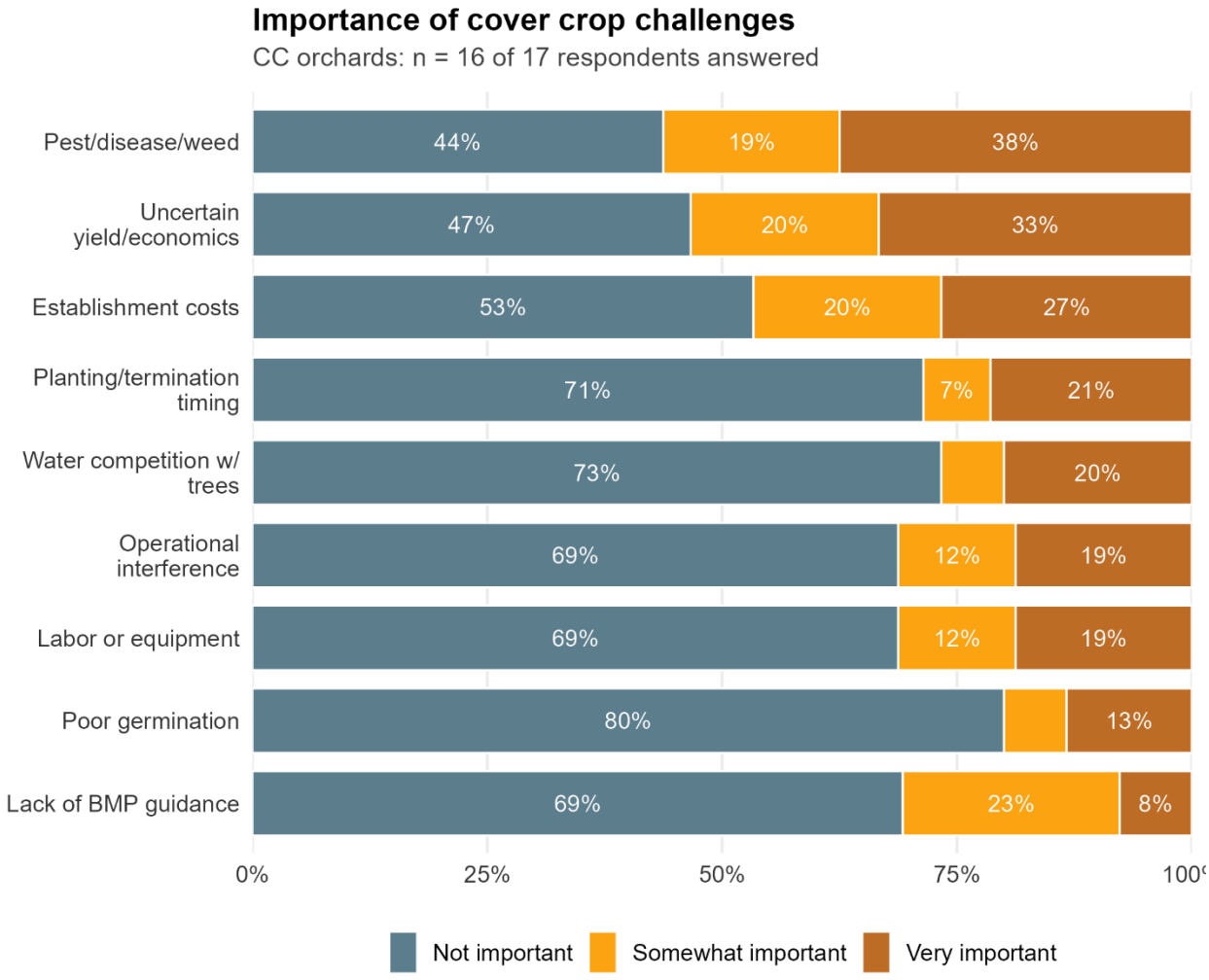


Figure 8. Importance ratings for nine cover crop related challenges among respondents reporting on a cover cropped orchard (n = 16). Each bar shows the share of respondents rating that challenge as Not important, Somewhat important, or Very important. Items are ordered by the share rating each challenge Very important.

3.1.5 Concerns, benefits, and knowledge gaps

Seventeen respondents completed the concerns, benefits, and knowledge gaps blocks (Q83 to Q87). Among agronomic concerns (Figure 8a), water use and competition with trees was

the most frequently rated "extremely concerned" item (35 percent), followed by pest, disease, and weed pressure (29 percent) and nutrient immobilization (12 percent). Operational concerns (Figure 8b) were generally lower: equipment costs and availability had the highest "extremely concerned" share (24 percent), while interference with harvest (88 percent), complicated transition to cover cropping (76 percent), and establishment and termination timing (76 percent) were each rated "not concerned" by a large majority. Economic concerns (Figure 8c) were the most polarized of the three blocks. Uncertainty of economic returns and cost of water under groundwater allocations were tied as the highest "extremely concerned" items, each at 41 percent, with seed costs (25 percent) and higher labor and equipment costs (24 percent) following.

Respondents valued CC benefits highly across nearly all categories (Figure 9). Soil health and organic matter improvement and soil moisture management and erosion control each rated “highly” valued by 82 percent of respondents, with soil moisture management and erosion control (82 percent) and environmental stewardship and sustainability (76 percent) close behind. Reduced inputs (irrigation, fertilizer, and herbicide) was the least valued benefit, with only 44 percent rating it highly.

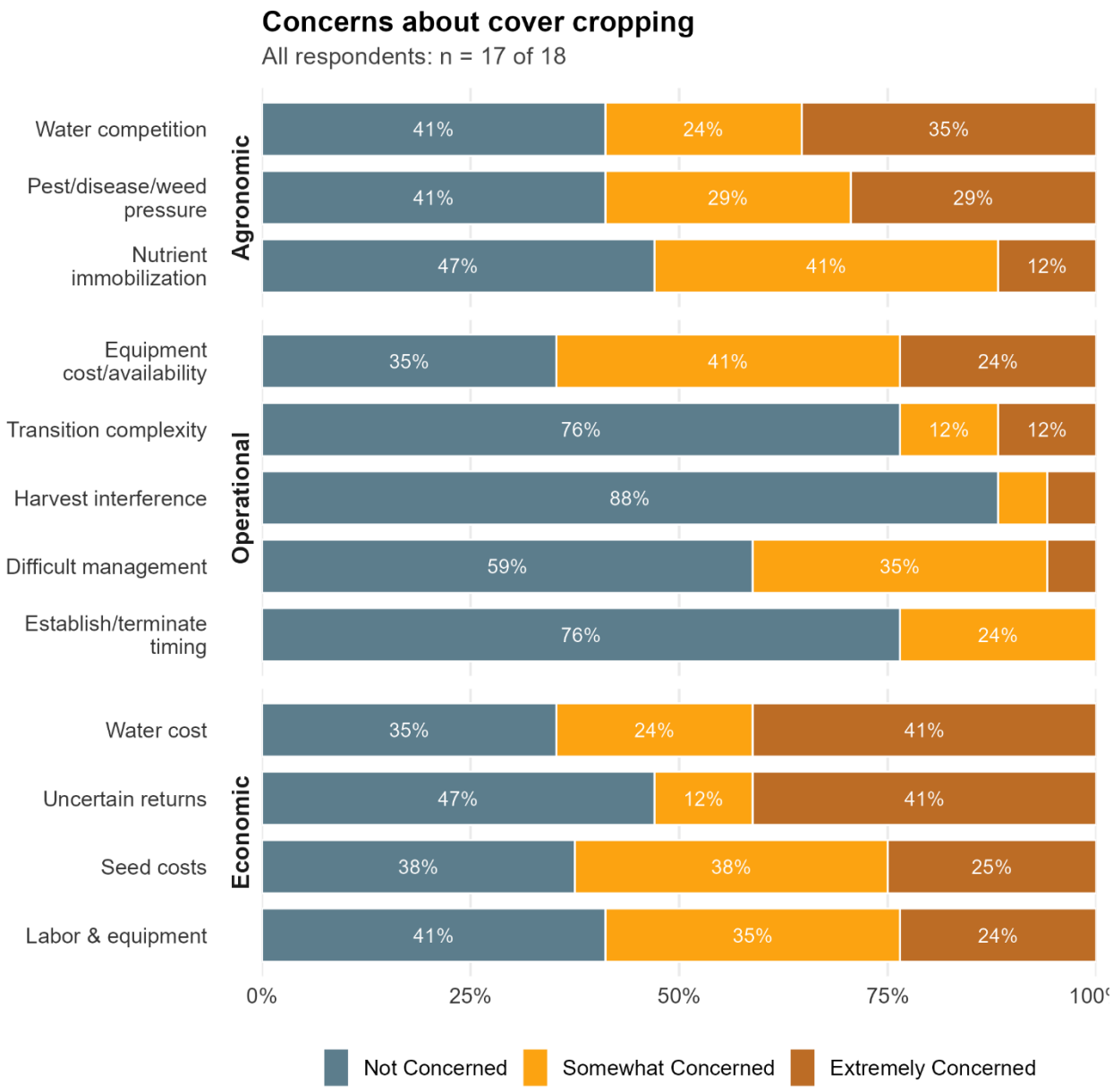


Figure 9. Level of concern across three classes of cover cropping issues: (a) agronomic; (b) operational; (c) economic concerns. n = 17 per panel. Each bar shows the share rating that item as Not Concerned, Somewhat Concerned, or Extremely Concerned. Items ordered by the share rating Extremely Concerned.

Knowledge gap rankings (Figure 10) were headed clearly by tree nutrition, soil health, and biological activity, which was rated "high priority" by 82 percent of respondents and selected as the single highest priority gap by 8 of 17 respondents. Subsequent rankings differed slightly between the two questions. In panel (a), water use and pest, weed, and disease control tied at 71

percent rating each as High priority, with economic return third at 60 percent. In panel (b), economic return placed second (4 of 17 votes) and water use third (2 votes). The items rated lowest priority were seed selection and traits (21 percent High priority) and seeding, maintenance, and termination (27 percent).

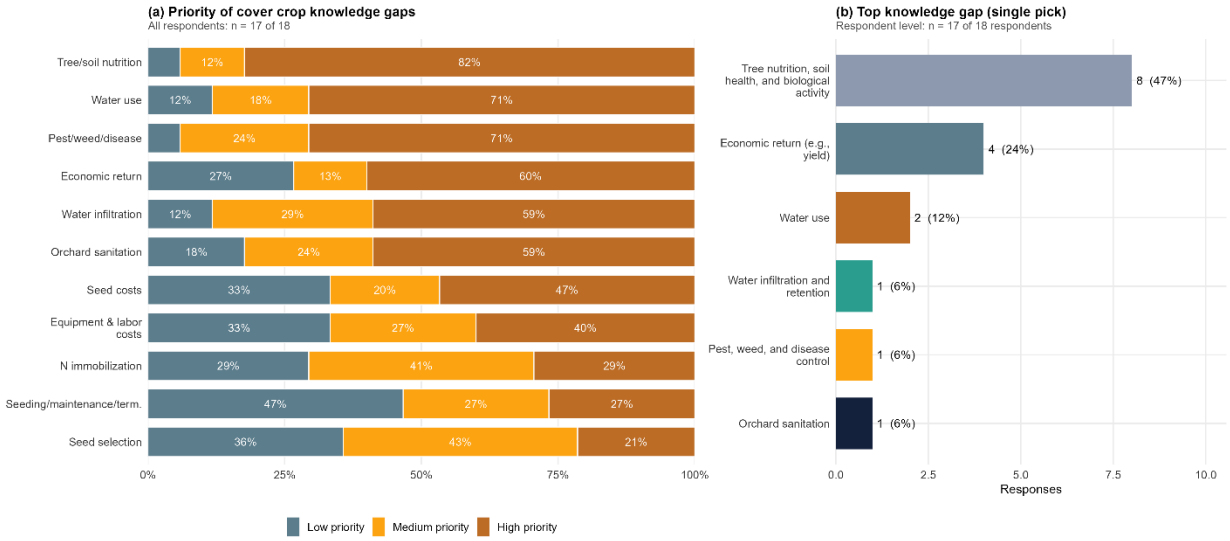


Figure 10. Priority of knowledge gaps in winter cover cropping (n = 17). (a) Priority assigned to each of eleven specific knowledge gaps (Low / Medium / High priority). (b) Single highest-priority gap selected from the list. Five gaps received no votes and are omitted from panel (b).

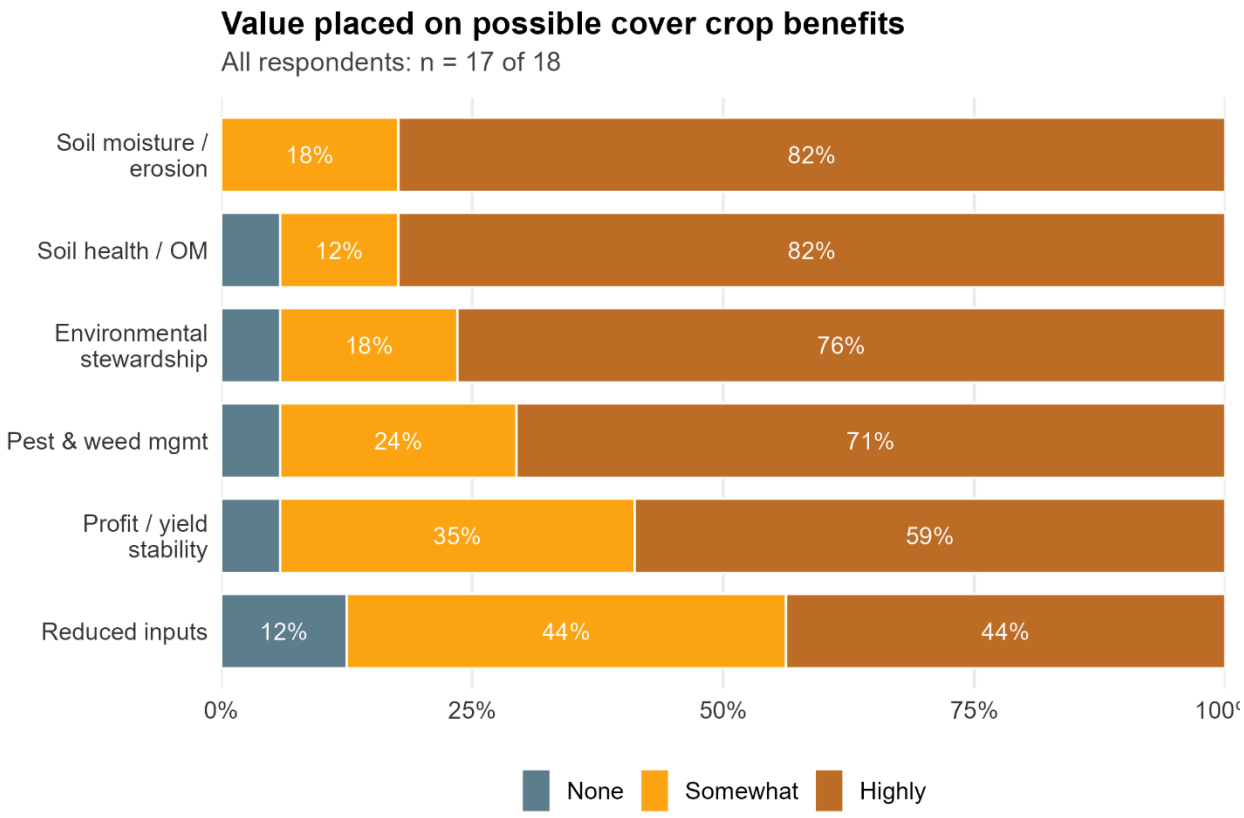


Figure 11. Value placed on six potential cover crop benefits among the 17 respondents who completed the benefits block. Each bar shows the share rating that benefit as None, Somewhat valued, or Highly valued.

3.1.6 Information sources and benefit prioritization

The same 17 respondents who completed the concerns and benefits blocks also ranked the information sources they rely on for cover crop decisions (Q81, n = 15 of 17 ranked all items) and the broad categories of cover crop benefits they prioritize (Q82, n = 13 of 17). Information source rankings (Figure 12) place practitioner facing sources at the top: farm advisors and Cooperative Extension specialists had the lowest mean rank (most important) at 2.20, followed by PCAs, CCAs, or independent consultants (2.80) and research collaborations or university studies (3.47). Passive media sources, including agricultural publications, books, and online materials, clustered at the bottom of the rankings, with books and online materials having

the highest mean rank (least important) at 5.60. Workshops and field days fell between these clusters at a mean rank of 4.73.

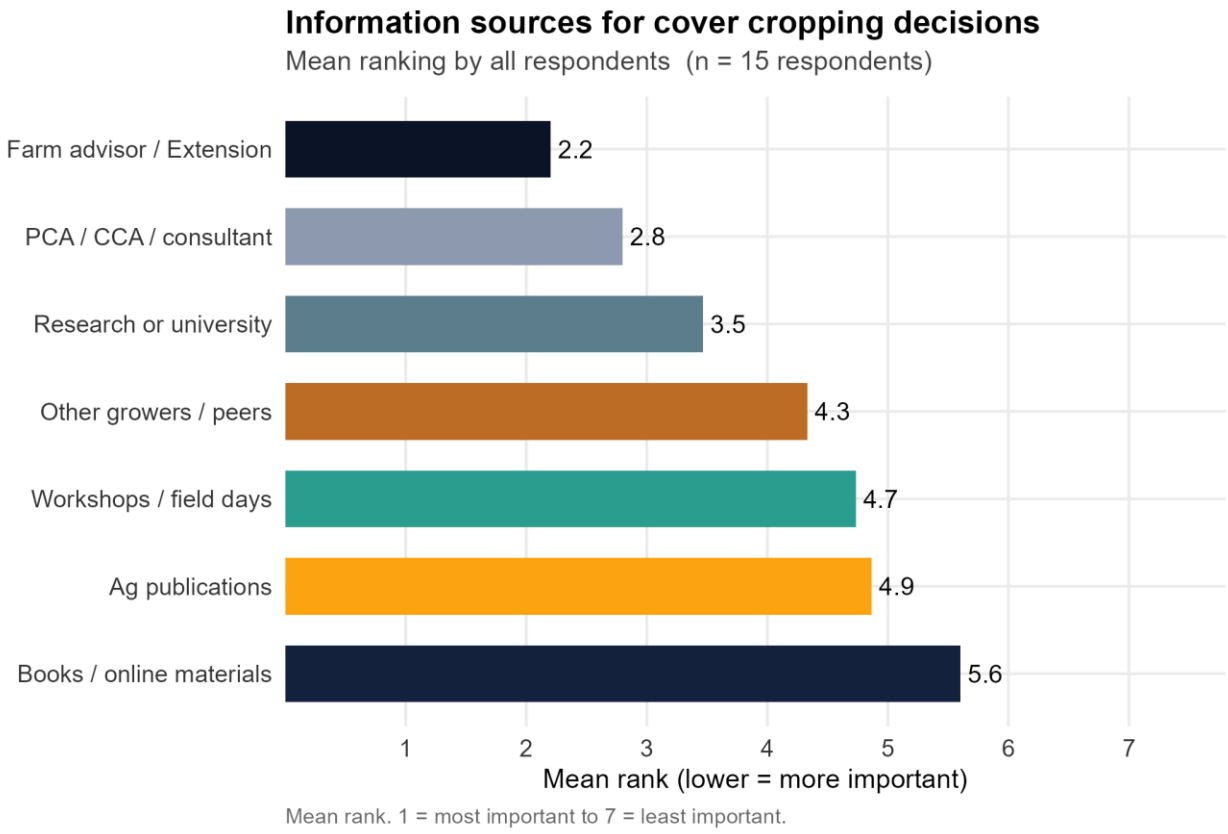


Figure 12. Ranking of trusted information sources for cover cropping decisions (Q81, n = 15). Mean rank shown; lower mean rank corresponds to higher importance.

Benefit category prioritization (Figure 13) was strongly weighted toward agronomic benefits, which 11 of 13 respondents ranked first and the remaining 2 ranked second, for a mean rank of 1.15. Economic and operational benefits were nearly tied in mean rank (2.38 and 2.46) but the underlying distributions differ: 2 respondents ranked Economic benefits first while no respondent ranked Operational benefits first, indicating that Economic benefits have a more polarized reception while Operational benefits are consistently rated as secondary.

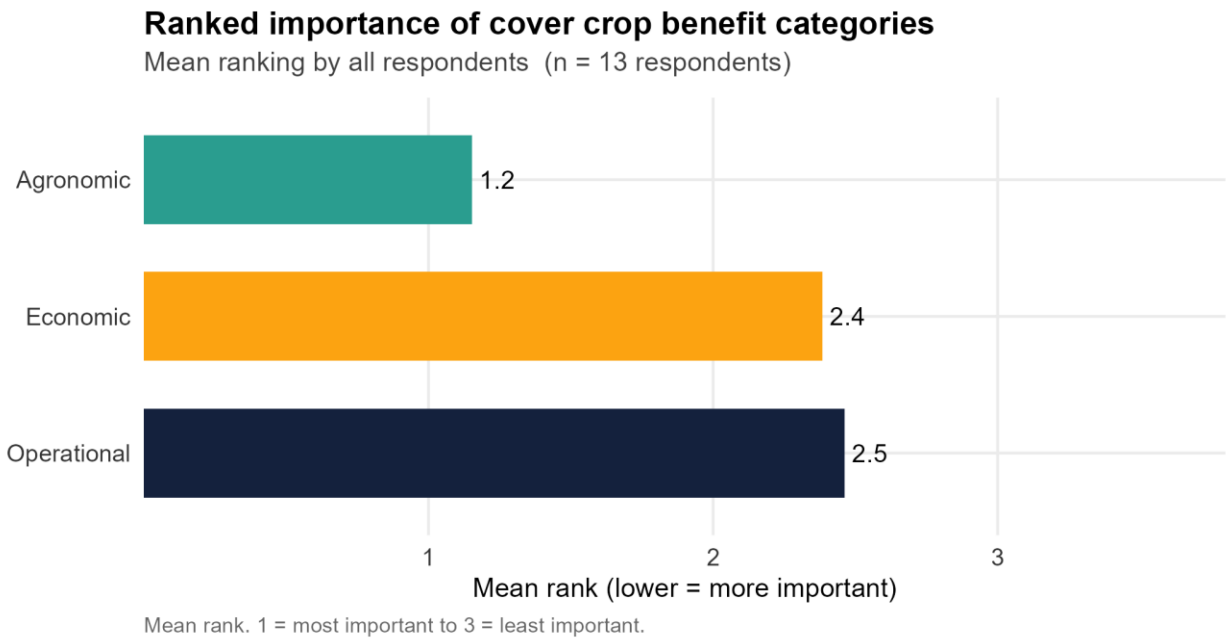


Figure 13. Ranking of cover crop benefit categories (Q82, n = 13 respondents who ranked all three). Each bar shows the mean rank assigned to each of the three categories (Agronomic, Economic, Operational), with lower mean rank corresponding to higher prioritization.

3.1.7 Observed yield response and irrigation practices

Of 17 respondents reporting on yield change since cover crop adoption (Figure 12a), 5 reported no significant change (within ±5 percent), 3 reported an increase greater than 5 percent, and 2 reported a decrease greater than 5 percent; 7 were unsure or preferred not to answer.

Cover crops in this sample were managed largely without supplemental irrigation. Of 16 orchards reporting on irrigation regime, 11 relied entirely on rainfall, 4 irrigated only for establishment, and 1 irrigated once or twice during the season (Figure 12b).

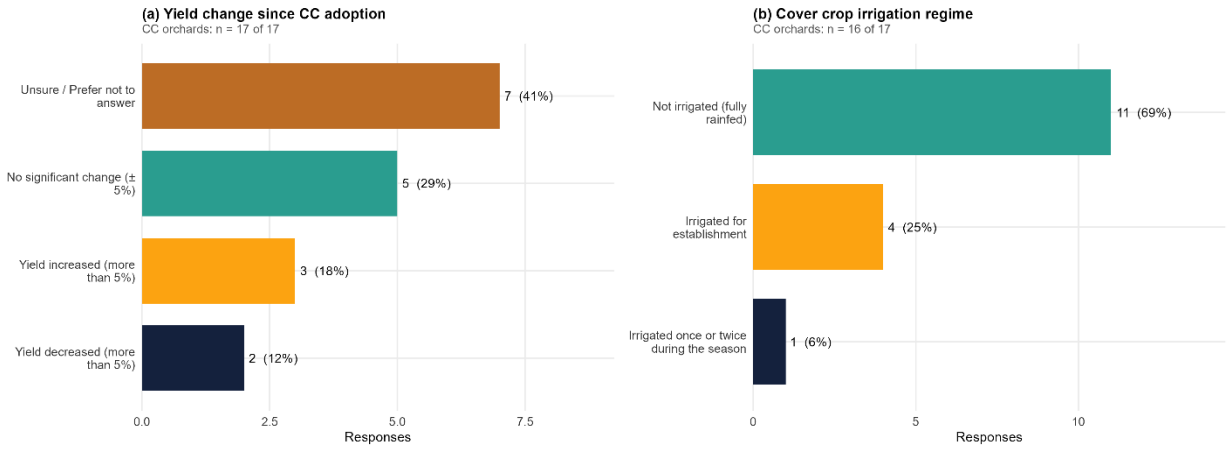


Figure 14. Observed cover crop outcomes among orchards using cover crops. (a) Yield change since CC adoption (n = 17). (b) Cover crop irrigation regime (n = 16).

3.1.8 Irrigation and water management

To contextualize the water cost and water competition concerns that motivate the climate-scenario analysis (Section 3.5), respondents were asked about the orchard scale irrigation system, water source, applied depth, irrigation cost, and use of deficit irrigation. All 18 CC orchards used drip irrigation, split between single-line drip (10 of 18) and double-line drip (8 of 18) configurations (Figure 15). Primary water source was distributed across surface water only (6 of 18), groundwater only (4 of 18), and two mixed categories (4 of 18 each), so 12 of 18 orchards (67 percent) report at least partial reliance on groundwater. Applied irrigation depth was concentrated between 26 and 40 inches (13 of 18 orchards, 72 percent), with 3 orchards reporting more than 40 inches and 2 reporting less than 25 inches. Reported irrigation cost was bimodal at the top of the scale: 6 of 14 respondents reported more than $10 per acre-inch and 5 of 14 reported $8 to $10 per acre-inch, with the remaining 3 distributed at lower price points. Eight of 18 respondents reported irrigating at or above full ET_a, while the remaining 10 practiced deficit irrigation of some kind: 2 reported slight deficits of less than 10 percent, 5 reported moderate

deficits of 10 to 25 percent, and 1 reported a severe deficit of more than 25 percent (the remaining 2 selected Unsure).

Cover crop activity costs reported by respondents fell predominantly in the less than $25 and $25 to $50 per acre range (n = 8 to 12 depending on activity). Cost-share or other financial assistance was reported by 5 of 17 respondents (29 percent): 3 used the California Healthy Soils Program, 3 used NRCS or EQIP, and 1 respondent used both; the remaining 12 of 17 (71 percent) reported self-funding all cover crop activity.

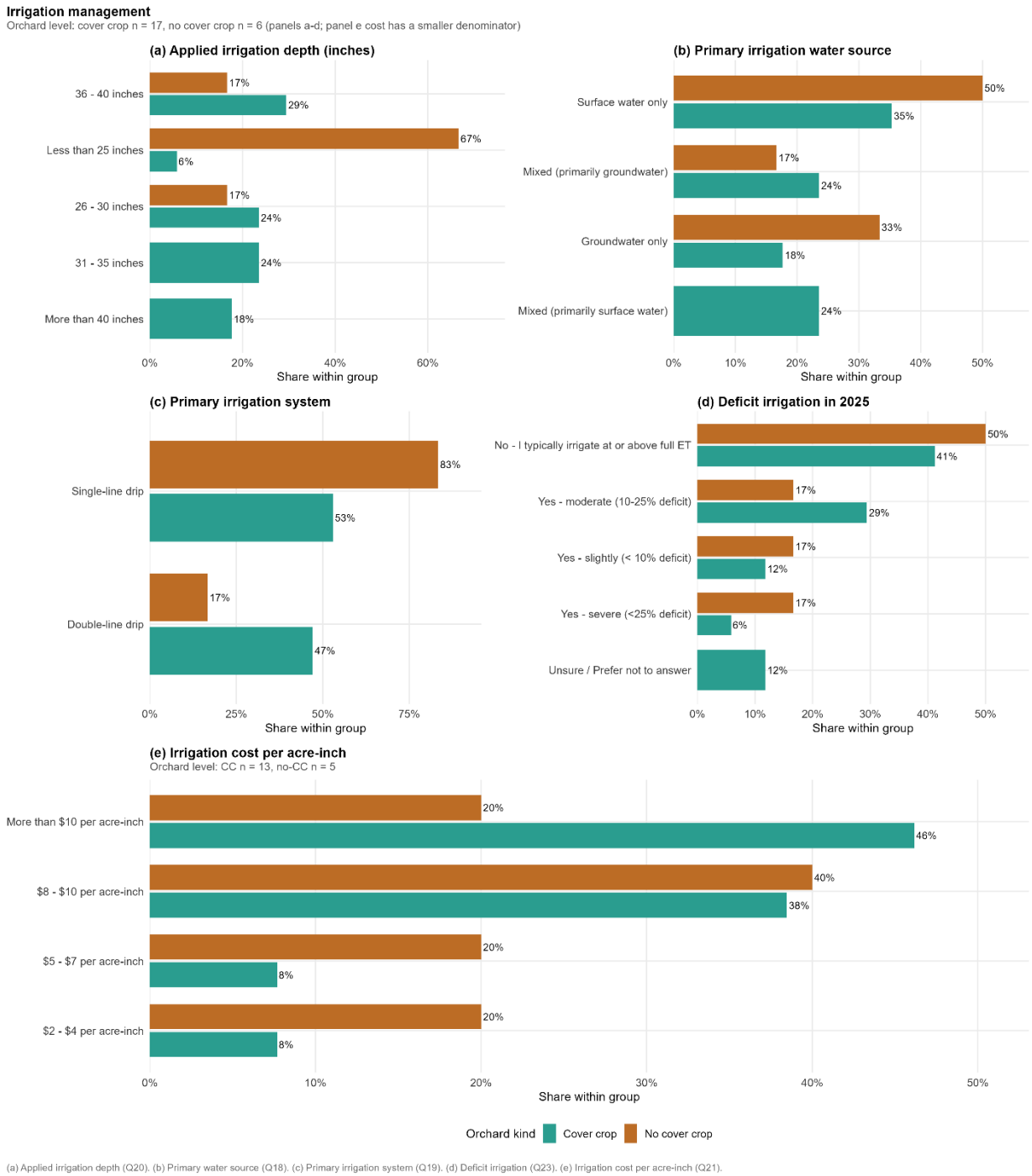


Figure 15. Irrigation and water management for the 18 CC orchards. (a) Primary irrigation system (Q19, n = 18). (b) Primary water source for irrigation (Q18, n = 18); the two "mixed" categories indicate orchards using both surface and groundwater with the indicated source as primary. (c) Applied irrigation depth (Q20, n = 18). (d) Irrigation cost per acre-inch (Q21, n = 14, with 4 NaN). (e) Deficit irrigation practice (Q23, n = 18, including 2 Unsure responses).

3.1.9 Reasons for non-adoption among NC respondents

A small subset of the survey (n = 4 of 9 no cover (NC) respondents) provided reasons for not using CC in their orchards (Figure 14). The most cited reason was pest, disease, or weed management concerns (3 of 4 respondents), followed by limited water availability or competition concerns and high cost or uncertain economic return (2 of 4 each), and lack of information or technical guidance and additional equipment and labor requirements (1 of 4 each). The small sample limits inferential interpretation.

The same NC respondents were asked how likely each of six types of support would be to move them toward adoption (Figure 16b, n = 6 respondents who answered Q65). Financial assistance and economic case studies were the strongest movers: 4 of 6 respondents rated each as "Very Likely" to lead to adoption, with the remaining 2 rating each as "Somewhat Likely" or "Unlikely". Demonstration sites, technical guidance, peer or consultant advice, and water and irrigation information each had 1 of 6 "Very Likely" and 3 of 6 "Somewhat Likely" responses, with the remaining 2 each rating "Unlikely".

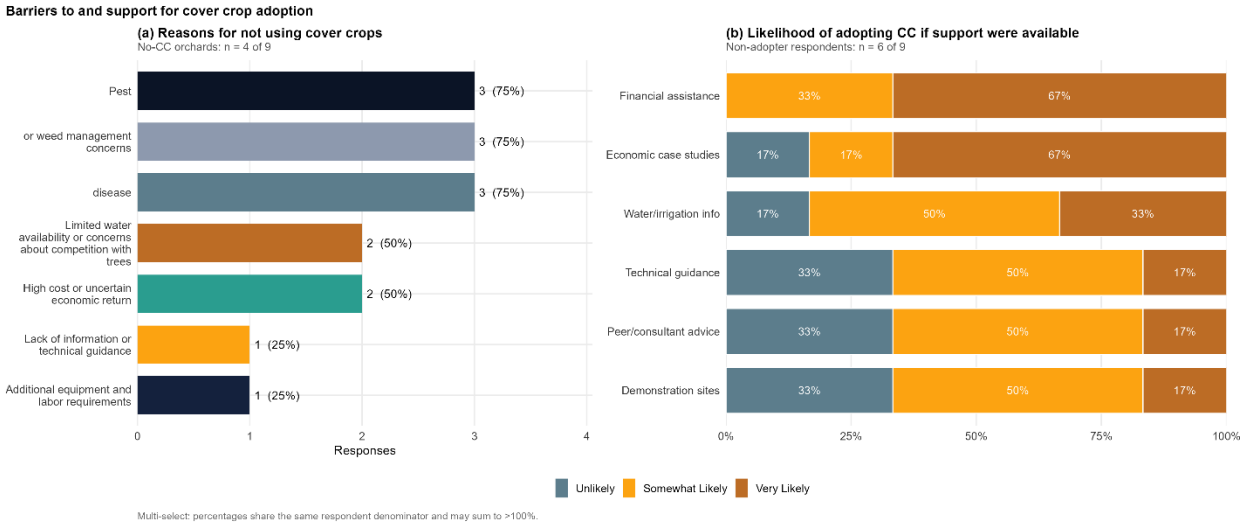


Figure 16. Non-adoption of cover cropping among NC respondents. (a) Main reasons cited for not using cover crops in the NC orchard (Q64). (b) Self-reported likelihood of adopting cover cropping if each of six types of information or support were provided (Q65).

3.2 APEX sensitivity analysis

PARM2 (root growth-soil strength) is the dominant parameter in both orchards, with substantially stronger sensitivity in NC (SI_Total = 0.77) than in CC (SI_Total = 0.43; Table 10). PARM2 controls how aggressively the model permits root expansion through soil layers with mechanical impedance. Its dominance in NC indicates that pistachio root response to soil strength is a critical physiological process driving simulated outputs when no competing vegetation is present; the lower CC sensitivity reflects the impact of the cover crop's root system or other external factors. PARM17 (soil evaporation-plant cover factor) is the second-most influential parameter, but with a strong CC vs NC contrast: in CC it is nearly co-dominant with PARM2 (SI_Total = 0.41), while in NC it drops to roughly two-thirds of the CC value (SI_Total = 0.26). This contrast is consistent with the CC impacting the partitioning of evaporative demand between bare soil and vegetation cover. PARM1 (Penman-Monteith canopy PET factor) is the third parameter (SI_Total = 0.12 in CC, 0.09 in NC), and PARM12 (soil evaporation coefficient)

is the least sensitive of the four parameters (SI_Total = 0.02 in both orchards). PARM1, PARM2, PARM12, and PARM17 were selected as the primary calibration targets.

3.3 APEX baseline model outputs

A useful first step in evaluating an APEX simulation is to characterize the overall behavior of the model before formal calibration. The baseline simulations use the management records provided by the orchard manager (irrigation, fertilization, tillage, harvest, and cover crop operations from 2019 onward, with the 2007 to 2018 warm-up running on default tree establishment management), and the CIMIS Davis weather record. No site-specific parameter adjustments have been applied at this stage. Examining these uncalibrated outputs serves three purposes. It provides a sanity check that the model is internally consistent and reproducing the basic mass balance. It shows whether any major variables are clearly out of range and need attention before quantitative calibration. And it identifies which parameters are the most plausible candidates for adjustment when the model is fit to observed ET_a, soil water content, leaf area index, and yield.

The APEX simulation in this study runs from 2007 through 2026, but the 2026 calendar year is still in progress at the time of writing and is excluded from all baseline figures and annual-summary tables. The figures in this section therefore cover the 2018 to 2025 pistachio + cover crop period (year 1 onward after the December 2018 transplant). The full 2007 to 2025 simulation provides spin-up of the soil carbon and nitrogen pools and historical climate context for the climate-scenario analysis in Section 3.5; full-simulation versions of each baseline figure are presented as paired supplementary figures (S6a, S7a, and so on), as are versions focused on the 2023 to 2025 field data window where direct comparison with EC, neutron probe, and LI-2200 observations is possible.

Table 10. Sensitive parameters identified by the output-category-targeted Sobol sensitivity analysis for the no cover (NC) and cover crop (CC) orchards. PARM identifiers follow the APEX 1501 user manual (Williams et al., 2023).

Parameter	Description	NC SI_First	NC SI_Total	NC Rank	CC SI_First	CC SI_Total	CC Rank
PARM1	Penman-Monteith canopy PET factor	0.08	0.09	3	0.11	0.12	3
PARM2	Root growth-soil strength	0.65	0.77	1	0.39	0.43	1
PARM12	Soil evaporation coefficient	0.04	0.02	4	0.02	0.02	4
PARM17	Soil evaporation-plant cover factor	0.29	0.26	2	0.44	0.41	2

In the figures that follow, standard colors denote variable type: water-related quantities (precipitation, percolation, evapotranspiration, soil water content) are shown in blue, temperature-related quantities in red, and crop yield and biomass in green. The two orchards share most physical conditions (soil texture, slope, climate, tree spacing, and pistachio cultivar), so differences between their baseline outputs are interpretable as the model response to the cover crop and its associated management rather than to underlying site differences.

3.3.1 Daily scale evaluation

At the daily scale, baseline performance differs substantially between the two treatments (Table 11). The NC orchard tracks the eddy covariance record with R^2 = 0.57, RMSE = 1.08 mm day^{-1}, NSE = 0.06, PBIAS = +38.3 percent, and RSR = 0.97, with the large positive PBIAS indicating a substantial underestimation in the baseline. The CC orchard performance is weaker, with R^2 = 0.23, RMSE = 1.12 mm day^{-1}, NSE = −0.43, PBIAS = +17.9 percent, and RSR = 1.20. The large positive PBIAS in both treatments indicates that the baseline systematically underestimates ET, while the negative NSE and RSR > 1 in CC indicate substantial day-to-day scatter that the baseline parameter set does not capture. Inspection of the daily series shows that the largest CC residuals occur on ten high-PET days between January and mid-March 2024 to 2026, when simulated daily ET reaches 6 to 9 mm day^{-1} while observed values remain at 2 to 3 mm day^{-1}. On these days, the CC is transpiring at near-potential rates with no water stress feedback (WPEA water stress factor = 1.0), reflecting an unstressed canopy in the baseline parameter set rather than a structural problem with the model. This pattern identifies the cover crop transpiration ceiling as a primary calibration target through adjustment of PARM17 (the soil evaporation plant cover factor) and PARM1 (the Penman-Monteith canopy PET factor) identified by the Sobol sensitivity analysis as the dominant ET_a parameters.

Table 11. Evaluation metrics for simulated daily and monthly evapotranspiration against eddy covariance observations for the no cover (NC) and cover crop (CC) treatments over February 2023 to December 2025. RSR is the RMSE–observations standard deviation ratio per Moriasi et al. (2007).

Treatment	Time scale	*n*	R^2	RMSE	NSE	PBIAS (%)	RSR
NC	Daily	1063	0.57	1.08	0.06	+38.3	0.97
CC	Daily	1063	0.23	1.12	−0.43	+17.9	1.20
NC	Monthly	35	0.74	29.7	0.11	+38.3	0.94
CC	Monthly	35	0.25	27.6	-0.18	+17.8	1.09

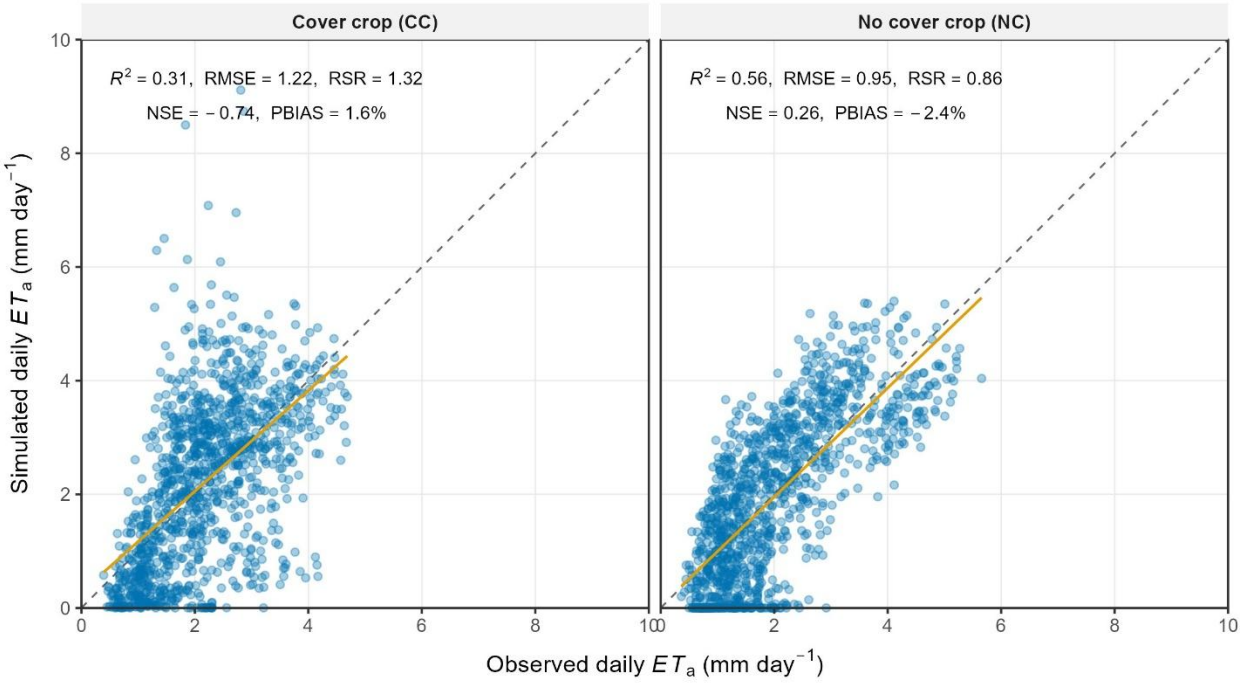


Figure 17. Daily 1:1 performance for the cover crop (CC) and no cover (NC) treatment simulations.

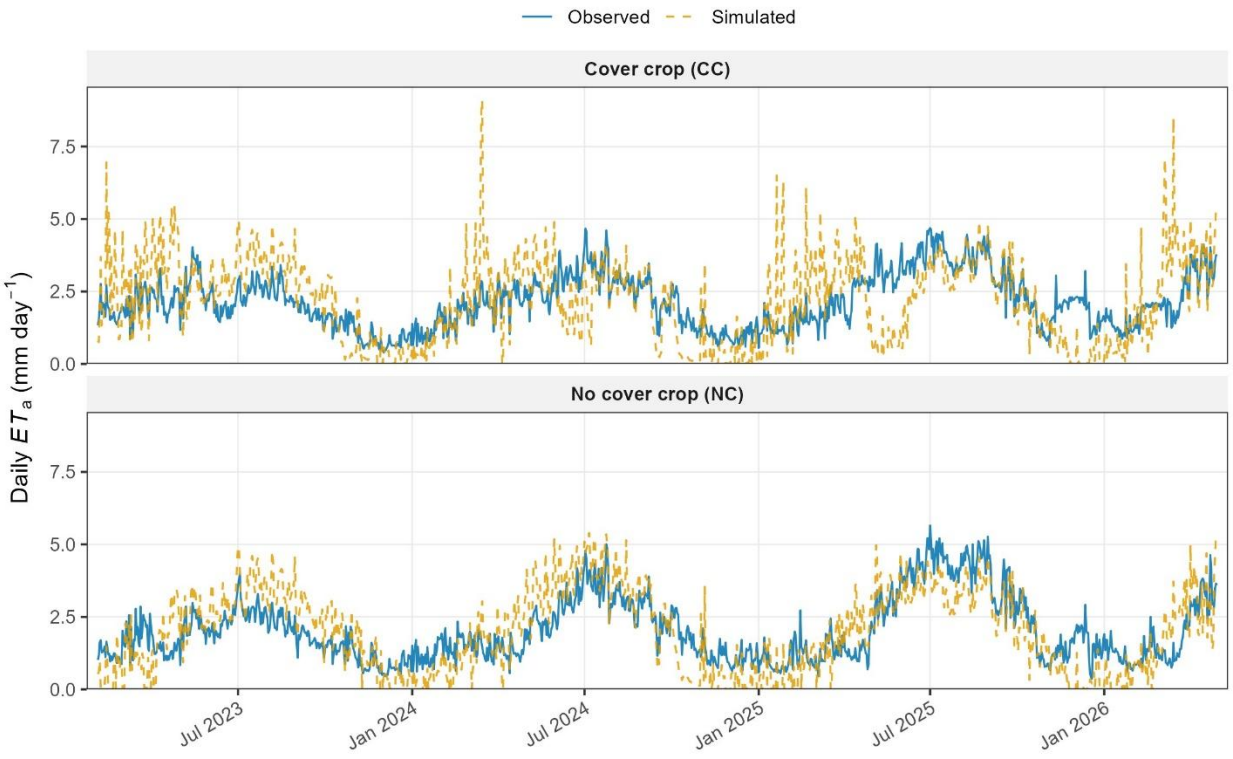


Figure 18. Daily time series of observed ET_a compared to simulated ET_a for the cover crop (CC) and no cover (NC) treatment simulations for March 2023 to April 2026.

3.3.2 Monthly scale evaluation

At the monthly scale, the baseline simulation misses the satisfactory thresholds for monthly evaluation in both orchards (Table 11) Moriasi et al. (2016). The NC orchard achieves R^2 = 0.74, RMSE = 29.7 mm month^{-1}, NSE = 0.11, PBIAS = +38.3 percent, and RSR = 0.94, with NSE marginally below the satisfactory threshold. The CC orchard achieves R^2 = 0.25, RMSE = 27.6 mm month^{-1}, NSE = -0.18, PBIAS = +17.8 percent, and RSR = 1.09, with NSE below the satisfactory threshold.

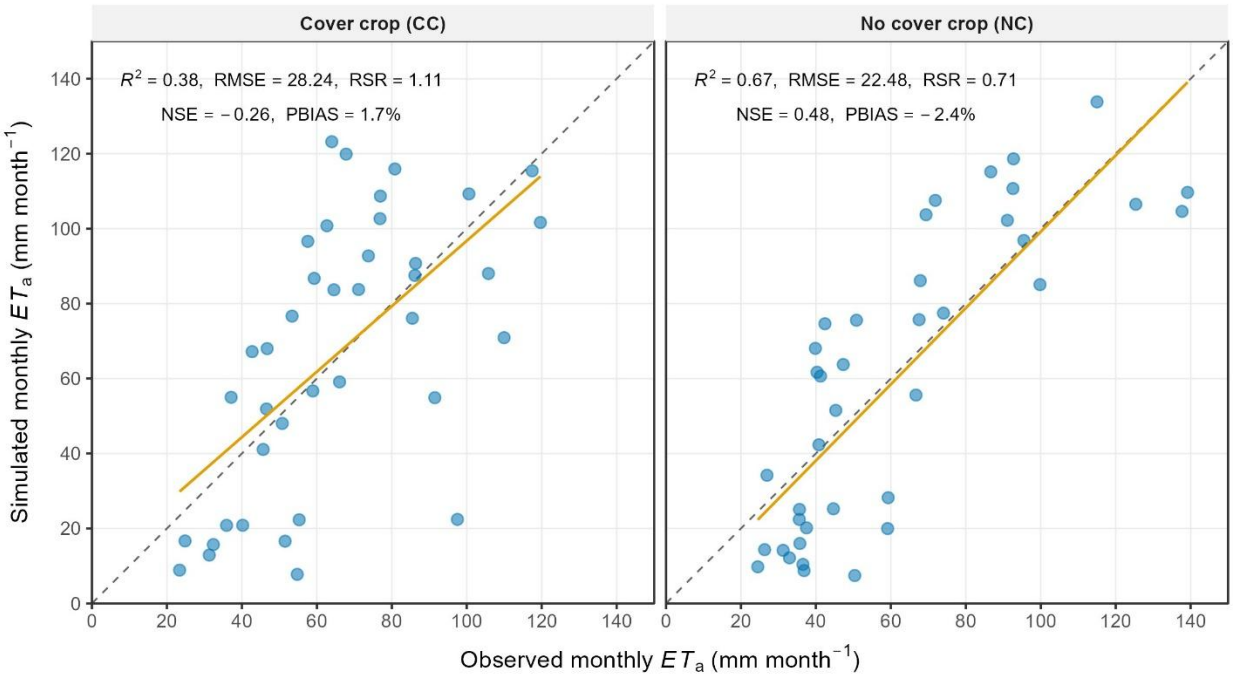


Figure 19. Monthly 1:1 evaluation performance for the cover crop (CC) and no cover (NC) treatment for February 2023 to April 2026.



Figure 20. Monthly time series for the cover crop (CC) and no cover (NC) treatment simulations from February 2023 to April 2026.

3.3.3 No cover (NC) orchard

Figure 21 summarizes the cumulative water inputs and outputs of the NC orchard over the 2023 to 2025 period. Total precipitation was 1,510 mm, total irrigation was 961 mm, and evapotranspiration accounted for 2,165 mm or about 86 percent of total water outputs. Total deep percolation over the same period was 183 mm, concentrated in the wet 2023 winter. On an annual basis during the field data period, simulated ET_a ranged from 685 to 741 mm, consistent with the magnitude expected for a young, drip irrigated pistachio orchard in the Sacramento Valley.

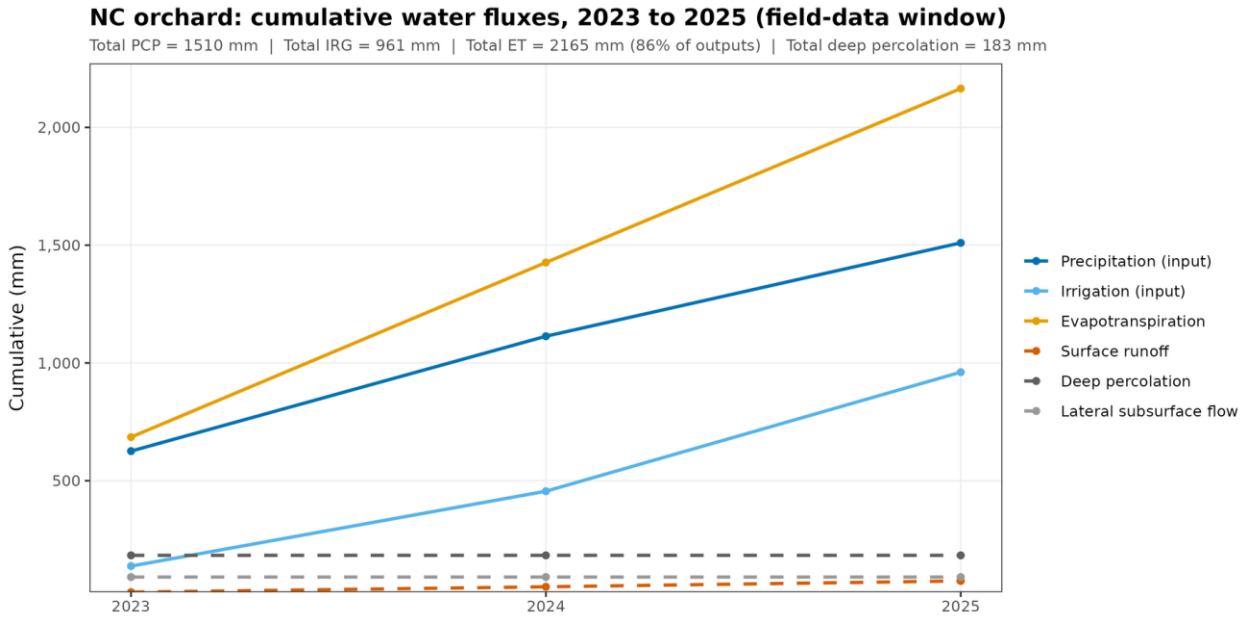


Figure 21. Cumulative water fluxes for the NC orchard over the 2023 to 2025 (field data window) period. Solid lines = water inputs (precipitation, irrigation); orange line = ET; dashed lines = surface runoff, deep percolation, and lateral subsurface flow.

Figure 22 shows the annual water flux time series for the NC orchard over the same period. Annual fluxes track precipitation, with 2023 showing the largest deep percolation pulse

(183 mm) and 2024 and 2025 essentially zero. Annual ET_a ranged from approximately 685 to 741 mm across 2023 to 2025.

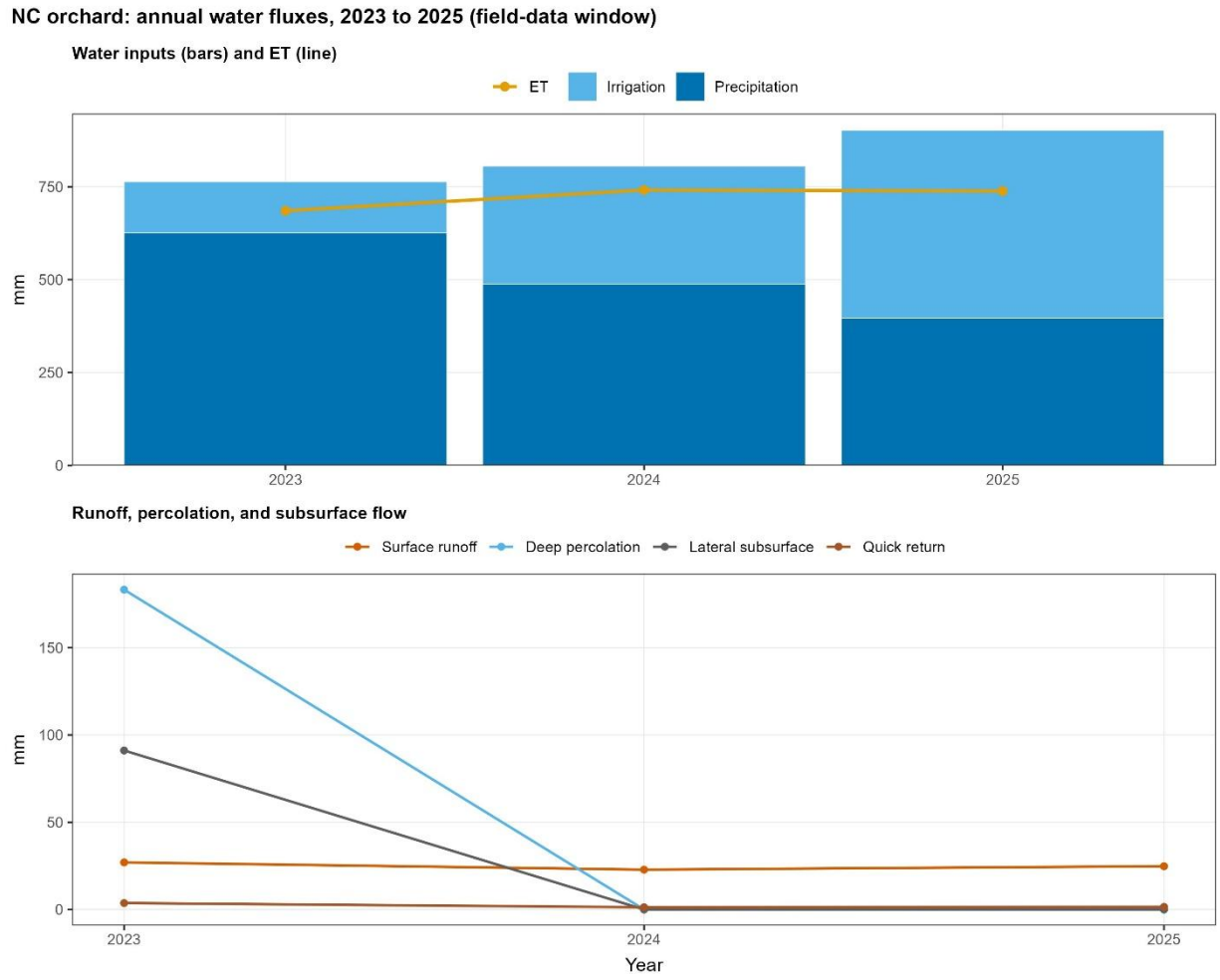


Figure 22. Annual water fluxes for the NC orchard over the 2023 to 2025 (field data window) period. Top panel: precipitation and irrigation (stacked bars) with ET overlaid as an orange line. Bottom panel: surface runoff, deep percolation, lateral subsurface flow, and quick return flow.

Figure 23 plots annual pistachio yield and precipitation for the NC orchard. Commercial yield begins in 2024 (modeled yield 1.10 t ha^{-1} in 2024 and 1.41 t ha^{-1} in 2025), consistent with the typical year-6 onset of commercial yield in young pistachio orchards.

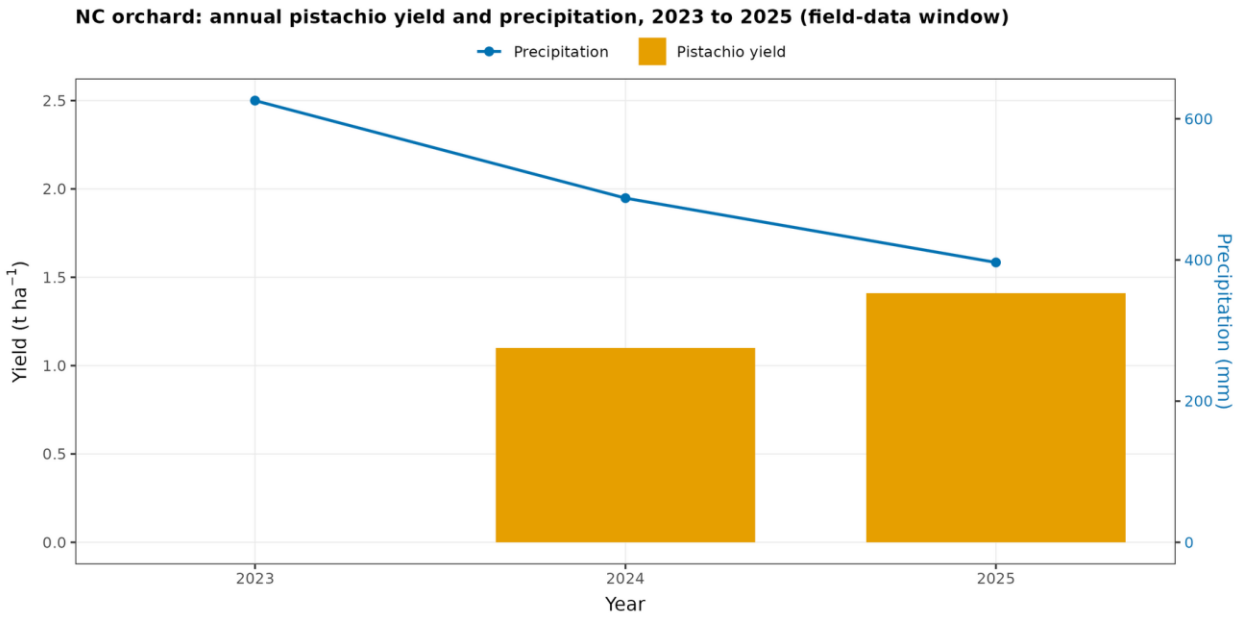


Figure 23. Annual pistachio yield and precipitation for the NC orchard. Window: 2023 to 2025 (field data window).

Figure 24 plots the daily pistachio heat unit index (HUI) for the NC orchard. HUI accumulates from zero at dormancy break to approximately 1.0 at physiological maturity. In the baseline simulation, the pistachio HUI rises only to approximately 0.45 by the end of 2025.

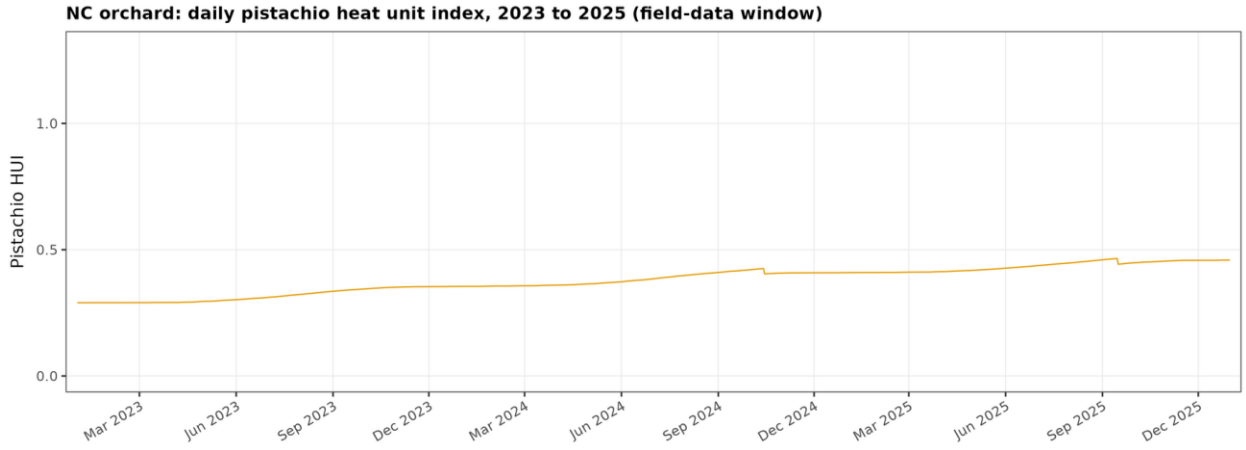


Figure 24. Daily pistachio heat unit index for the NC baseline simulation. Window: 2023 to 2025 (field data window). HUI accumulates from zero at dormancy break each year; values approaching 1.0 indicate progress toward physiological maturity.

Figure 25 plots weekly mean pistachio water, nitrogen, and temperature stress factors for the NC orchard. Daily values were averaged to weekly resolution to make seasonal patterns visible without the day-to-day noise. The temperature stress factor falls substantially below 1.0 during each winter and partially during the shoulder seasons, identifying TBS, TOP, and the temperature stress function as calibration targets in Section 3.4. Water stress is intermittent and primarily winter-driven, consistent with the orchard manager's irrigation schedule keeping summer root-zone moisture adequate.

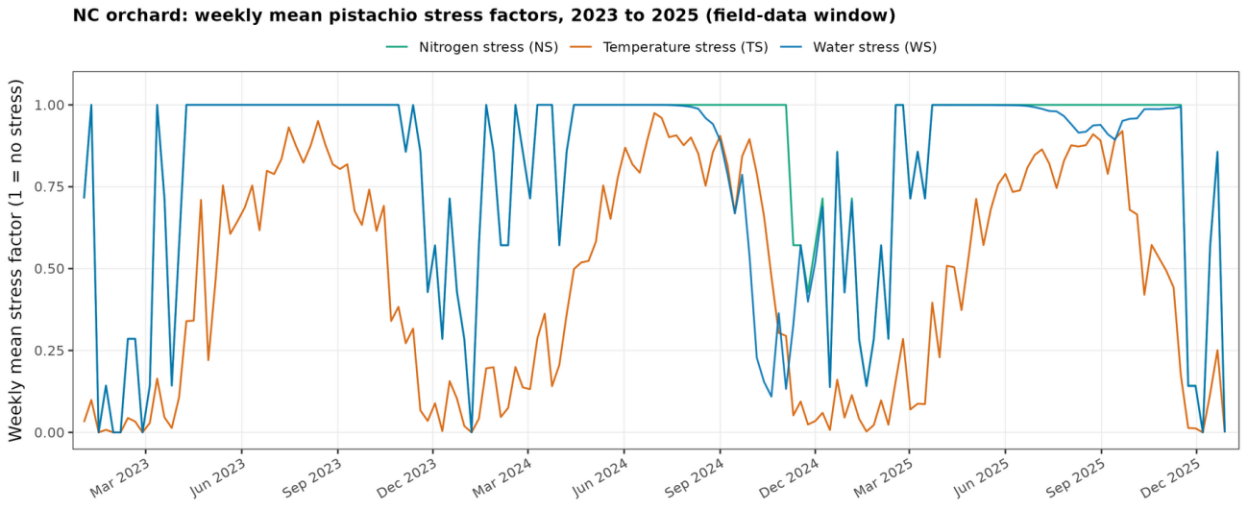


Figure 25. Weekly mean pistachio stress factors for the NC baseline simulation. Window: 2023 to 2025 (field data window).

Figure 26 plots daily pistachio standing live biomass (STL, top panel) and LAI (bottom panel) for the NC orchard, with observed LI-2200 LAI measurements overlaid on the LAI panel as blue points. Simulated pistachio LAI reached peak values of 1.34 in 2023, 1.45 in 2024, and 1.49 in 2025, with the LAI observations spanning 0 to 1.81 (mean approximately 0.6). Peak standing pistachio biomass reached 38 t ha^{-1} in 2023, 39 t ha^{-1} in 2024, and 49 t ha^{-1} in 2025.

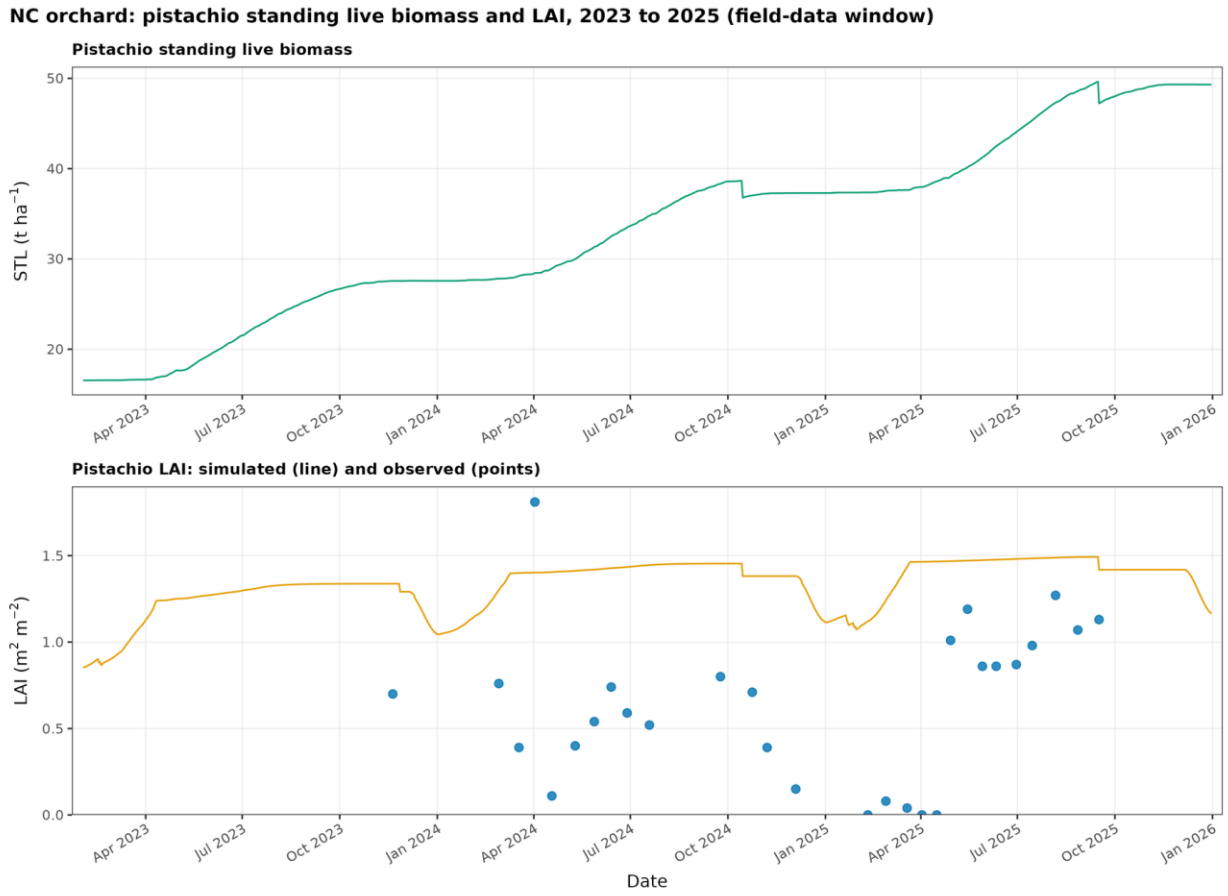


Figure 26. Daily pistachio standing live biomass and LAI for the NC baseline simulation. Window: 2023 to 2025 (field data window).

3.3.4 Cover crop (CC) orchard

Figure 27 summarizes the cumulative water balance for the CC orchard over the 2023 to 2025 field data period. ET accounts for approximately 97 percent of total water outputs (2,351 mm), and total *DP* was 0 mm. Compared to NC over the same period, the CC orchard shows higher cumulative ET (2,351 mm vs 2,165 mm) and lower cumulative deep percolation (0 mm vs 183 mm), reflecting the additional water use by the winter cover crop and the associated reduction in winter drainage. On an annual basis during the field data period, simulated ET_a for CC ranged from 695 to 857 mm in 2023 to 2025, slightly higher than NC (685 to 741 mm).

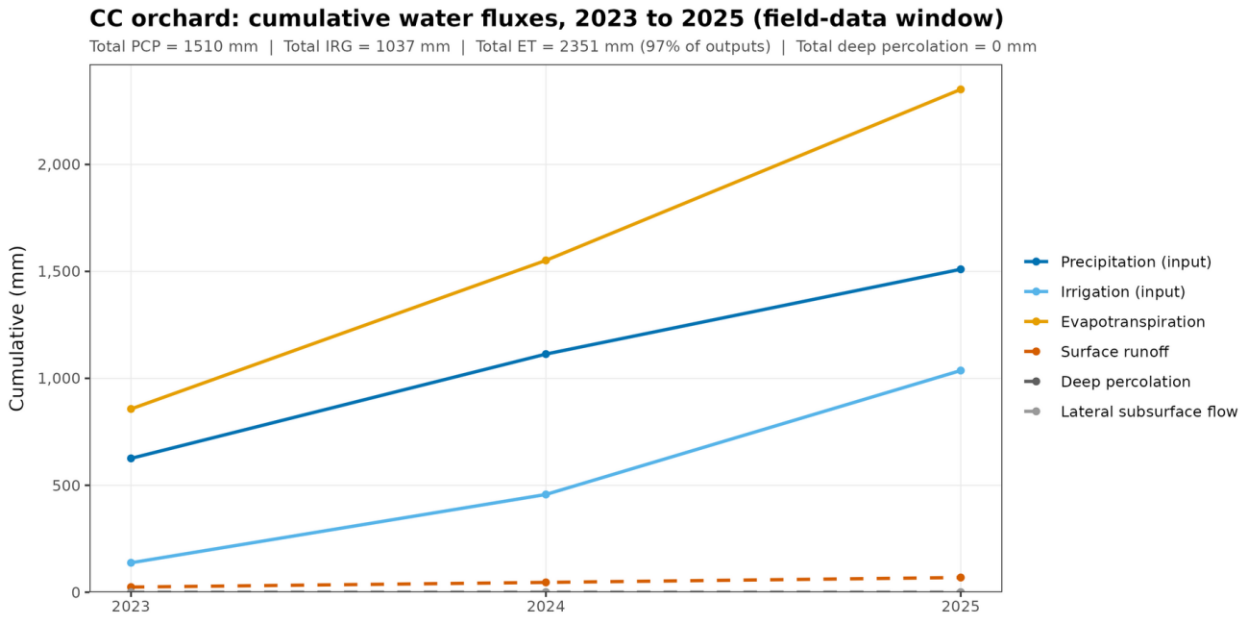


Figure 27. Cumulative water fluxes for the CC orchard. Window: 2023 to 2025 (field data window).

The CC orchard had a slightly different soil texture from the NC orchard but shared its slope, climate, and pistachio management, adding a winter CC seeded in November and terminated by mowing in early spring (Table 2). No supplemental irrigation is applied to the winter CC, which relies entirely on winter precipitation for establishment and growth. The mowing schedule in the baseline run follows the orchard manager's reported pattern of an initial cut in April and subsequent monthly cuts through July or August.

On an annual basis during the field data period, simulated ET_a ranged from 695 to 857 mm in 2023 to 2025, slightly higher than NC (685 to 741 mm), reflecting the additional water use by the winter cover crop. Simulated cover crop biomass at termination ranged from 4 to 9 t ha^{-1} across simulation years, within the field observed range of 0.75 to 12.4 t ha^{-1} reported in Table 3. WPEA water stress was essentially zero in all years (WS factor approximately 1.0 throughout). As discussed at the daily scale evaluation above, this unstressed cover crop

response is the immediate driver of the high simulated daily ET_a on the ten high PET days in January, February, and early March 2024 to 2026.

The carbon balance closes within 1.1 percent and shows a slight net accumulation of soil organic carbon in the CC orchard (beginning total C = 277,000 t, final = 277,800 t). As in the NC orchard, the nitrogen balance does not close in the CC baseline (PER = −286 percent), with simulated cumulative volatilization (489,751 kg total, or 1,790 kg ha^{-1} yr^{-1}) and runoff N (662,255 kg total, or 2,421 kg ha^{-1} yr^{-1}) far exceeding expected physical ranges.

Simulated pistachio LAI in the CC orchard followed the same growth trajectory as NC, reaching 1.31 in 2023, 1.43 in 2024, and 1.47 in 2025. Peak standing pistachio biomass reached 34 t ha^{-1} in 2023, 43 t ha^{-1} in 2024, and 55 t ha^{-1} in 2025, compared with NC values (38, 39, and 49 t ha^{-1}). Simulated pistachio yield was higher in CC than NC in both 2024 (1.44 vs. 1.10 t ha^{-1}) and 2025 (1.81 vs. 1.41 t ha^{-1}). Unlike NC, simulated CC pistachio water stress (PIST_WS) was substantial across the summer growing season (June through September), with mean monthly values of 0.46 in June 2024 and 0.67 in July 2024 and 100 percent of days at WS < 0.9, contrasting with NC where pistachio WS remained near 1.0 throughout. Inspection of soil moisture traces shows that the CC top 30 cm soil water content entered June 2024 at 0.14 m^3 m^{-3} against 0.21 m^3 m^{-3} in NC, reflecting cumulative drawdown from winter cover crop transpiration carrying into the pistachio growing season.

3.4 Calibration and validation against field observations

Calibration used the 2023 to 2024 field record (n = 23 monthly observations for ET_a), with 2025 retained as an independent validation year (n = 12). Performance was assessed using Nash-Sutcliffe efficiency (NSE), percent bias (PBIAS), coefficient of determination (R^2), and root mean square error (RMSE), and was judged satisfactory using the thresholds of Moriasi et

al. (2016): NSE greater than 0.50, R^2 greater than 0.60, and PBIAS within ±15 percent for daily streamflow-equivalent processes, with relaxed PBIAS limits of ±25 percent for crop yield (Wang et al., 2012). Full performance statistics for both calibration targets, both orchards, and both periods are reported in Table 13.

Table 12 Performance criteria ranges.

Rating	Monthly NSE	Daily SWC NSE	PBIAS (%)	Monthly R^2	Daily R^2	RSR
Very good	> 0.80	> 0.75	< 5	> 0.85	> 0.85	< 0.50
Good	> 0.70	> 0.60	< 10	> 0.80	> 0.75	< 0.60
Satisfactory	> 0.50	> 0.40	< 15	> 0.70	> 0.60	< 0.70
Unsatisfactory	≤ 0.50	≤ 0.40	≥ 15	≤ 0.70	≤ 0.60	≥ 0.70

Table 13 Model performance statistics for the CC and NC orchard calibration and validation, by output and period. Cal = calibration period (2023 to 2024); Val = validation year (2025). For yield, the two-year record (2024 and 2025) does not support a meaningful split-sample evaluation and is reported jointly; NSE and RSR are not informative at this sample size and are marked n/a.

Orchard	Output (time step)	Period	*n*	Obs. mean	NSE	PBIAS (%)	R^2	RSR	RMSE	Rating
NC	ET_a (monthly)	Cal	23	57.1 mm	0.60	4.9	0.70	0.63	20.0 mm	Satisfactory
NC	ET_a (monthly)	Val	12	74.2 mm	0.69	-10.27	0.73	0.54	22.8 mm	Satisfactory
NC	SWC (daily)	Cal	37	0.32 $m^3 m^{-3}$	-44.9	+38.9	0.43	6.68	0.12 $m^3 m^{-3}$	Diagnostic*
NC	SWC (daily)	Val	21	0.33 $m^3 m^{-3}$	-166.6	+36.7	0.68	12.63	0.12 $m^3 m^{-3}$	Diagnostic*
NC	LAI (monthly)	Cal	28	0.63 $m^2 m^{-2}$	-2.87	+120.1	0.16	n/a	n/a	Unsatisfactory
NC	LAI (monthly)	Val	n/a	n/a	-2.87	+120.1	0.16	n/a	n/a	Unsatisfactory
NC	Yield (annual)	Cal+Val	2	1.07 t ha^{-1}	n/a	-33.6	n/a	n/a	n/a	Unsatisfactory
CC	ET_a (monthly)	Cal	23	60.3 mm	0.55	11.1	0.78	0.67	17.0 mm	Satisfactory
CC	ET_a (monthly)	Val	12	75.9 mm	-1.06	-6.49	0.12	1.37	40.0 mm	Unsatisfactory
CC	SWC (daily)	Cal	37	0.32 $m^3 m^{-3}$	-116.5	+58.1	0.10	10.69	0.18 $m^3 m^{-3}$	Diagnostic*
CC	SWC (daily)	Val	22	0.32 $m^3 m^{-3}$	-135.6	+54.4	0.11	11.42	0.18 $m^3 m^{-3}$	Diagnostic*
CC	LAI (monthly)	Cal	28	0.71 $m^2 m^{-2}$	-3.74	+149.9	0.28	n/a	n/a	Unsatisfactory
CC	LAI (monthly)	Val	n/a	n/a	-3.74	+149.9	0.28	n/a	n/a	Unsatisfactory
CC	Yield (annual)	Cal+Val	2	1.07 t ha^{-1}	n/a	−1.87	n/a	n/a	n/a	Satisfactory
CC	Cover crop biomass	Cal+Val	19	6.8 t ha^{-1}	-3.27	-72.4	0.15	n/a	5.59 t ha^{-1}	Unsatisfactory
CC	Cover crop biomass	Val	n/a	n/a	n/a	n/a	n/a	n/a	n/a	n/a

For the NC orchard, calibration adjusted the four parameters identified as most sensitive: PARM1, PARM2, PARM12, and PARM17. The calibrated NC values were PARM1 = 1.00, PARM2 = 1.99, PARM12 = 1.84, and PARM17 = 0.10. The match between modeled and EC-derived monthly ET_a for the NC orchard is shown in Figure 28. These adjustments brought monthly ET_a into agreement with observations, improving NSE from a baseline of 0.11 to 0.60, changing PBIAS from +38.3 percent to +4.9 percent, and reducing RMSE from 22.5 to 20.0 mm month^{-1}, with $R^2 = 0.70$ (Table 13), meeting the satisfactory thresholds of Moriasi et al. (2016) for NSE and PBIAS. The seasonal cycle is well captured: the model reproduces the low winter values driven by limited dormant-season demand and the summer peak associated with full canopy and active drip irrigation.

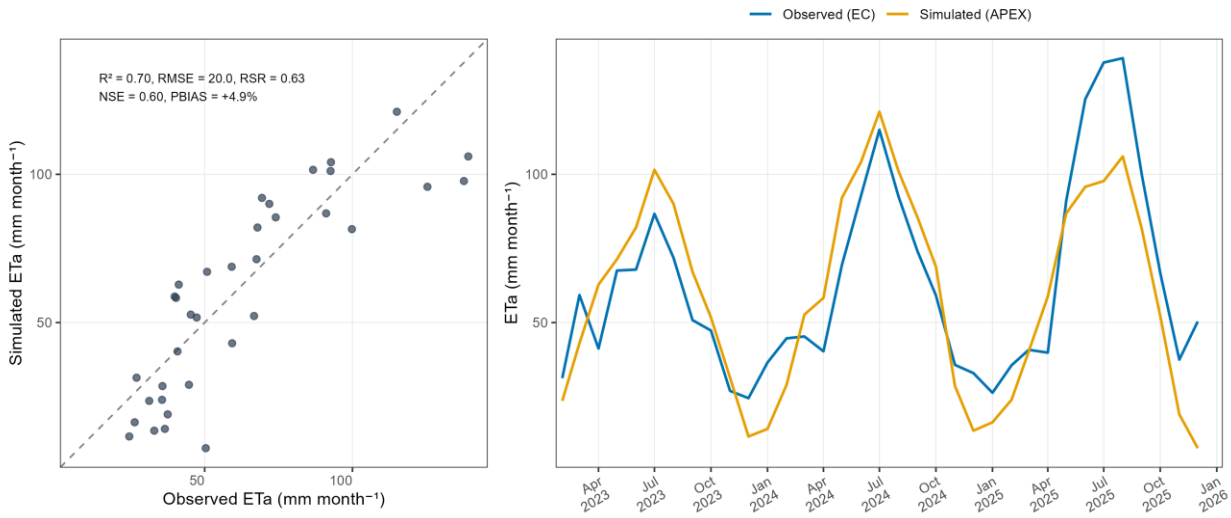


Figure 28. Calibrated no cover (NC) orchard monthly actual evapotranspiration (ET_a): (left) simulated versus eddy-covariance observed 1:1; (right) monthly time series, February 2023 to December 2025. Performance statistics as in Table 13.

The pistachio LAI diagnostic for the NC orchard is shown in Figure 29. Because the DDS objective function targeted monthly ETa rather than LAI directly, pistachio canopy development was not a primary calibration target. The calibrated model achieves LAI NSE = −2.87 and

PBIAS = +120 percent (Table 13), indicating systematic overestimation of peak LAI. This is consistent with the known difficulty of simulating year-on-year LAI accumulation in young deciduous nut trees in APEX without site-specific heat-unit parameterization. Calibration statistics are reported in Table 13.

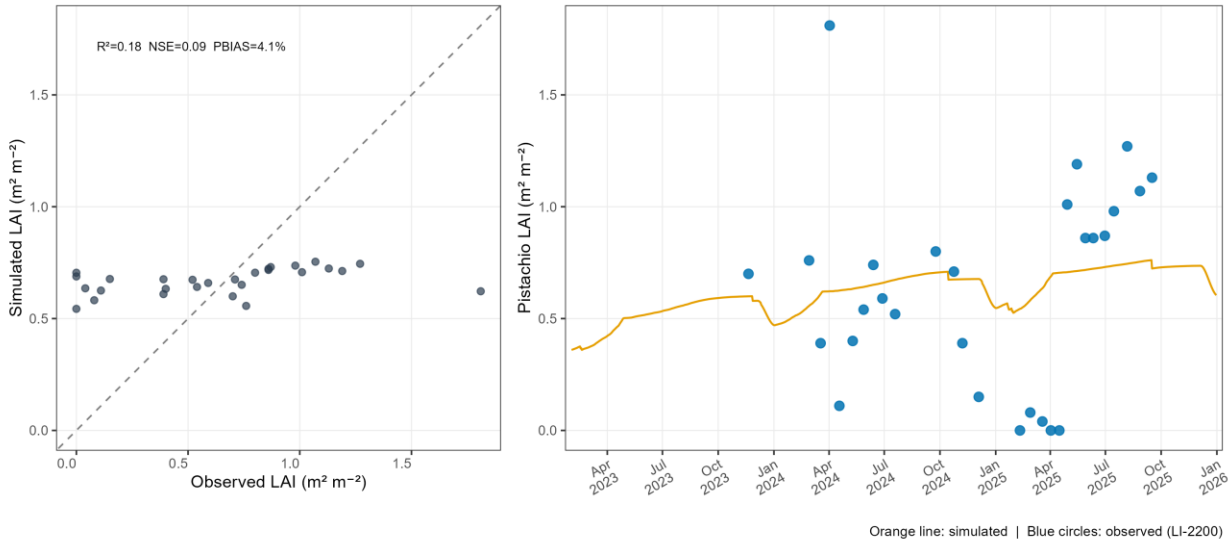


Figure 29. Calibrated NC orchard pistachio leaf area index (LAI): (left) simulated versus LI-2200 observed 1:1; (right) time series with observed data.

Pistachio yield for the NC orchard is compared to orchard manager records in Figure 30. Because the 2024 harvest was the first commercial event and yielded anomalously low at 0.20 t ha^{-1} (year-6 establishment year), yield calibration rests on the single 2025 observation of 1.07 t ha^{-1}. The calibrated NC orchard simulates 2025 yield with PBIAS = −33.6 percent, exceeding the relaxed ±25 percent threshold of Wang et al. (2012). Table 13 reports PBIAS as the primary metric in this single-observation context.

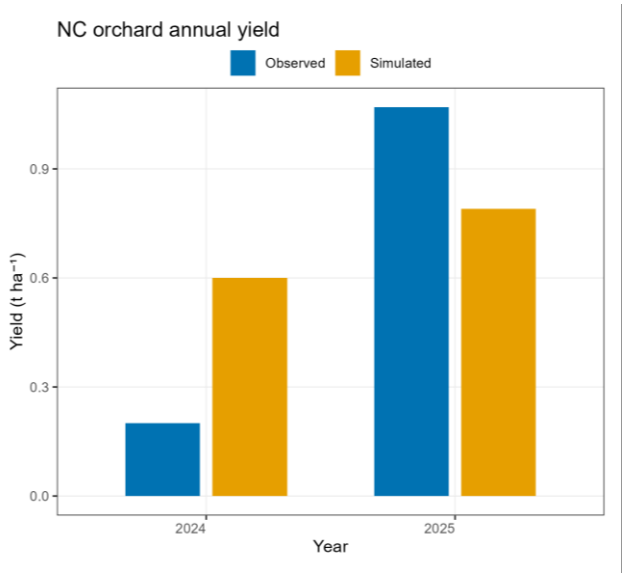


Figure 30. Calibrated NC orchard pistachio yield versus orchard records (2024 = 0.20 t ha^{-1} excluded as an anomalous first-harvest year; calibration anchored on 2025 = 1.07 t ha^{-1}).

Profile-mean soil water content was compared against neutron probe observations at campaign dates across the 0.3-3.0 m profile. The calibrated model systematically overestimates observed profile-mean SWC in both orchards (NC PBIAS = +38.9 percent, CC PBIAS = +58.1 percent; Table 13). SWC was treated as a diagnostic variable rather than a primary calibration target; the ET_a calibration is independent of this SWC bias because PARM17 controls evaporation partitioning as a function of ground cover fraction, not through the simulated SWC value directly. Site-specific adjustment of the layer-by-layer soil hydraulic parameters is identified as a priority for improving the SWC simulation in future work.

The CC orchard adds the cover crop as both a calibration target and a perturbation on the pistachio calibration targets. The CC pistachio calibration was performed first using the same parameter set and adjustment sequence as for NC, with subsequent fine-tuning of cover crop parameters (DMLA and DLAI) to match observed cover crop biomass and LAI without disturbing the pistachio fit.

The match between modeled and EC-derived monthly ET_a for the CC orchard is shown in Figure 31. The CC orchard's ET_a profile differs from NC primarily during the late winter and early spring window, when the cover crop adds transpiring biomass on top of the dormant or early leaf out tree canopy, raising total ET_a above NC levels for that part of the year. The CC orchard was calibrated over the same four parameters, with calibrated values of PARM1 = 1.00, PARM2 = 1.25, PARM12 = 1.82, and PARM17 = 0.10. The calibrated model reproduces this seasonal offset, improving NSE from a baseline of -0.18 to 0.55, reducing PBIAS from +17.8 percent to +11.1 percent, and reducing RMSE from 27.6 to 17.0 mm month^{-1}, with R^2 = 0.78 (Table 13).

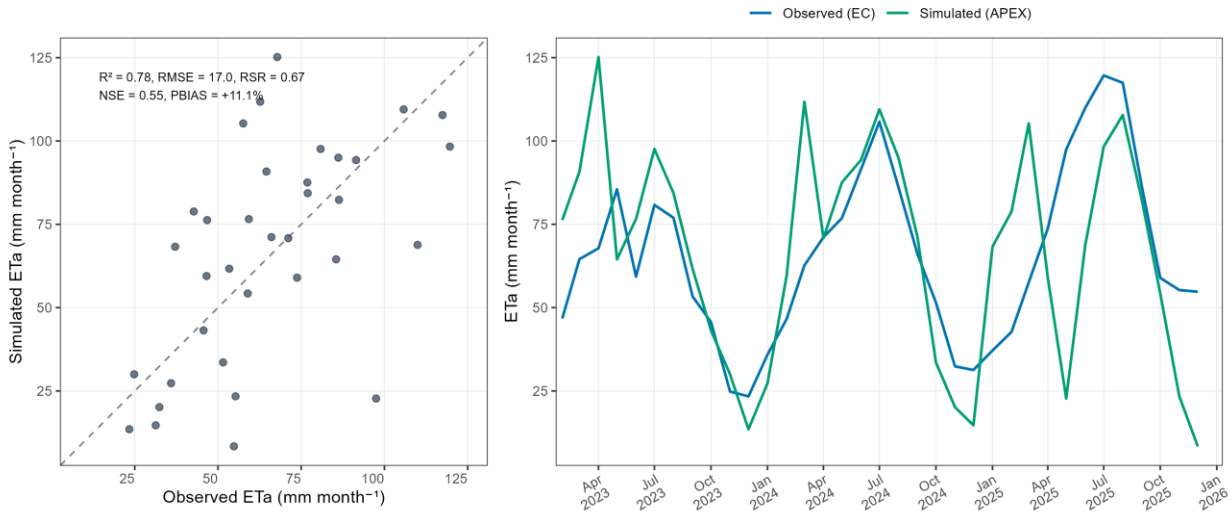


Figure 31. Calibrated cover crop (CC) orchard monthly ET_a: (left) simulated versus eddy-covariance observed 1:1; (right) monthly time series. Performance statistics as in Table 13.

The match between modeled and neutron probe-derived soil water content for the CC orchard was also examined. The calibrated model reproduces the seasonal drawdown pattern under the cover crop and subsequent summer depletion, with profile-mean SWC calibration NSE = -116.5, PBIAS = +58.1 percent, and RMSE = 0.18 m³ m⁻³ (Table 13). The NC orchard shows similar systematic underestimation (NSE = -44.9, PBIAS = +38.9 percent). The positive

PBIAS indicates the model overestimates the observed profile-mean SWC in both orchards, with the largest discrepancy in the 0.6–3.0 m layers where the Rincon silty clay loam retains substantially more water than the default NCSS-derived FC and WP values represent. SWC was treated as a diagnostic variable rather than a primary calibration target: the ET_a-targeted DDS calibration adjusts PARM17, which partitions evaporative demand between canopy transpiration and bare soil evaporation as a function of fractional ground cover, independently of the simulated SWC profile. The SWC bias therefore does not propagate into the ET_a simulation and does not invalidate the climate-scenario water balance comparisons, which are driven by the ET partition rather than by absolute soil water storage. Site-specific layer-by-layer adjustment of FC, WP, and K_{sat} is identified as a priority for a subsequent calibration iteration.

The match between modeled and observed pistachio LAI for the CC orchard is shown in Figure 32. The calibrated model systematically overestimates observed pistachio LAI (PBIAS = +150 percent, NSE = -3.74; Table 13).

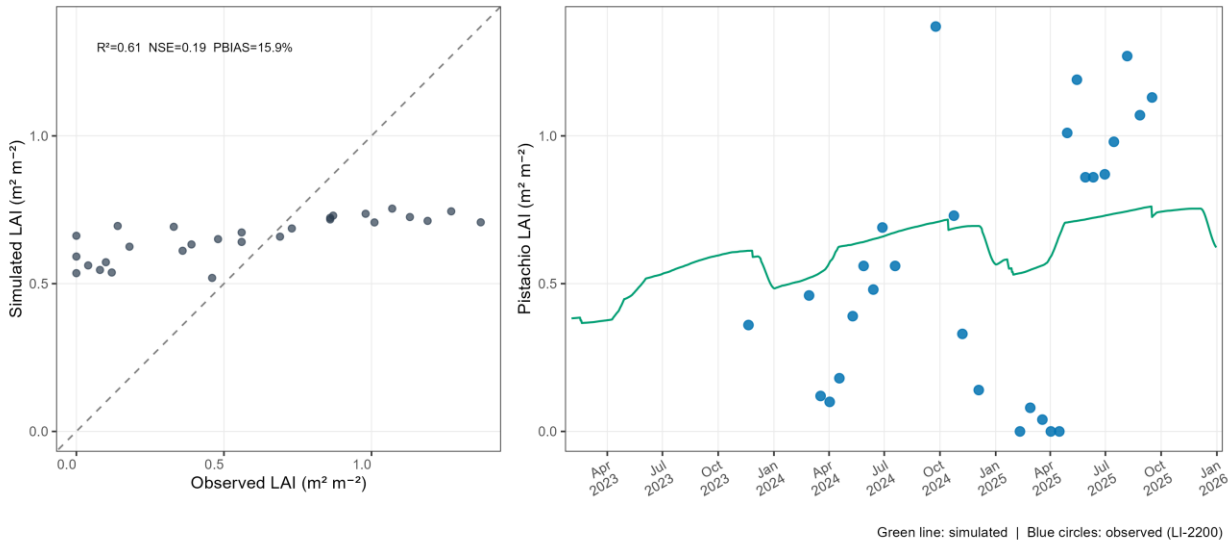


Figure 32. Calibrated CC orchard pistachio LAI: (left) simulated versus LI-2200 observed 1:1; (right) time series with observed campaigns overlaid.

Pistachio yield for the CC orchard is compared to orchard manager records in Figure 33. The calibrated CC orchard simulates 2025 yield with PBIAS = −1.87 percent against the observed 1.07 t ha⁻¹, well within the ±25 percent threshold of Wang et al. (2012).

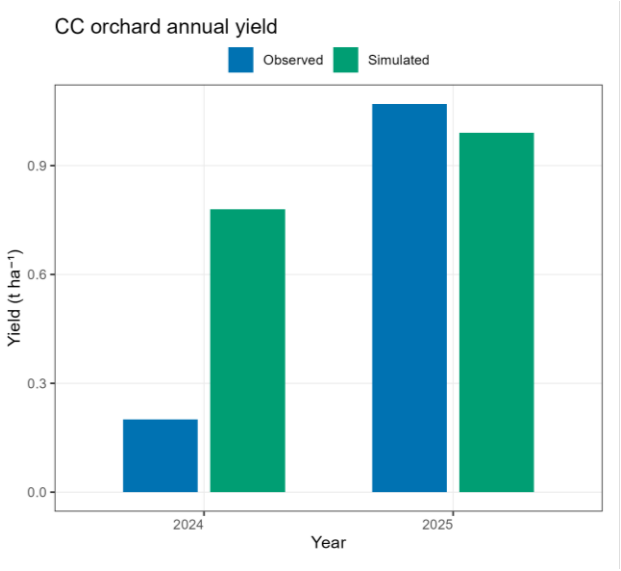


Figure 33. Calibrated CC orchard pistachio yield versus orchard records (calibration anchored on 2025 = 1.07 t ha^{-1}).

The match between modeled and observed cover crop biomass and LAI for the CC orchard is shown in Figure 34. Cover crop biomass samples were collected from the field on a monthly basis and LAI was derived from the LI-2200 LAI measurements. The calibrated cover crop module reproduces the observed November-to-April establishment and growth pattern, the timing of peak standing biomass, and the rapid decline at termination. Heat unit timing was set by tuning PHU within the bracketed range: values from 1600 to 2500 were tested, and PHU = 1600 produced the lowest RMSE across the pre-mow LAI measurement series, matching the 2025-02-27 observation (4.47 LAI). This value sits approximately 20 percent above the upper end of the published GDD-to-maturity range for late-maturing pea cultivars (Oregon State University, 2010), reflecting the modeling simplification of representing the multi-species cover crop mix (legumes, cereals, and brassicas; Table 2) with WPEA as a single proxy species. Cereal

components of the mix have GDD-to-maturity values above pure winter pea (e.g., winter wheat at approximately 1850 GDD; Tadesse et al. (2019)), so the proxy PHU was elevated to keep the simulated CC canopy active through the persistence window of the later maturing real components.

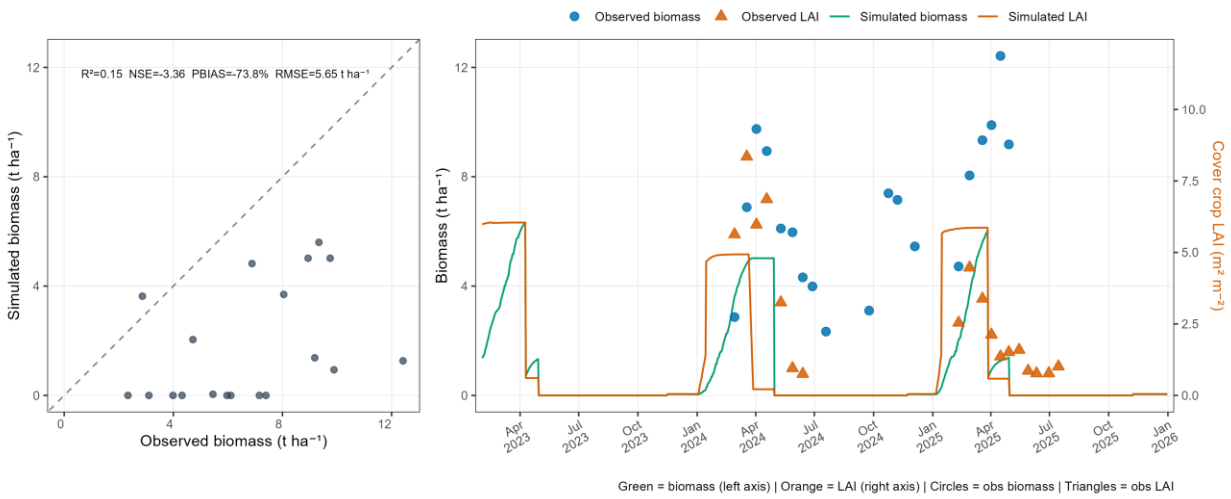


Figure 34. Calibrated CC orchard cover crop standing biomass and LAI versus destructive-sampling biomass and LI-2200 LAI observations.

Across the CC calibration targets, the calibrated model partially meets the Moriasi et al. (2016) satisfactory thresholds, with the strongest performance on ET_a and the largest residuals on soil water content, LAI, and cover crop biomass.

3.4.1 Calibrated parameter values

The calibrated parameter values (Table 14) are compared against the published APEX 1501 User Manual and APEX literature (Tadesse et al., 2019; Talebizadeh et al., 2018; Mason et al., 2020; Tadesse et al., 2021; Williams et al., 2023). For ET_a parameters, the calibrated PARM17 (soil evaporation plant cover factor) falls within the range reported by Tadesse et al. (2019) for irrigated row crops at Bushland and Talebizadeh et al. (2018) for cotton and grain

sorghum, and the calibrated PARM1 (Penman Monteith canopy PET factor) is within the 1.0 to 2.0 range cited by Tadesse et al. (2019).

Table 14. Calibrated APEX parameter values for the no cover (NC) and cover crop (CC) orchards. Parameters are organized by APEX input file. APEX defaults, calibrated NC and CC values, and the literature range from published APEX calibrations are reported. Parameters not calibrated remained at APEX defaults (Williams et al., 2023).

Parameter	Description	APEX default	NC calibrated	CC calibrated	Literature range / Comments
PARM file (PARMCOM.DAT)					
PARM1	Crop canopy-PET factor (Penman-Monteith)	1.5	1.00	1.00	1.0-2.0; Tadesse et al. (2019) reported 1.4-1.7 for irrigated row crops
PARM17	Soil evaporation-plant cover factor	0.25	0.10	0.10	0.00-0.5; dominant ET_a parameter
PARM12	Soil evaporation coefficient	2.5	1.84	1.82	1.5-2.5
PARM2	Root growth-soil strength	2.0	1.99	1.25	1.0-2.0; secondary yield parameter
Crop file (CROPCOM.DAT) - pistachio (PIST)					
DMLA	Maximum potential leaf area index	5	5.0	5.0	Year-7 peak LAI fit to LI-2200 range of 1.13-1.27
PPLP1	Population to LAI scaling, first point	1000.95	1.95	1.95	Reconfigured for tree density of 0.03 plants m^{-2}
PPLP2	Population to LAI scaling, second point	100.10	0.10	0.10	Reconfigured for tree density of 0.03 plants m^{-2}
TBS	Base temperature for plant growth (°C)	10	10	10	Default retained, consistent with Rahemi and Pakkish (2009); Zhang et al. (2015)
TOP	Optimum temperature for plant growth (°C)	30	30	30	Zhang et al. (2015) bloom-phase upper bound
IDC	Land-use / crop category code	8 (deciduous)	8 (deciduous)	8 (deciduous)	Pistachio is a deciduous nut tree
Crop file (CROPCOM.DAT) - cover crop (WPEA)					
PHU	Potential heat units to maturity (°C-days)	1000	n/a	1600	Bracketed by 1200-1800 from Oregon State University (2010)
DMLA	Maximum potential leaf area index	4	n/a	8	Refined by iterative fit against LI-2200 cover crop LAI series

3.5 Climate scenario outcomes

The calibrated APEX model was projected onto the seven-scenario set. Results are organized into three subsections aligned with the survey identified grower concerns: seasonal water use and the climate signal embedded in each scenario, the treatment-level cover crop effect on the annual water balance, and pistachio yield across scenarios and treatments. All comparisons are made relative to the 1996 to 2025 baseline.

The seasonal pattern of evapotranspiration under the CC treatment is shown for each scenario as both an absolute monthly cycle (Figure 35) and as a scenario minus baseline monthly difference (Figure 35). The absolute cycles reveal a bimodal seasonal structure that is consistent across all seven scenarios: a spring peak in March reflecting active cover crop transpiration overlapping with early pistachio bud break, a dip in April and May following cover crop termination, and a dominant summer peak in July driven by full pistachio canopy at peak atmospheric demand. The persistence of this bimodal structure across all scenarios indicates that the cover crop and pistachio phenology encoded in the calibrated APEX setup are robust to the range of warming imposed.

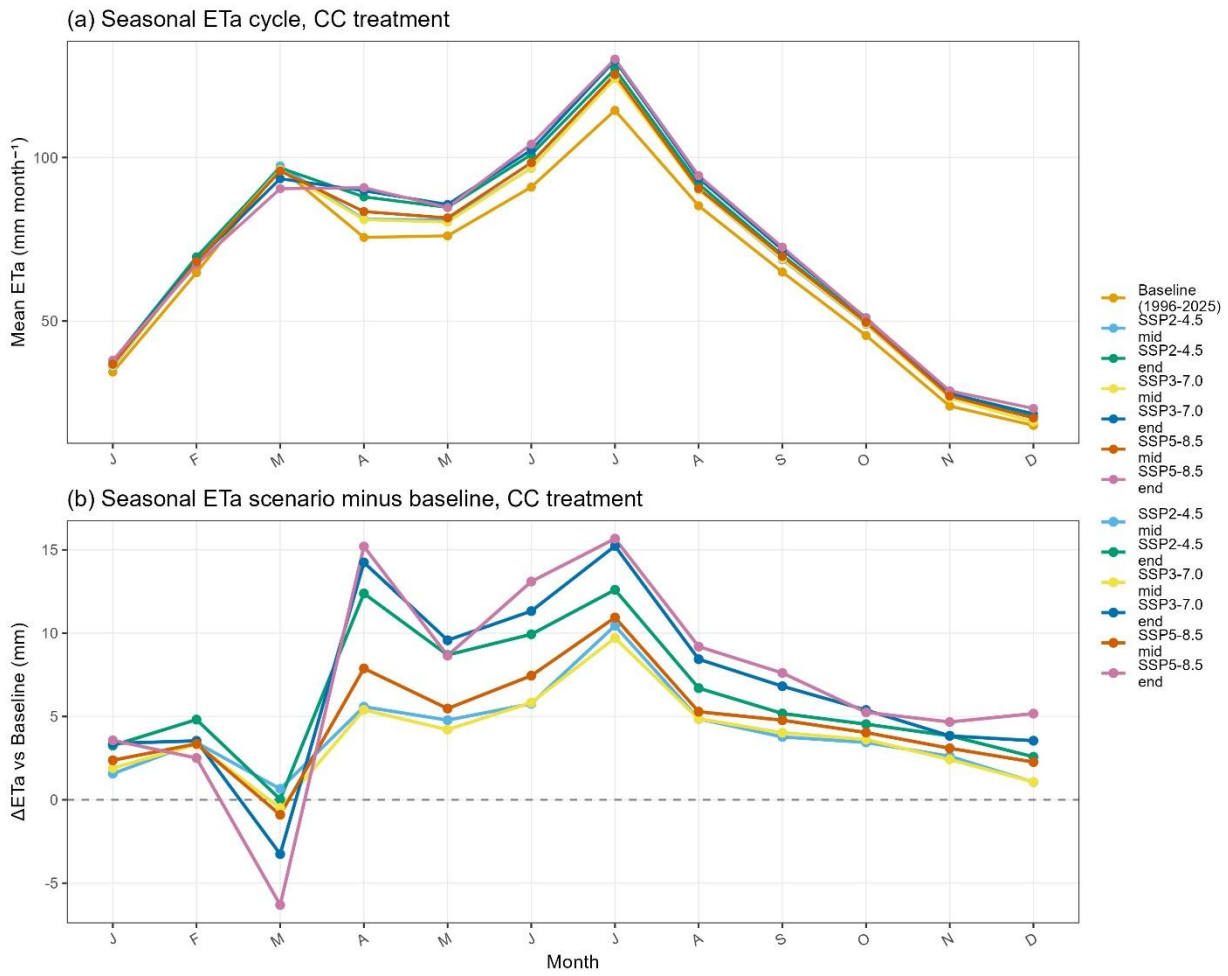


Figure 35. Climate effect on seasonal evapotranspiration under the cover crop (CC) treatment. (a) Absolute monthly ET_a cycle by scenario; (b) scenario minus baseline (1996 to 2025) monthly ET_a difference.

The scenario minus baseline difference figure isolates the climate signal from that background seasonal cycle. The warming imposed by all six future scenarios increases monthly ET relative to the Historical baseline throughout the year, but the increase is not uniform. The largest absolute increases occur in April to May and in July, where the ensemble mean difference ranges from approximately 10.4 mm per month under SSP2-4.5 mid-century to 15.7 mm per month under SSP5-8.5 end-of-century. The smallest increases occur in late autumn and early winter, when low atmospheric demand limits the ET response regardless of temperature. A

notable dip below baseline appears in March for the highest-emissions end-of-century scenarios, which reflects accelerated cover crop phenological development under elevated heat accumulation causing the cover crop to reach maturity earlier and reducing its late-winter transpiration contribution relative to the baseline. End-of-century scenarios (SSP3-7.0 end and SSP5-8.5 end) are consistently elevated above mid-century scenarios, while mid-century scenarios cluster together with modest separation, consistent with the moderate divergence among SSP pathways in the 2035 to 2065 window. The annual sum of monthly ET differences ranges from 46 mm under SSP2-4.5 mid-century to 84 mm under SSP5-8.5 end-of-century (Table 15).

Seasonal precipitation shifts are shown in Figure 36. Winter precipitation (January through March) is projected to increase under most scenarios relative to the baseline, with the largest increases in January reaching approximately 30 mm per month under SSP2-4.5 end-of-century and SSP3-7.0 end-of-century. The late-season window (November and December) shows greater inter-scenario divergence, with SSP3-7.0 end-of-century projecting a decrease in November and a substantial decrease in December of approximately 6 mm relative to baseline, while SSP2-4.5 end-of-century projects increases of similar magnitude in the same months. This divergence reflects the different precipitation responses embedded in the GCM ensemble across SSP pathways and does not resolve to a clear directional signal for late fall precipitation at this site. The inter-scenario spread in precipitation is substantially larger than the spread in ET_a, reflecting the higher intrinsic variability of precipitation projections at the regional scale relative to temperature-driven ET projections.

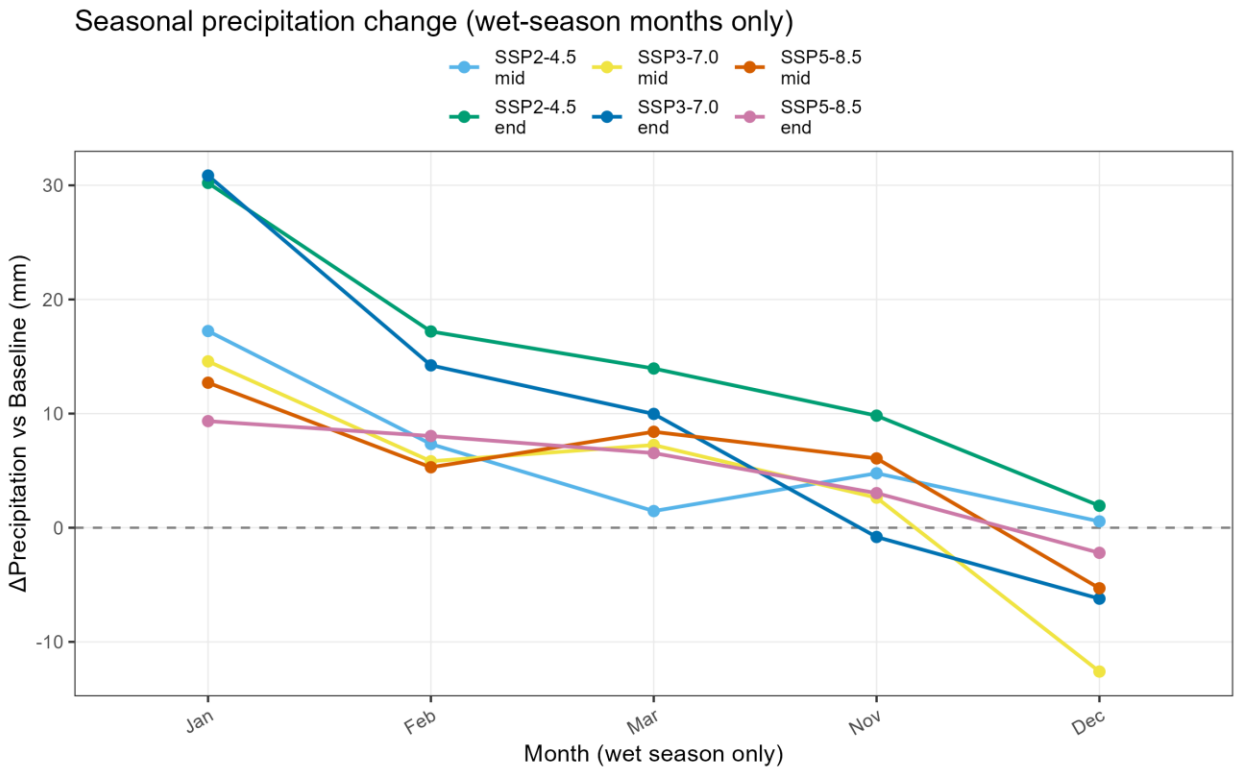


Figure 36. Climate effect on seasonal precipitation. Scenario minus baseline (1996 to 2025) monthly precipitation difference.

The CC treatment consistently increased total annual ET_a relative to the NC treatment across all seven scenarios. The ensemble median CC minus NC ET_a difference, representing the annual water cost of the cover crop, was approximately 93 mm under the Historical baseline and ranged from approximately 70 to 84 mm across the six future scenarios, about 12 percent above the NC treatment (Figure 37). The scenario-to-scenario variation in this difference is small relative to the ensemble spread within each scenario, indicating that the annual water cost of the CC is stable across the range of climates examined and is determined primarily by the CC growing season length and the calibrated CC parameterization rather than by the magnitude of future warming.

The CC treatment slightly increased annual deep percolation relative to the NC treatment under most scenarios. The ensemble median CC minus NC deep percolation differences was

approximately +5.5 mm under the Historical baseline and ranged from approximately -0.2 mm under SSP2-4.5 end-of-century to +9.1 mm under SSP5-8.5 end-of-century, so the CC adds a small amount of drainage in most scenarios rather than suppressing it. The largest positive differences occur under the scenarios with the highest winter precipitation increases (Figure 37). The pattern in the percolation panel is non-monotonic across scenarios and does not follow the same SSP ordering as the ET_a panel, because percolation depends jointly on winter precipitation totals, the cover crop's water uptake during the establishment and active growth period, and soil water storage capacity. The largest positive CC minus NC difference occurs under SSP5-8.5 end-of-century (+9.1 mm), while SSP2-4.5 end-of-century is the only scenario in which the cover crop slightly reduces percolation relative to no cover (-0.2 mm).

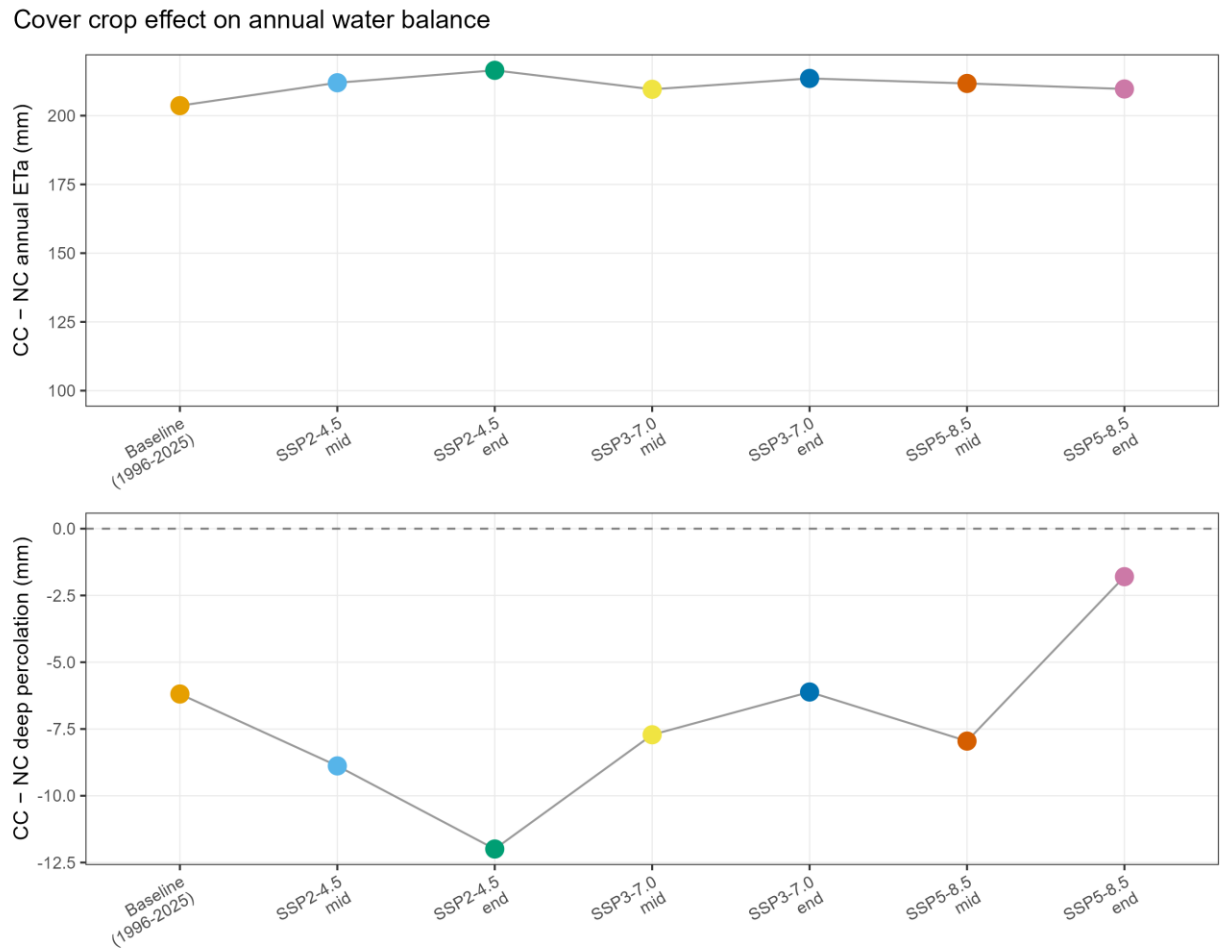


Figure 37. Cover crop effect on the annual water balance by scenario. (a) CC minus NC evapotranspiration difference; (b) CC minus NC deep percolation difference.

Taken together, the paired water balance results indicate that the CC adds approximately 70 to 93 mm of annual ET_a demand across all scenarios examined, an increase of roughly 12 percent relative to the NC treatment, while having only a small effect on deep percolation. Total orchard ET_a rises by about 14 percent in NC and 9 percent in CC from the Historical baseline to SSP5-8.5 end-of-century, an increase of roughly 66 to 89 mm across the warming gradient. The stability of the ET_a offset across scenarios supports the interpretation that the grower concern about CC water competition identified in the survey is not strongly amplified by the warming projected under any of the six future scenarios evaluated here.

Table 15. Ensemble median annual NC and CC actual evapotranspiration (ETa), the CC minus NC ETa offset, and the CC minus NC deep percolation (DP) difference for each climate scenario, expressed relative to the 1996 to 2025 baseline.

Scenario	**NC ET_a (mm/yr)**	**CC ET_a (mm/yr)**	**CC – NC ET_a (mm/yr)**	**CC – NC *DP* (mm/yr)**
Historical	634	727	93	+5.5
SSP245_Mid	676	760	84	+2.6
SSP245_End	701	780	79	-0.2
SSP370_Mid	677	756	79	+3.9
SSP370_End	714	787	73	+4.6
SSP585_Mid	686	764	78	+4.0
SSP585_End	723	793	70	+9.1

Pistachio yield distributions across scenarios and treatments are summarized in Figure 38, filtered to productive years only (YLDG greater than 0.01 t/ha) to exclude the near-zero yields characteristic of the off-cycle year in pistachio's biennial bearing pattern. The productive-year median yield under the Historical baseline is approximately 1.27 to 1.30 t per ha in both the CC and NC treatments, with the NC median slightly above the CC median, consistent with the slight soil water deficit introduced by cover crop ET during the establishment window. Yield variability within each scenario, represented by the interquartile range of the boxplot, is substantial in both treatments, reflecting the combined effect of interannual climate variability embedded in the 1000 stochastic realizations and the biennial bearing pattern that the productive-year filter does not entirely eliminate from the sample.

Across future scenarios, the median productive-year yield in both treatments declines modestly with increasing emissions and time horizon, with the largest reductions under SSP5-8.5 end-of-century where the median falls to approximately 1.14 t ha^{-1} in CC and 1.20 t ha^{-1} in NC. The yield trajectory under SSP3-7.0 end-of-century closely tracks SSP5-8.5 end-of-century, while mid-century scenarios and SSP2-4.5 end-of-century show smaller changes from the baseline. The CC treatment tends to have a slightly lower median productive year yield than NC under all scenarios, but the distributions overlap substantially, and the treatment difference is

small relative to the scenario-driven decline under the highest emissions end-of-century pathways.

The yield figure should be interpreted with the caveat regarding calibration constraints: pistachio yield in this APEX simulation was calibrated against a single observed harvest year (2025; 1.07 t ha^{-1}), because the 2024 harvest was the first harvest for the orchard and the data is not representative. The calibrated yield response therefore captures the central tendency of the 2025 observation, but the year-to-year variability and the shape of the yield distribution across the 1000-member ensemble are not independently validated against multi-year field data. The directional scenario response (yield declining with increasing warming) is consistent with the mechanisms represented in APEX (increased temperature stress days, earlier phenological development reducing the effective grain fill period), but the absolute magnitude of the scenario differences should be treated as indicative rather than precisely calibrated.

Distributions of annual pistachio yield and annual days of water and temperature stress for the CC and NC orchards across the seven scenarios are shown in Figure 38. APEX reports the regulating stress for each day of the simulation as the lowest stress factor among water, temperature, nitrogen, phosphorus, and aeration; in this orchard system, water and temperature are the dominant regulating stresses across all scenarios, while nitrogen, phosphorus, and aeration stresses are negligible (each accounting for fewer than 1 day per year on average across all scenarios). Median and standard deviation of yield, and median annual days of water and temperature stress, are reported in Table 16.

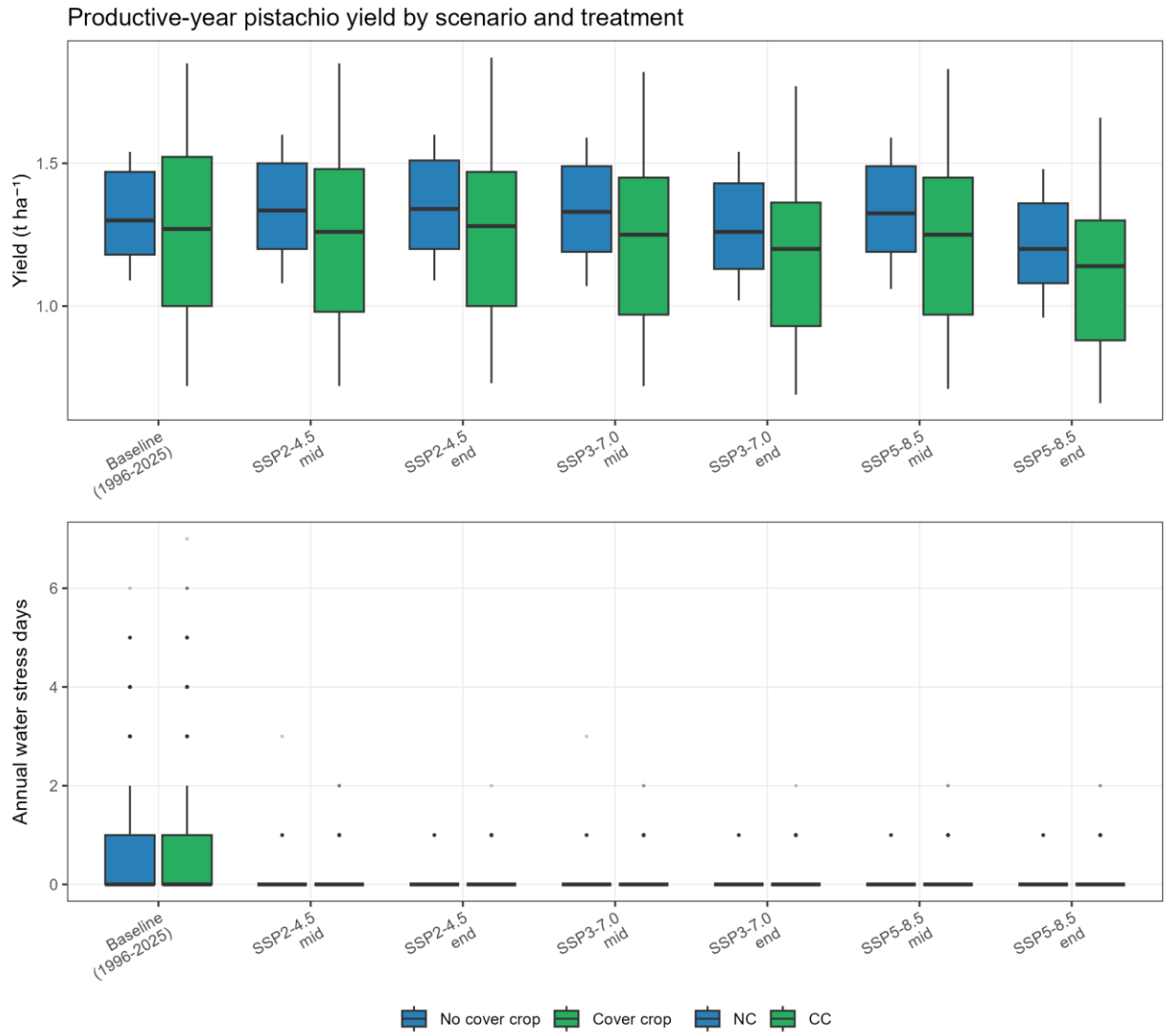


Figure 38. Productive-year pistachio outcomes by scenario and treatment. (a) Yield distributions for the no cover (NC) and cover crop (CC) treatments; (b) annual water stress days.

The Baseline scenario (observed 1996 to 2025, 5 GCM ensemble mean) produces a median productive-year pistachio yield of 1.30 t ha^{-1} in NC and 1.27 t ha^{-1} in CC, with the CC minus NC offset of -0.03 t ha^{-1}. Under SSP2-4.5 mid century, median yield changes by +2.7 percent in NC and -0.8 percent in CC; under SSP3-7.0 mid century by +2.3 percent in NC and -1.6 percent in CC; and under SSP5-8.5 mid century by +1.9 percent in NC and -1.6 percent in CC.

The end of century cells show clearer pathway separation. SSP2-4.5 end of century produces median yield changes of +3.1 percent in NC and +0.8 percent in CC; SSP3-7.0 end of century produces changes of -3.1 percent in NC and -5.5 percent in CC; and SSP5-8.5 end of century produces the largest changes at -7.7 percent in NC and -10.2 percent in CC, with median water stress days rising from a Baseline of 0.0 to 30.7 in NC and from 60.8 to 101.7 in CC. The yield variability (standard deviation across stochastic realizations) changes only modestly under the warmer scenarios, with the all-year SD ranging from 0.557 to 0.616 t ha^{-1} in NC and from 0.525 to 0.589 t ha^{-1} in CC across the seven scenarios.

Table 16 Median and standard deviation of annual pistachio yield, and median annual days of water and temperature stress, for each climate scenario and orchard.

Scenario	Orchard	Yield median (kg ha^{-1})	Yield SD (kg ha^{-1})	Water stress days, median	Temperature stress days, median
Historical	NC	1.30	0.597	0.0	199.9
Historical	CC	1.27	0.584	60.8	172.5
SSP245_Mid	NC	1.33	0.614	0.6	172.2
SSP245_Mid	CC	1.26	0.581	78.2	149.5
SSP245_End	NC	1.34	0.616	0.2	162.3
SSP245_End	CC	1.28	0.589	77.1	142.7
SSP370_Mid	NC	1.33	0.609	5.2	168.0
SSP370_Mid	CC	1.25	0.575	82.9	145.7
SSP370_End	NC	1.26	0.584	16.9	146.3
SSP370_End	CC	1.20	0.554	91.2	130.1
SSP585_Mid	NC	1.33	0.609	6.5	163.9
SSP585_Mid	CC	1.25	0.576	83.9	143.0
SSP585_End	NC	1.20	0.557	30.7	136.2
SSP585_End	CC	1.14	0.525	101.7	122.2

3.5.1 Soil water content and ET

Distributions of monthly potential evapotranspiration (PET) and actual evapotranspiration (ET_a), and of daily volumetric soil water content, for the CC and NC orchards across the seven scenarios are shown in Figure 35. PET responds primarily to the temperature signal embedded in each scenario, so the increases scale roughly with the magnitude of warming

relative to the Historical baseline. Monthly peak ET_a increases by approximately 13 percent under SSP245_Mid and by 19 percent under SSP585_End in both orchards, with intermediate increases under SSP370_Mid, SSP245_End, SSP370_End, and SSP585_Mid. ET_a rises across the same warming gradient but at a smaller proportional rate than PET because plant water uptake is constrained by canopy size and because the irrigation supply is held at the calibrated 2019 to 2024 schedule, so the ET_a response under the warmer scenarios is bounded by available soil water rather than by atmospheric demand.

The CC-NC ET_a offset, which represents CC transpiration on top of the dormant or early-leaf-out tree canopy, is most pronounced in late winter and early spring under all scenarios. The peak monthly offset (CC minus NC monthly ET_a) is approximately 38 mm under Historical and shifts to approximately 41 mm under SSP585_End, with intermediate values across the other future cells. The change in the offset reflects the combined effect of altered winter precipitation totals, altered winter precipitation timing, and accelerated cover crop phenology under higher accumulated heat units.

Daily soil water content distributions integrate the water balance signal of each scenario. The fraction of days with soil water below the wilting point in NC rises modestly under SSP585_End relative to Historical, with intermediate values that track the warming gradient through SSP245_Mid, SSP370_Mid, SSP245_End, SSP585_Mid, and SSP370_End; corresponding fractions in CC are consistently higher than in NC under every scenario. The fraction of dry days is consistently higher in CC than in NC under every scenario, which represents the cover crop's transpiration competing with available soil water during the establishment window.

3.5.2 Cover crop response under altered climates

Distributions of CC standing biomass at termination and establishment success rate for the CC treatment across the seven scenarios are shown in Figure 39. This subsection responds directly to the survey identified concern that water competition between CC and trees is the top agronomic issue, and to the survey finding that 11 of 16 CC orchards in the sample rely entirely on rainfall for CC establishment.

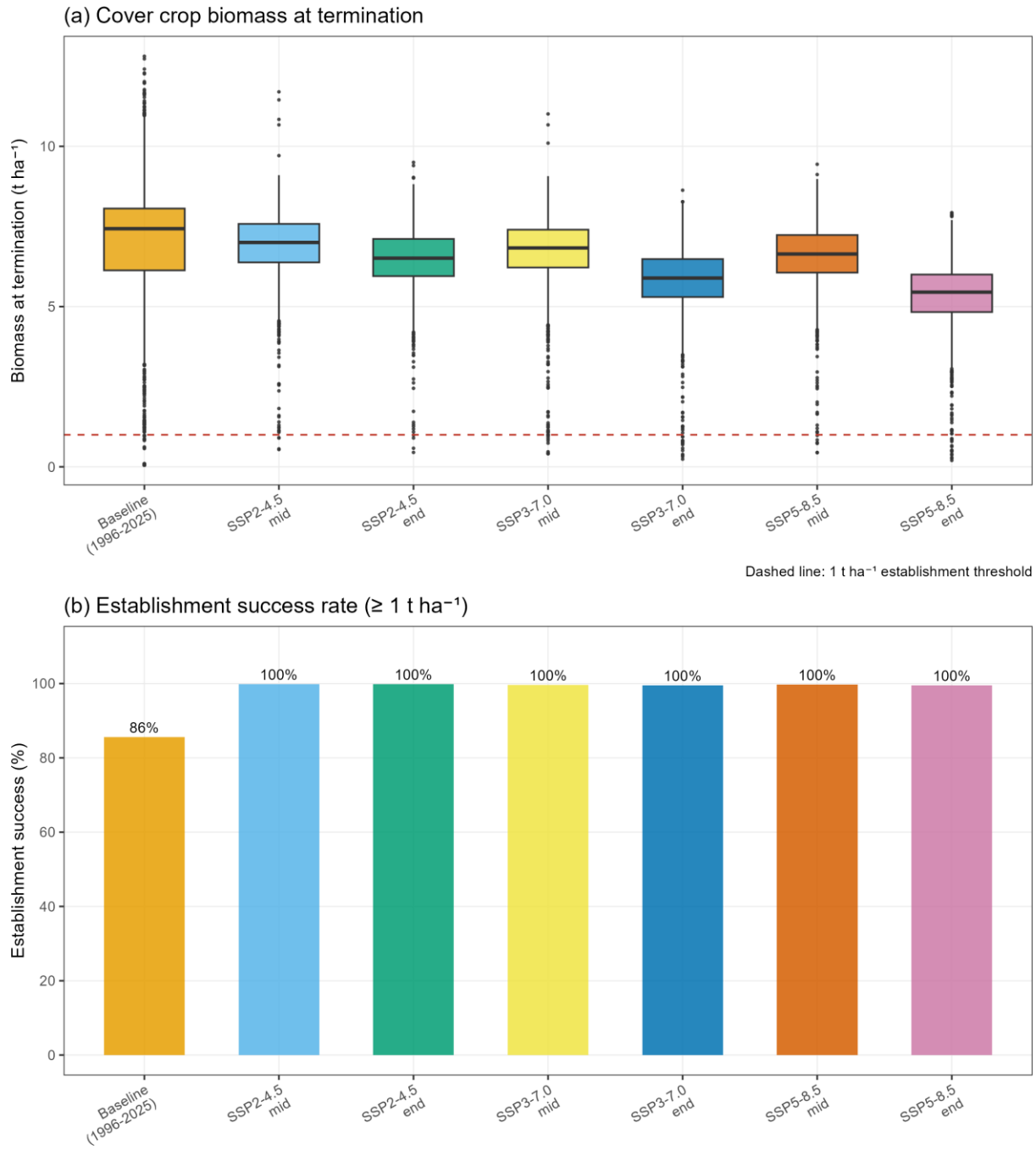


Figure 39. Cover crop response under altered climate, CC treatment across the seven scenarios. (a) cover crop biomass at termination; (b) establishment success rate (share of years at or above the 1 t ha⁻¹ establishment threshold).

Under the Historical scenario, cover crop biomass at termination has a median of 7.43 t ha⁻¹ and a standard deviation of 2.84 t ha⁻¹, with establishment success in 85.6 percent of

simulated years. Under the moderate emissions scenarios at mid-century (SSP245_Mid and SSP370_Mid), median biomass changes by -5.1 percent and -6.9 percent respectively relative to Historical, with establishment success in 99.9 percent and 99.7 percent of years. The mid-century response reflects the tradeoff between modestly higher winter temperatures and lower cover crop biomass.

The high emissions and end of century scenario produce the most consequential CC responses. Under SSP585_Mid, median cover crop biomass changes by -8.2 percent relative to Historical and establishment success is 99.8 percent of simulated years; under SSP585_End, median biomass changes by -20.5 percent and establishment success is 99.5 percent, with simulated biomass at termination falling below the 1 t ha^{-1} effective-ground-cover threshold in approximately 0.5 percent of years. The corresponding figures for SSP245_End and SSP370_End fall between the mid century and SSP585_End values; establishment success remains above 99 percent across all six future scenarios, with the dominant change being a reduction in median peak biomass rather than a change in establishment frequency.

4. Discussion

4.1 Survey findings in the broader context

The survey results align closely with the broader California cover crop adoption literature on the prevailing pattern of grower concerns, but they also expose a tension between grower perception and the most recent empirical evidence on the practice's actual water cost. The dominant agronomic concern identified by respondents, water use and competition with trees (35 percent extremely concerned), reproduces a pattern that has been documented across California specialty crops for at least two decades. Carlisle (2016), in a narrative review of soil health practice adoption in U.S. agriculture, identifies water uncertainty as a recurrent driver of grower

hesitation in semi-arid systems and concludes that rational actor models are inadequate to explain the persistence of the adoption gap. Mitchell et al. (1999) similarly identified water cost concerns as the primary barrier to cover crop adoption in the Central Valley, and DeVincentis et al. (2020), in a benefit-cost analysis of California specialty crops, found that the economic case for cover cropping is strongly conditioned on whether growers expect a water cost penalty. The survey's identification of cost of water under groundwater allocations as tied for the top economic concern (41 percent extremely concerned) extends this pattern explicitly into the SGMA compliance era, in which water itself, rather than only the water cost of cover cropping, has become a limiting constraint.

The empirical evidence on the size of the water cost is more reassuring than the survey responses suggest. DeVincentis et al. (2022), a multi-site study of winter cover cropping in California specialty crop fields, reports that water losses from winter cover crops were negligible relative to clean cultivated soil and that soil moisture differences between cover cropped and control fields were not significant at the end of the winter. They conclude that California growers of high-value specialty crops can likely adopt winter cover cropping without altering their irrigation plans. Borum et al. (2024), summarizing expert consensus from the Soil-Water Interface Expert Convening Series, reframes the question by noting that the water impact of cover crops in orchards is best understood not as a single seasonal mean difference but as a structural shift in the timing of ET across the calendar year, with potentially different implications for winter soil moisture recharge and for spring soil water availability at bud break. Both syntheses suggest that the water cost concern most often expressed by growers is not well supported as a steady state seasonal mean effect, but that it has merit as a concern about timing and about establishment period dynamics. The survey results are consistent with that reframing:

respondents identified water use as the top agronomic concern but also reported that 11 of 16 cover cropped orchards rely entirely on rainfall for cover crop establishment. Grower concerns and the expert reframing therefore meet at the same operational pinch point, the establishment window, even when their language differs.

The benefits hierarchy reported by respondents fits a pattern noted by Carlisle (2016) and others: soil health and environmental stewardship are valued more highly than financial gains. Soil health and organic matter improvement was rated highly valued by 82 percent of respondents in this study, soil moisture management and erosion control by 82 percent, and environmental stewardship by 76 percent, while reduced inputs in the form of irrigation, fertilizer, and herbicide was the least valued category at 44 percent. Carlisle's review explicitly identifies noneconomic farmer motives as one of five emergent themes underlying soil health practice adoption, and the present sample's preference for additive (improving soil) rather than substitutive (replacing inputs) framings of winter cover crop benefits reproduces that pattern in California pistachio orchards. This finding has practical implications for outreach: messaging that emphasizes input substitution as the primary value of cover cropping is likely to underperform messaging that emphasizes additive soil health and stewardship outcomes among orchard operators with profiles similar to those in this sample.

Two caveats limit the generalizability of these findings. First, the sample is biased toward experienced cover crop adopters: 8 of 17 CC orchards in the sample reported 6 to 10 years of cover crop history, and 3 reported more than 15 years. The very low priority that respondents placed on information gaps about seed selection and traits, seeding and termination management, and lack of technical guidance almost certainly reflects this accumulated experience rather than the state of knowledge available to a non-adopter contemplating the practice for the first time.

Additionally, most of the respondents seemed to have used resident vegetation, so the low interest could be due to most of the respondents not needing to learn about those types of information gaps. Studies of California cover crop adoption that have surveyed broader grower populations, including Gould and Rudnick (2018) and DeVincentis et al. (2020), routinely find information access and technical guidance among the most frequently cited barriers, with proportions roughly inverse to those reported here. The present sample's findings should therefore be interpreted as characterizing the residual concerns of practitioners who have already overcome the early adoption knowledge barriers, not as evidence that those barriers are no longer important industry-wide. Second, the sample size (n = 18 completing respondents, with subsample n values down to 9) does not support inferential statistics, so the rank order of concerns and benefits should be read as descriptive rather than as a precise estimate of population level priorities.

Taken together, the survey results corroborate the broad pattern reported in the California cover crop adoption literature, with one substantive interpretive shift driven by the recent SGMA era empirical work. The concern about water competition identified in the survey is best understood not as a generalized water cost penalty but as a concern about establishment period dynamics under variable winter precipitation, and that interpretation directly motivates the climate scenario design and the cover crop response analysis.

Findings should be read as characterizing what concerns and priorities arise among practitioners who have already engaged with the practice, not as estimates of the prevalence of those concerns across the industry.

The sample is best understood as characterizing experienced CC adopters rather than the broader pistachio industry; in particular it contains very few orchards in the early establishment

window during which the most acute uncertainty about water competition is reported in the literature (DeVincentis et al., 2020; Borum et al., 2024).

The prominence of native vegetation in the sample reflects a substantial subset of respondents who do not seed a CC mix at all but instead manage the resident understory through mowing alone, an approach intermediate between bare ground and seeded cover cropping that is not always captured in surveys structured around a binary cover or no cover question.

The pattern of challenges, with poor germination and lack of information rated low and pest/disease/weed and economic uncertainty rated high, suggests that the established practitioners in this sample have largely worked through the early adoption barriers most often cited in the California CC literature (Mitchell et al., 1999; DeVincentis et al., 2020), and that their ongoing concerns are concentrated on system integration issues rather than on agronomic feasibility.

The high "Highly valued" share for soil health and the comparatively low share for reduced inputs suggest that respondents view winter CC primarily as additive, improving soil and environmental outcomes, rather than as substitutive for purchased inputs.

The overlap between leading non-adopter concerns (Figure 16a) and leading adopter economic concerns (Figure 9c) on water cost and uncertain returns suggests the same concerns persist in both groups but that adopters have either accepted those tradeoffs or developed practices to manage them.

Cross-cluster reading: the dominance of agronomic benefits in the benefit-category ranking (Figure 13, mean rank 1.15) is consistent with the dominance of tree nutrition and soil health items in the knowledge-gap rankings (Figure 11), but stands in tension with the high

economic concern share (Figure 9c). The gap between what growers value (agronomic) and what they worry about (economic) is the central framing tension of these survey results.

Self-reported yield attribution is noisy in this sample (41 percent Unsure / Prefer not to answer in Figure 14a) even among multi-year adopters. This is itself a finding: it indicates that yield attribution to cover cropping is difficult to make confidently from orchard observation alone, which strengthens the case for using a process-based model to isolate the CC signal.

4.2 Calibrated parameter values and sensitivity in the broader APEX literature

The sensitivity analysis results and the calibrated parameter values invite explicit comparison with the published APEX literature for other cropping systems. The closest methodological analogues are the four studies cited extensively already: Tadesse et al. (2018, 2019) for irrigated and dryland row crops at Bushland, Texas; Tadesse et al. (2021) for conservation tillage wheat in the same setting; Talebizadeh et al. (2018) for cotton and grain sorghum under multi-objective ET and yield calibration; and Mason et al. (2020) for dairy farm rotations in Vermont. Comparing the present orchard simulation against these four analogues yields patterns of agreement and divergence.

First, the unified Sobol ranking promotes PARM2 (root growth-soil strength) ahead of PARM17 (soil evaporation-plant cover factor) in both orchards (Table 10). PARM2 dominates in NC at SI_Total = 0.77 and in CC at SI_Total = 0.43; PARM17 follows at SI_Total = 0.26 in NC and SI_Total = 0.41 in CC, with PARM17 nearly co-dominant with PARM2 in CC. The cited literature consistently identifies PARM17 as the dominant parameter for monthly ETa in annual cropping systems (Tadesse et al. 2018, 2019, 2021; Talebizadeh et al. 2018), so the present orchard system departs from that consensus in two specific ways. The PARM2 dominance, at SI_Total around 0.77 in NC, exceeds the second-rank PARM2 sensitivity reported in the cited

row crop studies by a factor of two or more, and is interpreted here as a perennial-system signature: pistachio root response to soil mechanical impedance is the single most influential physiological process driving simulated outputs over a multi-year horizon. The CC vs NC contrast in PARM17 sensitivity (~1.6x stronger in CC) is also a treatment-specific finding that single-treatment row-crop calibrations could not detect, and it suggests that cover crop ground cover variability is a meaningful modulator of evaporation partitioning in the orchard floor.

Second, the unified ranking confirms that, once the model's primary outputs (ET_a, SWC, LAI, Cover crop biomass, and yield) are aggregated, hydrology and root-growth processes carry most of the parameter sensitivity. The implication for APEX's transferability to perennial tree crops is that PARM2 should be included in the primary sensitivity target parameter set rather than treated as a second-tier yield parameter, and that treatment specific PARM17 contrasts should be tested whenever paired CC versus NC systems are simulated.

Third, the presence of a winter cover crop redirects soil carbon and soil nitrogen parameter sensitivity toward residue-related parameters. The implications for APEX's transferability to perennial tree crops are mixed and partial.

4.3 Model performance and what we can and cannot conclude

This section provides a candid assessment of the APEX modeling work in this study, distinguishing model outputs that calibrated to within accepted performance thresholds from those that did not, and identifying the conclusions that the model can and cannot defensibly support. The structure follows Mason et al. (2020), who recommended that documented APEX calibrations include explicit discussion of components that fall short of satisfactory thresholds, and who themselves reported satisfactory calibration of mean silage yield (PBIAS = 2 percent)

but unsatisfactory calibration of year-to-year yield variation (NSE = -1.6) on dairy farms in Vermont.

The model met the Moriasi et al. (2016) satisfactory thresholds for monthly ET_a in both orchards (Table 13). For ET_a, the calibrated NSE of 0.60 in NC and 0.55 in CC, with PBIAS of 4.9 percent and 11.1 percent respectively, indicate that the model reproduces the seasonal ET_a cycle and the inter-treatment offset with reasonable fidelity. The LAI diagnostic shows NSE = -2.87 and PBIAS = +120 percent in NC and NSE = -3.74 and PBIAS = +150 percent in CC, indicating systematic overestimation of peak LAI that is consistent with known APEX scaling limitations at low tree densities.

Yield calibration is constrained by data availability. The orchard produced its first commercial harvest in 2024 at 0.20 t ha^{-1} (excluded as an anomalously low establishment year); calibration rests on the single 2025 observation of 1.07 t ha^{-1}. The CC orchard achieved PBIAS = −1.87 percent, within the ±25 percent threshold of Wang et al. (2012); the NC orchard showed PBIAS = −33.6 percent, outside the threshold. Year-to-year yield variability cannot be assessed from a single observation, and the conventional NSE statistic reported in Table 13 is not informative at this sample size.

4.4 Climate scenario implications, viewed through grower concerns

The framing of the scenario results requires one important clarification. The Baseline is the observed 1996 to 2025 ensemble mean. This section juxtaposes the climate scenario results with the grower concerns. The dominant agronomic concern from the survey, water competition between the cover crop and the trees (35 percent extremely concerned), is most directly tested by the warmer and drier corner of the scenario ensemble, namely SSP585_End. Under that scenario, median cover crop biomass changes by -20.5 percent relative to Historical. The CC versus NC

ET_a offset (peak monthly) changes from approximately 38 mm month^{-1} under Historical to approximately 41 mm month^{-1} under SSP585_End.

The economic concern about cost of water under SGMA (41 percent extremely concerned, tied for top economic concern) is most directly tested by the warming increase from SSP245_Mid through SSP585_End, which spans a range of plausible future water demand increases against a fixed irrigation schedule. Section 3.5.2 reports that total orchard ET_a rises by 14.0 percent in NC and 9.1 percent in CC under SSP585_End relative to Historical. Pistachio productive-year median yield changes by -7.7 percent and -10.2 percent respectively along the same gradient.

The economic concern about uncertainty of returns (41 percent extremely concerned, tied for top economic concern) is tested by yield variability across the seven scenarios. Section 3.5.2 reports that the yield standard deviation changes only modestly relative to the Historical scenario in both orchards under all six future scenarios, with the largest deviations being a decrease of approximately 7 percent under SSP5-8.5 end-of-century in NC and a comparable decrease of approximately 10 percent under SSP5-8.5 end-of-century in CC. The CC orchard's yield standard deviation tracks NC closely across scenarios, with CC slightly lower than NC under every scenario.

The survey finding that 11 of 16 CC orchards rely entirely on rainfall for CC establishment is tested across the seven scenarios by examining how the Cover crop biomass distribution shifts in response to combined changes in winter temperature, winter precipitation totals, and winter precipitation timing. Section 3.5.3 reports that median cover crop biomass changes by -20.5 percent under SSP585_End to Historical, because warmer winters reduce the frequency of cold-limited establishment failures even as peak biomass declines.

The five concerns identified in the survey frame how the scenario results should be read; each concern maps to a specific axis or corner of the seven scenario set.

The water competition concern between the CC and trees, raised by 11 of 16 CC adopters and 7 of 9 NC respondents, motivates examination of the CC versus NC ET_a offset across the warming gradient. The concern is sharpest where atmospheric demand is highest and winter precipitation is most variable, namely the SSP5-8.5 mid-century and end-of-century cells.

The SGMA era water cost concern, raised by every NC respondent and by 12 of 16 CC adopters as a top three concern, motivates examination of total ET_a and the modeled irrigation demand across all six future scenarios.

The uncertainty of economic returns concern, ranked highest among economic concerns, motivates examination of yield variability both within each scenario (across stochastic realizations) and across the six future scenarios.

The CC establishment concern, raised by 9 of 16 CC adopters as a concrete operational worry, motivates examination of cover crop biomass at termination and peak CC LAI across the seven scenarios.

The heat stress and phenology concern, raised in connection with chilling hour reductions, motivates examination of water and temperature stress day counts across the warming gradient.

The dominance of fully rainfed cover cropping shown in Figure 14b means that CC establishment in these orchards is highly sensitive to the timing of seasonal precipitation rather than to seasonal totals alone.

4.5 Grower communication implications

The integrated survey and modeling results carry concrete implications for grower communication under SGMA. The survey indicates that growers already prioritize water cost as a top three concern about cover cropping, so outreach material that frames cover cropping primarily as a soil health practice without addressing water competition risks losing the conversation early.

The low priority placed on operational knowledge gaps (seed selection, seeding/maintenance/termination) is consistent with a sample of experienced practitioners who have already worked through those details. Research and outreach effort should therefore prioritize the dominant gap of tree nutrition, soil health, and biological activity (Q88, Figure 11b) rather than the operational details that experienced adopters have already worked through.

Workshops and field days fell between the practitioner facing and passive media clusters in the information-source ranking (Figure 12, mean rank 4.7). Some respondents rate them as central while others rate them as peripheral, suggesting that the impact of in-person events depends heavily on the targeting of the audience.

The strongest movers for non-adopters (Figure 16b) were financial assistance and economic case studies (4 of 6 "Very Likely"), pointing to financial assistance and concrete economic evidence as the most actionable points of leverage for CC adoption among the non-adopters in this sample.

Cost-share or other financial assistance was used by only 29 percent of CC adopters in this sample, with the remaining 71 percent self-funding all CC activity. The high self-funded share alongside the high economic concern suggests that available cost-share programs are not reaching the majority of adopters.

4.6 Limitations

Three major limitations of this study warrant explicit acknowledgment beyond those already discussed.

First, model calibration was performed at a single field site. The Bullseye orchard near Davis is a young commercial orchard on Rincon silty clay loam in the Sacramento Valley, with a Mediterranean climate that is somewhat cooler and wetter than the southern San Joaquin Valley pistachio belt. Most California pistachio production occurs in the counties of Kern, Fresno, Tulare, Kings, and Madera, where summer temperatures are higher, winter precipitation is lower, and soils differ in texture, salinity, and organic matter content from those at Davis. The calibrated parameter set is therefore site-specific in the strict sense, and extending the climate scenario conclusions to the southern San Joaquin Valley pistachio belt requires additional calibration and validation against orchards in those settings. The survey sample, concentrated in the southern San Joaquin Valley counties (91 percent of orchards in Kern, Fresno, Tulare, and Madera), anchors the regional context of the modeling work but does not substitute for site-specific calibration there.

Second, the survey sample of 18 completing respondents is small, geographically concentrated in the major pistachio-producing counties, and biased toward experienced cover crop adopters. The geographic concentration mirrors statewide production but does not capture peripheral pistachio-producing counties such as Butte, Yolo, and Merced, where soil and climate differ from the production core.

Third, the cover crop was represented in APEX as a single species (winter pea), while the actual cover crop at the Bullseye orchard is a multi-species mix (Table 2). APEX can simulate up to ten plant species growing simultaneously with competition for light, water, and nutrients

(Williams et al., 2023), but the practical difficulty of parameterizing a multi-species mix with the limited mix-specific calibration data available led to the single-species simplification. Winter pea was selected as a single-species proxy because the legume fraction of the actual mix (bell beans, peas, and vetch combined) constitutes 75 percent of the seeded mass, but the simplification has consequences. The actual mix produces different total biomass, fixes nitrogen at a different rate, and roots to different depths than a pure pea stand would. Climate scenario conclusions about cover crop biomass and establishment success should therefore be read as outcomes for the simplified model representation, with the qualitative direction of the scenario response likely to apply to multi-species mixes but with absolute biomass and nitrogen values requiring adjustment.

The non-adoption reasons (Figure 16a) draw on only 4 of 9 NC respondents who answered Q64. At this denominator, percentages should be read as raw counts and the directional results treated as suggestive only.

Although the sample is biased toward experienced adopters, the geographic distribution mirrors statewide pistachio acreage (CDFA, 2025), so the sample has geographic representativeness even though it lacks adoption-stage representativeness.

5. Conclusion

This study set out to address three objectives. First, to characterize current cover crop practices, perceived challenges, and information priorities among California pistachio operators through an online survey, providing practitioner context for an evaluation that would otherwise rest on a single instrumented orchard. Second, to calibrate and validate the Agricultural Policy/Environmental eXtender (APEX) model for a young commercial pistachio orchard near Davis, CA, with and without a winter cover crop, against actual evapotranspiration, soil water

content, leaf area index, and yield observations. Third, to use the calibrated model to evaluate cover crop performance and tree versus cover crop water dynamics under six future climate scenarios derived from the LOCA2 downscaled CMIP6 ensemble plus a historical baseline, with particular attention to scenarios motivated by survey-identified grower concerns. The structure of this conclusion follows the order of the objectives.

The survey characterized the concerns of 18 experienced California pistachio operators and identified water use and competition with trees as the dominant agronomic concern (35 percent rated it "extremely concerned"), with cost of water under SGMA era groundwater allocations and uncertainty of economic returns tied as the top economic concerns at 41 percent each. Respondents valued CC benefits highly, particularly soil health, soil moisture management, and environmental stewardship, while assigning the lowest value to direct input substitution. The survey also documented that 11 of 16 CC orchards rely entirely on rainfall for CC establishment, identifying precipitation timing as an implicit binding constraint on the practice that the survey instrument did not ask about explicitly.

The calibrated APEX model met the Moriasi et al. (2016) satisfactory thresholds for monthly ET_a in both the NC and CC treatments (NSE = 0.60 and 0.55 respectively), supported by the eddy covariance observations used as the primary calibration target. CC yield calibration achieved PBIAS = −1.87 percent against the 2025 harvest, within the Wang et al. (2012) threshold; NC yield PBIAS of −33.6 percent exceeded the threshold. Pistachio LAI, SWC, and cover crop biomass remained diagnostic rather than primary calibration targets.

The climate scenario analysis evaluated six future scenarios of CMIP6 SSP pathways (SSP2-4.5, SSP3-7.0, SSP5-8.5) and time periods (mid century 2035 to 2065, end of century 2070 to 2099) against an observed 1996 to 2025 baseline. Across scenarios, the cover crop water

cost remained near 70 to 93 mm per year (about 12 percent) and stable, pistachio yield declined modestly with the largest reduction of 8 to 10 percent under SSP5-8.5 end of century, and cover crop establishment remained high.

Three lines of future work follow directly from the limitations. First, the survey should be expanded both geographically (to include the southern San Joaquin Valley counties more thoroughly and to capture peripheral pistachio producing regions) and demographically (to reach prospective and recent adopters, not only experienced ones). Second, multi-site model calibration is needed before the climate scenario conclusions can be extended beyond the Davis study site; a coordinated effort with eddy covariance and soil moisture instrumentation deployed at one orchard per major pistachio-producing county would substantially expand the geographic envelope of confident inference. Third, cover crop species selection should itself be examined as a variable because the present study collapsed a multi-species mix to a single-species proxy. The integration of the APEX modeling framework with the remote-sensing ETa products evaluated by Chen et al. (in preparation) would also allow distributed orchard-scale water budget accounting that neither approach can accomplish alone. Taken together, these extensions build on the study's central observation: that linking practitioner-side survey work with process-based modeling produces results neither component would deliver alone, and that the pattern of confirmation and complication observed here is the kind of nuanced answer that real grower decisions and SGMA era policy choices both require.

Acknowledgements

This work was fully funded by USDA NIFA Award #2021-68012-35914. Thank you to Bullseye Farms for allowing us to conduct this research on their private orchard. Special thanks to Aaron Guerra, Ali Ghorbanpour, Anish Sapkota, Benny Briggs, Cassandra Bonfil, Felix Ogunmokun, Floyid Nicolas, Gento Shimamura, Ian Gomez, Isabella Burnett, Krista Blide, Matthew Maciosek, Nicolas Almeida, Sidd Dala, Usama Al-Dughaishi, William Lennon, and Zixuan Gan for assistance with equipment installation and data collection.

References

Abatzoglou, J.T., 2013. Development of gridded surface meteorological data for ecological applications and modelling. Intl Journal of Climatology 33, 121–131. https://doi.org/10.1002/joc.3413.

Adams, C.B., Cosner, J., 2025. Field pea cardinal temperatures, growth and vigor traits of winter- and spring-adapted germplasm at germination and seedling stages. Sci Rep 15, 21759. https://doi.org/10.1038/s41598-025-06342-w.

Alfieri, J.G., Kustas, W.P., Prueger, J.H., McKee, L.G., Hipps, L.E., Gao, F., 2019. A multi-year intercomparison of micrometeorological observations at adjacent vineyards in california's central valley during grapex. Irrig Sci 37, 345–357. https://doi.org/10.1007/s00271-018-0599-3.

Allen, R., Irmak, A., Trezza, R., Hendrickx, J.M.H., Bastiaanssen, W., Kjaersgaard, J., 2011. Satellite-based et estimation in agriculture using sebal and metric. Hydrological Processes 25, 4011–4027. https://doi.org/10.1002/hyp.8408.

Allen, R.G., Burnett, B., Kramber, W., Huntington, J., Kjaersgaard, J., Kilic, A., Kelly, C., Trezza, R., 2013. Automated calibration of the metric-landsat evapotranspiration process. J American Water Resour Assoc 49, 563–576. https://doi.org/10.1111/jawr.12056.

Allen, R.G., Pereira, L.S., 2009. Estimating crop coefficients from fraction of ground cover and height. Irrig Sci 28, 17–34. https://doi.org/10.1007/s00271-009-0182-z.

Allen, R.G., Pereira, L.S., Raes, D., Smith, M., 1998. FAO irrigation and drainage paper no. 56. crop evapotranspiration (guidelines for computing crop water requirements). FAO, Rome.

Allen, R.G., Tasumi, M., Morse, A., Trezza, R., 2005. Satellite-based evapotranspiration by energy balance for western states water management, in: Impacts of Global Climate Change. Presented at the World Water and Environmental Resources Congress 2005, American Society of Civil Engineers, Anchorage, Alaska, United States, pp. 1–18. https://doi.org/10.1061/40792(173)556.

Allen, R.G., Tasumi, M., Trezza, R., 2007. Satellite-based energy balance for mapping evapotranspiration with internalized calibration (metric)—model. J. Irrig. Drain Eng. 133, 380–394. https://doi.org/10.1061/(ASCE)0733-9437(2007)133:4(380).

Anderson, M., Gao, F., Knipper, K., Hain, C., Dulaney, W., Baldocchi, D., Eichelmann, E., Hemes, K., Yang, Y., Medellin-Azuara, J., Kustas, W., 2018. Field-scale assessment of land and water use change over the california delta using remote sensing. Remote Sensing 10, 889. https://doi.org/10.3390/rs10060889.

Anderson, M.C., Norman, J.M., Mecikalski, J.R., Otkin, J.A., Kustas, W.P., 2007. A climatological study of evapotranspiration and moisture stress across the continental united states based on thermal remote sensing: 1. model formulation. J. Geophys. Res. 112, 2006JD007506. https://doi.org/10.1029/2006JD007506.

Baldwin, R., Battany, M., Beede, R., Brar, G.S., Culumber, M., Ferguson, L., Fichtner, E., Gordon, P., Hanson, B., Havliand, D., Hembree, K., Kallsen, C.E., Sanden, B., Michailidas, T.J., Trouillas, F., Zaccaria, D., Harris, L., Stewart, D., 2020. Sample costs to establish and produce pistachios. Technical Report, UCCE ANR Agricultural Issues Center.

Bambach, N., Kustas, W., Alfieri, J., Prueger, J., Hipps, L., McKee, L., Castro, S.J., Volk, J., Alsina, M.M., McElrone, A.J., 2022. Evapotranspiration uncertainty at

micrometeorological scales: the impact of the eddy covariance energy imbalance and correction methods. Irrig Sci 40, 445–461. https://doi.org/10.1007/s00271-022-00783-1.
Basche, A.D., Kaspar, T.C., Archontoulis, S.V., Jaynes, D.B., Sauer, T.J., Parkin, T.B., Miguez, F.E., 2016. Soil water improvements with the long-term use of a winter rye cover crop. Agricultural Water Management 172, 40–50. https://doi.org/10.1016/j.agwat.2016.04.006.
Bastiaanssen, W.G.M., Menenti, M., Feddes, R.A., Holtslag, A.A.M., 1998. A remote sensing surface energy balance algorithm for land (sebal). 1. formulation. Journal of Hydrology 212–213, 198–212. https://doi.org/10.1016/S0022-1694(98)00253-4.
Bellvert, J., Adeline, K., Baram, S., Pierce, L., Sanden, B., Smart, D., 2018. Monitoring crop evapotranspiration and crop coefficients over an almond and pistachio orchard throughout remote sensing. Remote Sensing 10, 2001. https://doi.org/10.3390/rs10122001.
Bergtold, J.S., Ramsey, S., Maddy, L., Williams, J.R., 2019. A review of economic considerations for cover crops as a conservation practice. Renew. Agric. Food Syst. 34, 62–76. https://doi.org/10.1017/S1742170517000278.
Bethune, M.G., Selle, B., Wang, Q.J., 2008. Understanding and predicting deep percolation under surface irrigation. Water Resources Research 44, 2007WR006380. https://doi.org/10.1029/2007WR006380.
Blanco-Canqui, H., Mikha, M.M., Presley, D.R., Claassen, M.M., 2011. Addition of cover crops enhances no-till potential for improving soil physical properties. Soil Science Soc of Amer J 75, 1471–1482. https://doi.org/10.2136/sssaj2010.0430.
Blanco-Canqui, H., Ruis, S.J., 2020. Cover crop impacts on soil physical properties: a review. Soil Science Soc of Amer J 84, 1527–1576. https://doi.org/10.1002/saj2.20129.
Blanco-Canqui, H., Shaver, T.M., Lindquist, J.L., Shapiro, C.A., Elmore, R.W., Francis, C.A., Hergert, G.W., 2015. Cover crops and ecosystem services: insights from studies in temperate soils. Agron. J. 107, 2449–2474. https://doi.org/10.2134/agronj15.0086.
Bodner, G., Loiskandl, W., Kaul, H.-P., 2007. Cover crop evapotranspiration under semi-arid conditions using fao dual crop coefficient method with water stress compensation. Agricultural Water Management 93, 85–98. https://doi.org/10.1016/j.agwat.2007.06.010.
Borum, J., Bruno, E., Castle, S., Chiartas, J., Crowley, R., Decock, C., Delgado, C., DeVincentis, A., Dufour, R., Edwards, A., Flaherty, R., Flynn, M., Grimm, R., Hale, L., Light, S., Little, C., Lowell, K., Minshew, H., Nocco, M., Peterson, C., Roby, M., Roseman, J., Roth, A., Sandoval, S., Silva, S.A., Smet, E., Smither-Kopperl, M., Suvocarev, K., Waterhouse, H., Wauters, V., Williams, S., Zaccaria, D., 2024. Cover cropping in the SGMA era: a comprehensive overview of water impacts, policy implications, and recommendations for California's water managers, The Soil-Water Interface Expert Convening Series: Cover Crop Impacts on Water Budgets. California.
California Department of Food and Agriculture (CDFA), 2025. 2023-2024 California agricultural statistics review.
California Department of Water Resources (DWR), 2025. California's groundwater: bulletin 118 — update 2025. Public Draft, October 2025. California Department of Water Resources, Sacramento, CA.
Cao, Q., Wang, Z., Yang, X., Shen, Y., 2021. The effects of cocksfoot cover crop on soil water balance, evapotranspiration partitioning, and system production in an apple orchard on

the loess plateau of china. Soil and Tillage Research 205, 104788. https://doi.org/10.1016/j.still.2020.104788.
Carlisle, L., 2016. Factors influencing farmer adoption of soil health practices in the United States: a narrative review. Agroecol. Sustain. Food Syst. 40, 583–613. https://doi.org/10.1080/21683565.2016.1156596.
Chakraborty, P., Singh, J., Singh, N., Kumar, S., 2022. Assessing the influence of cover crop on soil water dynamics using soil moisture measurements and hydrus-1d simulations. Soil Science Soc of Amer J 86, 1538–1552. https://doi.org/10.1002/saj2.20477.
DeVincentis, A., Solis, S.S., Rice, S., Zaccaria, D., Snyder, R., Maskey, M., Gomes, A., Gaudin, A., Mitchell, J., 2022. Impacts of winter cover cropping on soil moisture and evapotranspiration in California's specialty crop fields may be minimal during winter months. Calif. Agr. 76, 37–45. https://doi.org/10.3733/ca.2022a0001.
DeVincentis, A.J., Solis, S.S., Bruno, E.M., Leavitt, A., Gomes, A., Rice, S., Zaccaria, D., 2020. Using cost-benefit analysis to understand adoption of winter cover cropping in california's specialty crop systems. Journal of Environmental Management 261, 110205. https://doi.org/10.1016/j.jenvman.2020.110205.
Dhungel, R., Anderson, R.G., French, A.N., Skaggs, T.H., Ajami, H., Wang, D., 2024. Intercomparison of citrus evapotranspiration among eddy covariance, openet ensemble models, and the water and energy balance model (baitsss). Agricultural Water Management 304, 109066. https://doi.org/10.1016/j.agwat.2024.109066.
Diffenbaugh, N.S., Swain, D.L., Touma, D., 2015. Anthropogenic warming has increased drought risk in California. Proc. Natl. Acad. Sci. U.S.A. 112, 3931–3936. https://doi.org/10.1073/pnas.1422385112.
Drechsler, K., Fulton, A., Kisekka, I., 2022. Crop coefficients and water use of young almond orchards. Irrig Sci 40, 379–395. https://doi.org/10.1007/s00271-022-00786-y.
Dunn, M., Ulrich-Schad, J.D., Prokopy, L.S., Myers, R.L., Watts, C.R., Scanlon, K., 2016. Perceptions and use of cover crops among early adopters: findings from a national survey. Journal of Soil and Water Conservation 71, 29–40. https://doi.org/10.2489/jswc.71.1.29.
Evett, S.R., Steiner, J.L., 1995. Precision of neutron scattering and capacitance type soil water content gauges from field calibration. Soil Science Soc of Amer J 59, 961–968. https://doi.org/10.2136/sssaj1995.03615995005900040001x.
Faunt, C.C., Sneed, M., Traum, J., Brandt, J.T., 2016. Water availability and land subsidence in the central valley, california, usa. Hydrogeol J 24, 675–684. https://doi.org/10.1007/s10040-015-1339-x.
Fernando, M., Scott, N., Shrestha, A., Gao, S., Hale, L., 2024. A native plant species cover crop positively impacted vineyard water dynamics, soil health, and vine vigor. Agriculture, Ecosystems & Environment 367, 108972. https://doi.org/10.1016/j.agee.2024.108972.
Firoozi, F., Alavipanah, S.K., Hosseini, S.Z., Asgari, S., Malamiri, H.R.G., Rahimi, K., 2023. Remotely sensed and empirical reference evapotranspiration models to derive crop coefficients for pistachios in the central basin of iran. Iran J Sci Technol Trans Civ Eng 47, 3999–4019. https://doi.org/10.1007/s40996-023-01169-9.
Fisher, J.B., Melton, F., Middleton, E., Hain, C., Anderson, M., Allen, R., McCabe, M.F., Hook, S., Baldocchi, D., Townsend, P.A., Kilic, A., Tu, K., Miralles, D.D., Perret, J., Lagouarde, J.-P., Waliser, D., Purdy, A.J., French, A., Schimel, D., Famiglietti, J.S., Stephens, G., Wood, E.F., 2017. The future of evapotranspiration: global requirements

for ecosystem functioning, carbon and climate feedbacks, agricultural management, and water resources: the future of evapotranspiration. Water Resour. Res. 53, 2618–2626. https://doi.org/10.1002/2016WR020175.
Fisher, J.B., Tu, K.P., Baldocchi, D.D., 2008. Global estimates of the land–atmosphere water flux based on monthly avhrr and islscp-ii data, validated at 16 fluxnet sites. Remote Sensing of Environment 112, 901–919. https://doi.org/10.1016/j.rse.2007.06.025.
Flynn, M.T., Guerrero-Medina, O., McDonald, I.F., Anika, J.T., Ware, E.C., Paw U, K.T., Gaudin, A.C., Fenster, T.L., Lundgren, J.G., Harter, T., Sandoval Solis, S., Suvočarev, K., 2025. A case study of evapotranspiration at five almond orchards on a spectrum of conventional to regenerative management. California Agriculture 79. https://doi.org/10.3733/001c.133243.
Foken, T., Aubinet, M., Leuning, R., 2012. The eddy covariance method, in: Aubinet, M., Vesala, T., Papale, D. (Eds.), Eddy Covariance. Springer Netherlands, Dordrecht, pp. 1–19. https://doi.org/10.1007/978-94-007-2351-1_1.
Folorunso, O.A., Rolston, D.E., Prichard, T., Loui, D.T., 1992. Soil surface strength and infiltration rate as affected by winter cover crops. Soil Technology 5, 189–197. https://doi.org/10.1016/0933-3630(92)90021-R.
Gabriel, J.L., Muñoz-Carpena, R., Quemada, M., 2012. The role of cover crops in irrigated systems: water balance, nitrate leaching and soil mineral nitrogen accumulation. Agriculture, Ecosystems & Environment 155, 50–61. https://doi.org/10.1016/j.agee.2012.03.021.
Garba, I.I., Bell, L.W., Williams, A., 2022. Cover crop legacy impacts on soil water and nitrogen dynamics, and on subsequent crop yields in drylands: a meta-analysis. Agron. Sustain. Dev. 42, 34. https://doi.org/10.1007/s13593-022-00760-0.
Gassman, P.W., Williams, J.R., Wang, X., Saleh, A., Osei, E., Hauck, L.M., Izaurralde, R.C., Flowers, J.D., 2010. Invited review article: the agricultural policy/environmental extender (apex) model: an emerging tool for landscape and watershed environmental analyses. Transactions of the ASABE 53, 711–740. https://doi.org/10.13031/2013.30078.
Gaze, S.R., Stalham, M.A., Allen, E.J., 2002. Accuracy of the neutron probe for measuring changes in soil water storage under potatoes. J. Agric. Sci. 138, 135–152. https://doi.org/10.1017/S0021859601001654.
Goldhamer, D.A., Kjelgren, R.K., Beede, R.H., Williams, L.E., Moore, J.M., Lane, J., Weinberger, G., Menezes, J., Jr., 1985. Water use requirements of pistachio trees and response to water stress. Annual Report of the California Pistachio Commission, Crop Year 1984-1985, 85–92.
Goring, D.G., Nikora, V.I., 2002. Despiking acoustic doppler velocimeter data. J. Hydraul. Eng. 128, 117–126. https://doi.org/10.1061/(ASCE)0733-9429(2002)128:1(117).
Gould, K., Rudnick, J., 2018. Adoption of cover crops in california.
Gribov, A., Krivoruchko, K., 2020. Empirical bayesian kriging implementation and usage. Sci. Total Environ. 722, 137290. https://doi.org/10.1016/j.scitotenv.2020.137290.
Hao, X., Abou Najm, M., Steenwerth, K.L., Nocco, M.A., Basset, C., Daccache, A., 2023. Are there universal soil responses to cover cropping? a systematic review. Science of The Total Environment 861, 160600. https://doi.org/10.1016/j.scitotenv.2022.160600.
Haruna, S.I., Eichas, R.C., Peters, O.M., Farmer, A.C., Lackey, D.Q., Nichols, J.E., Peterson, W.H., Slone, N.A., 2022. In situ water infiltration: influence of cover crops after growth termination. Soil Science Soc of Amer J 86, 769–780. https://doi.org/10.1002/saj2.20390.

Iniesta, F., Testi, L., Goldhamer, D.A., Fereres, E., 2008. Quantifying reductions in consumptive water use under regulated deficit irrigation in pistachio (pistacia vera l.). Agricultural Water Management 95, 877–886. https://doi.org/10.1016/j.agwat.2008.01.013.

Irmak, A., Ratcliffe, I., Ranade, P., Hubbard, K.G., Singh, R.K., Kamble, B., Kjaersgaard, J., 2011. Estimation of land surface evapotranspiration with a satellite remote sensing procedure. Great Plains Research 21, 73–88.

Izaurralde, R.C., Williams, J.R., McGill, W.B., Rosenberg, N.J., Jakas, M.C.Q., 2006. Simulating soil c dynamics with epic: model description and testing against long-term data. Ecological Modelling 192, 362–384. https://doi.org/10.1016/j.ecolmodel.2005.07.010.

Jensen, M.E., Allen, R.G. (Eds.), 2016. Evaporation, evapotranspiration, and irrigation water requirements, Second. ed. American Society of Civil Engineers, Reston, VA. https://doi.org/10.1061/9780784414057.

Jin, Y., He, R., Marino, G., Whiting, M., Kent, E., Sanden, B.L., Culumber, M., Ferguson, L., Little, C., Grattan, S., Paw U, K.T., Lagos, L.O., Snyder, R.L., Zaccaria, D., 2018. Spatially variable evapotranspiration over salt affected pistachio orchards analyzed with satellite remote sensing estimates. Agricultural and Forest Meteorology 262, 178–191. https://doi.org/10.1016/j.agrformet.2018.07.004.

Joyce, B.A., Wallender, W.W., Mitchell, J.P., Huyck, L.M., Temple, S.R., Brostrom, P.N., Hsiao, T.C., 2002. Infiltration and soil water storage under winter cover cropping in span class="nocase">california's span class="nocase">sacramentovalley. Transactions of the ASAE 45. https://doi.org/10.13031/2013.8526.

Kader, M.A., Singha, A., Begum, M.A., Jewel, A., Khan, F.H., Khan, N.I., 2019. Mulching as water-saving technique in dryland agriculture: review article. Bull Natl Res Cent 43, 147. https://doi.org/10.1186/s42269-019-0186-7.

Kaimal, J.C., Finnigan, J.J., 1994. Atmospheric boundary layer flows: their structure and measurement. Oxford University Press, New York.

Kanber, R., Yazar, A., □Nder, S., K□ksal, H., 1993. Irrigation response of pistachio (pistacia vera l.). Irrig Sci 14. https://doi.org/10.1007/BF00195000.

Kandhway, A., Scarpare, F., Liu, M., Nelson, R., Adam, J.C., Anderson, R.G., Conklin, M.H., Safeeq, M., 2025. Water use dynamics of almond and pistachio crops in the mediterranean region amid climate change. Agric. Water Manage. 307, 109219. https://doi.org/10.1016/j.agwat.2024.109219.

Kermani, M.M., Salehi, F., 2006. Determination of pistachio crop evapotranspiration (etc). Acta Hortic. 441–448. https://doi.org/10.17660/ActaHortic.2006.726.71.

Kiniry, J.R., Williams, J.R., Gassman, P.W., Debaeke, P., 1992. A general, process-oriented model for two competing plant species. Transactions of the ASAE 35, 801–810. https://doi.org/10.13031/2013.28665.

Kljun, N., Calanca, P., Rotach, M.W., Schmid, H.P., 2015. A simple two-dimensional parameterisation for flux footprint prediction (ffp). Geosci. Model Dev. 8, 3695–3713. https://doi.org/10.5194/gmd-8-3695-2015.

Knipper, K., Anderson, M., Bambach, N., Kustas, W., Gao, F., Zahn, E., Hain, C., McElrone, A., Belfiore, O.R., Castro, S., Alsina, M.M., Saa, S., 2022. Evaluation of partitioned evaporation and transpiration estimates within the disalexi modeling framework over irrigated crops in california. Remote Sensing 15, 68. https://doi.org/10.3390/rs15010068.

Knipper, K., Anderson, M., Bambach, N., Melton, F., Ellis, Z., Yang, Y., Volk, J., McElrone, A.J., Kustas, W., Roby, M., Carrara, W., Castro, S., Kilic, A., Fisher, J.B., Ruhoff, A., Senay, G.B., Morton, C., Saa, S., Allen, R.G., 2024. A comparative analysis of openet for evaluating evapotranspiration in california almond orchards. Agricultural and Forest Meteorology 355, 110146. https://doi.org/10.1016/j.agrformet.2024.110146.

Koudahe, K., Allen, S.C., Djaman, K., 2022. Critical review of the impact of cover crops on soil properties. International Soil and Water Conservation Research 10, 343–354. https://doi.org/10.1016/j.iswcr.2022.03.003.

Krivoruchko, K., Gribov, A., 2019. Evaluation of empirical bayesian kriging. Spatial Statistics 32, 100368. https://doi.org/10.1016/j.spasta.2019.100368.

Laipelt, L., Henrique Bloedow Kayser, R., Santos Fleischmann, A., Ruhoff, A., Bastiaanssen, W., Erickson, T.A., Melton, F., 2021. Long-term monitoring of evapotranspiration using the sebal algorithm and google earth engine cloud computing. ISPRS Journal of Photogrammetry and Remote Sensing 178, 81–96. https://doi.org/10.1016/j.isprsjprs.2021.05.018.

Leys, C., Ley, C., Klein, O., Bernard, P., Licata, L., 2013. Detecting outliers: do not use standard deviation around the mean, use absolute deviation around the median. Journal of Experimental Social Psychology 49, 764–766. https://doi.org/10.1016/j.jesp.2013.03.013.

Lobell, D.B., Field, C.B., Cahill, K.N., Bonfils, C., 2006. Impacts of future climate change on california perennial crop yields: model projections with climate and crop uncertainties. Agricultural and Forest Meteorology 141, 208–218. https://doi.org/10.1016/j.agrformet.2006.10.006.

Lu, Y.C., Watkins, K.B., Teasdale, J.R., Abdul-Baki, A.A., 2000. Cover crops in sustainable food production. Food Reviews International 16, 121–157. https://doi.org/10.1081/FRI-100100285.

Lubell, M., Blomquist, W., Beutler, L., 2020. Sustainable groundwater management in california: a grand experiment in environmental governance. Society & Natural Resources 33, 1447–1467. https://doi.org/10.1080/08941920.2020.1833617.

Mall, N.K., Herman, J.D., 2019. Water shortage risks from perennial crop expansion in california's central valley. Environ. Res. Lett. 14, 104014. https://doi.org/10.1088/1748-9326/ab4035.

Marino, G., Zaccaria, D., Lagos, L.O., Souto, C., Kent, E.R., Grattan, S.R., Shapiro, K., Sanden, B.L., Snyder, R.L., 2021. Effects of salinity and sodicity on the seasonal dynamics of actual evapotranspiration and surface energy balance components in mature micro-irrigated pistachio orchards. Irrig Sci 39, 23–43. https://doi.org/10.1007/s00271-020-00694-z.

Marino, G., Zaccaria, D., Snyder, R.L., Lagos, O., Lampinen, B.D., Ferguson, L., Grattan, S.R., Little, C., Shapiro, K., Maskey, M.L., Corwin, D.L., Scudiero, E., Sanden, B.L., 2019. Actual evapotranspiration and tree performance of mature micro-irrigated pistachio orchards grown on saline-sodic soils in the san joaquin valley of california. Agriculture 9, 76. https://doi.org/10.3390/agriculture9040076.

Mason, R., Gorres, J., Faulkner, J.W., Doro, L., Merrill, S.C., 2020. Calibrating the apex model for simulations of environmental and agronomic outcomes on dairy farms in the northeast u.s.: a step-by-step example. Applied Engineering in Agriculture 36, 281–301. https://doi.org/10.13031/aea.13679.

Massman, W.J., 2000. A simple method for estimating frequency response corrections for eddy covariance systems. Agricultural and Forest Meteorology 104, 185–198. https://doi.org/10.1016/S0168-1923(00)00164-7.

Melton, F.S., Huntington, J., Grimm, R., Herring, J., Hall, M., Rollison, D., Erickson, T., Allen, R., Anderson, M., Fisher, J.B., Kilic, A., Senay, G.B., Volk, J., Hain, C., Johnson, L., Ruhoff, A., Blankenau, P., Bromley, M., Carrara, W., Daudert, B., Doherty, C., Dunkerly, C., Friedrichs, M., Guzman, A., Halverson, G., Hansen, J., Harding, J., Kang, Y., Ketchum, D., Minor, B., Morton, C., Ortega-Salazar, S., Ott, T., Ozdogan, M., ReVelle, P.M., Schull, M., Wang, C., Yang, Y., Anderson, R.G., 2022. OpenET: filling a critical data gap in water management for the western united states. J American Water Resour Assoc 58, 971–994. https://doi.org/10.1111/1752-1688.12956.

Melton, F.S., Johnson, L.F., Lund, C.P., Pierce, L.L., Michaelis, A.R., Hiatt, S.H., Guzman, A., Adhikari, D.D., Purdy, A.J., Rosevelt, C., Votava, P., Trout, T.J., Temesgen, B., Frame, K., Sheffner, E.J., Nemani, R.R., 2012. Satellite irrigation management support with the terrestrial observation and prediction system: a framework for integration of satellite and surface observations to support improvements in agricultural water resource management. IEEE J. Sel. Top. Appl. Earth Observations Remote Sensing 5, 1709–1721. https://doi.org/10.1109/JSTARS.2012.2214474.

Mitchell, J.P., Peters, D.W., Shennan, C., 1999. Changes in soil water storage in winter fallowed and cover cropped soils. J. Sustain. Agric. 15, 19–31. https://doi.org/10.1300/J064v15n02_04.

Mitchell, J.P., Shrestha, A., Irmak, S., 2015. Trade-offs between winter cover crop production and soil water depletion in the San Joaquin valley, California. J. Soil Water Conserv. 70, 430–440. https://doi.org/10.2489/jswc.70.6.430.

Monteith, J.L., 1965. Evaporation and environment. Symposia of the Society for Experimental Biology 19, 205–234.

Moore, C.J., 1986. Frequency response corrections for eddy correlation systems. Boundary-Layer Meteorol 37, 17–35. https://doi.org/10.1007/BF00122754.

Moore, E.A., Norton, U., 2024. Improving semi-arid agroecosystem services with cover crop mixes. PLoS ONE 19, e0306567. https://doi.org/10.1371/journal.pone.0306567.

Moriasi, D.N., Arnold, J.G., Liew, M.W.V., Bingner, R.L., Harmel, R.D., Veith, T.L., 2007. Model evaluation guidelines for systematic quantification of accuracy in watershed simulations. Transactions of the ASABE 50, 885–900. https://doi.org/10.13031/2013.23153.

Moriasi, D.N., King, K.W., Bosch, D.D., Bjorneberg, D.L., Teet, S., Guzman, J.A., Williams, M.R., 2016. Framework to parameterize and validate apex to support deployment of the nutrient tracking tool. Agric. Water Manage. 177, 146–164. https://doi.org/10.1016/j.agwat.2016.07.009.

Munna, M.N.H., Lal, R., 2025. Impacts of cover cropping and organic amendments on soil physical quality under temperate climate. Cogent Food & Agriculture 11, 2467452. https://doi.org/10.1080/23311932.2025.2467452.

Nash, J.E., Sutcliffe, J.V., 1970. River flow forecasting through conceptual models part i — a discussion of principles. Journal of Hydrology 10, 282–290. https://doi.org/10.1016/0022-1694(70)90255-6.

Nielsen, D.C., Lyon, D.J., Hergert, G.W., Higgins, R.K., Calderón, F.J., Vigil, M.F., 2015. Cover crop mixtures do not use water differently than single-species plantings. Agron. J. 107, 1025–1038. https://doi.org/10.2134/agronj14.0504.

Oregon State University, 2010. Peas - Western Oregon. https://horticulture.oregonstate.edu/oregon-vegetables/peas-western-oregon-0 (accessed 9 May 2026).

Papale, D., Reichstein, M., Aubinet, M., Canfora, E., Bernhofer, C., Kutsch, W., Longdoz, B., Rambal, S., Valentini, R., Vesala, T., Yakir, D., 2006. Towards a standardized processing of net ecosystem exchange measured with eddy covariance technique: algorithms and uncertainty estimation. Biogeosciences 3, 571–583. https://doi.org/10.5194/bg-3-571-2006.

Pastorello, G., Trotta, C., Canfora, E., Chu, H., Christianson, D., Cheah, Y.-W., Poindexter, C., Chen, J., Elbashandy, A., Humphrey, M., Isaac, P., Polidori, D., Reichstein, M., Ribeca, A., Van Ingen, C., Vuichard, N., Zhang, L., Amiro, B., Ammann, C., Arain, M.A., Ardö, J., Arkebauer, T., Arndt, S.K., Arriga, N., Aubinet, M., Aurela, M., Baldocchi, D., Barr, A., Beamesderfer, E., Marchesini, L.B., Bergeron, O., Beringer, J., Bernhofer, C., Berveiller, D., Billesbach, D., Black, T.A., Blanken, P.D., Bohrer, G., Boike, J., Bolstad, P.V., Bonal, D., Bonnefond, J.-M., Bowling, D.R., Bracho, R., Brodeur, J., Brümmer, C., Buchmann, N., Burban, B., Burns, S.P., Buysse, P., Cale, P., Cavagna, M., Cellier, P., Chen, S., Chini, I., Christensen, T.R., Cleverly, J., Collalti, A., Consalvo, C., Cook, B.D., Cook, D., Coursolle, C., Cremonese, E., Curtis, P.S., D'Andrea, E., Da Rocha, H., Dai, X., Davis, K.J., Cinti, B.D., Grandcourt, A.D., Ligne, A.D., De Oliveira, R.C., Delpierre, N., Desai, A.R., Di Bella, C.M., Tommasi, P.D., Dolman, H., Domingo, F., Dong, G., Dore, S., Duce, P., Dufrêne, E., Dunn, A., Dušek, J., Eamus, D., Eichelmann, U., ElKhidir, H.A.M., Eugster, W., Ewenz, C.M., Ewers, B., Famulari, D., Fares, S., Feigenwinter, I., Feitz, A., Fensholt, R., Filippa, G., Fischer, M., Frank, J., Galvagno, M., Gharun, M., Gianelle, D., Gielen, B., Gioli, B., Gitelson, A., Goded, I., Goeckede, M., Goldstein, A.H., Gough, C.M., Goulden, M.L., Graf, A., Griebel, A., Gruening, C., Grünwald, T., Hammerle, A., Han, S., Han, X., Hansen, B.U., Hanson, C., Hatakka, J., He, Y., Hehn, M., Heinesch, B., Hinko-Najera, N., Hörtnagl, L., Hutley, L., Ibrom, A., Ikawa, H., Jackowicz-Korczynski, M., Janouš, D., Jans, W., Jassal, R., Jiang, S., Kato, T., Khomik, M., Klatt, J., Knohl, A., Knox, S., Kobayashi, H., Koerber, G., Kolle, O., Kosugi, Y., Kotani, A., Kowalski, A., Kruijt, B., Kurbatova, J., Kutsch, W.L., Kwon, H., Launiainen, S., Laurila, T., Law, B., Leuning, R., Li, Yingnian, Liddell, M., Limousin, J.-M., Lion, M., Liska, A.J., Lohila, A., López-Ballesteros, A., López-Blanco, E., Loubet, B., Loustau, D., Lucas-Moffat, A., Lüers, J., Ma, S., Macfarlane, C., Magliulo, V., Maier, R., Mammarella, I., Manca, G., Marcolla, B., Margolis, H.A., Marras, S., Massman, W., Mastepanov, M., Matamala, R., Matthes, J.H., Mazzenga, F., McCaughey, H., McHugh, I., McMillan, A.M.S., Merbold, L., Meyer, W., Meyers, T., Miller, S.D., Minerbi, S., Moderow, U., Monson, R.K., Montagnani, L., Moore, C.E., Moors, E., Moreaux, V., Moureaux, C., Munger, J.W., Nakai, T., Neirynck, J., Nesic, Z., Nicolini, G., Noormets, A., Northwood, M., Nosetto, M., Nouvellon, Y., Novick, K., Oechel, W., Olesen, J.E., Ourcival, J.-M., Papuga, S.A., Parmentier, F.-J., Paul-Limoges, E., Pavelka, M., Peichl, M., Pendall, E., Phillips, R.P., Pilegaard, K., Pirk, N., Posse, G., Powell, T., Prasse, H., Prober, S.M., Rambal, S., Rannik, Ü., Raz-Yaseef, N., Rebmann, C., Reed, D., Dios, V.R.D., Restrepo-Coupe, N., Reverter, B.R., Roland, M., Sabbatini, S., Sachs, T.,

Saleska, S.R., Sánchez-Cañete, E.P., Sanchez-Mejia, Z.M., Schmid, H.P., Schmidt, M., Schneider, K., Schrader, F., Schroder, I., Scott, R.L., Sedlák, P., Serrano-Ortíz, P., Shao, C., Shi, P., Shironya, I., Siebicke, L., Šigut, L., Silberstein, R., Sirca, C., Spano, D., Steinbrecher, R., Stevens, R.M., Sturtevant, C., Suyker, A., Tagesson, T., Takanashi, S., Tang, Y., Tapper, N., Thom, J., Tomassucci, M., Tuovinen, J.-P., Urbanski, S., Valentini, R., Van Der Molen, M., Van Gorsel, E., Van Huissteden, K., Varlagin, A., Verfaillie, J., Vesala, T., Vincke, C., Vitale, D., Vygodskaya, N., Walker, J.P., Walter-Shea, E., Wang, H., Weber, R., Westermann, S., Wille, C., Wofsy, S., Wohlfahrt, G., Wolf, S., Woodgate, W., Li, Yuelin, Zampedri, R., Zhang, J., Zhou, G., Zona, D., Agarwal, D., Biraud, S., Torn, M., Papale, D., 2020. The fluxnet2015 dataset and the oneflux processing pipeline for eddy covariance data. Sci Data 7, 225. https://doi.org/10.1038/s41597-020-0534-3.

Pathak, T., Maskey, M., Dahlberg, J., Kearns, F., Bali, K., Zaccaria, D., 2018. Climate change trends and impacts on California agriculture: a detailed review. Agronom. 8, 25. https://doi.org/10.3390/agronomy8030025.

Peddinti, S.R., 2026. Flux gap filling tool: mds and ml gap-filling for micrometeorological data.

Pereira, L.S., Paredes, P., Melton, F., Johnson, L., Wang, T., López-Urrea, R., Cancela, J.J., Allen, R.G., 2020. Prediction of crop coefficients from fraction of ground cover and height. background and validation using ground and remote sensing data. Agricultural Water Management 241, 106197. https://doi.org/10.1016/j.agwat.2020.106197.

Pruitt, W.O., Doorenbos, J., 1977. Empirical calibration, a requisite for evapotranspiration formulae based on daily or longer mean climatic data? Presented at the International Commission on Irrigation and Drainage.

Rahemi, M., Pakkish, Z., 2009. Determination of chilling and heat requirements of pistachio (pistacia vera l.) cultivars. Agricultural Sciences in China 8, 803–807. https://doi.org/10.1016/S1671-2927(08)60281-3.

Rahimzadegan, M., Janani, A., 2019. Estimating evapotranspiration of pistachio crop based on sebal algorithm using landsat 8 satellite imagery. Agric. Water Manag. 217, 383–390. https://doi.org/10.1016/j.agwat.2019.03.018.

Reichstein, M., Falge, E., Baldocchi, D., Papale, D., Aubinet, M., Berbigier, P., Bernhofer, C., Buchmann, N., Gilmanov, T., Granier, A., Grünwald, T., Havránková, K., Ilvesniemi, H., Janous, D., Knohl, A., Laurila, T., Lohila, A., Loustau, D., Matteucci, G., Meyers, T., Miglietta, F., Ourcival, J., Pumpanen, J., Rambal, S., Rotenberg, E., Sanz, M., Tenhunen, J., Seufert, G., Vaccari, F., Vesala, T., Yakir, D., Valentini, R., 2005. On the separation of net ecosystem exchange into assimilation and ecosystem respiration: review and improved algorithm. Global Change Biology 11, 1424–1439. https://doi.org/10.1111/j.1365-2486.2005.001002.x.

Sabiston, L., Sabie, R., Buenemann, M., Stringam, B., Fernald, A., 2024. Comparing field-scale eddy covariance measurements and crop coefficient estimates of alfalfa evapotranspiration to openet model estimates and exploring water budget implications in a dryland environment. Irrig Sci. https://doi.org/10.1007/s00271-024-00941-7.

Sainju, U.M., Singh, B.P., 1997. Winter cover crops for sustainable agricultural systems: influence on soil properties, water quality, and crop yields. HortSci 32, 21–28. https://doi.org/10.21273/HORTSCI.32.1.21.

Saleh, A., Niraula, R., Marek, G.W., Gowda, P.H., Brauer, D.K., Howell, T.A., 2018. Lysimetric evaluation of the apex model to simulate daily et for irrigated crops in the texas high plains. Transactions of the ASABE 61, 65–74. https://doi.org/10.13031/trans.11938.

Sanden, B.L., Ferguson, L., Reyes, H.C., Grattan, S.R., 2004. Effect of salinity on evapotranspiration and yield of san joaquin valley pistachios. Acta Hortic. 583–589. https://doi.org/10.17660/ActaHortic.2004.664.73.

Sastre, B., Marques, M.J., García-Díaz, A., Bienes, R., 2018. Three years of management with cover crops protecting sloping olive groves soils, carbon and water effects on gypsiferous soil. CATENA 171, 115–124. https://doi.org/10.1016/j.catena.2018.07.003.

Schomberg, H.H., White, K.E., Thompson, A.I., Bagley, G.A., Burke, A., Garst, G., Bybee-Finley, K.A., Mirsky, S.B., 2023. Interseeded cover crop mixtures influence soil water storage during the corn phase of corn-soybean-wheat no-till cropping systems. Agricultural Water Management 278, 108167. https://doi.org/10.1016/j.agwat.2023.108167.

Senay, G.B., 2018. Satellite psychrometric formulation of the operational simplified surface energy balance (ssebop) model for quantifying and mapping evapotranspiration. Applied Engineering in Agriculture 34, 555–566. https://doi.org/10.13031/aea.12614.

Senay, G.B., Bohms, S., Singh, R.K., Gowda, P.H., Velpuri, N.M., Alemu, H., Verdin, J.P., 2013. Operational evapotranspiration mapping using remote sensing and weather datasets: a new parameterization for the SSEB approach. J. American Water Resour. Assoc. 49, 577–591. https://doi.org/10.1111/jawr.12057.

Senay, G.B., Parrish, G.E.L., Schauer, M., Friedrichs, M., Khand, K., Boiko, O., Kagone, S., Dittmeier, R., Arab, S., Ji, L., 2023. Improving the operational simplified surface energy balance evapotranspiration model using the forcing and normalizing operation. Remote Sensing 15, 260. https://doi.org/10.3390/rs15010260.

Snapp, S.S., Swinton, S.M., Labarta, R., Mutch, D., Black, J.R., Leep, R., Nyiraneza, J., O'Neil, K., 2005. Evaluating cover crops for benefits, costs and performance within cropping system niches. Agron. J. 97, 322–332. https://doi.org/10.2134/agronj2005.0322a.

Soil Health Institute, 2019. Progress report: adoption of soil health systems based on data from the 2017 U.S. census of agriculture. https://soilhealthinstitute.org/app/uploads/2022/01/Soil-Health-Adoption-Overview_2017-Census-Report_FINAL.pdf (accessed 30 October 2024).

Steele, M.K., Coale, F.J., Hill, R.L., 2012. Winter annual cover crop impacts on no-till soil physical properties and organic matter. Soil Science Soc of Amer J 76, 2164–2173. https://doi.org/10.2136/sssaj2012.0008.

Steglich, E.M., Osorio, J., Doro, L., Jeong, J., Williams, J.R., 2023. Agricultural policy/environmental extender user's manual version 1501.

Tadesse, H.K., Moriasi, D.N., Gowda, P.H., Marek, G., Steiner, J.L., Brauer, D., Talebizadeh, M., Nelson, A., Starks, P., 2018. Evaluating evapotranspiration estimation methods in apex model for dryland cropping systems in a semi-arid region. Agricultural Water Management 206, 217–228. https://doi.org/10.1016/j.agwat.2018.04.007.

Tadesse, H.K., Moriasi, D.N., Gowda, P.H., Steiner, J.L., Talebizadeh, M., Nelson, A.M., Starks, P.J., Marek, G., 2019. Comparison of evapotranspiration simulation performance by apex model in dryland and irrigated cropping systems. J American Water Resour Assoc 55, 1009–1023. https://doi.org/10.1111/1752-1688.12759.

Tadesse, H.K., Moriasi, D.N., Gowda, P.H., Wagle, P., Starks, P.J., Steiner, J.L., Talebizadeh, M., Neel, J.P.S., Nelson, A.M., 2021. Comparison of evapotranspiration and biomass simulation in winter wheat under conventional and conservation tillage systems using

apex model. Ecohydrology & Hydrobiology 21, 55–66. https://doi.org/10.1016/j.ecohyd.2020.08.003.
Talebizadeh, M., Moriasi, D., Gowda, P., Steiner, J.L., Tadesse, H.K., Nelson, A.M., Starks, P., 2018. Simultaneous calibration of evapotranspiration and crop yield in agronomic system modeling using the apex model. Agricultural Water Management 208, 299–306. https://doi.org/10.1016/j.agwat.2018.06.043.
Tawalbeh, Z.M., Bawazir, A.S., Fernald, A., Sabie, R., Heerema, R.J., 2024. Assessing satellite-derived openet platform evapotranspiration of mature pecan orchard in the mesilla valley, new mexico. Remote Sensing 16, 1429. https://doi.org/10.3390/rs16081429.
Teasdale, J.R., Mohler, C.L., 1993. Light transmittance, soil temperature, and soil moisture under residue of hairy vetch and rye. Agronomy Journal 85, 673–680. https://doi.org/10.2134/agronj1993.00021962008500030029x.
Timlin, D., Chun, J.A., Meisinger, J., Kang, K., Fleisher, D., Staver, K., Doherty, C., Russ, A., 2019. Evaluation of the agricultural policy environmental extender (apex) for the chesapeake bay watershed. Agricultural Water Management 221, 477–485. https://doi.org/10.1016/j.agwat.2019.03.046.
Tootelian, D.H., 2023a. Projected pistachio production: 2023 through 2031.
Tootelian, D.H., 2023b. Projected pistachio production: 2023 through 2031.
Unger, P.W., Vigil, M.F., 1998. Cover crop effects on soil water relationships. Journal of Soil and Water Conservation.
United Nations University Institute for Water, Environment and Health (UNU INWEH), Madani, K., 2026. Global water bankruptcy: living beyond our hydrological means in the post crisis era. United Nations University Institute for Water, Environment and Health (UNU INWEH). https://doi.org/10.53328/INR26KAM001.
United States Department of Agriculture (USDA), 2026. Pistachios. https://www.fas.usda.gov/data/production/commodity/0577907 (accessed 13 January 2026).
Vanella, D., Peddinti, S.R., Kisekka, I., 2022. Unravelling soil water dynamics in almond orchards characterized by soil-heterogeneity using electrical resistivity tomography. Agricultural Water Management 269, 107652. https://doi.org/10.1016/j.agwat.2022.107652.
Vendig, I., Guzman, A., De La Cerda, G., Esquivel, K., Mayer, A.C., Ponisio, L., Bowles, T.M., 2023. Quantifying direct yield benefits of soil carbon increases from cover cropping. Nat Sustain 6, 1125–1134. https://doi.org/10.1038/s41893-023-01131-7.
Volk, J.M., Huntington, J.L., Melton, F.S., Allen, R., Anderson, M., Fisher, J.B., Kilic, A., Ruhoff, A., Senay, G.B., Minor, B., Morton, C., Ott, T., Johnson, L., Comini De Andrade, B., Carrara, W., Doherty, C.T., Dunkerly, C., Friedrichs, M., Guzman, A., Hain, C., Halverson, G., Kang, Y., Knipper, K., Laipelt, L., Ortega-Salazar, S., Pearson, C., Parrish, G.E.L., Purdy, A., ReVelle, P., Wang, T., Yang, Y., 2024. Assessing the accuracy of openet satellite-based evapotranspiration data to support water resource and land management applications. Nat Water 2, 193–205. https://doi.org/10.1038/s44221-023-00181-7.
Vukicevich, E., Lowery, T., Bowen, P., Úrbez-Torres, J.R., Hart, M., 2016. Cover crops to increase soil microbial diversity and mitigate decline in perennial agriculture. a review. Agron. Sustain. Dev. 36, 48. https://doi.org/10.1007/s13593-016-0385-7.

Wang, J., Zhang, S., Sainju, U.M., Ghimire, R., Zhao, F., 2021. A meta-analysis on cover crop impact on soil water storage, succeeding crop yield, and water-use efficiency. Agricultural Water Management 256, 107085. https://doi.org/10.1016/j.agwat.2021.107085.

Wang, X., Jeong, J., 2019. APEX-cute 4 user manual.

Wang, X., Williams, J.R., Gassman, P.W., Baffaut, C., Izaurralde, R.C., Jeong, J., Kiniry, J.R., 2012. EPIC and apex: model use, calibration, and validation. Transactions of the ASABE 55, 1447–1462. https://doi.org/10.13031/2013.42253.

Ward, P.R., Dunin, F.X., Micin, S.F., Williamson, D.R., 1998. Evaluating drainage responses in duplex soils in a mediterranean environment. Australian Journal of Soil Research 36, 509–524. https://doi.org/10.1071/S97082.

Ward, P.R., Flower, K.C., Cordingley, N., Weeks, C., Micin, S.F., 2012. Soil water balance with cover crops and conservation agriculture in a mediterranean climate. Field Crops Research 132, 33–39. https://doi.org/10.1016/j.fcr.2011.10.017.

Webb, E.K., Pearman, G.I., Leuning, R., 1980. Correction of flux measurements for density effects due to heat and water vapour transfer. Quart J Royal Meteoro Soc 106, 85–100. https://doi.org/10.1002/qj.49710644707.

Westling, F., Underwood, J., Örn, S., 2018. Light interception modelling using unstructured lidar data in avocado orchards. Computers and Electronics in Agriculture 153, 177–187. https://doi.org/10.1016/j.compag.2018.08.020.

Williams, J.R., Izaurralde, R.C., Williams, C., Steglich, E.M., 2023. Agricultural policy / environmental extender model theoretical documentation version 1501.

Wilson, K., Goldstein, A., Falge, E., Aubinet, M., Baldocchi, D., Berbigier, P., Bernhofer, C., Ceulemans, R., Dolman, H., Field, C., Grelle, A., Ibrom, A., Law, B.E., Kowalski, A., Meyers, T., Moncrieff, J., Monson, R., Oechel, W., Tenhunen, J., Valentini, R., Verma, S., 2002. Energy balance closure at fluxnet sites. Agricultural and Forest Meteorology 113, 223–243. https://doi.org/10.1016/S0168-1923(02)00109-0.

Wutzler, T., Lucas-Moffat, A., Migliavacca, M., Knauer, J., Sickel, K., Šigut, L., Menzer, O., Reichstein, M., 2018. Basic and extensible post-processing of eddy covariance flux data with reddyproc. Biogeosciences 15, 5015–5030. https://doi.org/10.5194/bg-15-5015-2018.

Wyland, L., 1996. Winter cover crops in a vegetable cropping system: impacts on nitrate leaching, soil water, crop yield, pests and management costs. Agriculture, Ecosystems & Environment 59, 1–17. https://doi.org/10.1016/0167-8809(96)01048-1.

Yang, W., Feng, G., Read, J.J., Ouyang, Y., Han, J., Li, P., 2020. Impact of cover crop on corn–soybean productivity and soil water dynamics under different seasonal rainfall patterns. Agronomy Journal 112, 1201–1215. https://doi.org/10.1002/agj2.20110.

Yost, J.L., Huang, J., Hartemink, A.E., 2019. Spatial-temporal analysis of soil water storage and deep drainage under irrigated potatoes in the central sands of wisconsin, usa. Agricultural Water Management 217, 226–235. https://doi.org/10.1016/j.agwat.2019.02.045.

Zaccaria, D., 2023. Updated information on water use and water productivity of pistachio grown on non-saline and salt-affected soils. Statewide Pistachio Day, Visalia Convention Center, Visalia, CA.

Zhang, J., Ranford, T., Taylor, C., 2015. Heat model for pistachio bloom and harvest. Scientia Horticulturae 186, 47–53. https://doi.org/10.1016/j.scienta.2015.02.005.

Zhang, J., Taylor, C., 2011. The dynamic model provides the best description of the chill process on ‘sirora’ pistachio trees in australia. horts 46, 420–425. https://doi.org/10.21273/HORTSCI.46.3.420.

Chapter 4: Concluding remarks

This dissertation set out to evaluate the soil water, evapotranspiration, and grower perceived consequences of winter cover cropping in California pistachio orchards under the operational and regulatory pressures of the Sustainable Groundwater Management Act (SGMA) and a changing climate. It approached that question along a single observation–detection–projection arc (Figure 4.1): a multi-year field campaign that measured what cover crops (CC) do to the orchard water balance (Chapter 1), an evaluation of whether the satellite tools used for SGMA water accounting can actually see those effects (Chapter 2), and a grower-anchored, process-based projection of how the effects persist under a changing climate (Chapter 3). The three studies share one experimental backbone, the paired CC and no cover (NC) orchards, so that each builds directly on the measurements and findings of the one before it rather than standing as an independent result.

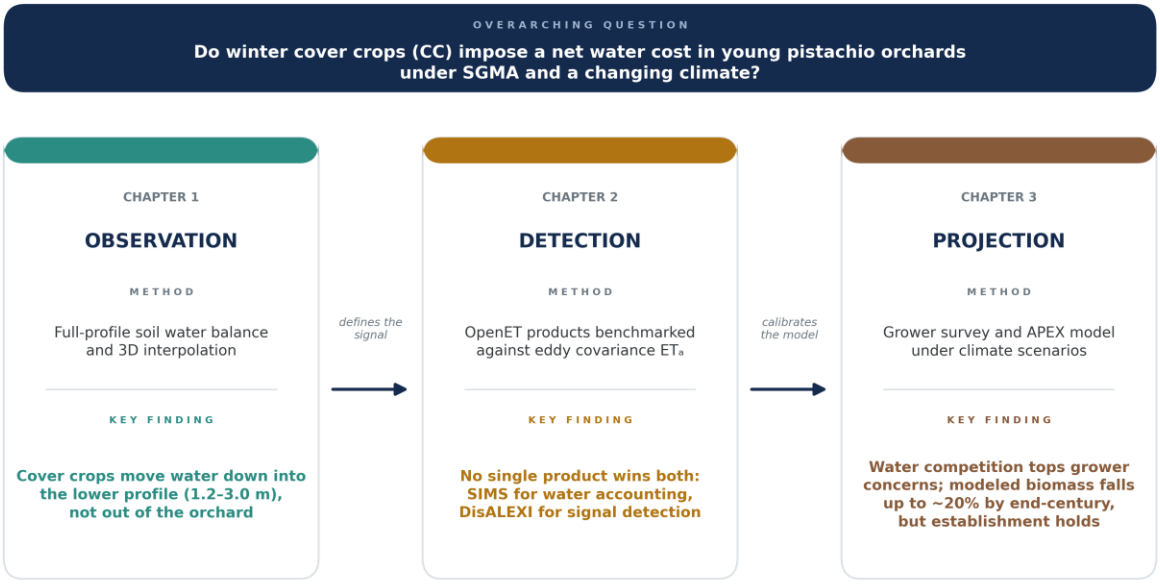


Figure 1 The dissertation as a single observation–detection–projection arc. Field observation (Chapter 1) establishes where cover crop water goes, remote sensing (Chapter 2) determines which tools can track it, and process-based

modeling (Chapter 3) projects its persistence under a changing climate, on one shared paired cover crop (CC) and no cover (NC) orchard instrumented with eddy covariance.

Briefly, the three studies established the following. Chapter 1 showed that the soil water cost of winter cover cropping in young pistachio is mischaracterized by the shallow (0 to 1.2 m), endpoint-based design carried over from the annual cropping literature: CC increased winter ET_a by 15 to 30 mm and dried the upper (0 to 1.2 m) profile, but redistributed that water downward into the lower (1.2 to 3.0 m) profile (8 to 17 percent wetter under the CC in every season) rather than removing it from the orchard. Post-termination mulch also lowered summer ET_a by 32 to 76 mm and interval-based deep percolation (*DP*) exceeded endpoint estimates by 1.3 to 7.7 times. Chapter 2 showed that no single OpenET product serves both SGMA use cases: SIMS gave the lowest monthly error (19 versus 23 mm per month for the Ensemble) for volumetric accounting, whereas DisALEXI most reliably recovered the CC signal (six of six seasons versus five of six for SIMS), and eddy covariance actual crop coefficients (K_a) rose from 0.57 to 0.95 between the fifth and seventh leaf. Chapter 3 coupled an IRB-approved grower survey to an APEX model calibrated on the same orchards and projected CC performance under climate scenarios built from the concerns growers themselves raised.

The connective thread among the three studies is that the physical behavior documented in Chapter 1 sets the terms for everything that follows. Because CC move water down the soil profile rather than out of the orchard, the quantity a RSET model must resolve in Chapter 2 is not a simple loss but a redistribution whose surface expression is muted: the deep storage gain that dominates the Chapter 1 water balance is, by construction, largely invisible to sensors that infer ET_a from canopy temperature and greenness. This is one reason the product that best reproduces absolute ET is not the product that best detects the treatment difference, and it is why the Chapter 2 recommendation is framed around the use case rather than a single accuracy ranking. The same

logic carries into Chapter 3: an APEX model asked to project CC water effects must first reproduce the full-profile partitioning measured in Chapter 1, which is why it was calibrated not only to ET_a but also to soil water through the 3.0 m profile, leaf area index (LAI), Cover crop biomass, and pistachio yield.

A second thread is temporal. The seasonal structure of the CC effect, evapotranspiration elevated from late winter through early spring, near zero by late May, and reversing sign through summer as pistachio canopy demand overtakes residue evaporation, appears in all three chapters: as the monthly ET_a difference in Chapter 1, as the bi-monthly K_a divergence in Chapter 2, and as the within-year dynamics the model must capture in Chapter 3. None of these structures survives reduction to a single annual mean, which is the form in which CC water costs are most often reported and most often misjudged. Taken together, the chapters describe one SGMA accounting problem viewed at three scales: the depth and interval of field monitoring (Chapter 1), the choice of satellite model used to scale that accounting to the basin (Chapter 2), and the projection of long-term performance under climate change and grower behavior (Chapter 3). The unifying conclusion is that monitoring depth, accounting interval, RSET model, and projection framework should each be matched to the management question being asked.

The experimental design has limitations that point to its natural extensions. The field measurement campaign was conducted at a single orchard with a specific CC species mix, and the transferability of the resulting full-profile findings to the more saline and more arid soils of the southern San Joaquin Valley, where the bulk of California's pistachio acreage is in fact concentrated, has not been established. The RSET validation was conducted in young (fifth- to seventh-leaf) trees, and the relative performance of SIMS and DisALEXI may shift as the orchard reaches the mature canopy structure. A coordinated multi-site campaign, instrumented at

one orchard per major pistachio producing county and paired by management treatment where possible, would expand the confidence of these results.

Pistachio acreage in California is projected to grow by approximately 47 percent between 2023 and 2031, concentrating future water demand in basins that are simultaneously subject to mandatory groundwater allocations under SGMA. The questions this dissertation has addressed, how CC alter the orchard water balance, whether the RSET models that account for that water under SGMA can resolve the relevant treatment-scale signals, and how grower perspectives and a changing climate should shape the projected long-term performance of orchard floor management, are not specialized methodological questions. They are central to the operating conditions of an industry that already represents a billion-dollar share of California's agricultural economy and that will be making CC decisions on hundreds of thousands of acres over the next decade. The integrated picture developed here is offered to support those decisions with evidence that is both technically defensible and practitioner-relevant.

Appendices

1. Support Materials for Chapter 1

1.1 Empirical Bayesian Kriging (EBK)

Empirical Bayesian Kriging (EBK) integrates Bayesian statistics with kriging to estimate values at unmeasured locations based on observed data. The method accounts for measurement errors and applies a Gaussian process transformation using Equation SS1:

$$z_i = t^{-1}(y_i|\Theta) = t^{-1}(y(s_i) + \epsilon_i|\Theta)\ , i = \overline{1 \dots K} \quad \text{(S1)}$$

where z_i is the measured value at the observed location s_i, $y_i = y(s_i) + \epsilon_i$ is the transformed measured value, $y(s)$ is the transformed Gaussian process under study at location s, ϵ_i is the normally distributed measurement error of the transformed z_i with mean zero, $t(\bullet \mid \Theta)$ is a transformation to Gaussian process, Θ are the parameters describing the process, and K is the number of measurements (Gribov and Krivoruchko, 2020).

1.2 Neutron probe

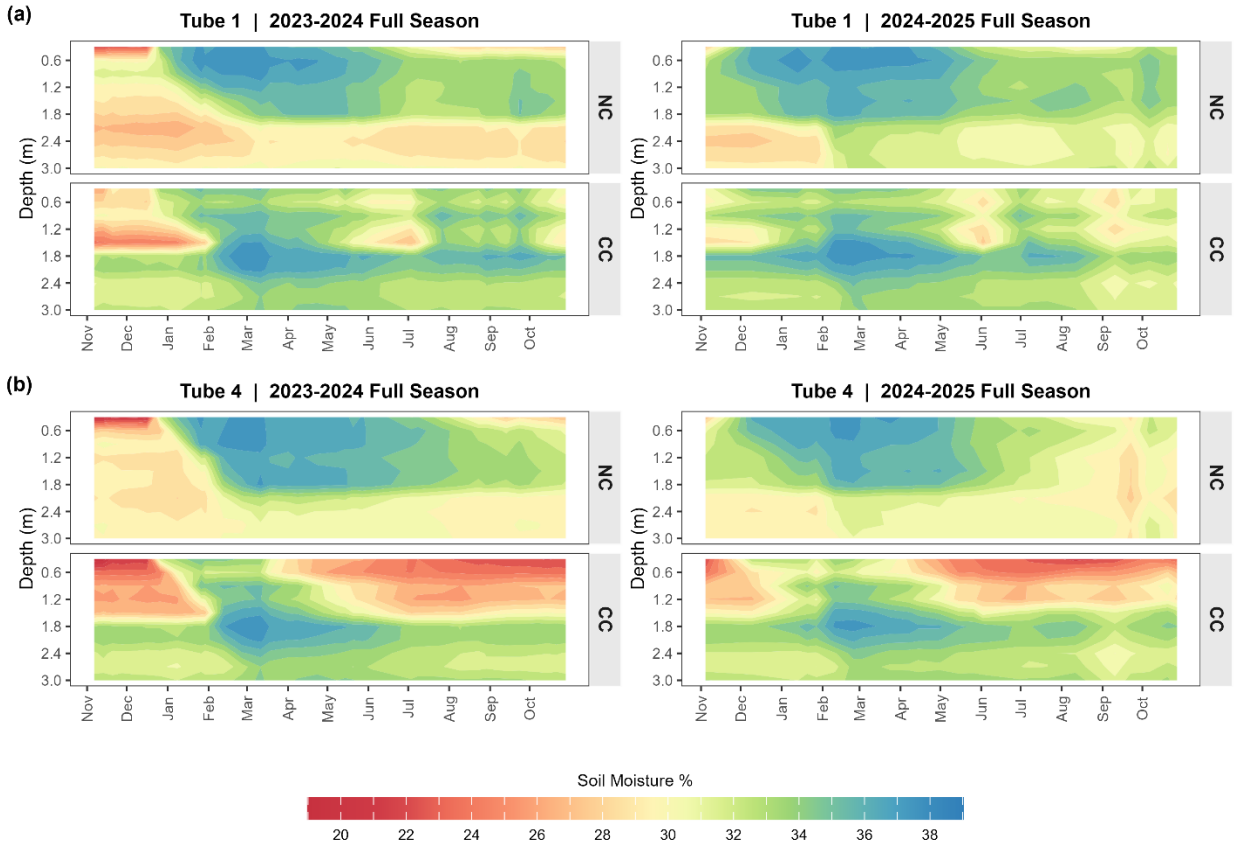


Figure S1. Full season (November to April) full-profile (0.3-3.0 m) soil moisture for the cover crop (CC) and no cover crop (NC) treatments for 2023-24 and 2024-25 seasons.

1.3 Cosmic Ray

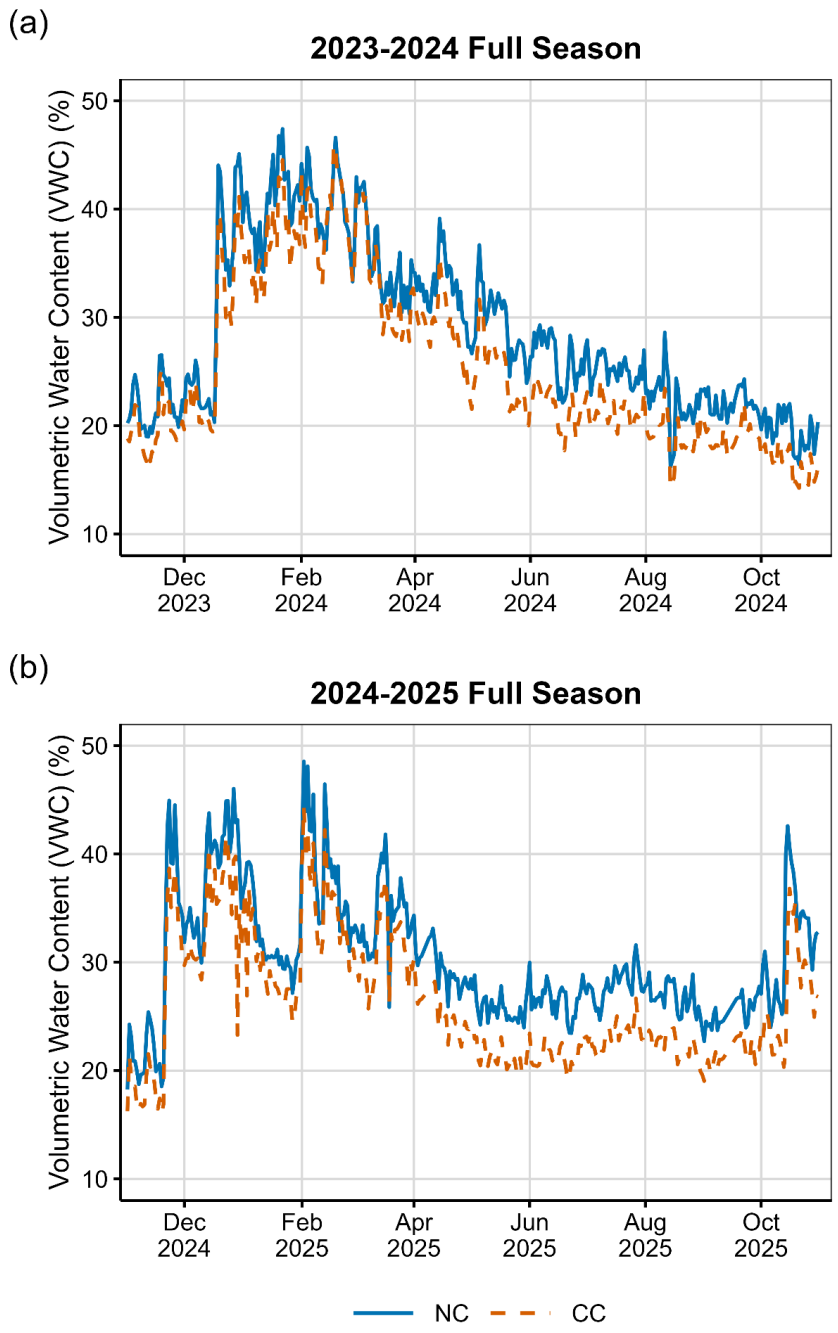


Figure S2. Daily volumetric water content (VWC, %) dynamics measured by cosmic-ray soil moisture sensors for two consecutive pistachio growing cycles: (a) 2023–2024 full season and (b) 2024–2025 full season. Data represent the comparison between two management treatments: NC (blue, solid line) and CC (orange, dashed line). X-axis labels represent the beginning of the respective months.

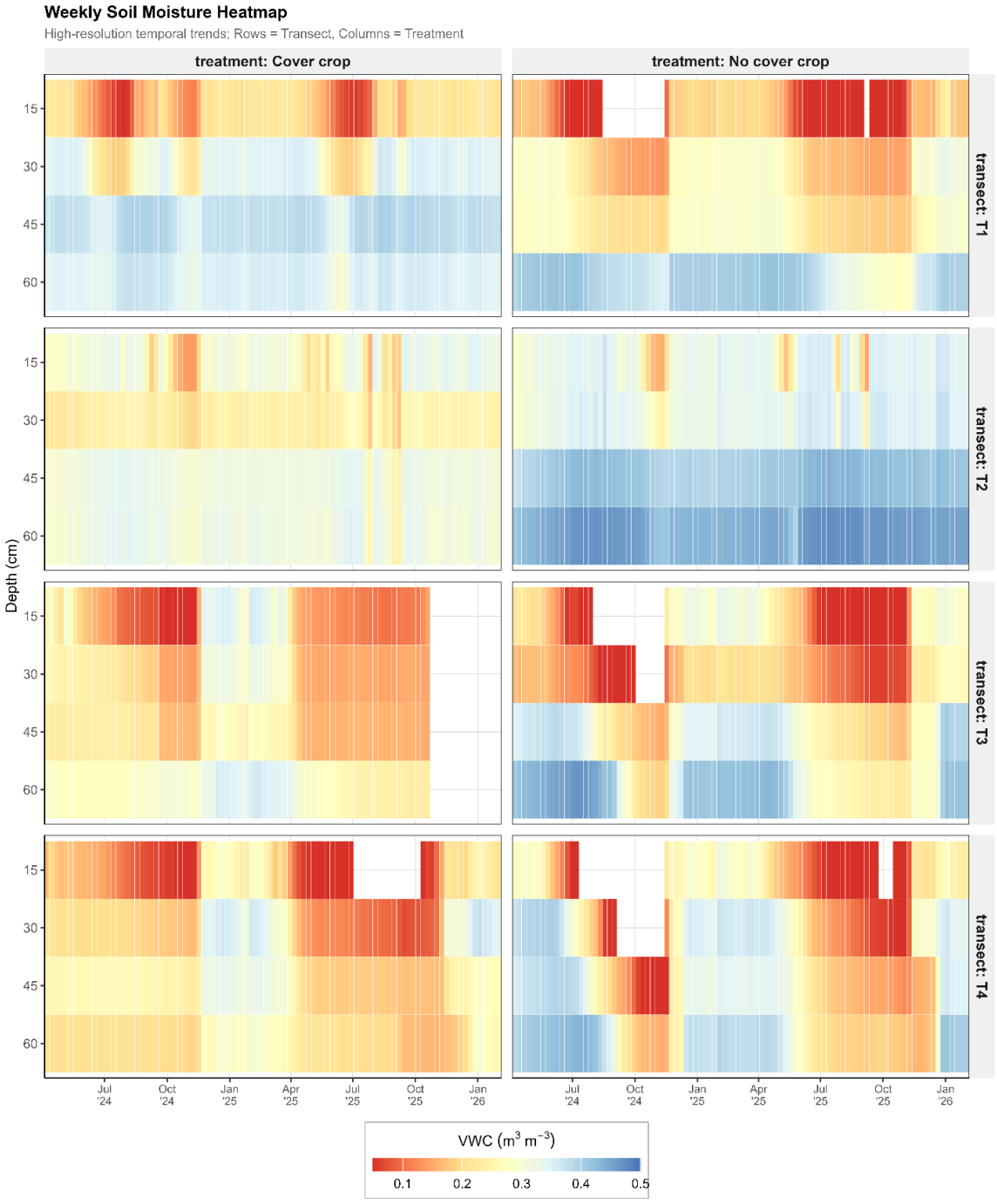


Figure S3. Spatiotemporal dynamics of weekly soil volumetric water content (VWC). Heatmaps illustrate the intensity and duration of soil moisture at four depths (15, 30, 45, and 60 cm) across a spatial transect (T1: tree line to T4: interrow center) for cover crop (left) and no cover crop (right) treatments. Color scales represent VWC ranging from 0.05 m^3m^{-3} (red/dry) to 0.50 m^3m^{-3} (blue/wet). White gaps indicate periods of missing data or sensor maintenance. Data spans from mid-2024 through early 2026, capturing seasonal wetting fronts from winter precipitation and subsequent drying cycles during the growing seasons.

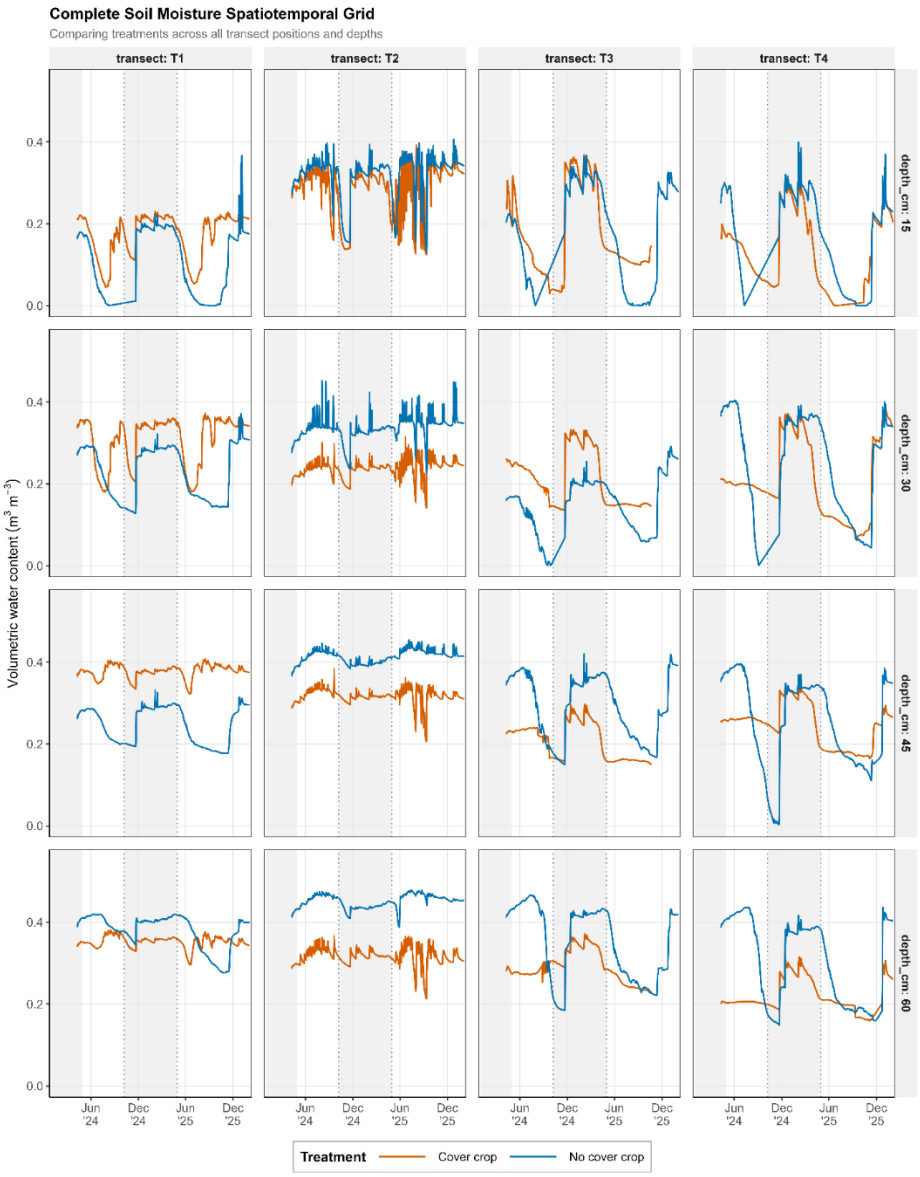


Figure S4. A 4x4 matrix of daily mean volumetric water content (VWC) time series. Columns denote spatial transect positions (T1: Tree line to T4: Interrow center), and rows indicate sensor depths (15, 30, 45, and 60 cm). Time spans from mid-2024 to late-2025. Data is shown for two treatments: Cover crop (orange lines) and no cover crop (blue lines). Light grey background shading indicates winter precipitation/dormant periods. This visualization reveals distinct interactive effects of treatment, depth, and spatial position on soil moisture dynamics and water infiltration patterns throughout the study period.

1.4 OpenET

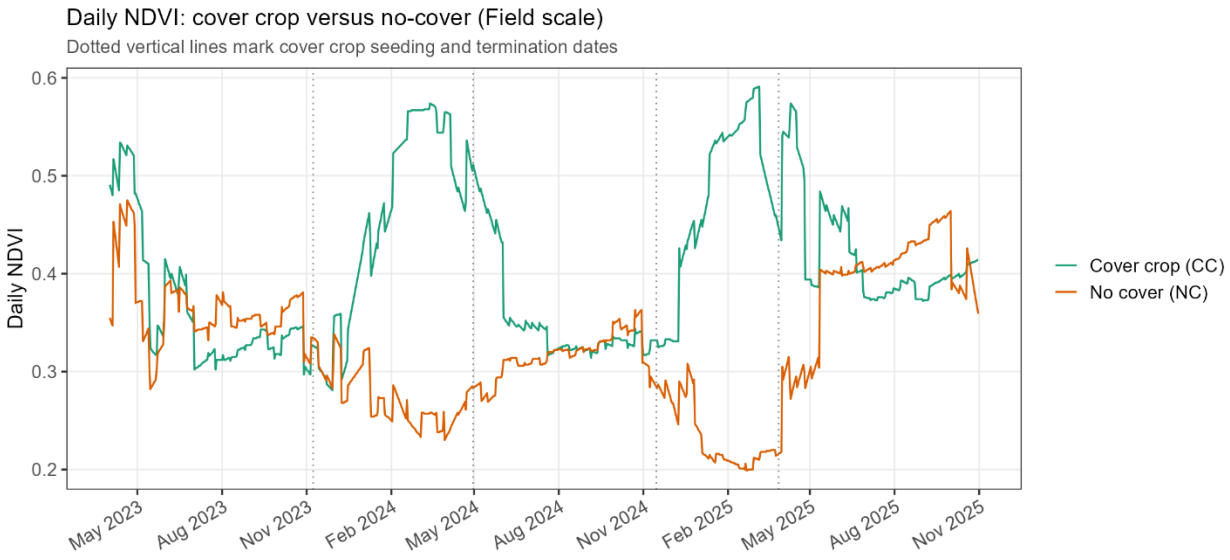


Figure S5. OpenET daily NDVI from April 2023 to November 2025.

2. Support Materials for Chapter 2

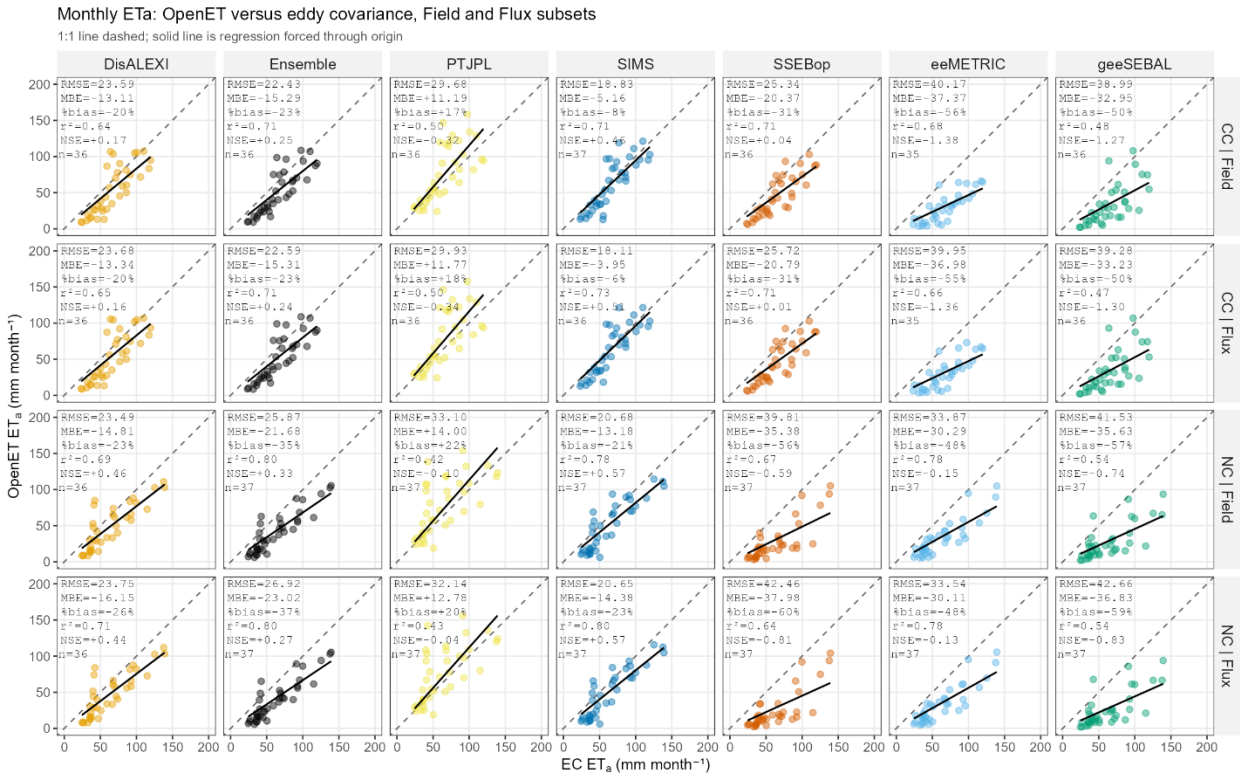


Figure S1 Monthly ET_a from the seven OpenET products versus eddy covariance ET_a across the cover crop (CC) and no cover crop (NC) treatments and the Field and Flux subsets at the orchard. Monthly values are computed as the sum of daily values within each calendar month. Each panel shows the seven products in columns (DisALEXI, OpenET Ensemble, PT-JPL, SIMS, SSEBop, eeMETRIC, geeSEBAL) and the four region-by-subset combinations in rows (CC Field, CC Flux, NC Field, NC Flux). The dashed line is the 1:1 reference; the solid line is the regression forced through the origin. Per-panel statistics report the slope of the regression forced through the origin (Slope), root mean square error (RMSE), mean bias error (MBE), percent bias, the coefficient of determination (r^2), Nash-Sutcliffe efficiency (NSE), and the number of paired monthly observations.

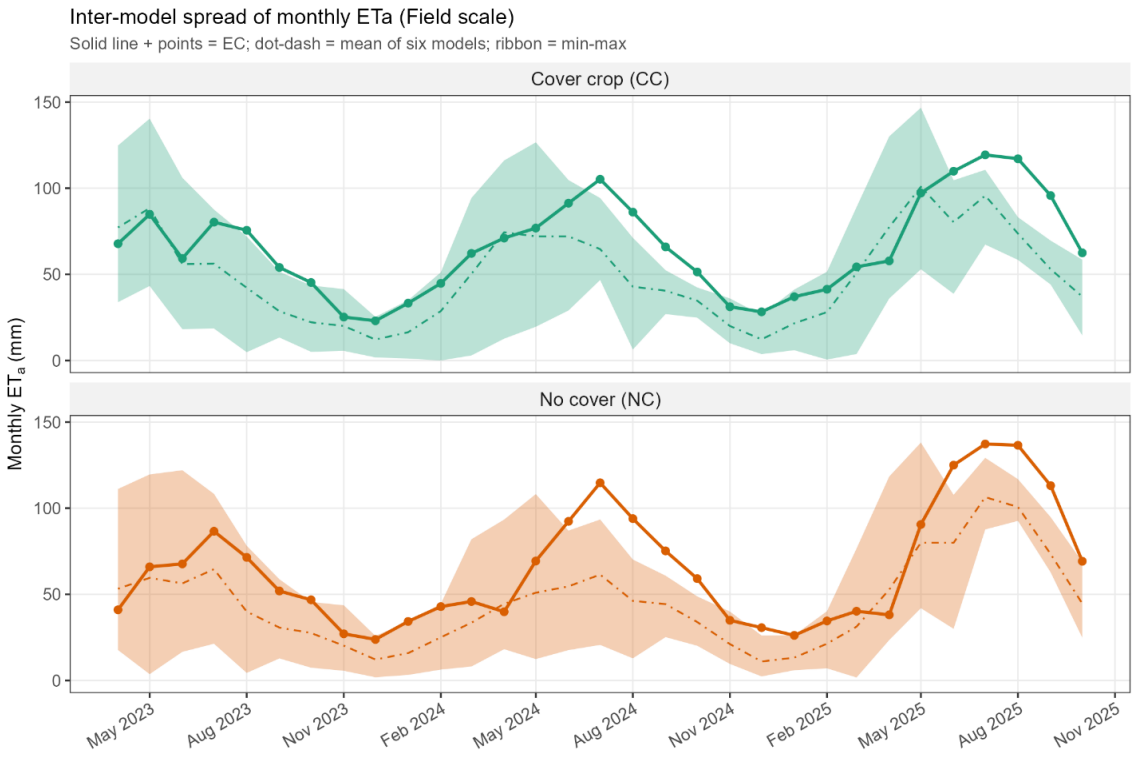


Figure S2. Inter-model spread of monthly ET_a across the six OpenET products at the field scale, for the cover cropped (CC, top panel, green) and no cover crop (NC, bottom panel, orange) treatments. The solid line and points show EC monthly ET_a, the dot-dash line shows the mean of the six OpenET models, and the shaded ribbon shows the min-max envelope across the six products.

Table S1. Three-year mean monthly NDVI by treatment (Field subset, 2023 to 2025).

Month	CC NDVI	NC NDVI	CC minus NC
Jan	0.48	0.25	+0.23
Feb	0.55	0.23	+0.32
Mar	0.53	0.23	+0.30
Apr	0.51	0.33	+0.18
May	0.43	0.33	+0.10
Jun	0.39	0.36	+0.03
Jul	0.34	0.36	-0.02
Aug	0.34	0.37	-0.03
Sep	0.35	0.38	-0.03
Oct	0.36	0.37	-0.01
Nov	0.33	0.32	+0.01
Dec	0.38	0.29	+0.09

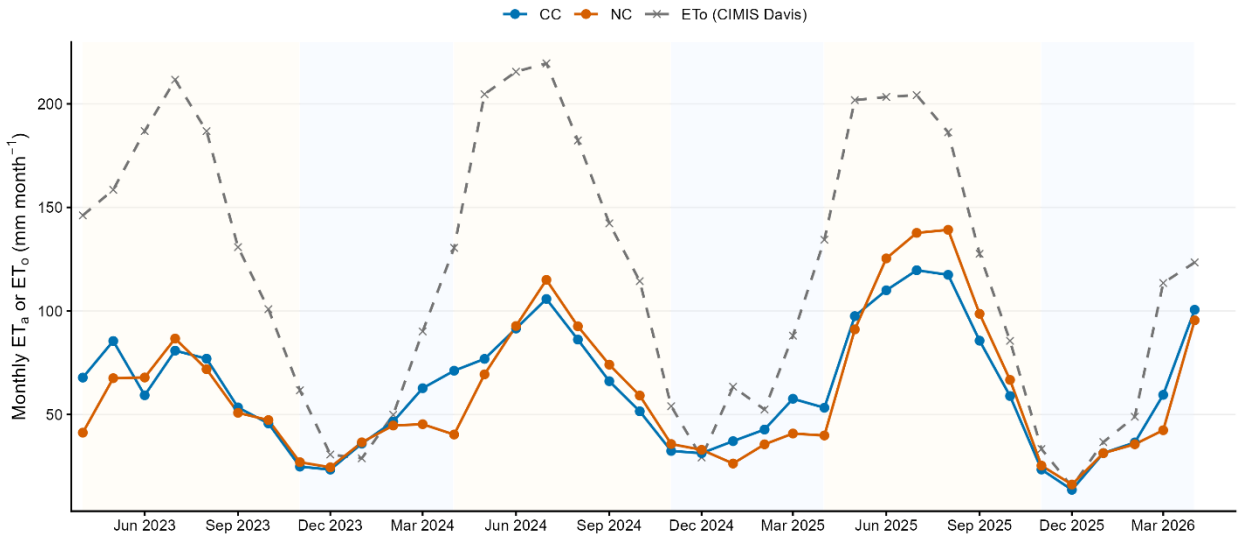


Figure S3. Monthly eddy covariance ET_a for the cover cropped (CC, blue) and no cover crop (NC, orange) treatments at the orchard, with CIMIS Davis Station #006 monthly ET_o overlaid (gray dashed). Background bands distinguish growing seasons (light yellow) from cover crop winter seasons (light blue).

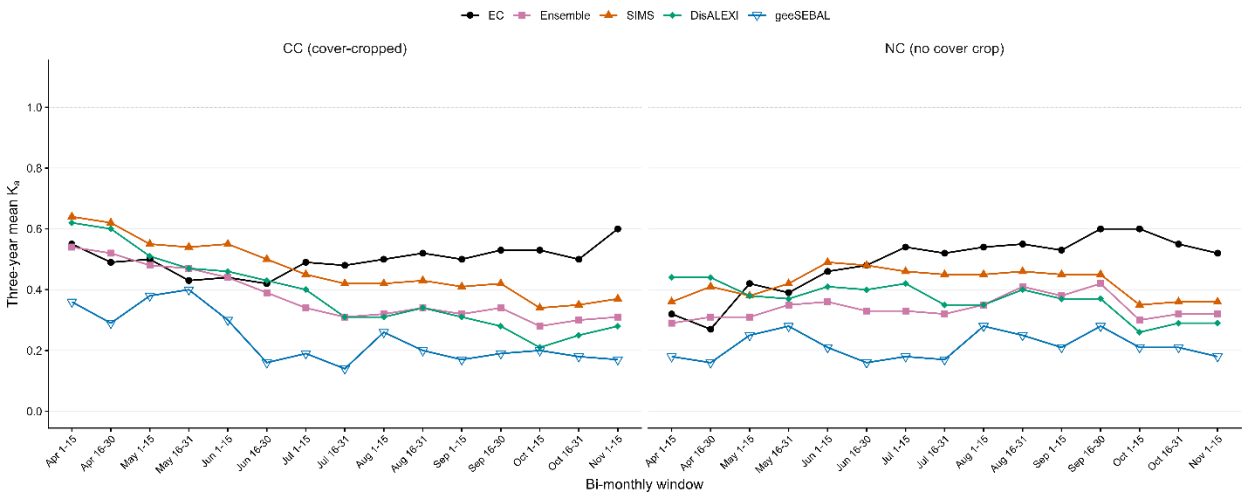


Figure S4. Three-year-mean (2023 to 2025) bi-monthly actual crop coefficient (K_a) by treatment and source. Two panels: cover crop (CC, left) and no cover crop (NC, right). EC (black, filled circles) is the ground reference. Top OpenET performers are shown: OpenET Ensemble (purple, squares), SIMS (vermillion, triangles), DisALEXI (green, diamonds), and geeSEBAL (blue, inverted triangles). Each window-K_a is computed as the ratio of summed daily ET_a to summed daily ET_o over each of 15 bi-monthly windows from April 1-15 through November 1-15. The dotted gray line at K_a = 1.0 marks the reference ET equivalence threshold.

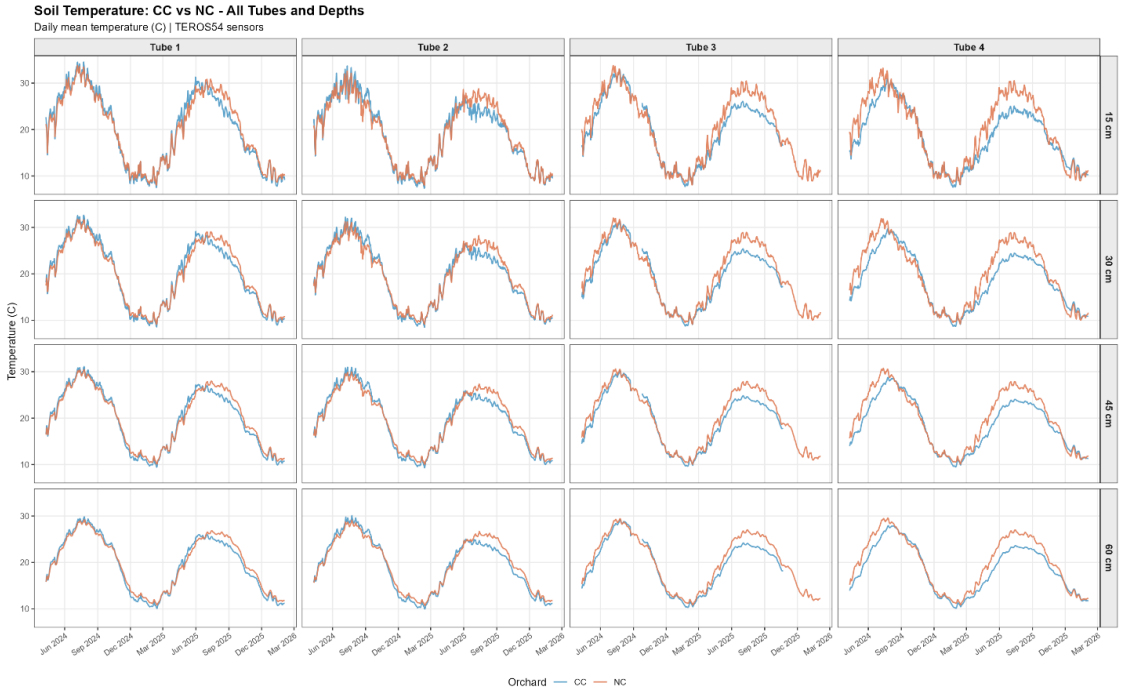


Figure S5. Daily mean soil temperature (°C) recorded by TEROS-54 sensors at the cover crop (CC, blue) and no cover crop (NC, orange) treatments across the 2024 and 2025 growing seasons (April through October). Measurements are shown at the 15, 30, 45 and 60 cm depths in the active root zone, where CC summer values averaged 1 to 2 °C cooler than NC.

Table S2. Daily RMSE by model, treatment, and season (mm/d, Field subset). Models ordered by overall daily RMSE within each treatment.

Model	Treatment	2023 Grow	2023-24 Winter	2024 Grow	2024-25 Winter	2025 Grow
SIMS	CC	0.71	0.44	0.76	0.43	0.93
Ensemble	CC	0.92	0.56	0.94	0.62	0.99
DisALEXI	CC	1.04	0.54	0.93	0.59	0.98
SSEBop	CC	1.17	0.63	1.05	0.60	0.92
PT-JPL	CC	1.26	0.64	1.15	0.56	1.38
eeMETRIC	CC	1.23	1.22	1.56	1.14	1.48
geeSEBAL	CC	1.38	0.98	1.80	0.89	1.75
SIMS	NC	0.64	0.73	0.69	0.72	0.92
DisALEXI	NC	0.92	0.62	1.03	0.70	0.96
Ensemble	NC	0.88	0.77	1.18	0.81	1.02
PT-JPL	NC	1.39	0.83	1.20	0.68	1.37
eeMETRIC	NC	1.21	0.94	1.34	0.85	1.32
SSEBop	NC	1.46	0.90	2.04	0.97	1.22
geeSEBAL	NC	1.52	0.97	2.00	0.89	1.80

Table S3. Three-year mean of bi-monthly Ka by source and treatment (2023 to 2025).

Window	EC		Ensemble		DisALEXI		PT-JPL		SIMS		SSEBop		eeMETRIC		geeSEBAL	
	CC	NC	CC	NC	CC	NC	CC	NC	CC	NC	CC	NC	CC	NC	CC	NC
Apr 1-15	0.51	0.32	0.54	0.29	0.62	0.44	0.88	0.77	0.64	0.36	0.50	0.17	0.15	0.14	0.37	0.18
Apr 16-30	0.46	0.27	0.52	0.31	0.60	0.44	0.84	0.76	0.62	0.41	0.49	0.21	0.18	0.14	0.29	0.16
May 1-15	0.49	0.41	0.48	0.31	0.51	0.38	0.78	0.70	0.55	0.38	0.42	0.16	0.21	0.18	0.38	0.25
May 16-31	0.43	0.39	0.47	0.35	0.47	0.37	0.68	0.62	0.54	0.42	0.41	0.22	0.25	0.20	0.40	0.28
Jun 1-15	0.44	0.46	0.44	0.36	0.46	0.41	0.60	0.58	0.55	0.49	0.41	0.22	0.27	0.25	0.30	0.21
Jun 16-30	0.42	0.48	0.39	0.33	0.43	0.40	0.57	0.58	0.50	0.48	0.35	0.21	0.26	0.24	0.16	0.16
Jul 1-15	0.48	0.54	0.34	0.33	0.40	0.42	0.46	0.51	0.45	0.46	0.29	0.21	0.23	0.25	0.19	0.18
Jul 16-31	0.48	0.53	0.31	0.32	0.31	0.35	0.38	0.45	0.42	0.45	0.27	0.23	0.23	0.29	0.14	0.18
Aug 1-15	0.49	0.54	0.32	0.35	0.31	0.35	0.39	0.47	0.42	0.45	0.27	0.24	0.24	0.31	0.26	0.28
Aug 16-31	0.51	0.55	0.34	0.41	0.34	0.40	0.44	0.54	0.43	0.46	0.31	0.31	0.28	0.41	0.20	0.25
Sep 1-15	0.54	0.59	0.32	0.38	0.31	0.37	0.42	0.52	0.41	0.45	0.34	0.31	0.30	0.43	0.17	0.21
Sep 16-30	0.54	0.61	0.34	0.42	0.28	0.37	0.51	0.62	0.42	0.45	0.33	0.36	0.32	0.47	0.19	0.28
Oct 1-15	0.54	0.60	0.28	0.30	0.21	0.26	0.46	0.52	0.34	0.35	0.27	0.22	0.27	0.36	0.20	0.21
Oct 16-31	0.51	0.56	0.30	0.33	0.25	0.29	0.65	0.70	0.35	0.36	0.29	0.25	0.31	0.40	0.18	0.21
Nov 1-15	0.47	0.52	0.31	0.32	0.28	0.29	0.64	0.68	0.37	0.36	0.30	0.24	0.33	0.40	0.17	0.18

Table S4. Field subset versus flux footprint extraction sensitivity, daily RMSE (mm/d). Difference is computed as (Flux minus Field) divided by Field, in percent.

Model	Treatment	Field subset	Flux subset	Difference (%)
SIMS	CC	0.708	0.718	+1.4
Ensemble	CC	0.850	0.859	+1.1
DisALEXI	CC	0.873	0.877	+0.5
SSEBop	CC	0.936	0.950	+1.5
PT-JPL	CC	1.098	1.111	+1.2
eeMETRIC	CC	1.356	1.352	-0.3
geeSEBAL	CC	1.464	1.479	+1.0
SIMS	NC	0.749	0.740	-1.2
DisALEXI	NC	0.886	0.893	+0.8
Ensemble	NC	0.961	0.987	+2.7
PT-JPL	NC	1.172	1.116	-4.8
eeMETRIC	NC	1.179	1.164	-1.3
SSEBop	NC	1.429	1.512	+5.8
geeSEBAL	NC	1.566	1.591	+1.6

3. Support Materials for Chapter 3

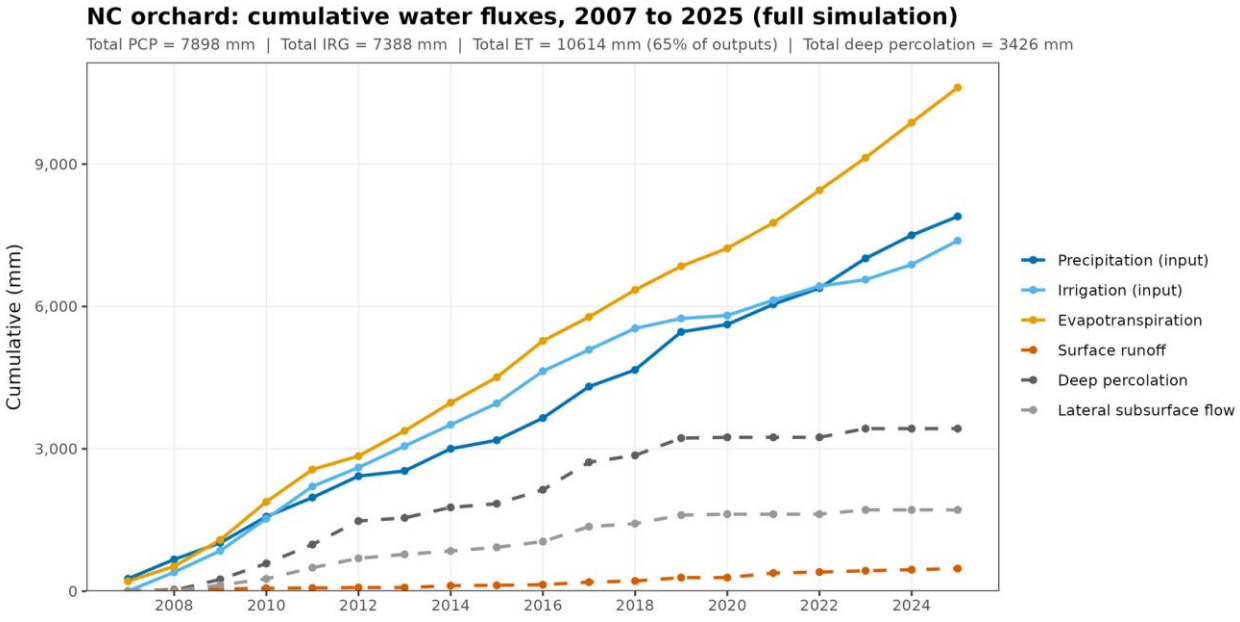


Figure S6. Cumulative water fluxes for the NC orchard. Window: 2007 to 2025 (full simulation).

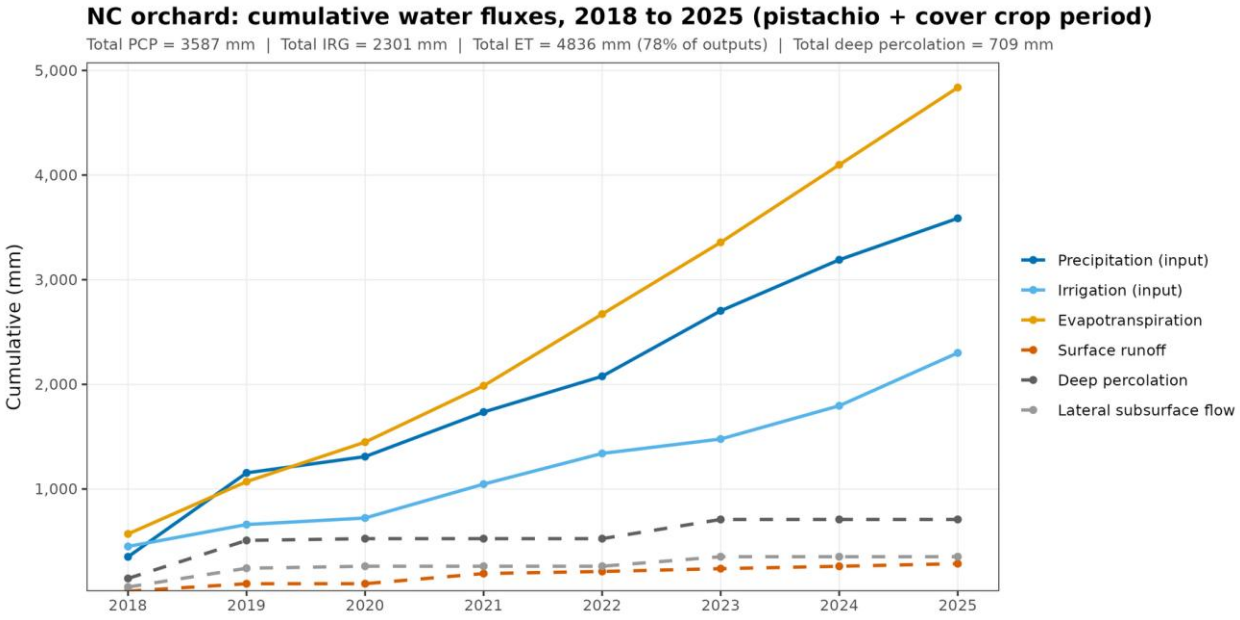


Figure S7. Cumulative water fluxes for the NC orchard. Window: 2018 to 2025 pistachio + winter period.

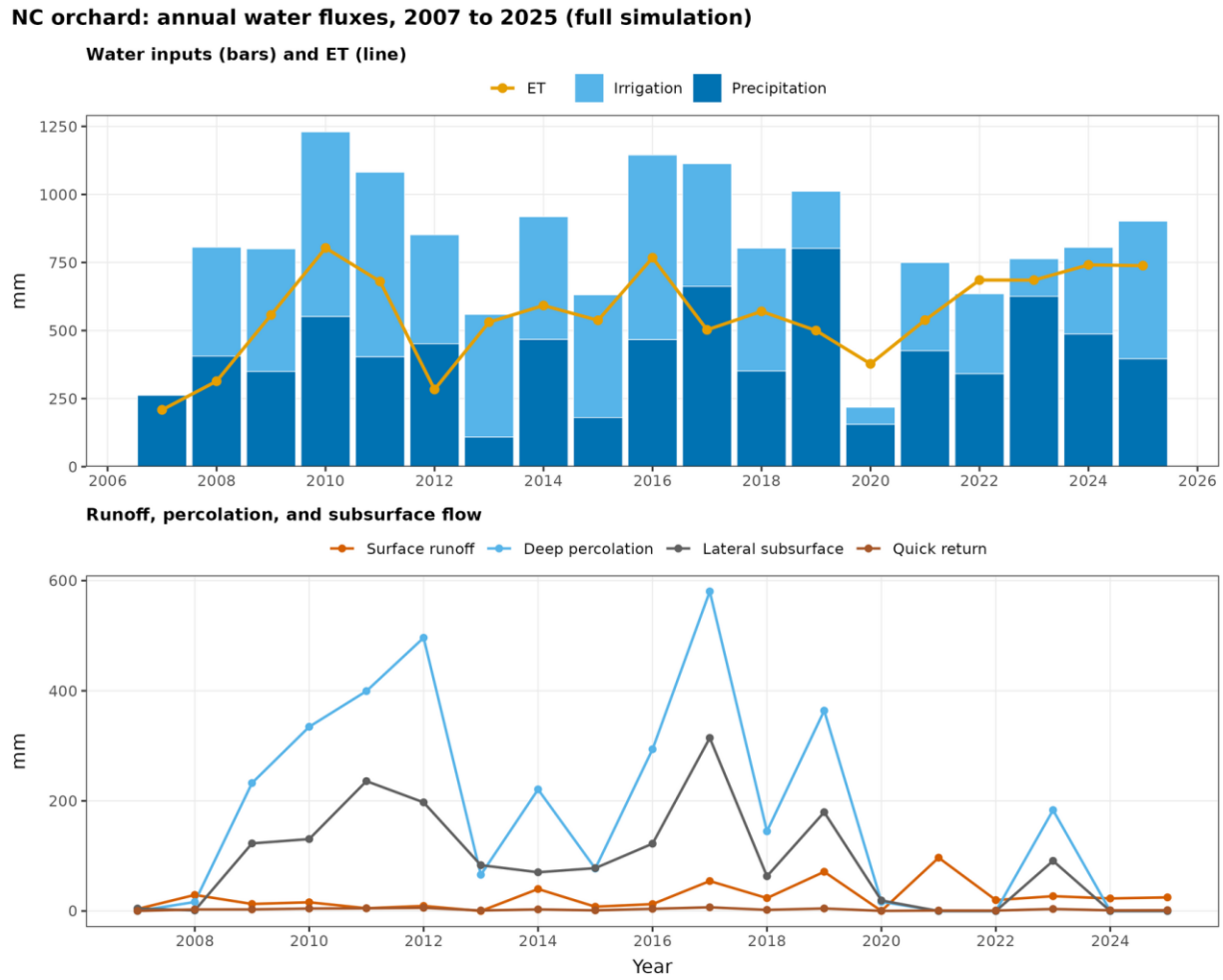


Figure S8. Annual water fluxes for the no cover (NC) orchard. Window: 2007 to 2025 (full simulation).

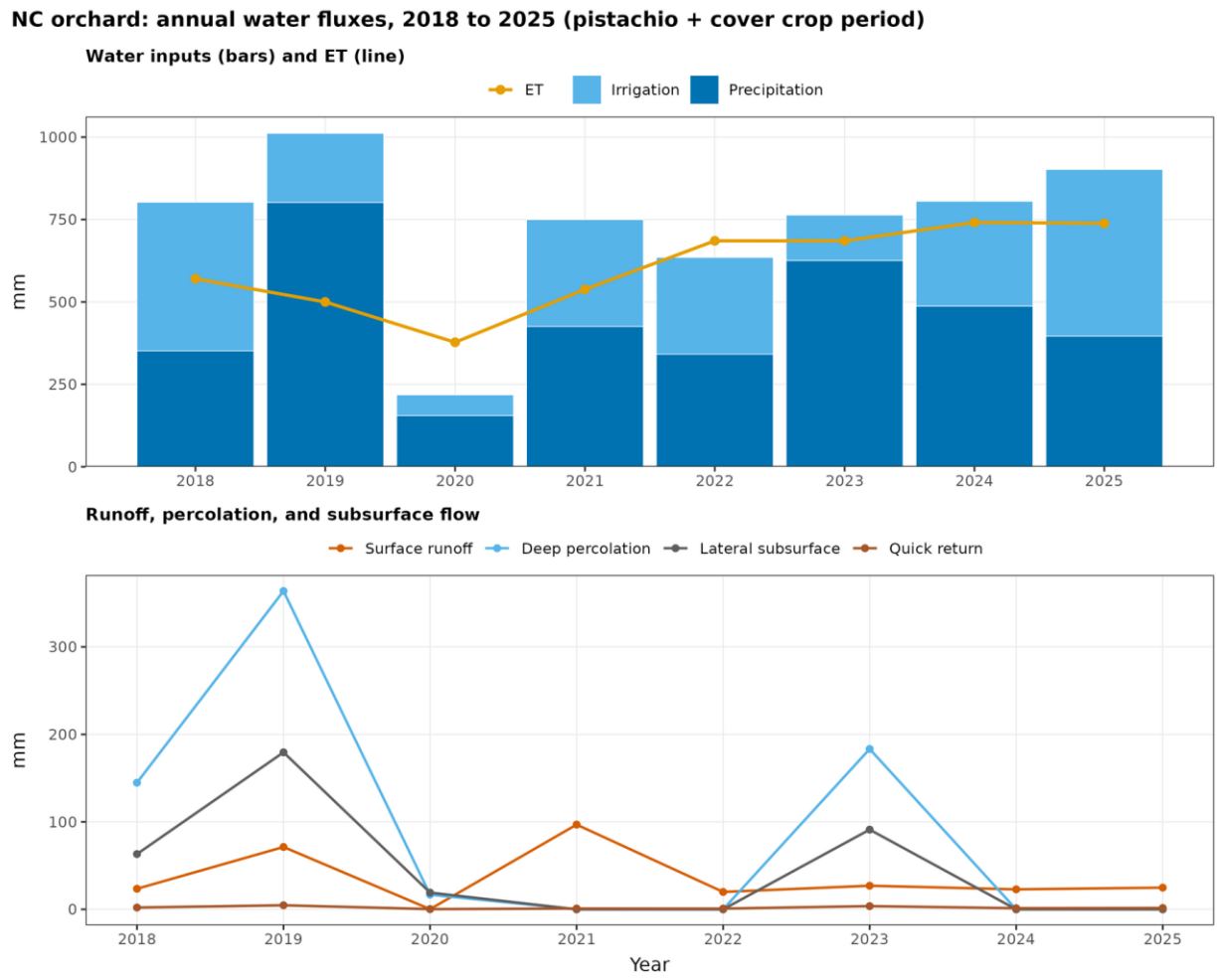


Figure S9. Annual water fluxes for the no cover (NC) orchard. Window: 2018 to 2025 pistachio + winter period.

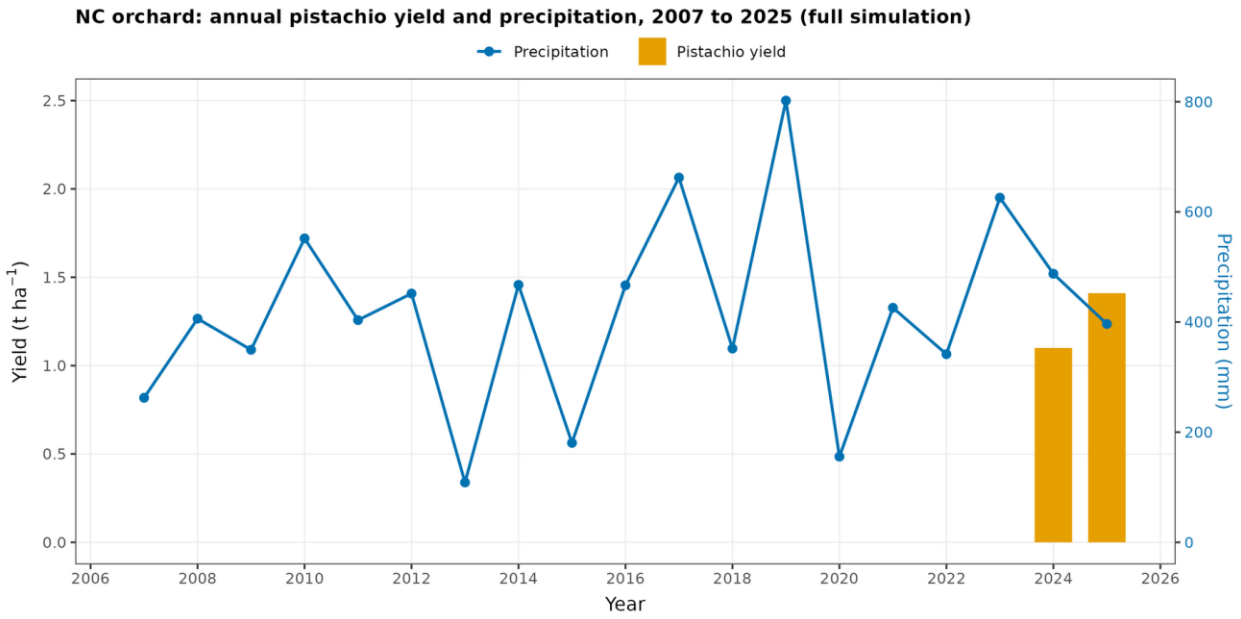


Figure S10. Annual pistachio yield and precipitation for the no cover (NC) orchard. Window: 2007 to 2025 (full simulation).

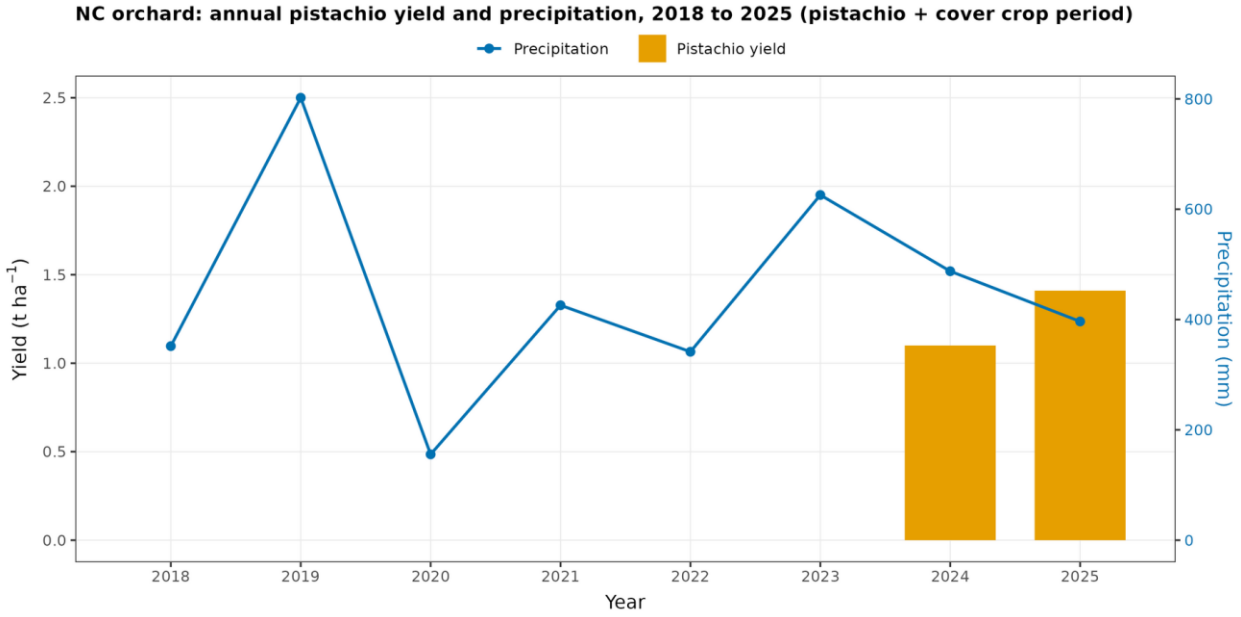


Figure S11. Annual pistachio yield (orange bars, left axis) and annual precipitation (blue line, right axis) for the no cover (NC) baseline simulation over the 2018 to 2025 pistachio + winter period.

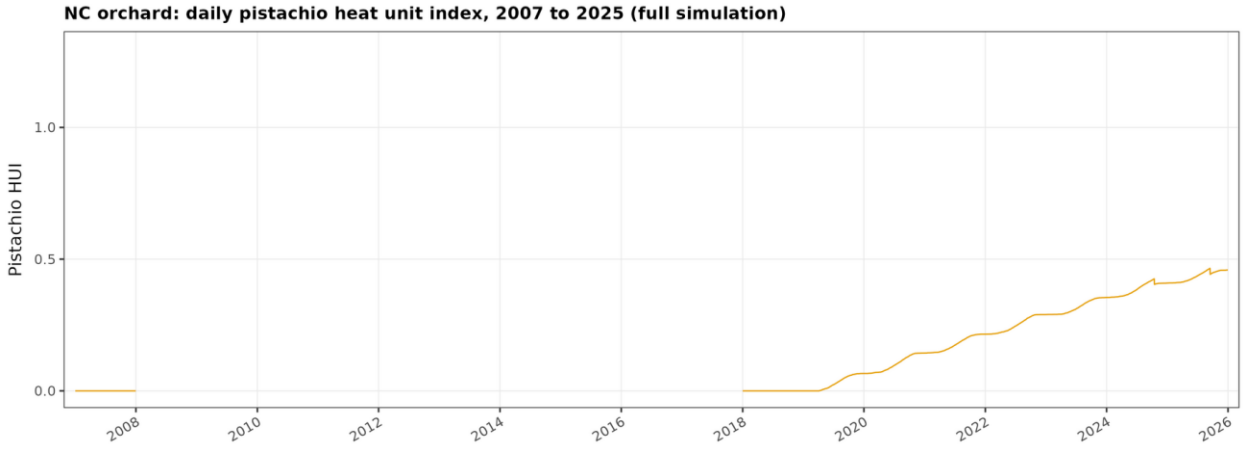


Figure S12. Daily pistachio heat unit index for the no cover (NC) baseline simulation. Window: 2007 to 2025 (full simulation).

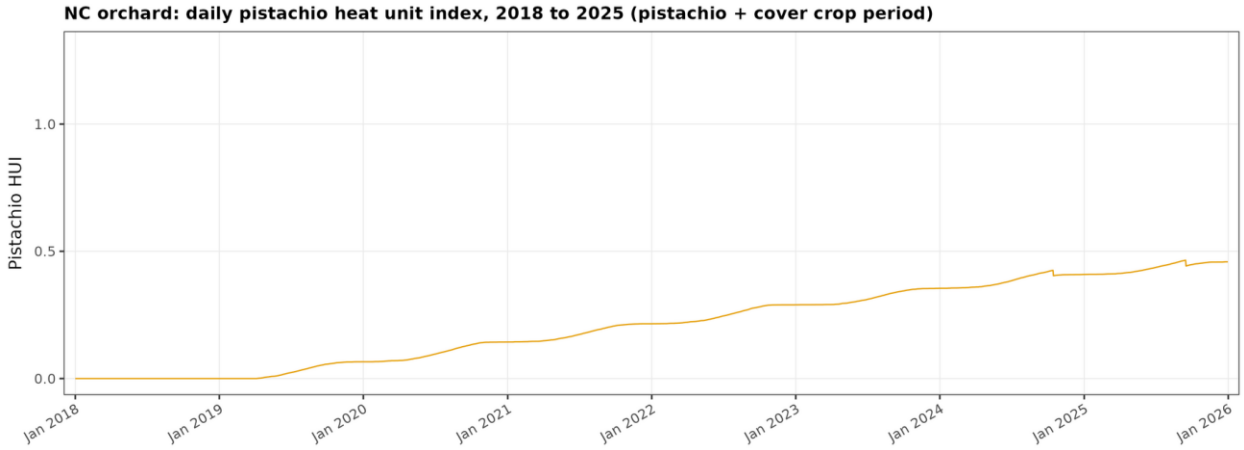


Figure S13. Daily pistachio heat unit index for the no cover (NC) baseline simulation. Window: 2018 to 2025 pistachio + winter period.

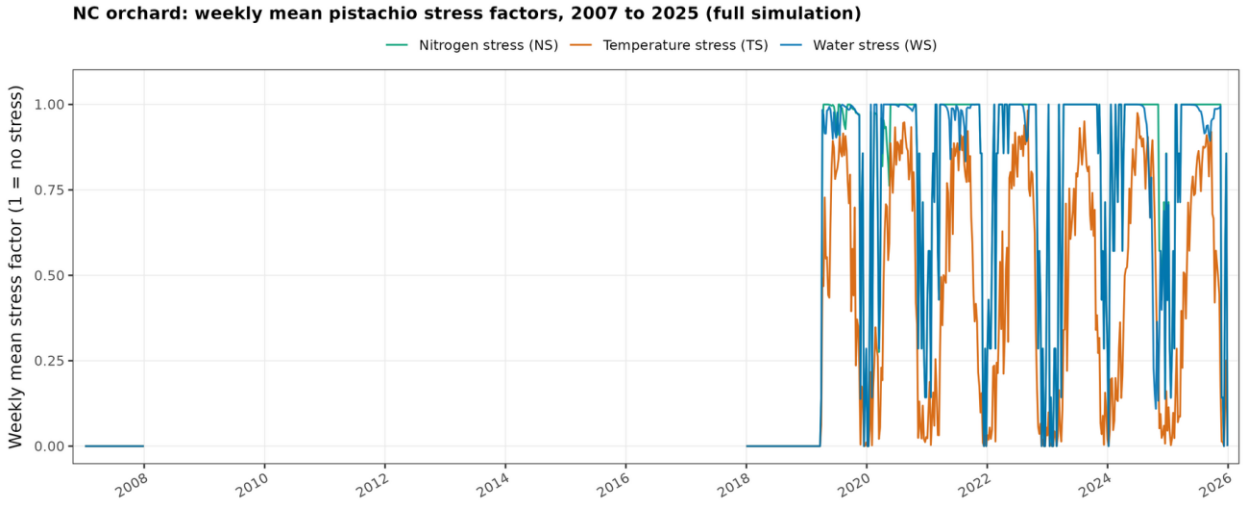


Figure S14. Weekly mean pistachio stress factors for the no cover (NC) baseline simulation. Window: 2007 to 2025 (full simulation).

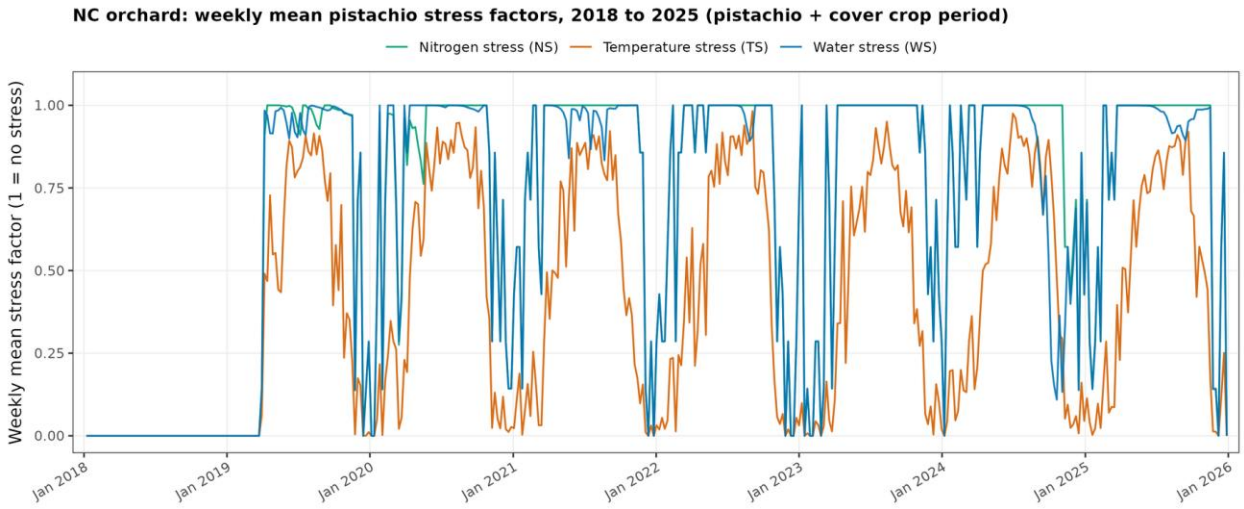


Figure S15. Weekly mean pistachio stress factors for the no cover (NC) baseline simulation over the 2018 to 2025 pistachio + winter period. Stress factors are scaled so that 1.0 indicates no stress. Daily PIST_WS, PIST_NS, and PIST_TS values were averaged over each calendar week.

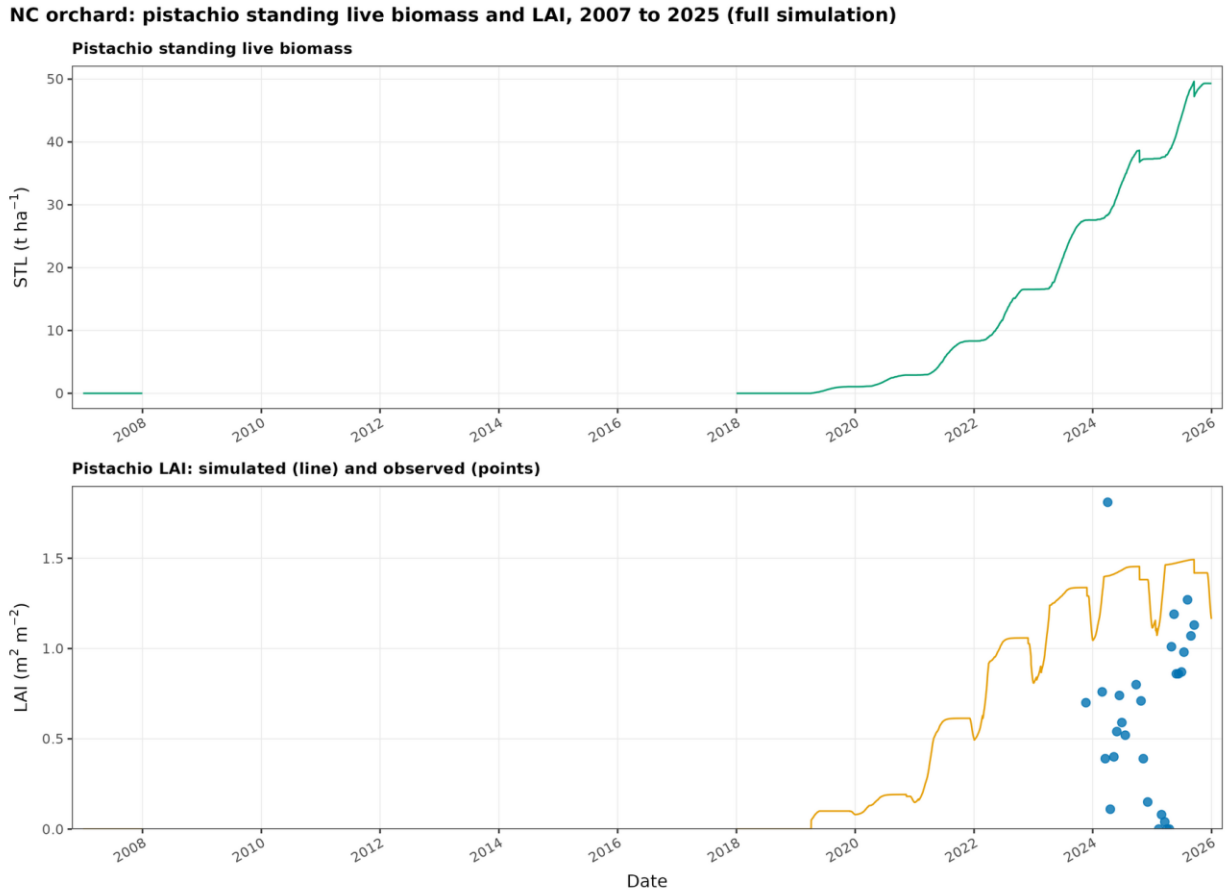


Figure S16. Daily pistachio standing live biomass and LAI for the no cover (NC) baseline simulation; the field data window panel (b) is clipped to Feb 1 2023 through Dec 31 2025. Window: 2007 to 2025 (full simulation).

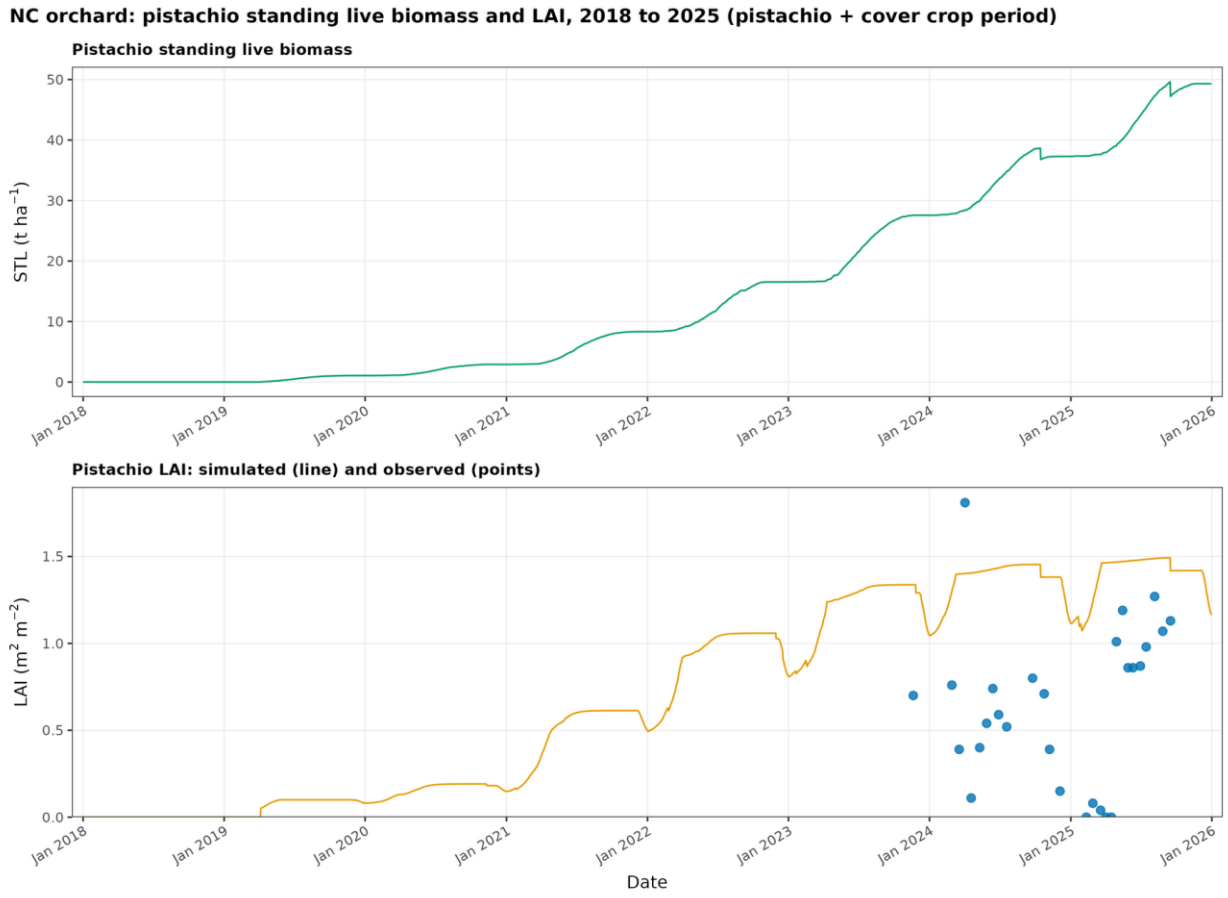


Figure S17. Daily pistachio standing live biomass (STL, t ha^{-1}; top panel) and LAI (m^2 m^{-2}; bottom panel) for the no cover (NC) baseline simulation over the 2018 to 2025 pistachio + winter period. Observed pistachio LAI from LI-2200 measurements is overlaid as blue points.

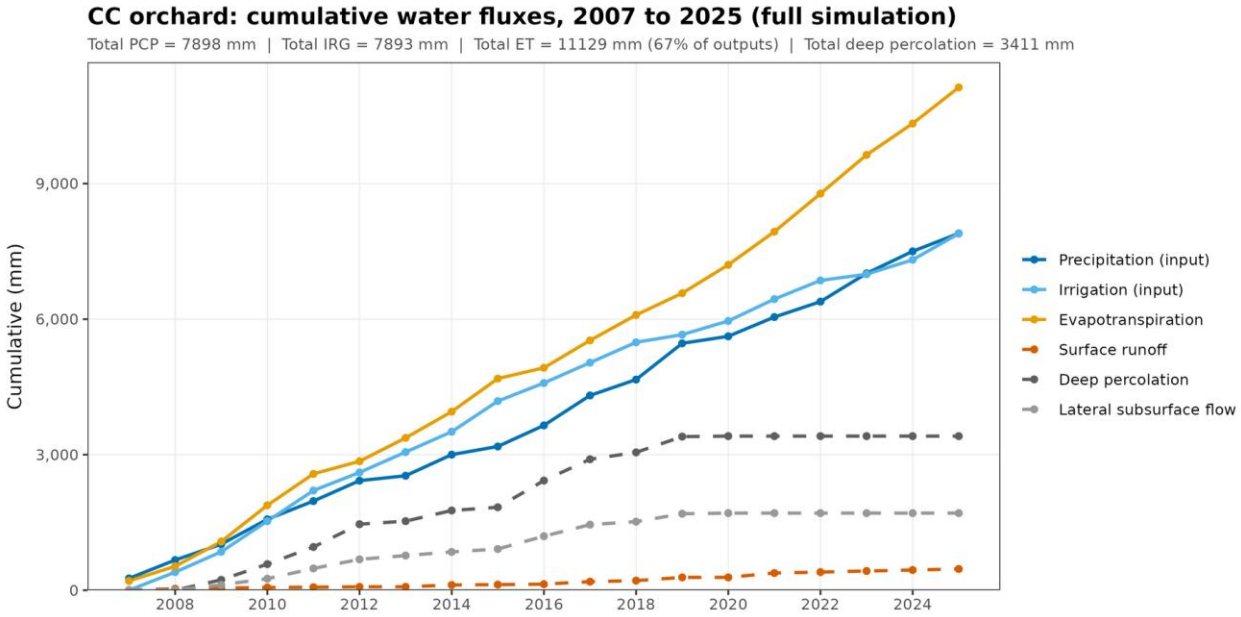


Figure S18. Cumulative water fluxes for the CC orchard. Window: 2007 to 2025 (full simulation).

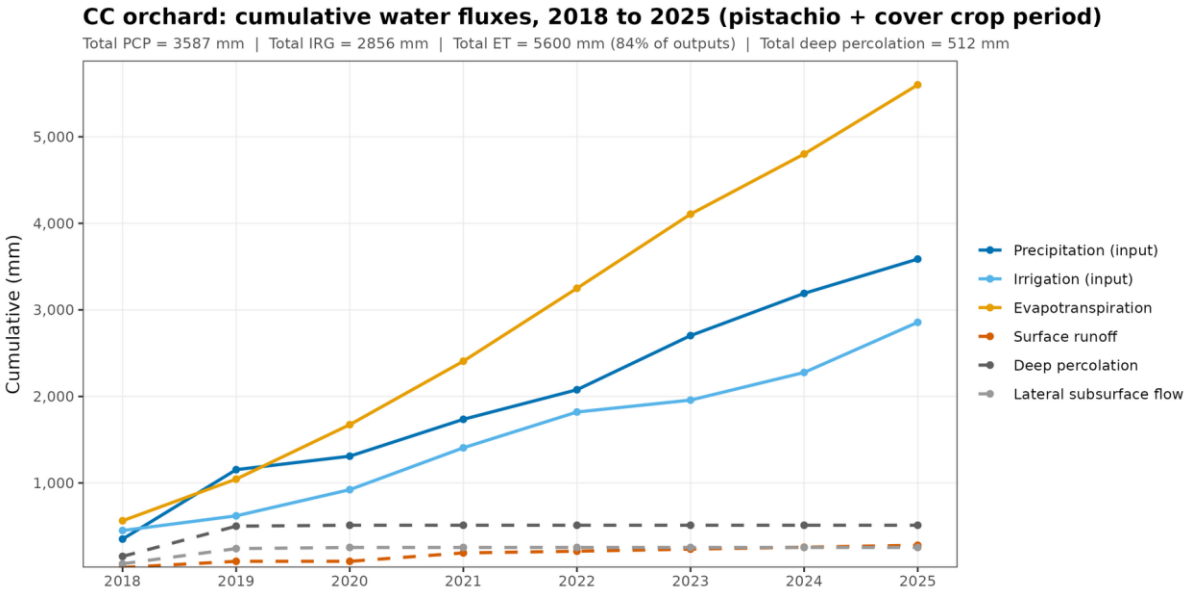


Figure S19. Cumulative water fluxes for the CC orchard over the 2018 to 2025 pistachio + winter period. The CC orchard differs from NC primarily in the partitioning between ET, surface runoff, and deep percolation during the winter-spring CC window.

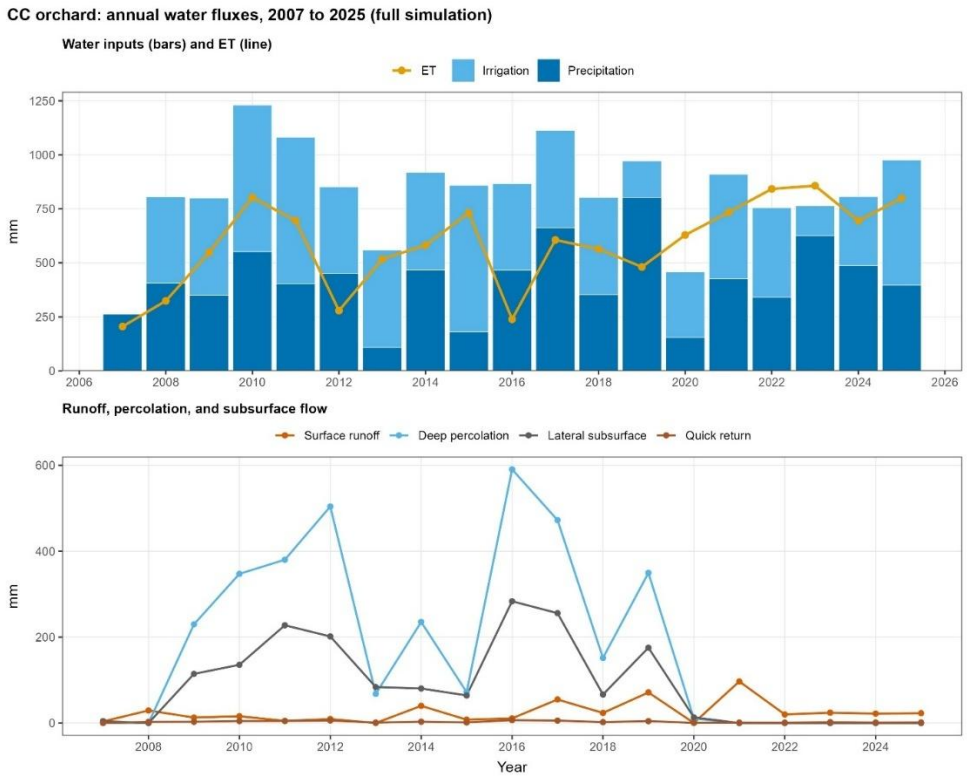


Figure S20. Annual water fluxes for the cover crop (CC) orchard. Window: 2007 to 2025 (full simulation).

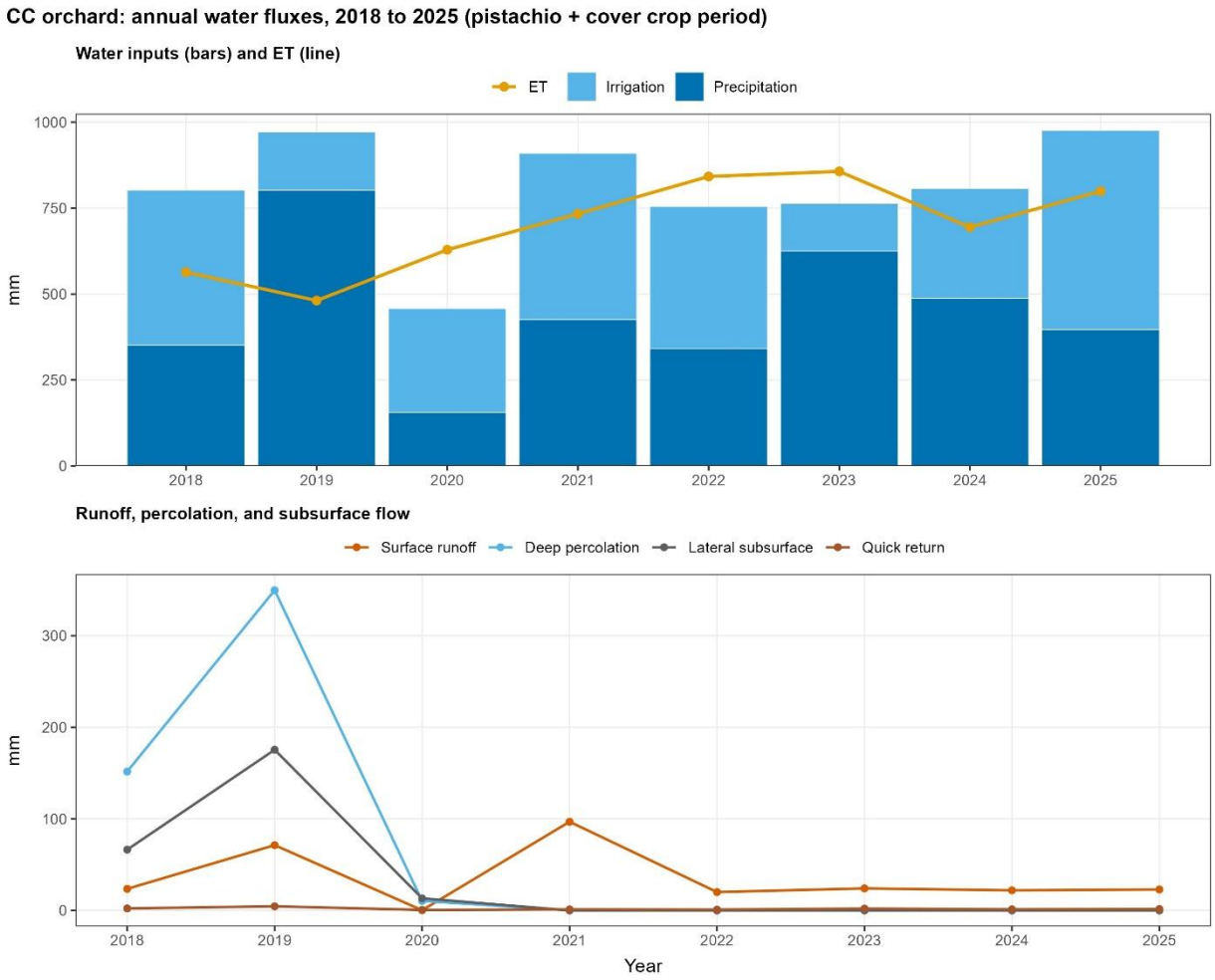


Figure S21. Annual water fluxes for the cover crop (CC) orchard. Window: 2018 to 2025 pistachio + winter period.

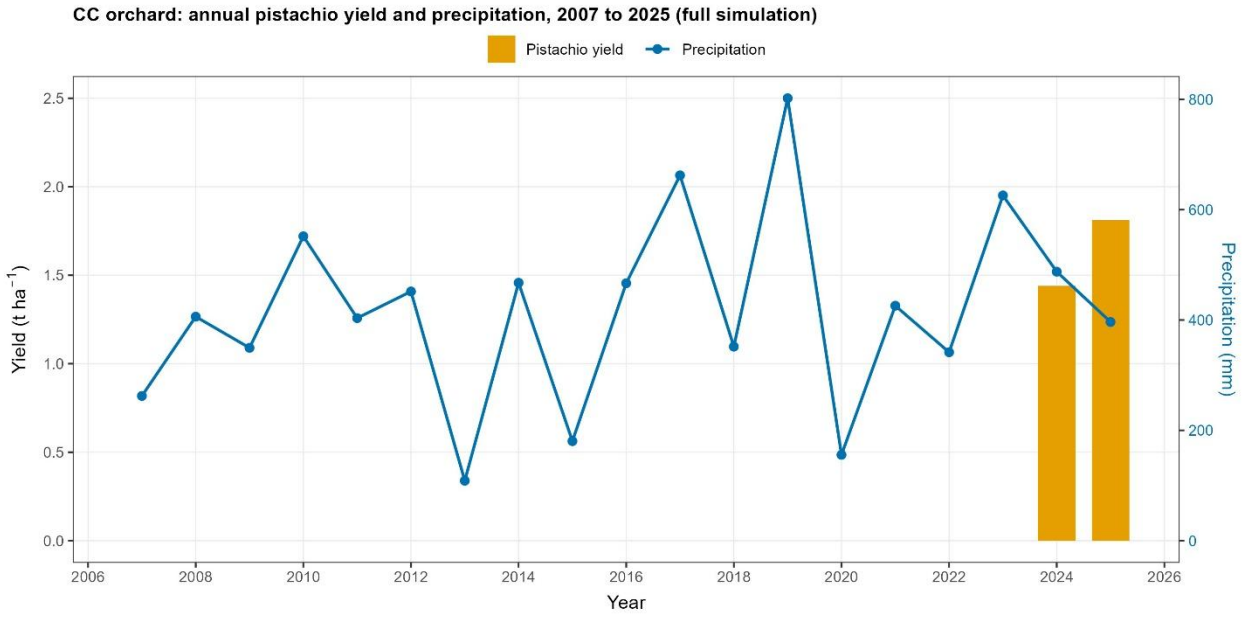


Figure S22. Annual pistachio yield and precipitation for the cover crop (CC) orchard. Window: 2007 to 2025 (full simulation).

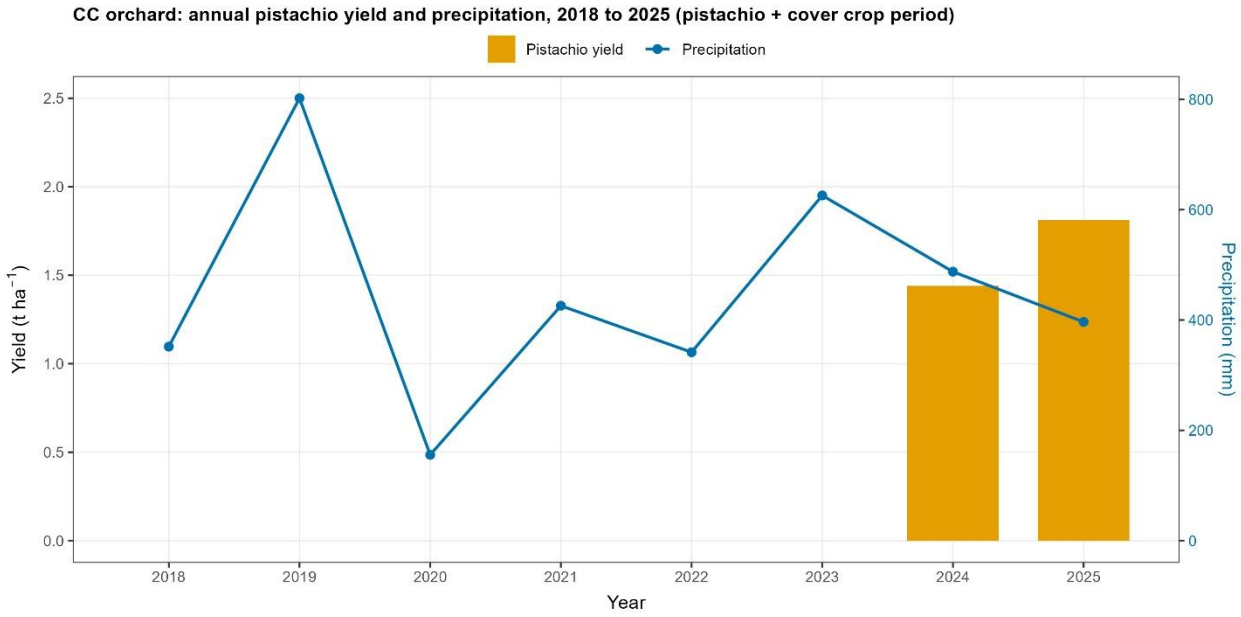


Figure S23. Annual pistachio yield (orange bars, left axis) and annual precipitation (blue line, right axis) for the cover crop (CC) baseline simulation over the 2018 to 2025 pistachio + winter period.

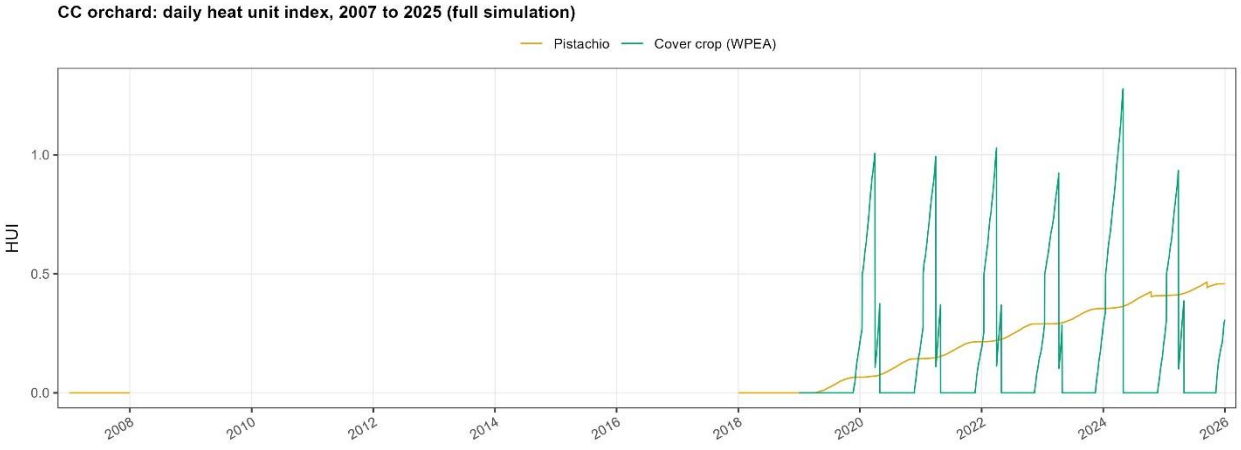


Figure S24. Daily pistachio heat unit index for the cover crop (CC) baseline simulation. Window: 2007 to 2025 (full simulation).

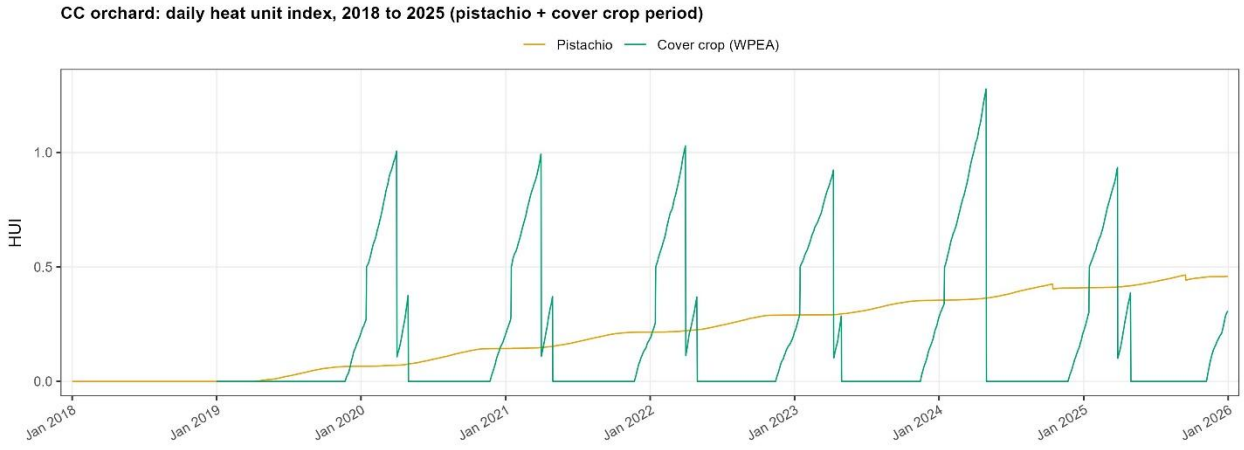


Figure S25. Daily pistachio heat unit index for the cover crop (CC) baseline simulation. Window: 2018 to 2025 pistachio + winter period.

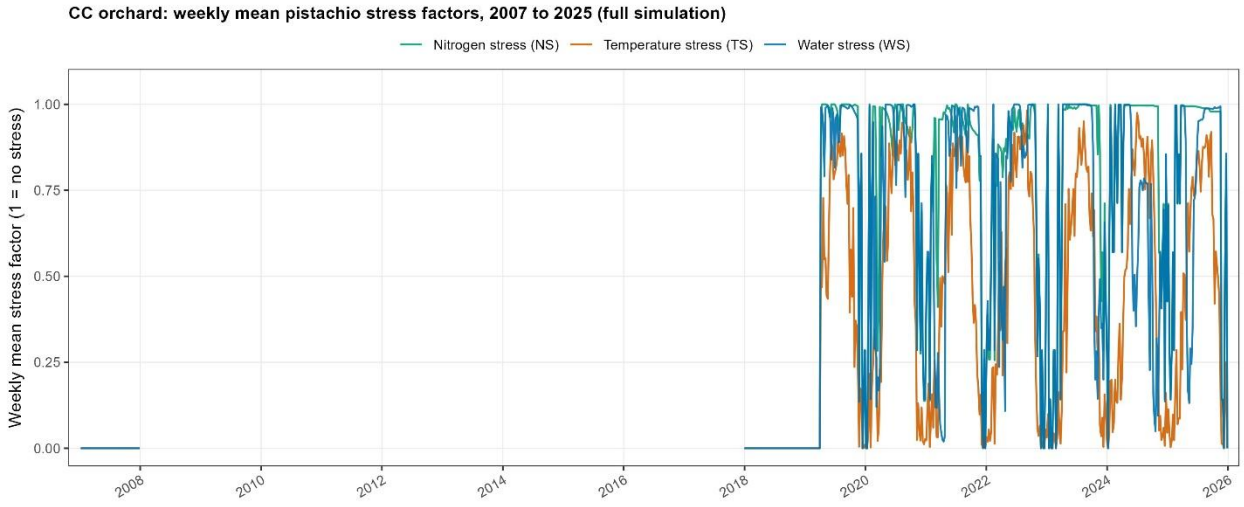


Figure S26. Weekly mean pistachio stress factors for the cover crop (CC) baseline simulation. Window: 2007 to 2025 (full simulation).

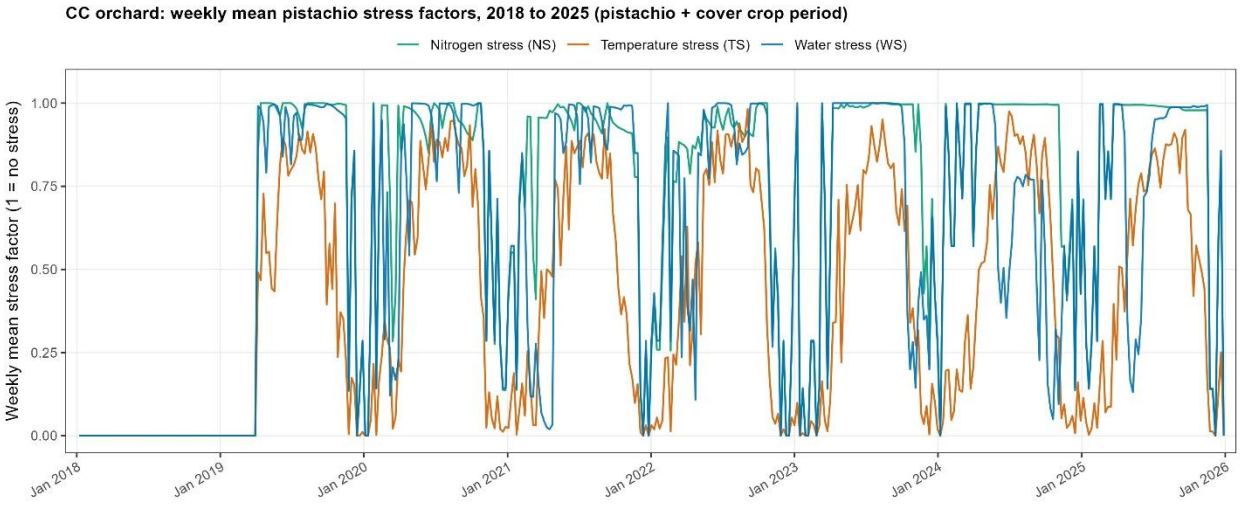


Figure S27. Weekly mean pistachio stress factors for the cover crop (CC) baseline simulation over the 2018 to 2025 pistachio + cover crop period. Stress factors are scaled so that 1.0 indicates no stress. Daily PIST_WS, PIST_NS, and PIST_TS values were averaged over each calendar week.

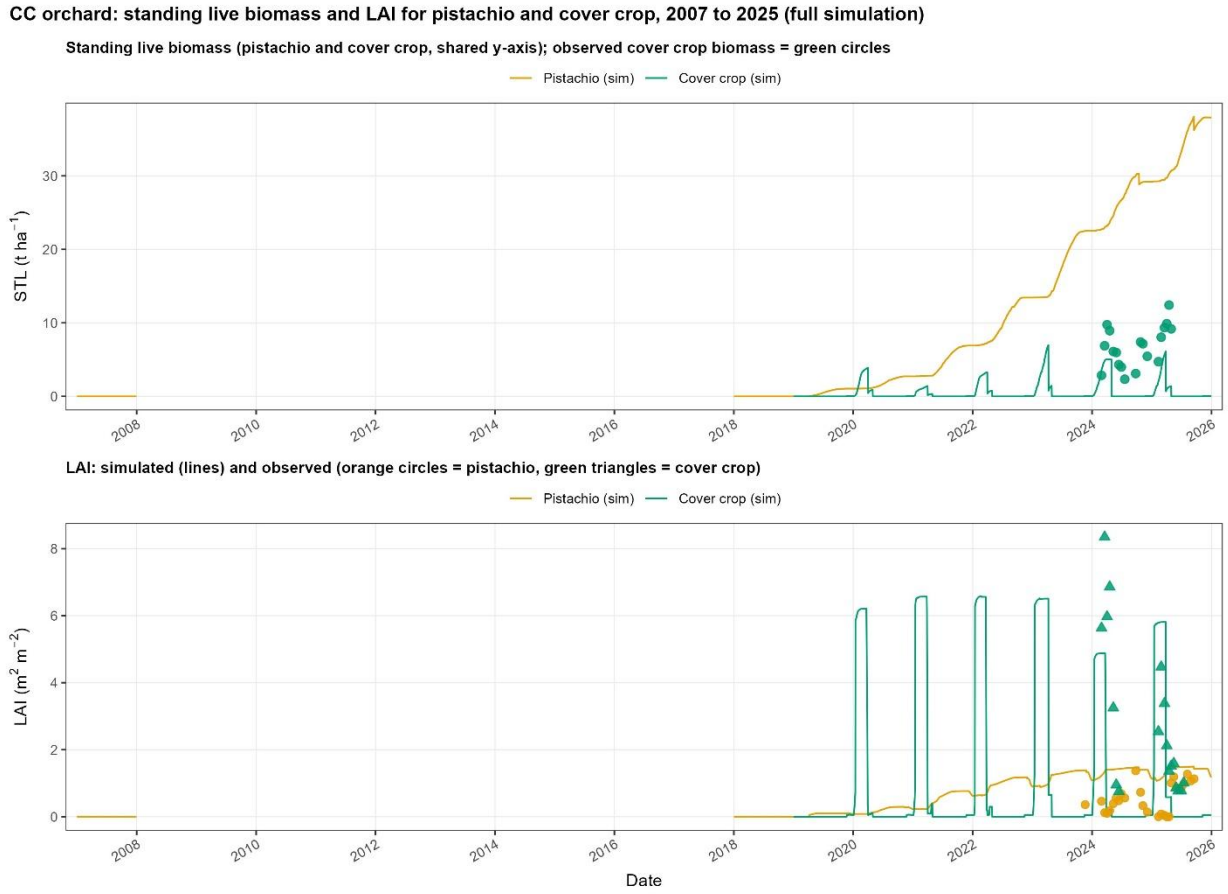


Figure S28. Daily pistachio standing live biomass and LAI for the cover crop (CC) baseline simulation; the field data window panel (b) is clipped to Feb 1 2023 through Dec 31 2025. Window: 2007 to 2025 (full simulation).

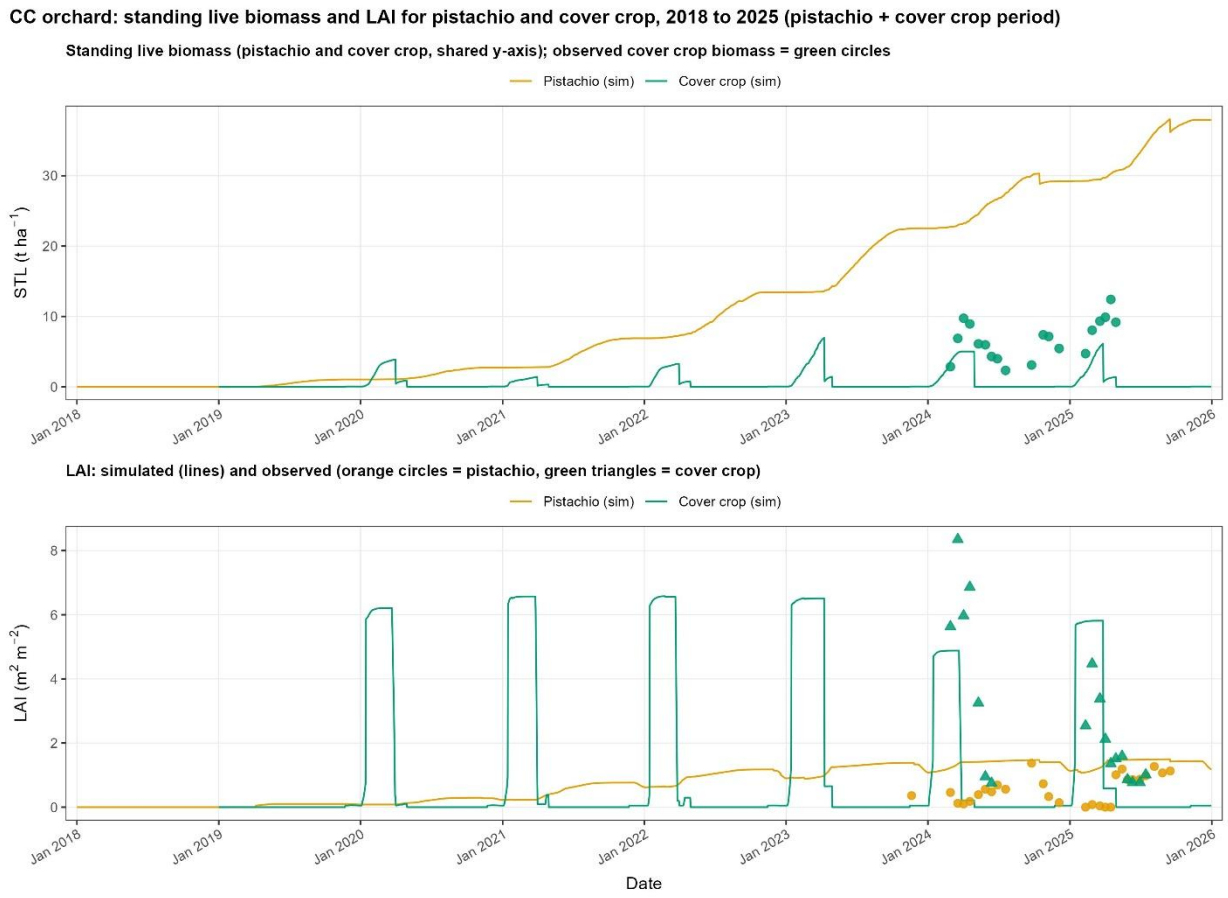


Figure S29. Daily pistachio standing live biomass (STL, t ha^{-1}; top panel) and LAI (m^2 m^{-2}; bottom panel) for the cover crop (CC) baseline simulation over the 2018 to 2025 pistachio + winter period. Observed pistachio LAI from LI-2200 measurements is overlaid as green points.